

Organic carbon transfer between coral reef micro- and macro-organisms under environmental change

Doctoral Thesis by

Bianca M. Thobor

For the attainment of the academic degree of

Doktor der Naturwissenschaften

- Dr. rer. nat. -

Submitted to the Department of Biology and Chemistry

at the University of Bremen

In May 2024

Supervised by Prof. Dr. Christian Wild



Supervisor

Prof. Dr. Christian Wild
Marine Ecology
FB2 Biology / Chemistry
University of Bremen

Reviewers

Prof. Dr. Christian Wild (FB2, University of Bremen)
Prof. Dr. Marko Rohlf (FB2, University of Bremen)
Jr. Prof. Dr. Claudia Pogoreutz (Université Perpignan Via Domitia, France)

Examiners

Prof. Dr. Juliane Filser (FB2, University of Bremen)
Prof. Dr. Christian Wild (FB2, University of Bremen)
Prof. Dr. Marko Rohlf (FB2, University of Bremen)
Jr. Prof. Dr. Claudia Pogoreutz (Université Perpignan Via Domitia, France)

Other members of the examination committee

Dr. Benjamin Müller (FB2, University of Bremen)
Jonna Holm (BSc student, University of Bremen)

Date of Defence: 5th of June 2024

The present work was carried out from February 2021 until May 2024 at the Centre of Environmental Research and Sustainable Technology (UFT), University of Bremen, Germany.

The work was financed by baseline funds from the University of Bremen.



*This thesis is dedicated to my mother Christina
who decided to get a second child (me) instead of a PhD.*

Abstract

Efficient organic carbon (OC) and nutrient cycling between coral reef-associated micro- and macro-organisms is vital for coral reef functioning and supports the ecosystems' exceptional productivity. However, global and local anthropogenic stressors interfere with the transfer of OC within the reef ecosystem (i.e., through altered benthic-pelagic coupling) as well as within its keystone species, the coral holobiont (i.e., between coral host and algal endosymbiont). Excess OC inputs through wastewater and/or algal blooms can stimulate microbe-mediated hypoxia and disease, supporting coral mortality and resulting in shifts towards macroalgae or soft coral dominance on many degraded reefs. While soft corals are generally understudied, carbohydrates exuded by macroalgae may support reef degradation by stimulating bacterioplankton respiration, but the role of carbohydrates released by benthic primary producers in shaping coral reef community metabolism is still poorly understood. This thesis aims to improve our knowledge on OC transfer between coral reef micro- and macro-organisms under environmental change by: i) assessing the effects of global and local stressors on the physiology of the increasingly widespread soft coral *Xenia umbellata*, ii) developing an indicator tool for the detection of OC eutrophication in reefs, and iii) investigating the carbohydrate compositions of hard coral- and macroalgae exudates and their effects on bacterioplankton communities. The experimental studies in this thesis include physiological, biogeochemical, and microbial parameters, and were carried out in aquarium facilities in Bremen and on Curaçao, Dutch Caribbean. Findings revealed a high resistance of *X. umbellata* to warming, phosphate eutrophication, and acidification, while nitrate eutrophication reduced its resistance to warming. A newly developed microbial fuel cell (MFC) successfully detected OC pulses by electrically quantifying microbial degradation of OC in coral reef sediment. Compositional analyses of coral mucus carbohydrates and comparisons with previously reported data revealed a correlation with hard coral phylogeny. When comparing hard coral- with macroalgae exudates, differences in carbohydrate compositions and responses of bacterioplankton communities emerged. Coral exudates enriched opportunistic microbial taxa commonly considered as stress indicators, while macroalgae exudates were compositionally similar to ambient reef water and did not induce any shift in bacterioplankton communities. In conclusion, the soft coral *X. umbellata* may replace less resistant hard corals on many reefs in the future, and may therefore sustain some ecosystem functions and services provided by reefs. However, coastal water quality management will become more important for hard- and soft corals with ongoing ocean warming. As such, the here presented MFCs could be used to detect OC eutrophication before benthic community shifts occur. Changes in hard coral assemblages may influence benthic-pelagic coupling in yet unexplored ways through their compositionally distinct mucus carbohydrates. Macroalgae exudates will likely reduce trophic transfer of OC compared to coral exudates due to their inefficient incorporation and/or resistance to microbial degradation. Results further suggest that not the origin of OC (i.e., coral- vs. macroalgae-derived) *per se*, but rather an alteration in OC composition relative to ambient reef water disrupts the stable bacterioplankton community and

supports the increase of opportunistic microbes. Overall, results presented here can be used by coral reef managers to target conservation strategies at a soft coral species with high resistance to environmental change and monitor OC eutrophication in reefs with the here developed MFC biosensors. Finally, this thesis provides new insights for understanding how benthic macro-organisms shape microbial communities by altering the OC composition of reef water. As shifts in benthic primary producers are not exclusive to coral reefs, altered OC compositions may influence microbial communities in a wide range of coastal ecosystems under environmental change.

Zusammenfassung

Ein effizienter Kreislauf von organischem Kohlenstoff und Nährstoffen zwischen Korallenriff-assoziierten Mikro- und Makroorganismen ist entscheidend für das Funktionieren von Korallenriffen und trägt zur außergewöhnlichen Produktivität dieser Ökosysteme bei. Globale und lokale anthropogene Stressfaktoren stören jedoch den Transfer von organischem Kohlenstoff im Riff-Ökosystem. Dies geschieht zum Beispiel durch eine veränderte benthisch-pelagische Kopplung, sowie innerhalb der Schlüsselart, dem Korallen-Holobionten, zwischen Korallenwirt und Algen-Endosymbiont. Ein übermäßiger Eintrag von organischem Kohlenstoff durch Abwässer und/oder Algenblüten kann durch Mikroben vermittelte Hypoxie und Krankheiten verursachen, welche das Korallensterben fördern und in vielen betroffenen Riffen zu einer Dominanz von Makroalgen oder Weichkorallen führen. Während Weichkorallen im Allgemeinen wenig erforscht sind, können von Makroalgen abgegebene Kohlenhydrate die Degradierung von Riffen unterstützen, indem sie die Atmung des Bakterioplanktons anregen. Die Rolle der Kohlenhydrate, die von benthischen Primärproduzenten freigesetzt werden, bei der Gestaltung des Stoffwechsels von Korallenriffgemeinschaften ist jedoch noch wenig erforscht. Das Ziel dieser Arbeit ist es, unser Wissen über den Transfer von organischem Kohlenstoff zwischen Mikro- und Makroorganismen in Korallenriffen unter veränderten Umweltbedingungen zu verbessern, indem: i) die Auswirkungen globaler und lokaler Stressfaktoren auf die Physiologie der zunehmend verbreiteten Weichkoralle *Xenia umbellata* getestet werden, ii) ein Indikatorinstrument für den Nachweis von Eutrophierung mit organischem Kohlenstoff in Riffen entwickelt wird und iii) die Kohlenhydratzusammensetzung von Hartkorallen- und Makroalgenexsudaten und ihre Auswirkungen auf Bakterioplanktongemeinschaften untersucht werden. Die experimentellen Untersuchungen in dieser Arbeit umfassen physiologische, biogeochemische und mikrobielle Parameter und wurden in Aquarienanlagen in Bremen und auf Curaçao in der niederländischen Karibik durchgeführt. Die Ergebnisse zeigen eine hohe Resistenz von *X. umbellata* gegenüber Erwärmung, Phosphat-Eutrophierung und Versauerung, während Nitrat-Eutrophierung die Resistenz gegenüber Erwärmung verringert. Eine neu entwickelte mikrobielle Brennstoffzelle (MBZ) konnte erfolgreich Pulse von organischem Kohlenstoff in Riff-Sediment nachweisen, indem sie den mikrobiellen Abbau von organischem Kohlenstoff elektrisch quantifizierte. Die Analyse der Zusammensetzung von Korallenschleim-Kohlenhydraten und der Vergleich mit bisherigen Daten ergaben eine Korrelation mit der Phylogenie der Steinkorallen. Der Vergleich von Steinkorallen- und Makroalgenexsudaten zeigte Unterschiede in der Kohlenhydratzusammensetzung und in den Reaktionen der Bakterioplanktongemeinschaften. Korallenexsudate reicherten opportunistische mikrobielle Taxa an, die gemeinhin als Stressindikatoren gelten, während Makroalgenexsudate in ihrer Zusammensetzung dem umgebenden Riffwasser ähnelten und keine Veränderung in den Bakterioplanktongemeinschaften bewirkten. Zusammenfassend lässt sich sagen, dass die Weichkoralle *X. umbellata* in Zukunft in vielen Riffen die weniger widerstandsfähigen Steinkorallen ersetzen und somit einige Ökosystemfunktionen

und -leistungen der Riffe aufrechterhalten könnte. Mit der fortschreitenden Erwärmung der Ozeane wird das Management der Wasserqualität in den Küstengebieten für Hart- und Weichkorallen jedoch immer wichtiger werden. Die hier vorgestellte MBZ könnte dazu verwendet werden, die Eutrophierung der Küstengewässer zu erkennen, bevor es zu einer Veränderung der benthischen Gemeinschaften kommt. Veränderungen in Hartkorallengemeinschaften könnten die benthisch-pelagische Kopplung auf noch unerforschte Weise durch ihre unterschiedlichen Schleimkohlenhydrate beeinflussen. Makroalgenexsudate verringern vermutlich den trophischen Transfer von organischem Kohlenstoff im Vergleich zu Korallenexsudaten, weil sie weniger effizient umgewandelt werden und/oder gegen den mikrobiellen Abbau resistent sind. Die Ergebnisse weisen außerdem darauf hin, dass nicht die Herkunft des organischen Kohlenstoffs, also ob er von Korallen oder Makroalgen stammt, entscheidend ist. Stattdessen stört eine Veränderung der Zusammensetzung im Vergleich zum Riffwasser die stabile Bakterioplanktongemeinschaft und fördert das Wachstum opportunistischer Mikroben. Insgesamt können die hier vorgestellten Ergebnisse von Korallenriffmanagern genutzt werden, um Erhaltungsstrategien auf eine Weichkorallenart mit hoher Resistenz gegenüber Umweltveränderungen auszurichten und die Eutrophierung durch organischen Kohlenstoff in Riffen mit den hier entwickelten MBZ-Biosensoren zu überwachen. Letztlich liefert diese Arbeit neue Erkenntnisse darüber, wie benthische Makroorganismen mikrobielle Gemeinschaften umformen, indem sie die Zusammensetzung von organischem Kohlenstoff im Riffwasser verändern. Da Veränderungen der benthischen Primärproduzenten nicht auf Korallenriffen beschränkt sind, können veränderte Zusammensetzungen des organischen Kohlenstoffs die mikrobiellen Gemeinschaften in einer Vielzahl von Küstenökosystemen unter sich wandelnden Umweltbedingungen beeinflussen.

Acknowledgements

First of all, I want to sincerely thank Christian Wild for choosing me to become a PhD student in his research group and trusting me to accomplish things I did not know I could. Thank you for your guidance, support, and also for the critical feedback, because it helped me to learn and grow into the person and scientist I am today.

Next, I want to thank Andreas Haas for advising and supporting me throughout my PhD, specifically for enabling me to extend my skillset from ecology to microbiology. Thank you for your help, valuable insights, and positive energy which was often a source of motivation during the grey months of Bremen's winter.

I want to express my appreciation to Benjamin Müller for being a key advisor and mentor throughout my PhD and for introducing me to the way things work on Curaçao. Thank you especially for the thoughtful feedback, inspiration, and encouragement you have provided during the final phase of writing this thesis.

I am grateful to Jan-Hendrik Hehemann for being an advisor on my GLOMAR thesis committee, and to the whole Marine Glycobiology research group at MPI & MARUM in Bremen for guiding me into the world of carbohydrate analyses, from initial advice and instructions to providing the resources and facilities to measure our samples. In addition, I want to thank Sven Kerzenmacher from the Environmental Process Engineering group at the University of Bremen for the fruitful collaboration which has given me the opportunity to go beyond my comfort zone and experience how interdisciplinary research can provide solutions to present-day problems.

Moreover, I want to thank the entire Marine Ecology research group at the University of Bremen. Selma Mezger and Arjen Tilstra, thank you for the great collaborations with many chats and laughs along the way. Special thanks also to my fellow PhD students Johanna Berlinghof, Claudia Hill, Ana Castrillon, and Malte Ostendarp for the cheerful lunch breaks we shared which often took my mind off some problem and generally provided comfort by sharing the ups and downs of the last three years. I also want to thank Milou Arts and Lisa Schellenberg for their invaluable assistance with my work on Curaçao, as well as during my stay at NIOZ on Texel, and for adding joy to my time there.

I would not have been able to complete this work without the love and support of my family and friends who provide me with a stable foundation throughout life. To my husband Robin: thank you for always being there for me, listening to my work-things you know nothing about, and believing in me unconditionally.

Lastly, I want to thank Juliane Filser, Marko Rohlf, Claudia Pogoreutz, and Jonna Holm to agree to be members of my PhD examination committee.

Table of contents

ABSTRACT	V
ZUSAMMENFASSUNG	VII
ACKNOWLEDGEMENTS	IX
TABLE OF CONTENTS	X
LIST OF PUBLICATIONS AND MANUSCRIPTS INCLUDED IN THIS THESIS	XI
DECLARATION ON THE CONTRIBUTION OF THE CANDIDATE TO A MULTI-AUTHOR ARTICLE/MANUSCRIPT WHICH IS INCLUDED AS A CHAPTER IN THE SUBMITTED DOCTORAL THESIS.....	XII
CHAPTER 1 GENERAL INTRODUCTION	14
CHAPTER 2 THE PULSATING SOFT CORAL <i>XENIA UMBELLATA</i> SHOWS HIGH RESISTANCE TO WARMING WHEN NITRATE CONCENTRATIONS ARE LOW.....	30
CHAPTER 3 PHOSPHATE ENRICHMENT INCREASES THE RESILIENCE OF THE PULSATING SOFT CORAL <i>XENIA UMBELLATA</i> TO WARMING.....	60
CHAPTER 4 THE WIDELY DISTRIBUTED SOFT CORAL <i>XENIA UMBELLATA</i> EXHIBITS HIGH RESISTANCE AGAINST PHOSPHATE ENRICHMENT AND TEMPERATURE INCREASE	83
CHAPTER 5 SHORT-TERM OCEAN ACIDIFICATION DECREASES PULSATION AND GROWTH OF THE WIDESPREAD SOFT CORAL <i>XENIA UMBELLATA</i>.....	106
CHAPTER 6 MICROBIAL FUEL CELLS IN CORAL REEF SEDIMENTS AS INDICATOR TOOLS FOR ORGANIC CARBON EUTROPHICATION	127
CHAPTER 7 CORRELATION BETWEEN MUCUS CARBOHYDRATE COMPOSITION AND PHYLOGENY SUGGESTS CO-DIVERSIFICATION WITHIN SCLERACTINIAN CORALS	149
CHAPTER 8 CORAL EXUDATES SHAPE BACTERIOPLANKTON COMMUNITY COMPOSITION AND FUNCTION IN AN ALGAE-DOMINATED CARIBBEAN REEF.....	168
CHAPTER 9 GENERAL DISCUSSION	202
APPENDIX SUPPLEMENTARY MATERIAL	220

List of publications and manuscripts included in this thesis

- Thobor, B. M.;** Tilstra, A.; Bourne, D. G.; Springer, K.; Mezger, S. D.; Struck, U.; Bockelmann, F.; Zimmermann, L.; Yáñez Suárez, A. B.; Klinke, A.; Wild, C. (2022). The pulsating soft coral *Xenia umbellata* shows high resistance to warming when nitrate concentrations are low. *Scientific Reports*, **12**(1): 16788, <https://doi.org/10.1038/s41598-022-21110-w>
- Klinke, A.; Mezger, S. D.; **Thobor, B. M.;** Tilstra, A.; El-Khaled, Y. C.; Wild, C. (2022). Phosphate enrichment increases the resilience of the pulsating soft coral *Xenia umbellata* to warming. *Frontiers in Marine Science*, **9**: 1026321, <https://doi.org/10.3389/fmars.2022.1026321>
- Mezger, S. D.; Klinke, A.; Tilstra, A.; El-Khaled, **Thobor, B. M.;** Wild, C. (2022). The widely distributed soft coral *Xenia umbellata* exhibits high resistance against phosphate enrichment and temperature increase. *Scientific Reports*, **12**(1):22135, <https://doi.org/10.1038/s41598-022-26325-5>
- Tilstra, A.; Braxator, L.; **Thobor, B. M.;** Mezger, S. D.; Hill, C. E. L.; El-Khaled, Y. C.; Caporale, G.; Kim, S.; Wild, C. (2023). Short-term ocean acidification decreases pulsation and growth of the widespread soft coral *Xenia umbellata*. *Plos one*, **18**(11): e0294470, <https://doi.org/10.1371/journal.pone.0294470>
- Thobor, B. M.;** Schanz, F. R.; Förster, A.; Kerzenmacher, S.; Wild, C. (2023). Microbial fuel cells in coral reef sediments as indicator tools for organic carbon eutrophication. *Ecological Indicators*, **153**: 110385, <https://doi.org/10.1016/j.ecolind.2023.110385>
- Thobor, B. M.;** Tilstra, A.; Mueller, B.; Haas, A.; Hehemann, J.-H.; Wild, C. (under review). Evidence for co-diversification of mucus carbohydrate composition with scleractinian coral phylogeny. *Scientific Reports*.

Manuscripts in preparation for submission included in this thesis

- Thobor, B. M.;** Haas, A.; Wild, C.; Nelson, C. E.; Wegles Kelly, L.; Hehemann, J.-H.; Arts, M. G. I.; Boer, M.; Buck-Wiese, H.; Nguyen, N. P.; Hellige, I.; Mueller, B. (in prep.). Coral exudates shape bacterioplankton community composition and function in an algae-dominated Caribbean reef

Declaration on the contribution of the candidate to a multi-author article/manuscript which is included as a chapter in the submitted doctoral thesis

Contribution of the candidate is given in % of the total work load (up to 100 % for each category).

Chapter 2: The pulsating soft coral *Xenia umbellata* shows high resistance to warming when nitrate concentrations are low

Experimental concept and design	50 %
Experimental work and/or acquisition of (experimental) data	50 %
Data analysis and interpretation	90 %
Preparation of figures and tables	100 %
Drafting of the manuscript	100 %

Chapter 3: Phosphate enrichment increases the resilience of the pulsating soft coral *Xenia umbellata* to warming

Experimental concept and design	10 %
Experimental work and/or acquisition of (experimental) data	10 %
Data analysis and interpretation	5 %
Preparation of figures and tables	0 %
Drafting of the manuscript	10 %

Chapter 4: The widely distributed soft coral *Xenia umbellata* exhibits high resistance against phosphate enrichment and temperature increase

Experimental concept and design	10 %
Experimental work and/or acquisition of (experimental) data	10 %
Data analysis and interpretation	5 %
Preparation of figures and tables	0 %
Drafting of the manuscript	10 %

Chapter 5: Short-term ocean acidification decreases pulsation and growth of the widespread soft coral *Xenia umbellata*

Experimental concept and design	0 %
Experimental work and/or acquisition of (experimental) data	0 %
Data analysis and interpretation	10 %
Preparation of figures and tables	0 %
Drafting of the manuscript	20 %

Chapter 6: Microbial fuel cells in coral reef sediments as indicator tools for organic carbon eutrophication

Experimental concept and design	0 %
Experimental work and/or acquisition of (experimental) data	0 %
Data analysis and interpretation	95 %
Preparation of figures and tables	100 %
Drafting of the manuscript	100 %

Chapter 7: Evidence for co-diversification of mucus carbohydrate composition with scleractinian coral phylogeny

Experimental concept and design	90 %
Experimental work and/or acquisition of (experimental) data	100 %
Data analysis and interpretation	100 %
Preparation of figures and tables	100 %
Drafting of the manuscript	100 %

Chapter 8: Coral exudates shape bacterioplankton community composition and function in an algae-dominated Caribbean reef

Experimental concept and design	50 %
Experimental work and/or acquisition of (experimental) data	100 %
Data analysis and interpretation	95 %
Preparation of figures and tables	100 %
Drafting of the manuscript	100 %

Date:

Signature:

Chapter 1 | General introduction

Chapter 1 | General introduction

1.1 Corals are essential for organic carbon cycling in coral reefs

Although inhabiting nutrient-poor waters¹, coral reefs are one of the most productive ecosystems on earth². This ‘Darwin’s Paradox’, named after its first observer Charles Darwin^{1,3}, can be explained by highly efficient nutrient cycling between the diverse microbes and macrobes making up coral reefs⁴⁻⁶. Corals are the main autogenic and allogenic ecosystem engineers of coral reefs, as they provide habitat for reef organisms and transform large amounts of inorganic- into organic carbon (OC)⁷. Shallow-water corals are mostly mixotrophic, acquiring energy from heterotrophic feeding⁸ and primary production, where OC is photosynthetically fixed by algal symbionts in the tissue of coral holobionts (see [Box 1.1](#)). Up to half of the fixed OC is released by the coral host to form a surface mucus layer (SML)^{9,10} which, among other functions, protects the underlying tissue from environmental stressors (reviewed by Brown and Bythell¹¹). Coral mucus partially dissolves in the water column and feeds bacterioplankton^{6,12,13}, facilitating trophic transfer of OC and other nutrients by supporting the microbial loop¹⁴. Dissolved coral mucus can further be taken up by sponges, fuelling trophic transfer via sponge detritus production^{15,16} (i.e., the sponge loop⁵). The non-dissolvable fraction of mucus traps particles from the water column and sinks to the reef benthos^{17,18}, where it supports benthic fauna and microbes⁶. Additionally, particulate and dissolved OC (POC and DOC, respectively) from coral mucus is transported into permeable calcareous reef sands, where sediment-dwelling microbes contribute to carbon cycling¹⁹. To summarize, coral holobionts are primary producers which transfer energy to higher trophic levels through the release of POC and DOC, thus facilitating the existence of highly diverse and productive ecosystems in a nutrient-poor marine environment.

Box 1.1 The coral holobiont

Like all animals, corals live in a mutualistic relationship with a diverse microbiome, combined making up a meta-organism²⁰ or holobiont²¹. Shallow-water corals harbour dinoflagellates of the family Symbiodiniaceae²² in their tissue, which transfer about 40 to 80 % of their photosynthetically fixed OC to the coral host²³⁻²⁵. In return, the coral host provides shelter and adjusts environmental conditions (e.g., supply of inorganic carbon and nutrients, removal of excess oxygen, exposure to light) to optimize algal photosynthesis²⁶. Additional members of the coral holobiont include bacteria, viruses, archaea, fungi, endolithic algae, and other protists (reviewed by Voolstra et al.²⁷). These other members of the coral holobiont provide benefits like inorganic nitrogen cycling^{28,29} and antimicrobial activity against pathogens^{30,31} (reviewed by Voolstra et al.³²).

1.2 Human stressors change the composition and functioning of coral reefs

Coral reefs provide livelihoods for millions of people worldwide by supporting fishery and tourism industries³³, but are severely threatened by anthropogenic threats including global (e.g., ocean warming, ocean acidification^{34,35}) and local stressors (e.g., coastal development, eutrophication, overfishing³⁶⁻³⁸).

It was estimated that 61 % of all coral reefs will soon be affected by global and local stressors simultaneously³⁹. About half of global hard coral cover was already lost since the 1950s⁴⁰ and remaining assemblages change towards more opportunistic, fast-growing hard coral species^{41–44}. Declining hard coral cover often coincides with shifts towards other benthic primary producers, where the dominating organism seems to depend on the biogeographic region^{45,46}. The most abundant shifts to alternative communities in the eastern and central Indo-Pacific are towards soft corals⁴⁵. Soft corals appear to be more resistant to ocean warming and ocean acidification compared to hard corals^{47–50} and can dominate reefs affected by natural and human-induced disturbances^{51–53}. Xenidiids are particularly opportunistic due to their fast asexual reproduction⁵⁴, making them strong invasive species^{55,56}. Although soft corals may provide less structural complexity and habitat for reef organisms compared to hard corals^{57,58}, recent studies suggest they also support reef fish assemblages^{59,60}. In the Atlantic, Caribbean reefs are especially vulnerable due to their low biodiversity, resulting in lower functional redundancy and resilience to disturbances⁶¹. Decades of coastal eutrophication and overfishing, combined with mass mortality of the herbivorous sea urchin *Diadema antillarum* and wide-spread coral disease outbreaks⁶², caused shifts to macroalgae dominance throughout the Caribbean in the 1980s^{63,64} and an 80% decline in hard coral cover from 1975 to 2000⁶⁵. This dominance of macroalgae in the Caribbean is still prevalent today^{45,46}, and is supported by continued global and local stressors affecting Caribbean reefs^{66,67}. These macroalgae-dominated reefs are less structurally complex⁶⁸ and support less fish diversity and biomass production⁶⁶.

1.3 Environmental change affects organic carbon cycling in coral reefs

Anthropogenic stressors affect the transfer of OC between the micro- and macro-organisms of the coral holobiont^{69,70} and the reef ecosystem^{71,72}, with feedback loops connecting processes on the holobiont- and ecosystem-scale (e.g.,^{73–75}, summarized in [Fig. 1.1](#)).

Organic carbon transfer within the coral holobiont

Environmental stressors like ocean warming⁷⁶, ocean acidification⁷⁷, and eutrophication^{78–80} can cause a breakdown of the coral-Symbiodiniaceae symbiosis, thus reducing the supply of OC to the coral host. This dysbiosis is commonly associated with coral bleaching, a loss of Symbiodiniaceae cells and/or pigmentation^{81,82}, and can cause coral mortality⁸³. Several mechanisms have been proposed to underlie coral bleaching (e.g., oxidative hypothesis, carbon limitation hypothesis, reviewed by Helgoe et al.⁸⁴), but here I will focus on the role of nitrogen (N) in mediating the coral-Symbiodiniaceae symbiosis. Excess inorganic N can be caused by coastal pollution^{85,86} and warming, i.e., by stimulating the metabolism of the coral host⁷⁰ and/or associated microbes⁸⁷. Symbiodiniaceae growth in coral tissue is normally N limited, allowing OC from photosynthesis to be transferred to the coral host⁸⁸, while an alleviation of N limitation can facilitate a dysbiosis^{69,70} where Symbiodiniaceae may become parasitic^{70,89}. Symbiodiniaceae can further become phosphorous (P) deficient under high N:P ratios,

which reduces their resistance to temperature- and light-induced bleaching⁸⁰. Availability of P may thus be important to stabilize coral holobiont metabolism during heat stress⁹⁰. Ocean acidification can have positive, negative, and neutral effects on coral holobiont OC cycling (reviewed by Krämer et al.⁹¹), but will likely add to the negative effects of ocean warming under continued climate change³⁴. Overall, human-induced stressors can disrupt the symbiotic transfer of OC from Symbiodiniaceae to the coral host, which weakens the coral host and can ultimately cause coral mortality.

Organic carbon transfer within the reef ecosystem and feedback loops

Elevated inorganic nutrient concentrations can induce micro- and macroalgae blooms^{86,92–94} and excess OC input can increase microbial oxygen consumption in sediment⁹⁵ and water column⁹⁶. Micro- and macroalgae growth exacerbates OC eutrophication through detritus production^{97,98} and high rates of OC exudation^{99–101}. Stimulated microbial degradation of OC is a main driver of hypoxia in coral reefs which can lead to mass coral mortality¹⁰². Warming can additionally increase OC release by corals¹⁰³ and algae^{74,104} and stimulates heterotrophic oxygen consumption by microbes¹⁰². Overall, organic eutrophication and warming may thus shift net ecosystem metabolism from autotrophy (production of OC) to heterotrophy (consumption of OC)³⁷. Indirect effects of human stressors on coral reef OC cycling are facilitated through shifts in benthic community composition, where the main research focus so far has been on coral-macroalgae shifts (e.g.,^{71,105,106}). Algae usually release more DOC than corals^{107,108} and stimulate more bacterioplankton growth and respiration, a process termed the microbialization of reefs^{106,109}. Increased DOC availability further stimulates nitrogen fixing bacteria, thus increasing N availability for Symbiodiniaceae which can reduce coral bleaching thresholds⁸⁷. Fleshy algae exudates can additionally support opportunistic microbes and potential pathogens in the coral holobiont^{75,110} and in the water column^{99,111}. Coral mortality due to bleaching, hypoxia and disease opens up new space for macroalgae to colonize, resulting in the **DDAM** (DOC, disease, algae, microbes) positive feedback loop^{73,74}. These differences in the response of bacterioplankton communities to coral- versus algae exudates may be explained by differing exudate compositions^{111,112}. Mainly composed of carbohydrates^{11,113,114}, coral and macroalgae exudates enrich distinct bacterioplankton lineages^{111,115,116}. Additionally, bacterioplankton communities of macroalgae-dominated reefs have been suggested to use less energy efficient metabolic pathways¹⁰⁶, reducing relative energy transfer to higher trophic levels¹⁰⁹. Thus, changes in benthic community composition affect microbial metabolism and OC cycling in the water column through the release of DOC which often differs in quantity and quality between corals and fleshy macroalgae.

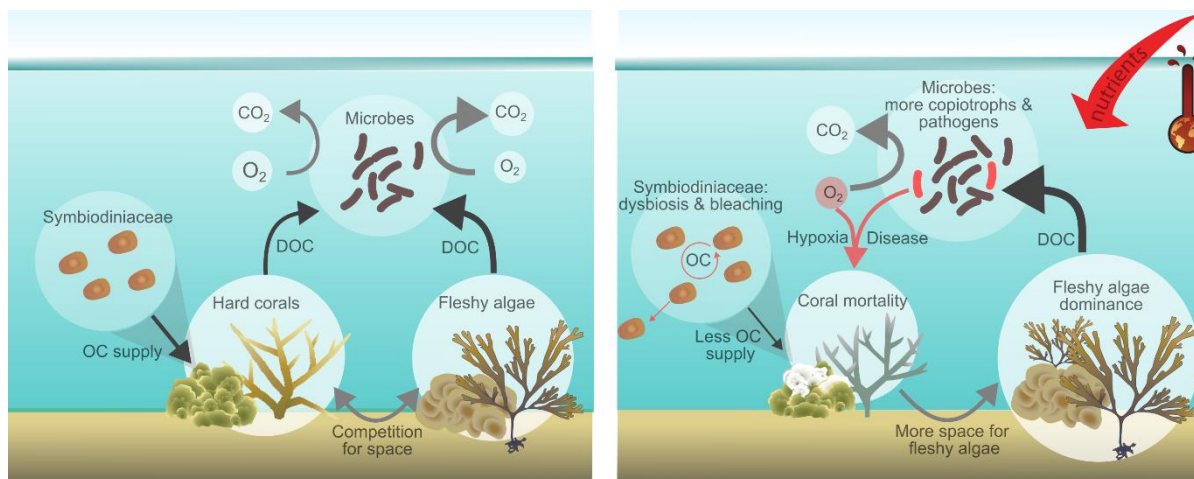


Figure 1.1 Organic carbon transfer between micro- and macro-organisms on an undisturbed reef (**left**) and on a reef affected by eutrophication and warming (**right**). **Left:** Coral holobionts receive OC from their Symbiodiniaceae and release DOC which fuels microbial growth in the water column. Fleshy algae release more DOC, resulting in higher microbial respiration. Algae compete for space with hard corals. **Right:** Corals receive less OC from Symbiodiniaceae due to dysbiosis and bleaching. Macroalgae increase in abundance due to excess nutrients, and thus release more DOC. Higher DOC release supports copiotrophic microbes which consume more oxygen, leading to hypoxia, and more pathogens, causing coral disease. Coral mortality due to hypoxia, disease and bleaching opens up new space for fleshy algae to grow, resulting in the DDAM feedback loop (DOC, disease, algae, microbes). Dark grey arrows indicate OC transfer between micro- and macro-organisms, red arrows mark processes which are detrimental to coral health, light grey arrows indicate microbial respiration and benthic competition, and the width of arrows indicates a relative increase or decrease of processes compared to the undisturbed reef. Adapted from Nelson and Altieri¹⁰². Icon attribution: Integration and Application Network (ian.umces.edu/media-library).

1.4 Specific knowledge gaps

1 | Shifts towards soft coral dominance on coral reefs are increasingly reported^{45,51}, but soft corals are understudied compared to hard corals^{45,53,117,118}. Xenidiids are particularly well adapted to opportunistic growth⁵⁴ and polyp pulsation in some xeniid taxa can improve conditions for Symbiodiniaceae photosynthesis by increasing gas exchange¹¹⁹. Evidence also suggests that the pulsating soft coral *Xenia umbellata* can compensate energy deficiency from warming through heterotrophic feeding on DOC¹²⁰. However, knowledge on the response of pulsating soft corals and their associated Symbiodiniaceae to combined warming and eutrophication, and to ocean acidification, is scarce.

2 | Eutrophication is one of the most common local stressors for coral reef ecosystems^{36,38,39}, with wastewater discharge alone affecting more than half of all coral reefs³⁸. Inorganic nutrient concentrations are poor indicators for eutrophication, because they are quickly transformed into OC by phytoplankton^{86,121}. Indicators for coastal eutrophication should ideally have fast response times and high temporal resolution¹²², yet no currently used indicator combines these traits. Microbial communities in reefs respond fast to environmental perturbations¹²³, but genomic analyses are not suited for continuous measurements. Microbial fuel cells (MFCs) can generate an electrical signal which is proportional to the microbial degradation of OC in marine sediments¹²⁴, but it is unknown whether MFCs can detect OC pulses in permeable coral reef sediment.

3 | The SML serves vital functions for the coral holobiont¹¹ and upon release, contributes to cycling of OC within the reef ecosystem¹²⁵. Mucus consists mainly of glycoproteins¹¹, and particularly the carbohydrates may contribute to shaping microbial communities in the SML^{126,127} and in the water surrounding corals¹¹¹. Hard coral assemblages are changing in species composition on many reefs worldwide¹²⁸, which could affect compositions of reef water because mucus carbohydrate compositions differ among species¹²⁹. Yet, no patterns could be discerned so far for the phylogenetic variation of coral mucus carbohydrate compositions¹³⁰.

4 | Many reefs worldwide shift in composition towards fleshy macroalgae dominance⁴⁶ which can affect bacterioplankton communities and ecosystem-wide cycling of OC¹⁰⁶. Carbohydrates are considered as especially important for shaping marine bacterioplankton communities¹³¹, yet few studies have investigated how different carbohydrates released by corals and macroalgae affect reef bacterioplankton composition and function. Thus, considerable knowledge gaps remain, particularly on the composition of high molecular weight (HMW, > 1 kDa) carbohydrates which belong to the most abundant fraction of DOC in the ocean¹³².

1.5 Aims and approach

Aims

Balanced OC transfer between micro- and macro-organisms is essential for the functioning of single coral holobionts (i.e., the transfer of photosynthates from algal symbionts to their coral host), as well as the whole coral reef ecosystem (i.e., the trophic transfer of OC from primary producers to consumers). Global and local anthropogenic stressors affect the flow of organic carbon on both levels, leading to increased coral mortality and reef degradation. The overall aim of my thesis is thus to investigate coral reefs under environmental change by studying OC transfer between coral reef micro- and macro-organisms.

Thereto, I investigated the following research questions:

1 | How does the pulsating soft coral *Xenia umbellata* respond to global and local environmental stressors? What are the ecological implications?

2 | Can microbial fuel cells be used to detect OC eutrophication in coral reefs sediments? What is the ecological relevance?

3 | How does the composition of mucosal carbohydrates vary among hard coral species? What are potential implications for coral holobiont functioning?

4 | How do carbohydrates exuded by hard corals and macroalgae affect bacterioplankton communities from an algae-dominated Caribbean reef? What are the ecological implications?

Approach

Experimental studies with *X. umbellata* were carried out in a tank system of the Marine Ecology department at the Centre for Environmental Research and Sustainable Technology (UFT), Bremen, where soft corals were exposed to single and combined global and local stressors. The MFC was developed and tested in the same laboratory facility, where artificial wastewater was added to experimental tanks containing MFCs and coral reef sediments. Coral mucus was sampled from hard corals grown in Bremen and from corals collected on Curaçao, Dutch Caribbean. Monosaccharide compositions of hydrolysed coral mucus, HMW coral and macroalgae exudates, and macroalgae tissue extracts were measured in the Marine Glycobiology Department at the Max Planck Institute for Marine Microbiology, Bremen using high-performance anion exchange chromatography with pulsed amperometric detection (HPAEC-PAD). For the final research question, we added HMW exudates to an ambient bacterioplankton community in four-day dark incubations and assessed the microbial community composition using 16S rRNA sequencing.

1.6 Thesis structure and outline

Chapters 1 and 9 are the general introduction and discussion of this thesis, which develop and discuss the main research questions. All other chapters are either submitted or already published manuscripts, or manuscripts in preparation for publication. These chapters are structured in three distinct thematic sections (see overview of chapters in Fig. 1.2):

Section 1 | Effects of global and local stressors on the soft coral *Xenia umbellata*

In chapters 2 – 5, we investigated the effects of global (warming and acidification) and local (nitrate and phosphate eutrophication) factors on the physiology of the cosmopolitan soft coral *Xenia umbellata*. Multiple parameters were measured to determine the health status of the coral host (i.e. survival, polyp pulsation, colony growth), Symbiodiniaceae (i.e., cell density, cellular chlorophyll *a* content, gross photosynthesis), and the coral holobiont (i.e., respiration, elemental and stable isotope composition). In chapter 2, we investigated the single and combined effects of nitrate eutrophication and warming on *X. umbellata*, while chapters 3 – 4 assessed the effects of phosphate enrichment on the soft coral's resistance to warming. In chapter 5, we studied the effects of ocean acidification on *X. umbellata*.

Section 2 | Development of an indicator tool for the detection of OC eutrophication

To enable real-time monitoring of wastewater-induced OC eutrophication of coral reefs, we developed and tested a new MFC in chapter 6. In a laboratory experiment, we measured the electrical current density of MFCs deployed in coral reef sands in response to three consecutive artificial wastewater pulses. OC content in the tank water was measured weekly with high-temperature catalytic oxidation, and electrical current density of MFCs was measured daily. We then assessed the suitability of the MFCs

for the indication of coral reef water quality using a framework of five characteristics developed by Cooper et al. ¹²²: specificity, monotonicity, variability, ecological relevance, and practicality.

Section 3 | Effects of hard corals and macroalgae on carbohydrate- and bacterioplankton community composition of reef water

In chapter 7, we compared the carbohydrate composition of mucus from five species of hard corals to previously reported data (for a total of 23 species). Subsequently, we used hierarchical cluster analysis to create a dendrogram based on similarity of mucus compositions, and compared the dendrogram to the phylogenetic tree of hard corals. In chapter 8, we compared the composition of HMW carbohydrates released by a mixed community of hard corals to that of brown macroalgae, all collected at an algae-dominated reef off Curaçao, Dutch Caribbean. Subsequently, we assessed the bacterioplankton community response to both types of HMW exudates and ambient HMW DOM.

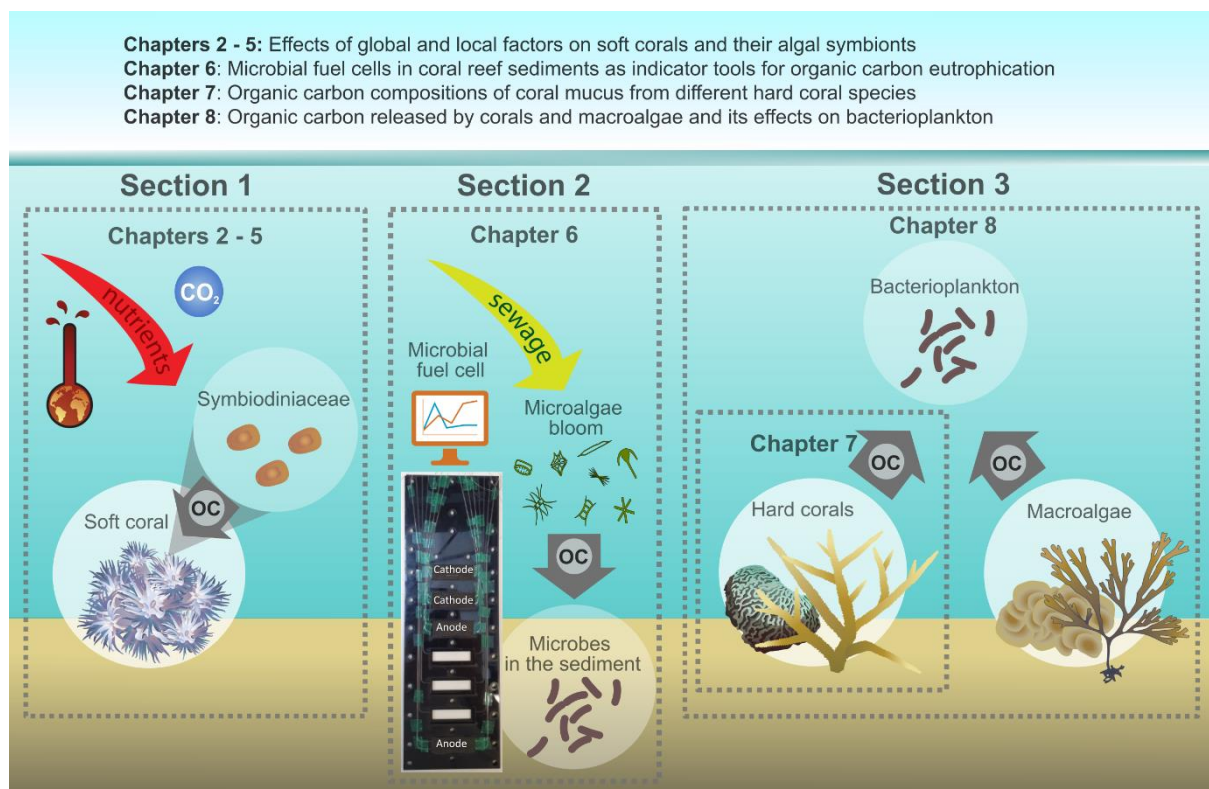


Figure 1.2. Overview of chapters in my dissertation, highlighting the transfer of organic carbon (OC) between micro- and macro-organisms. Icon attribution: Integration and Application Network (ian.umces.edu/media-library).

1.7 References

1. Sammarco, P. W., Risk, M. J., Schwarcz, H. P. & Heikoop, J. M. Cross-continental shelf trends in coral $\delta^{15}\text{N}$ on the Great Barrier Reef: further consideration of the reef nutrient paradox. *Mar. Ecol. Prog. Ser.* **180**, 131–138 (1999).
2. Odum, H. T. & Odum, E. P. Trophic structure and productivity of a windward coral reef community on Eniwetok Atoll. *Ecol. Monogr.* **25**, 291–320 (1955).

3. Tribble, G. W., Atkinson, M. J., Sansone, F. J. & Smith, S. V. Reef metabolism and endo-upwelling in perspective. *Coral Reefs* **13**, 199–201 (1994).
4. Cui, G. *et al.* Molecular insights into the Darwin paradox of coral reefs from the sea anemone *Aiptasia*. *Sci. Adv.* **9**, eadf7108 (2023).
5. de Goeij, J. M. *et al.* Surviving in a marine desert: the sponge loop retains resources within coral reefs. *Science* **342**, 108–110 (2013).
6. Wild, C. *et al.* Coral mucus functions as an energy carrier and particle trap in the reef ecosystem. *Nature* **428**, 66–70 (2004).
7. Wild, C. *et al.* Climate change impedes scleractinian corals as primary reef ecosystem engineers. *Mar. Freshw. Res.* **62**, 205 (2011).
8. Houlbrèque, F. & Ferrier-Pagès, C. Heterotrophy in tropical scleractinian corals. *Biol. Rev.* **84**, 1–17 (2009).
9. Crossland, C. J., Barnes, D. J. & Borowitzka, M. A. Diurnal lipid and mucus production in the staghorn coral *Acropora acuminata*. *Mar. Biol.* **60**, 81–90 (1980).
10. Davies, P. S. The role of zooxanthellae in the nutritional energy requirements of *Pocillopora eydouxi*. *Coral Reefs* **2**, 181–186 (1984).
11. Brown, B. E. & Bythell, J. C. Perspectives on mucus secretion in reef corals. *Mar. Ecol. Prog. Ser.* **296**, 291–309 (2005).
12. Allers, E., Niesner, C., Wild, C. & Pernthaler, J. Microbes enriched in seawater after addition of coral mucus. *Appl. Environ. Microbiol.* **74**, 3274–3278 (2008).
13. Taniguchi, A., Yoshida, T. & Eguchi, M. Bacterial production is enhanced by coral mucus in reef systems. *J. Exp. Mar. Biol. Ecol.* **461**, 331–336 (2014).
14. Azam, F. *et al.* The ecological role of water-column microbes in the sea. *Mar. Ecol. Prog. Ser.* **10**, 257–263 (1983).
15. Rix, L. *et al.* Reef sponges facilitate the transfer of coral-derived organic matter to their associated fauna via the sponge loop. *Mar. Ecol. Prog. Ser.* **589**, 85–96 (2018).
16. Rix, L. *et al.* Coral mucus fuels the sponge loop in warm- and cold-water coral reef ecosystems. *Sci. Rep.* **6**, 18715 (2016).
17. Huettel, M., Wild, C. & Gonelli, S. Mucus trap in coral reefs: formation and temporal evolution of particle aggregates caused by coral mucus. *Mar. Ecol. Prog. Ser.* **307**, 69–84 (2006).
18. Naumann, M., Richter, C., el-Zibdah, M. & Wild, C. Coral mucus as an efficient trap for picoplanktonic cyanobacteria: implications for pelagic–benthic coupling in the reef ecosystem. *Mar. Ecol. Prog. Ser.* **385**, 65–76 (2009).
19. Wild, C. *et al.* Degradation and mineralization of coral mucus in reef environments. *Mar. Ecol. Prog. Ser.* **267**, 159–171 (2004).
20. Bosch, T. C. G. & McFall-Ngai, M. J. Metaorganisms as the new frontier. *Zoology* **114**, 185–190 (2011).

21. Rohwer, F., Seguritan, V., Azam, F. & Knowlton, N. Diversity and distribution of coral-associated bacteria. *Mar. Ecol. Prog. Ser.* **243**, 1–10 (2002).
22. LaJeunesse, T. C. *et al.* Systematic revision of Symbiodiniaceae highlights the antiquity and diversity of coral endosymbionts. *Curr. Biol.* **28**, 2570–2580.e6 (2018).
23. Hatcher, B. Coral reef primary productivity: a beggar's banquet. **3**, 6 (1988).
24. Muscatine, L. The role of symbiotic algae in carbon and energy flux in reef corals. *Coral Reefs* (1990).
25. Tremblay, P., Naumann, M., Sikorski, S., Grover, R. & Ferrier-Pagès, C. Experimental assessment of organic carbon fluxes in the scleractinian coral *Stylophora pistillata* during a thermal and photo stress event. *Mar. Ecol. Prog. Ser.* **453**, 63–77 (2012).
26. Allemand, D. & Furla, P. How does an animal behave like a plant? Physiological and molecular adaptations of zooxanthellae and their hosts to symbiosis. *C. R. Biol.* **341**, 276–280 (2018).
27. Voolstra, C. R. *et al.* Extending the natural adaptive capacity of coral holobionts. *Nat. Rev. Earth Environ.* **2**, 747–762 (2021).
28. Lema, K. A., Willis, B. L. & Bourne, D. G. Corals form characteristic associations with symbiotic nitrogen-fixing bacteria. *Appl. Environ. Microbiol.* **78**, 3136–3144 (2012).
29. Tilstra, A. *et al.* Denitrification aligns with N₂ fixation in Red Sea corals. *Sci. Rep.* **9**, 19460 (2019).
30. Glasl, B., Herndl, G. J. & Frade, P. R. The microbiome of coral surface mucus has a key role in mediating holobiont health and survival upon disturbance. *ISME J.* **10**, 2280–2292 (2016).
31. Kvennefors, E. C. E. *et al.* Regulation of bacterial communities through antimicrobial activity by the coral holobiont. *Microb. Ecol.* **63**, 605–618 (2012).
32. Voolstra, C. R. *et al.* The coral microbiome in sickness, in health and in a changing world. *Nat. Rev. Microbiol.* 1–16 (2024) doi:10.1038/s41579-024-01015-3.
33. Woodhead, A. J., Hicks, C. C., Norström, A. V., Williams, G. J. & Graham, N. A. J. Coral reef ecosystem services in the Anthropocene. *Funct. Ecol.* **33**, 1023–1034 (2019).
34. Hoegh-Guldberg, O., Poloczanska, E. S., Skirving, W. & Dove, S. Coral Reef Ecosystems under Climate Change and Ocean Acidification. *Front. Mar. Sci.* **4**, 158 (2017).
35. Hughes, T. P. *et al.* Coral reefs in the Anthropocene. *Nature* **546**, 82–90 (2017).
36. Andrello, M. *et al.* A global map of human pressures on tropical coral reefs. *Conserv. Lett.* **15**, e12858 (2022).
37. Deininger, A. & Frigstad, H. Reevaluating the role of organic matter sources for coastal eutrophication, oligotrophication, and ecosystem health. *Front. Mar. Sci.* **6**, 210 (2019).
38. Tuholske, C. *et al.* Mapping global inputs and impacts from of human sewage in coastal ecosystems. *PLOS ONE* **16**, e0258898 (2021).
39. Guan, Y., Hohn, S., Wild, C. & Merico, A. Vulnerability of global coral reef habitat suitability to ocean warming, acidification and eutrophication. *Glob. Change Biol.* **26**, 5646–5660 (2020).

40. Eddy, T. D. *et al.* Global decline in capacity of coral reefs to provide ecosystem services. *One Earth* **4**, 1278–1285 (2021).
41. Courtney, T. A. *et al.* Disturbances drive changes in coral community assemblages and coral calcification capacity. *Ecosphere* **11**, e03066 (2020).
42. Cramer, K. L. *et al.* The transformation of Caribbean coral communities since humans. *Ecol. Evol.* **11**, 10098–10118 (2021).
43. De Bakker, D. M., Meesters, E. H., Bak, R. P. M., Nieuwland, G. & Van Duyl, F. C. Long-term shifts in coral communities on shallow to deep reef slopes of Curaçao and Bonaire: are there any winners? *Front. Mar. Sci.* **3**, (2016).
44. Green, D. H., Edmunds, P. J. & Carpenter, R. C. Increasing relative abundance of *Porites astreoides* on Caribbean reefs mediated by an overall decline in coral cover. *Mar. Ecol. Prog. Ser.* **359**, 1–10 (2008).
45. Reverter, M., Helber, S. B., Rohde, S., De Goeij, J. M. & Schupp, P. J. Coral reef benthic community changes in the Anthropocene: biogeographic heterogeneity, overlooked configurations, and methodology. *Glob. Change Biol.* **28**, 1956–1971 (2022).
46. Tebbett, S. B., Connolly, S. R. & Bellwood, D. R. Benthic composition changes on coral reefs at global scales. *Nat. Ecol. Evol.* **7**, 71–81 (2023).
47. Gabay, Y., Benayahu, Y. & Fine, M. Does elevated pCO₂ affect reef octocorals? *Ecol. Evol.* **3**, 465–473 (2013).
48. Inoue, S., Kayanne, H., Yamamoto, S. & Kurihara, H. Spatial community shift from hard to soft corals in acidified water. *Nat. Clim. Change* **3**, 683–687 (2013).
49. Lopes, A. R. *et al.* Physiological resilience of a temperate soft coral to ocean warming and acidification. *Cell Stress Chaperones* **23**, 1093–1100 (2018).
50. Sammarco, P. W. & Strychar, K. B. Responses to high seawater temperatures in zooxanthellate octocorals. *PLoS ONE* **8**, e54989 (2013).
51. Norström, A., Nyström, M., Lokrantz, J. & Folke, C. Alternative states on coral reefs: beyond coral–macroalgal phase shifts. *Mar. Ecol. Prog. Ser.* **376**, 295–306 (2009).
52. van de Water, J. A. J. M., Allemand, D. & Ferrier-Pagès, C. Host-microbe interactions in octocoral holobionts - recent advances and perspectives. *Microbiome* **6**, 64 (2018).
53. Schubert, N., Brown, D. & Rossi, S. Symbiotic versus non-symbiotic octocorals: physiological and ecological implications. in *Marine Animal Forests: The Ecology of Benthic Biodiversity Hotspots* 40 (2017).
54. Benayahu, Y. & Loya, Y. Settlement and recruitment of a soft coral: why is *Xenia macrospiculata* a successful colonizer? *Bull. Mar. Sci.* **36**, 12 (1985).
55. Mantelatto, M. C., Silva, A. G. da, Louzada, T. dos S., McFadden, C. S. & Creed, J. C. Invasion of aquarium origin soft corals on a tropical rocky reef in the southwest Atlantic, Brazil. *Mar. Pollut. Bull.* **130**, 84–94 (2018).

56. Ruiz-Allais, J. P., Amaro, M. E., McFadden, C. S., Halász, A. & Benayahu, Y. The first incidence of an alien soft coral of the family Xeniidae in the Caribbean, an invasion in eastern Venezuelan coral communities. *Coral Reefs* **33**, 287–287 (2014).
57. Richardson, L. E., Graham, N. A. J., Pratchett, M. S. & Hoey, A. S. Structural complexity mediates functional structure of reef fish assemblages among coral habitats. *Environ. Biol. Fishes* **100**, 193–207 (2017).
58. Syms, C. & Jones, G. P. Soft corals exert no direct effects on coral reef fish assemblages. *Oecologia* **127**, 560–571 (2001).
59. Epstein, H. E. & Kingsford, M. J. Are soft coral habitats unfavourable? A closer look at the association between reef fishes and their habitat. *Environ. Biol. Fishes* **102**, 479–497 (2019).
60. Moynihan, J. L., Hall, A. E. & Kingsford, M. J. Interrelationships between soft corals and reef-associated fishes on inshore-reefs of the Great Barrier Reef. *Mar. Ecol. Prog. Ser.* **698**, 15–28 (2022).
61. Bellwood, D. R., Hughes, T. P., Folke, C. & Nyström, M. Confronting the coral reef crisis. *Nature* **429**, 827–833 (2004).
62. Aronson, R. B. & Precht, W. F. White-band disease and the changing face of Caribbean coral reefs. in *The Ecology and Etiology of Newly Emerging Marine Diseases* (ed. Porter, J. W.) 25–38 (Springer Netherlands, Dordrecht, 2001). doi:10.1007/978-94-017-3284-0_2.
63. Carpenter, R. C. Mass mortality of *Diadema antillarum*. *Mar. Biol.* **104**, 67–77 (1990).
64. Hughes, T. P. Catastrophes, phase shifts, and large-scale degradation of a Caribbean coral reef. **265**, 6 (1994).
65. Gardner, T. A., Côté, I. M., Gill, J. A., Grant, A. & Watkinson, A. R. Long-term region-wide declines in Caribbean corals. *Science* **301**, 958–960 (2003).
66. Quezada-Perez, F., Mena, S., Fernández-García, C. & Alvarado, J. J. Status of coral reef communities on the Caribbean coast of Costa Rica: are we talking about corals or macroalgae reefs? *Oceans* **4**, 315–330 (2023).
67. Randazzo-Eisemann, Á., Garza-Pérez, J. R., Penié-Rodríguez, I. & Figueroa-Zavala, B. 25 years of multiple stressors driving the coral-algae phase shift in Akumal, Mexico. *Ocean Coast. Manag.* **214**, 105917 (2021).
68. Alvarez-Filip, L., Dulvy, N. K., Gill, J. A., Côté, I. M. & Watkinson, A. R. Flattening of Caribbean coral reefs: region-wide declines in architectural complexity. *Proc. R. Soc. B Biol. Sci.* (2009) doi:10.1098/rspb.2009.0339.
69. Rådecker, N., Escrig, S., Spangenberg, J. E., Voolstra, C. R. & Meibom, A. Coupled carbon and nitrogen cycling regulates the cnidarian–algal symbiosis. *Nat. Commun.* **14**, 6948 (2023).
70. Rådecker, N. *et al.* Heat stress destabilizes symbiotic nutrient cycling in corals. *Proc. Natl. Acad. Sci.* **118**, e2022653118 (2021).

71. Nelson, C. E., Wegley Kelly, L. & Haas, A. F. Microbial interactions with dissolved organic matter are central to coral reef ecosystem function and resilience. *Annu. Rev. Mar. Sci.* **15**, null (2023).
72. Silveira, C. B. *et al.* Microbial processes driving coral reef organic carbon flow. *FEMS Microbiol. Rev.* **41**, 575–595 (2017).
73. Barott, K. L. & Rohwer, F. L. Unseen players shape benthic competition on coral reefs. *Trends Microbiol.* **20**, 621–628 (2012).
74. Dinsdale, E. A. & Rohwer, F. Fish or germs? Microbial dynamics associated with changing trophic structures on coral reefs. in *Coral Reefs: An Ecosystem in Transition* (eds. Dubinsky, Z. & Stambler, N.) 231–240 (Springer Netherlands, Dordrecht, 2011). doi:10.1007/978-94-007-0114-4_16.
75. Smith, J. E. *et al.* Indirect effects of algae on coral: algae-mediated, microbe-induced coral mortality. *Ecol. Lett.* **9**, 835–845 (2006).
76. Hughes, T. P. *et al.* Global warming and recurrent mass bleaching of corals. *Nature* **543**, 373–377 (2017).
77. Anthony, K. R. N., Kline, D. I., Diaz-Pulido, G., Dove, S. & Hoegh-Guldberg, O. Ocean acidification causes bleaching and productivity loss in coral reef builders. *Proc. Natl. Acad. Sci.* **105**, 17442–17446 (2008).
78. Pogoreutz, C. *et al.* Sugar enrichment provides evidence for a role of nitrogen fixation in coral bleaching. *Glob. Change Biol.* **23**, 3838–3848 (2017).
79. Rosset, S., Wiedenmann, J., Reed, A. J. & D’Angelo, C. Phosphate deficiency promotes coral bleaching and is reflected by the ultrastructure of symbiotic dinoflagellates. *Mar. Pollut. Bull.* **118**, 180–187 (2017).
80. Wiedenmann, J. *et al.* Nutrient enrichment can increase the susceptibility of reef corals to bleaching. *Nat. Clim. Change* **3**, 160–164 (2013).
81. Fitt, W., Brown, B., Warner, M. & Dunne, R. Coral bleaching: interpretation of thermal tolerance limits and thermal thresholds in tropical corals. *Coral Reefs* **20**, 51–65 (2001).
82. Weis, V. M. Cellular mechanisms of Cnidarian bleaching: stress causes the collapse of symbiosis. *J. Exp. Biol.* **211**, 3059–3066 (2008).
83. Anthony, K. R. N., Connolly, S. R. & Hoegh-Guldberg, O. Bleaching, energetics, and coral mortality risk: effects of temperature, light, and sediment regime. *Limnol. Oceanogr.* **52**, 716–726 (2007).
84. Helgoe, J., Davy, S. K., Weis, V. M. & Rodriguez-Lanetty, M. Triggers, cascades, and endpoints: connecting the dots of coral bleaching mechanisms. *Biol. Rev.* **n/a**, (2024).
85. Cloern, J. Our evolving conceptual model of the coastal eutrophication problem. *Mar. Ecol. Prog. Ser.* **210**, 223–253 (2001).

86. D'Angelo, C. & Wiedenmann, J. Impacts of nutrient enrichment on coral reefs: new perspectives and implications for coastal management and reef survival. *Curr. Opin. Environ. Sustain.* **7**, 82–93 (2014).
87. Rådecker, N., Pogoreutz, C., Voolstra, C. R., Wiedenmann, J. & Wild, C. Nitrogen cycling in corals: the key to understanding holobiont functioning? *Trends Microbiol.* **23**, 490–497 (2015).
88. Dubinsky Z., Z. & Jokiel, P. L. Ratio of energy and nutrient fluxes regulates symbiosis between zooxanthellae and corals. *Pac. Sci.* **48**, 12 (1994).
89. Baker, D. M., Freeman, C. J., Wong, J. C. Y., Fogel, M. L. & Knowlton, N. Climate change promotes parasitism in a coral symbiosis. *ISME J.* **12**, 921–930 (2018).
90. Ezzat, L., Maguer, J.-F., Grover, R. & Ferrier-Pagès, C. Limited phosphorus availability is the Achilles heel of tropical reef corals in a warming ocean. *Sci. Rep.* **6**, 31768 (2016).
91. Krämer, W. E., Iglesias-Prieto, R. & Enríquez, S. Evaluation of the current understanding of the impact of climate change on coral physiology after three decades of experimental research. *Commun. Biol.* **5**, 1–11 (2022).
92. Adam, T. C. *et al.* Landscape-scale patterns of nutrient enrichment in a coral reef ecosystem: implications for coral to algae phase shifts. *Ecol. Appl.* **31**, e2227 (2021).
93. McCook, L. J. Macroalgae, nutrients and phase shifts on coral reefs: scientific issues and management consequences for the Great Barrier Reef. *Coral Reefs* **18**, 357–367 (1999).
94. Reopanichkul, P., Schlacher, T. A., Carter, R. W. & Worachananant, S. Sewage impacts coral reefs at multiple levels of ecological organization. *Mar. Pollut. Bull.* **58**, 1356–1362 (2009).
95. Ford, A. K. *et al.* High sedimentary oxygen consumption indicates that sewage input from small islands drives benthic community shifts on overfished reefs. *Environ. Conserv.* **44**, 405–411 (2017).
96. Silveira, C. B. *et al.* Biophysical and physiological processes causing oxygen loss from coral reefs. *eLife* **8**, e49114 (2019).
97. El Sayed, M. A., Al Farawati, R. Kh., El Maradny, A. A., Shaban, Y. A. & Rifaat, A. E. Environmental status and nutrients and dissolved organic carbon budget of two Saudi Arabian Red Sea coastal inlets: A snapshot statement. *Environ. Earth Sci.* **74**, 7755–7767 (2015).
98. Furnas, M., Mitchell, A., Skuza, M. & Brodie, J. In the other 90%: phytoplankton responses to enhanced nutrient availability in the Great Barrier Reef Lagoon. *Mar. Pollut. Bull.* **51**, 253–265 (2005).
99. Haas, A. F. *et al.* Influence of coral and algal exudates on microbially mediated reef metabolism. *PeerJ* **1**, e108 (2013).
100. Mueller, B. *et al.* Nocturnal dissolved organic matter release by turf algae and its role in the microbialization of reefs. *Funct. Ecol.* **36**, 2104–2118 (2022).

101. Wild, C., Niggel, W., Naumann, M. & Haas, A. Organic matter release by Red Sea coral reef organisms—potential effects on microbial activity and *in situ* O₂ availability. *Mar. Ecol. Prog. Ser.* **411**, 61–71 (2010).
102. Nelson, H. R. & Altieri, A. H. Oxygen: The universal currency on coral reefs. *Coral Reefs* **38**, 177–198 (2019).
103. Niggel, W., Glas, M., Laforsch, C., Mayr, C. & Wild, C. First evidence of coral bleaching stimulating organic matter release by reef corals. *Proc. 11th Int. Coral Reef Symp.* 905–911 (2009).
104. Haas, A. F. *et al.* Organic matter release by coral reef associated benthic algae in the Northern Red Sea. *J. Exp. Mar. Biol. Ecol.* **389**, 53–60 (2010).
105. Dinsdale, E. A. *et al.* Microbial ecology of four coral atolls in the Northern Line Islands. *PLOS ONE* **3**, e1584 (2008).
106. Haas, A. F. *et al.* Global microbialization of coral reefs. *Nat. Microbiol.* **1**, 16042 (2016).
107. Haas, A., Jantzen, C., Naumann, M., Iglesias-Prieto, R. & Wild, C. Organic matter release by the dominant primary producers in a Caribbean reef lagoon: implication for *in situ* O₂ availability. *Mar. Ecol. Prog. Ser.* **409**, 27–39 (2010).
108. Mueller, B. *et al.* Effect of light availability on dissolved organic carbon release by Caribbean reef algae and corals. *Bull. Mar. Sci.* **90**, 875–893 (2014).
109. McDole, T. *et al.* Assessing coral reefs on a Pacific-wide scale using the microbialization score. *PLoS ONE* **7**, e43233 (2012).
110. Zaneveld, J. R. *et al.* Overfishing and nutrient pollution interact with temperature to disrupt coral reefs down to microbial scales. *Nat. Commun.* **7**, 11833 (2016).
111. Nelson, C. E. *et al.* Coral and macroalgal exudates vary in neutral sugar composition and differentially enrich reef bacterioplankton lineages. *ISME J.* **7**, 962–979 (2013).
112. Wegley Kelly, L. *et al.* Distinguishing the molecular diversity, nutrient content, and energetic potential of exometabolomes produced by macroalgae and reef-building corals. *Proc. Natl. Acad. Sci.* **119**, e2110283119 (2022).
113. Buck-Wiese, H. *et al.* Furoid brown algae inject fucoidan carbon into the ocean. *Proc. Natl. Acad. Sci.* **120**, e2210561119 (2022).
114. Haas, A. & Wild, C. Composition analysis of organic matter released by cosmopolitan coral reef-associated green algae. *Aquat. Biol.* **10**, 131–138 (2010).
115. Taniguchi, A., Kuroyanagi, Y., Aoki, R. & Eguchi, M. Community structure and predicted functions of actively growing bacteria responsive to released coral mucus in surrounding seawater. *Microbes Environ.* **38**, ME23024 (2023).
116. Taniguchi, A., Yoshida, T., Hibino, K. & Eguchi, M. Community structures of actively growing bacteria stimulated by coral mucus. *J. Exp. Mar. Biol. Ecol.* **469**, 105–112 (2015).

117. Steinberg, R. K., Dafforn, K. A., Ainsworth, T. & Johnston, E. L. Know thy anemone: a review of threats to octocorals and anemones and opportunities for their restoration. *Front. Mar. Sci.* **7**, 590 (2020).
118. Derviche, P., Menegotto, A. & Lana, P. Carbon budget trends in octocorals: a literature review with data reassessment and a conceptual framework to understand their resilience to environmental changes. *Mar. Biol.* **169**, 159 (2022).
119. Kremien, M., Shavit, U., Mass, T. & Genin, A. Benefit of pulsation in soft corals. *Proc. Natl. Acad. Sci.* **110**, 8978–8983 (2013).
120. Vollstedt, S., Xiang, N., Simancas-Giraldo, S. M. & Wild, C. Organic eutrophication increases resistance of the pulsating soft coral *Xenia umbellata* to warming. *PeerJ* **8**, e9182 (2020).
121. Fabricius, K. E. *et al.* A bioindicator system for water quality on inshore coral reefs of the Great Barrier Reef. *Mar. Pollut. Bull.* **65**, 320–332 (2012).
122. Cooper, T. F., Gilmour, J. P. & Fabricius, K. E. Bioindicators of changes in water quality on coral reefs: Review and recommendations for monitoring programmes. *Coral Reefs* **28**, 589–606 (2009).
123. Glasl, B. *et al.* Microbial indicators of environmental perturbations in coral reef ecosystems. *Microbiome* **7**, 94 (2019).
124. Quek, S. B., Cheng, L. & Cord-Ruwisch, R. Microbial fuel cell biosensor for rapid assessment of assimilable organic carbon under marine conditions. *Water Res.* **77**, 64–71 (2015).
125. Bythell, J. C. & Wild, C. Biology and ecology of coral mucus release. *J. Exp. Mar. Biol. Ecol.* **408**, 88–93 (2011).
126. Lee, S. T. M., Davy, S. K., Tang, S.-L. & Kench, P. S. Mucus sugar content shapes the bacterial community structure in thermally stressed *Acropora muricata*. *Front. Microbiol.* **7**, 371 (2016).
127. Belzer, C. Nutritional strategies for mucosal health: the interplay between microbes and mucin glycans. *Trends Microbiol.* **30**, 13–21 (2022).
128. Edmunds, P. J. *et al.* Persistence and change in community composition of reef corals through present, past, and future climates. *PLOS ONE* **9**, e107525 (2014).
129. Wild, C., Naumann, M., Niggel, W. & Haas, A. Carbohydrate composition of mucus released by scleractinian warm- and cold-water reef corals. *Aquat. Biol.* **10**, 41–45 (2010).
130. Hadaidi, G., Gegner, H. M., Ziegler, M. & Voolstra, C. R. Carbohydrate composition of mucus from scleractinian corals from the central Red Sea. *Coral Reefs* **38**, 21–27 (2019).
131. Teeling, H. *et al.* Recurring patterns in bacterioplankton dynamics during coastal spring algae blooms. *eLife* **5**, e11888 (2016).
132. Benner, R. & Amon, R. M. W. The size-reactivity continuum of major bioelements in the ocean. *Annu. Rev. Mar. Sci.* **7**, 185–205 (2015).

Chapter 2 | The pulsating soft coral *Xenia umbellata* shows high resistance to warming when nitrate concentrations are low



Coral polyp of the soft coral *Xenia umbellata* harboring Symbiodiniaceae (400 x magnified). Photos by Lisa Zimmermann.

Chapter 2 | The pulsating soft coral *Xenia umbellata* shows high resistance to warming when nitrate concentrations are low

Bianca M. Thobor^{1*}, Arjen Tilstra¹, David G. Bourne^{2,3}, Karin Springer⁴, Selma Deborah Mezger¹, Ulrich Struck^{5,6}, Franziska Bockelmann¹, Lisa Zimmermann¹, Ana Belén Yáñez Suárez¹, Annabell Klinke¹, and Christian Wild¹

¹ University of Bremen, Faculty of Biology and Chemistry, Department of Marine Ecology, UFT Building, Leobener Str. 6, 28359 Bremen, Germany

² James Cook University, College of Science and Engineering, 1 Angus Smith Drive, Douglas, QLD, 4814, Australia

³ Australian Institute of Marine Science, Cape Ferguson, Townsville, QLD, 4810

⁴ University of Bremen, Faculty of Biology and Chemistry, Marine Botany, NW2 building, Leobener Str. 5, 28359 Bremen, Germany

⁵ Museum für Naturkunde, Leibniz Institute for Evolution and Biodiversity Science, Invalidenstr. 43, D-10115 Berlin, Germany

⁶ Free University Berlin, Department of Earth Sciences, Malteserstr. 74-100, Haus D, 12249 Berlin, Germany

*Corresponding author: thobor@uni-bremen.de

2.1 Abstract

The resistance of hard corals to warming can be negatively affected by nitrate eutrophication, but related knowledge for soft corals is scarce. We thus investigated the ecophysiological response of the pulsating soft coral *Xenia umbellata* to different levels of nitrate eutrophication (control = 0.6, medium = 6, high = 37 μM nitrate) in a laboratory experiment, with additional warming (27.7 to 32.8 °C) from days 17 to 37. High nitrate eutrophication enhanced cellular chlorophyll *a* content of Symbiodiniaceae by 168 %, while it reduced gross photosynthesis by 56 %. After additional warming, polyp pulsation rate was reduced by 100 % in both nitrate eutrophication treatments, and additional polyp loss of 7 % d^{-1} and total fragment mortality of 26 % was observed in the high nitrate eutrophication treatment. Warming alone did not affect any of the investigated response parameters. These results suggest that *X. umbellata* exhibits resistance to warming, which may facilitate ecological dominance over some hard corals as ocean temperatures warm, though a clear negative physiological response occurs when combined with nitrate eutrophication. This study thus confirms the importance of investigating combinations of global and local factors to understand and manage changing coral reefs.

Keywords: multiple stressors, soft coral, global stressor, local stressor, warming, eutrophication, nitrate

An adapted version of this chapter has been published in *Scientific Reports* **12**, 16788.

<https://doi.org/10.1038/s41598-022-21110-w>

2.2 Introduction

Anthropogenically caused accumulation of carbon dioxide (CO₂) results in excess heat in the atmosphere, which is absorbed by the ocean and ultimately causes ocean warming¹. Due to this, increased frequency of coral bleaching events is predicted over the next century, leaving less time for recovery². The loss and damage to coral reef ecosystems has serious economic consequences on the livelihoods of those who depend on fisheries and tourism².

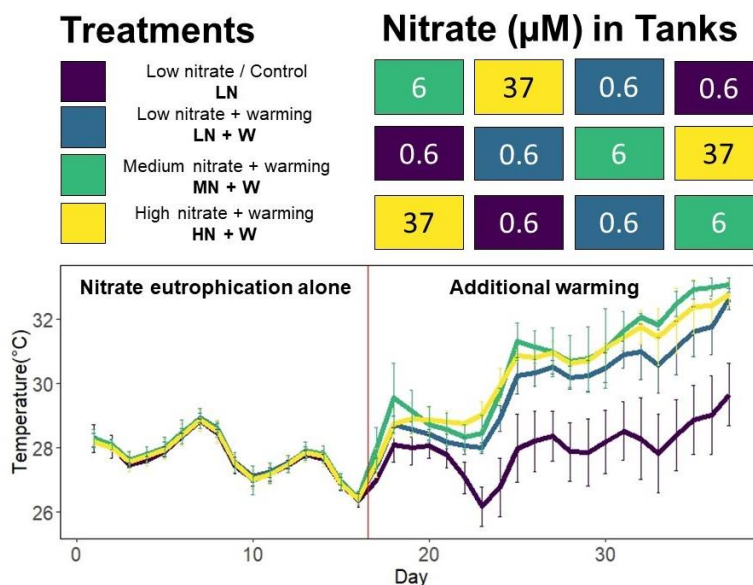
Coral bleaching is a stress response that is commonly described by a loss of algal symbiont pigmentation, loss of algal symbiont cell number or a combination of both, which in turn changes coral colour and constitutes the breakdown of the symbiosis^{3,4}. This stress response can be triggered by seawater warming⁵, which has been connected to increased production of reactive oxygen species (ROS) by algal symbionts³ and shifts in nutrient cycling between coral host and algal symbiont⁶. Fitness of shallow water corals depends on a stable nutritional exchange with their algal symbionts⁶ of the family Symbiodiniaceae⁷. When this symbiosis is disrupted, a reduction in the organisms energy budget can affect coral host health and subsequently cause an increase in mortality⁸.

The cell numbers of the endosymbiotic algae populations within coral tissues are controlled through nitrogen (N) limitation by the coral host⁸ and concentrated discharge of coastal wastewater may result in excess of dissolved inorganic nutrients such as nitrate⁹, one of the main forms of inorganic N in wastewater impacted sites¹⁰. It is now clear that such anthropogenic eutrophication causes disproportionate nutrient availability which can affect the stability of the coral-algae symbiosis (as reviewed by Morris et al.¹¹). Excess N may increase proliferation of algal symbiont cells¹², but may also increase the cellular demand for other nutrients which can potentially lead to relative phosphorus (P) starvation¹³. Nitrate assimilation in particular is associated with higher energetic costs than ammonium in plants¹⁴ and caused reduced photosynthesis in a hard coral, while ammonium enhanced photosynthesis¹⁵.

Predicted scenarios of ocean warming and increased inorganic eutrophication will affect most nearshore coral reefs worldwide simultaneously¹⁶. Furthermore, documented decline in coral cover varies between regions, indicating that local factors such as water quality may play a role in determining responses to ocean warming for some coral taxa^{17,18}. Due to these increasing synergistic pressures facing coral reefs, studies that investigate the interaction of eutrophication and ocean warming are becoming a priority^{9,19}. Previous studies show that the thermally-induced bleaching response may be exacerbated when combined with local eutrophication^{20,21}. Synergistic effects of warming and eutrophication on corals can result for example from P starvation^{9,15}, increased parasitic activity of algal symbionts²², or increased oxidative stress²³. A recent review by Morris et al.¹¹ summarises the effects of nutrient stress on corals and its implications for thermal tolerance. Most studies investigating the effects of temperature and eutrophication on corals have focused on scleractinian corals²⁰ with fewer studies investigating these combined effects on soft corals²⁴. Community shifts from hard coral to soft coral dominance have been

observed under a variety of disturbance regimes^{25,26}. Thus, soft corals may become more abundant on some reefs in the future which has implications for whole ecosystems, since soft corals do not have the ecosystem engineer characteristics of hard corals in supporting reef fish assemblages through structural complexity^{27,28}. However, Epstein & Kingsford²⁹ found increasing fish diversity with increasing soft coral, but not hard coral cover, for a reef in the Great Barrier Reef (GBR) and highlighted that soft corals could have higher ecological importance than previously assumed. Knowledge about processes benefiting soft corals under certain environmental conditions is needed to better understand and predict future coral reef community compositions.

To improve our understanding of the effects of inorganic eutrophication and warming on soft corals, this study aimed to answer the following research questions: (i) How does nitrate eutrophication affect *Xenia umbellata*? (ii) How does chronic nitrate eutrophication affect the response of *X. umbellata* to warming? We also discuss whether *X. umbellata* is more or less resistant to nitrate eutrophication and warming than hard corals, and the implications for coastal management. *X. umbellata* was used because this pulsating soft coral is common and widespread in the Indo-Pacific^{30,31} and the Red Sea³². Because a fully factorial experimental design was not possible with our aquarium facilities, we chose to primarily investigate the effects of nitrate eutrophication on the resistance of *X. umbellata* to warming. For this, *X. umbellata* was exposed to medium (6 μM) and high (37 μM) nitrate eutrophication (controls ~ 0.6 μM). After 17 days, temperatures were gradually increased from an average of 27.7 ± 0.7 °C from days 1-16, to 32.8 ± 0.3 °C on day 37 in all but control tanks (a total increase of 5 °C over 22 days; see Fig. 2.1 for detailed experimental design). To assess the coral health status in response to nitrate eutrophication and /or warming, we measured coral colony survival, growth rate, polyp pulsation rate, gross photosynthesis (P_{gross}), respiration (R), algal symbiont cell density, chlorophyll *a* (chl *a*) content, coral colouration, and elemental and stable isotope composition (to provide information about nutrient uptake and utilization).



◀ **Figure 2.1** Experimental design with development of temperatures per treatment. Tanks were arranged in the depicted order vertically, with four tanks on every level. The experiment lasted 37 days, and temperatures were increased gradually from day 17 in all but the low nitrate (LN) control tanks. During the first 16 days of the experiment, both low nitrate treatments (LN and LN + W) were exposed to the same conditions. This changed as temperatures in the LN + W treatment increased together with the MN + W and HN + W treatments.

2.3 Results

Colony survival and growth rate

The treatment effect on colony survival was significant (Wald-type statistic = 4.14, $p < 0.05$; ANOVA-type statistic = 4.14, $p < 0.05$). Survival was only affected by high nitrate eutrophication (HN + W) with additional warming (Fig. 2.2a). The first mortality was observed on day 22 (at 28.4 °C). On day 36 (at 32.4 °C), the average survival was 74 % (Table 2.1).

The overall treatment effect on growth rates was not significant. However, colonies exposed to high nitrate eutrophication and additional warming (HN + W) displayed partial mortality (mortality of some colony polyps, measured as negative growth rate), averaging 7.2 ± 4.1 % polyp loss d^{-1} during the last week of the experiment, with a mean temperature of 31.9 °C (Fig. 2.2b). This partial mortality was significantly higher than observed for all other treatments and controls (pwc, Bonferroni adjustment, t -test, $p < 0.05$). Colony growth rates decreased in all tanks shortly after the start of the experiment, and the time interval of the experiment significantly affected growth rates (2-way mixed ANOVA, $F = 29.21$, $p < 0.001$).

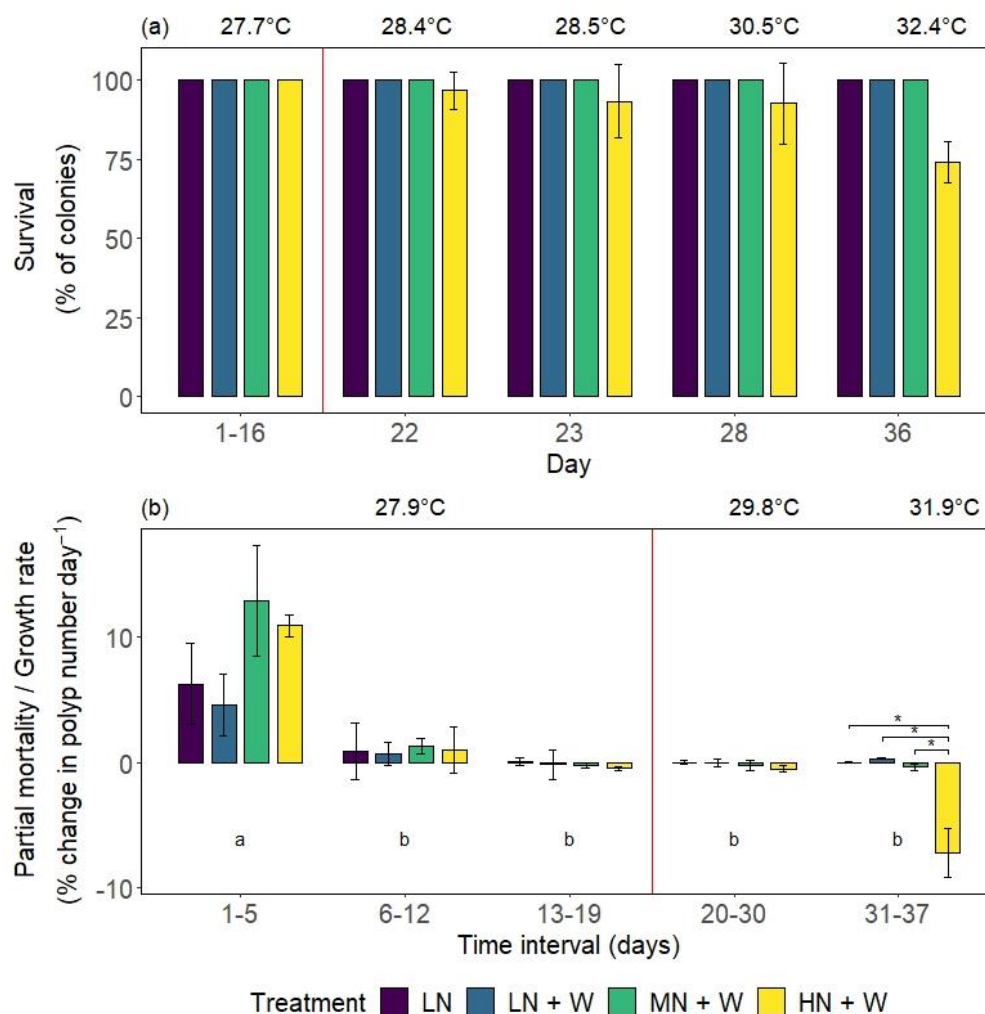


Figure 2.2 (a) Percent survival and (b) growth rates of *Xenia umbellata* colonies from control tanks with low nitrate (LN, $\sim 0.6 \mu\text{M}$) and three treatments: LN + W = low nitrate ($\sim 0.6 \mu\text{M}$) + warming from day 17;

MN + W = medium nitrate eutrophication (~6 μM) + warming from day 17; HN + W = high nitrate eutrophication (~37 μM) + warming from day 17. Error bars represent standard deviations of three replicates. Temperatures represent mean temperatures of the respective days or intervals, excluding controls. Different letters in (b) indicate significant differences between days (pwc, Bonferroni adjustment, t-test, $p < 0.05$). Asterisks indicate significant differences between treatments within days (pwc, Bonferroni adjustment, t-test, $* = p < 0.05$). For (a), only days with recorded colony mortalities were plotted (except day 1-16). No post-hoc analysis could be performed for (a) due to lack of variance within groups where all replicate tanks displayed 100% survival. Raw data is available in [Supplementary Table S2.3](#).

Table 2.1 Effect size (%) of ecophysiological parameters relative to controls (LN; ~ 0.6 μM NO_3 , no warming). Bold values indicate significant differences to controls (LN) and values in brackets indicate effect size relative to low nitrate-treated colonies exposed to warming (LN + W). Puls. rate = polyp pulsation rate, P_{gr} = gross photosynthesis, R = respiration, algae cells = algae symbiont cell density, C:N = carbon to nitrogen ratio, %N/C = percent nitrogen/carbon of tissue dry weight.

Warming	NO ₃ (μM)	Puls. rate	P _{gr}	R	Algae cells	Chl a	Colour score			C:N	% N	% C
							Red	Green	Blue			
No warming (Day 15-17)	6	+3	-11	+16	-17	+75	0	0	0	-10	+6	-12
	37	-34	-56	+19	-10	+168	-4	+16	+29	-28	+23	-18
+ 5 °C (Day 37)	0.6	-45	+15	+35	-12	+29	0	0	0	-9	+18	+8
	6	-100	-30	-4	-11	+59	-1	+2	+4	-16	+22	+2
		(-100)	(-40)	(-29)	(+1)	(+23)	(-1)	(+2)	(+4)	(-8)	(+3)	(-6)
	37	-100	0	-3	+36	+81	-6	+25	+44	-30	+58	+10
	(-100)	(-14)	(-28)	(+54)	(+40)	(-6)	(+25)	(+44)	(-24)	(+34)	(+2)	

Polyp pulsation rate

Overall, the effect of treatment on pulsation rates varied significantly between days of the experiment (Wald-type statistic = 81.87, $p < 0.001$; ANOVA-type statistic = 3.52, $p < 0.01$). Pulsation rates of colonies exposed to high nitrate eutrophication (HN + W) were reduced by 36 % compared to the medium nitrate eutrophication treatment (MN + W) after 15 days (Fig. 2.3a, Table 2.1; pwc, Bonferroni adjustment, Dunn's test, $p < 0.05$), but they did not significantly differ from controls. On day 22, after additional warming, pulsation rates of colonies exposed to high nitrate eutrophication decreased by 97 % compared to controls (at 28.4 °C). With medium nitrate eutrophication (MN + W), pulsation rates remained stable until day 28 (at 30.5 °C) and dropped to zero during the last week of the experiment (at > 30.6 °C). At the end of the experiment (day 36 at 32.4 °C), pulsation could not be observed under medium or high nitrate eutrophication. Corals exposed to warming alone (LN + W) exhibited no significant reduction in pulsation rates.

Coral holobiont gross photosynthesis and respiration rates

The overall effect of treatment on P_{gross} was not significant. Colonies exposed to high nitrate eutrophication (HN + W) exhibited reduced P_{gross} (by 56 %) compared to controls after 16 days (Fig. 2.3b, Table 2.1; pwc, Bonferroni adjustment, t-test, $p < 0.01$). With additional warming, no significant treatment effect was observed. P_{gross} values for all treatments varied significantly over time (2-way mixed ANOVA, $F = 29.35$, $p < 0.001$) with highest values on day 1 and lowest values on day 22 and 37.

Treatments did not significantly affect R, though there was a trend of declining R in all treatments throughout the experiment (2-way mixed ANOVA, $F = 12.08$, $p < 0.001$) with highest R on

day one and eight and lowest R on day 22 (Fig. 2.3b). Spearman's correlation analysis revealed a significant negative correlation of P_{gross} and R (Supplementary Fig. S2.1, $r_s = -0.63$, $n = 72$, $p < 0.001$).

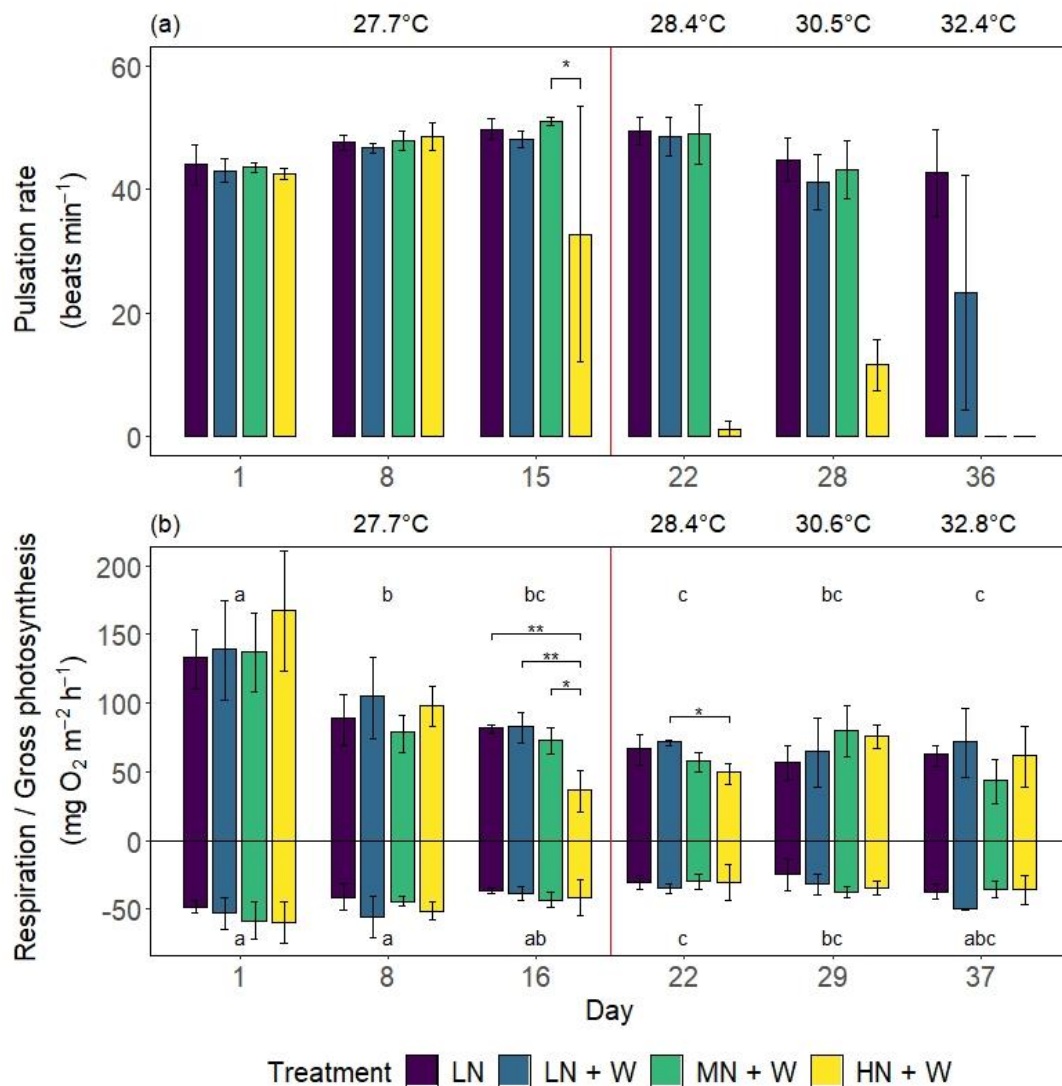


Figure 2.3 (a) Pulsation rates and (b) gross photosynthesis (P_{gross}) and respiration (R) of *Xenia umbellata* colonies from control tanks with low nitrate (LN, $\sim 0.6 \mu\text{M}$) and three treatments: LN + W = low nitrate ($\sim 0.6 \mu\text{M}$) + warming from day 17; MN + W = medium nitrate eutrophication ($\sim 6 \mu\text{M}$) + warming from day 17; HN + W = high nitrate eutrophication ($\sim 37 \mu\text{M}$) + warming from day 17. Error bars represent standard deviations of three replicates. Temperatures represent mean temperatures of the respective days, excluding controls. Different letters in (a) indicate significant differences between days (pwc, Bonferroni adjustment, t-test, $p < 0.05$). Asterisks represent significant differences between treatments within days (pwc, Bonferroni adjustment, (a) t-test & (b) Dunn's test, $** = p < 0.005$, $* = p < 0.05$). Raw data is available in Supplementary Table S2.3.

Algal symbiont cell density, chlorophyll *a* content, and coral colouration

None of the treatments resulted in significant differences in algal symbiont cell densities throughout the experiment (Fig. 2.4a, Table 2.1).

Treatments significantly affected algal symbiont chl *a* content (2-way ANOVA, $F = 6.648$, $p < 0.01$). Colonies exposed to high nitrate eutrophication (HN + W) exhibited 168 % higher chl *a* concentrations than controls (LN) after 15 days (Fig. 2.4b, Table 2.1; pwc, Bonferroni adjustment, t -

test, $p < 0.05$). Additional warming did not result in significant differences between treatments by the end of the experiment (pwc, Bonferroni adjustment, t -test, $p > 0.05$).

The effect of treatment on colour scores varied significantly between days of the experiment (Wald-type statistic = 731.95, $p < 0.001$; ANOVA-type statistic = 3.59, $p < 0.05$). The colour score of corals exposed to high nitrate eutrophication (HN + W) increased from 1.0 to 3.3 after 15 days (Fig. 2.4c). This was significantly higher compared to all other treatments and controls (pwc, Bonferroni adjustment, Dunn's test, $p < 0.05$). Based on the definition of each colour score (Supplementary Table S2.2), this was equivalent to a 16 % and 29 % increase in green and blue values, respectively, and reduced red values by 4 % (Table 2.1). After additional warming, the colour score of all corals exposed to high nitrate eutrophication was five, which was not significantly different from other treatments or controls. The change in colour score from one to five was equivalent to increased green and blue values by 25 % and 44 %, respectively, and reduced red values by 6 %.

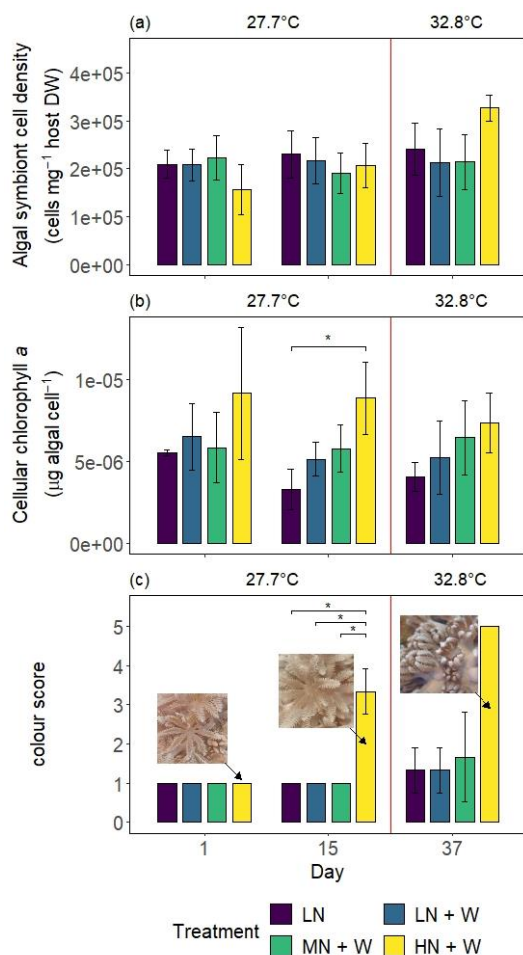


Figure 2.4 (a) Algal symbiont cell density, (b) chlorophyll *a* content standardized to cell density, and (c) colour scores (definitions in Supplementary Table S2.2, see also Supplementary Fig. S2.3) of *Xenia umbellata* colonies from control tanks with low nitrate (LN, $\sim 0.6 \mu\text{M}$) and three treatments: LN + W = low nitrate ($\sim 0.6 \mu\text{M}$) + warming from day 17; MN + W = medium nitrate eutrophication ($\sim 6 \mu\text{M}$) + warming from day 17; HN + W = high nitrate eutrophication ($\sim 37 \mu\text{M}$) + warming from day 17. Error bars represent standard deviations of three replicates, with one exception of two replicates for the warming treatment on day one for both, (a) and (b). Temperatures represent mean temperatures of the respective days, excluding controls. Asterisks represent significant differences between treatments within days (pwc, Bonferroni adjustment, t -test (b) or Dunn's test (c), $* = p < 0.05$). Post-hoc test in (c) was conducted excluding day 1. Pictures in (c) show representative polyps of one identical *X. umbellata* colony in the high nitrate treatment at the respective time points (as indicated by arrows). Images in (c) by Lisa Zimmermann. Raw data is available in Supplementary Table S2.3.

Nitrogen and carbon elemental composition, and stable isotope ratios

Treatments significantly affected the ratios of total carbon (C) to total N (C:N ratios) of coral colonies (2-way ANOVA, $F = 15.756$, $p < 0.001$). Nitrate eutrophication for 15 days alone did not affect C:N ratios (Fig. 2.5a, Table 2.1). After additional warming, colonies exposed to high nitrate eutrophication

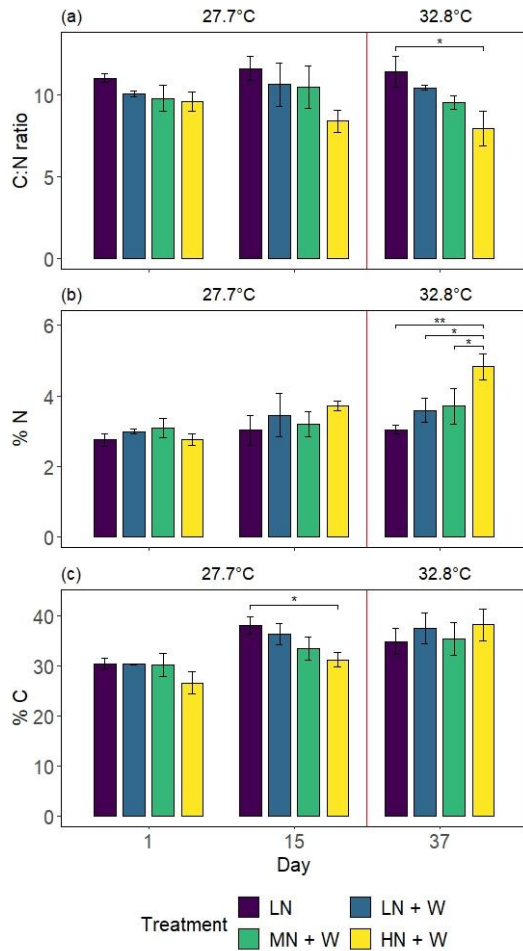
(HN + W) displayed 30 % lower C:N ratios compared to controls (pwc, Bonferroni adjustment, *t*-test, $p < 0.01$), and 24 % lower C:N ratios compared to colonies exposed to warming alone (LN + W; $p > 0.05$).

The effect of treatment on percent N content of coral colonies varied between days of the experiment (2-way ANOVA, $F = 4.294$, $p < 0.01$). Percent N contents were not affected after 15 days of nitrate eutrophication alone (Fig. 2.5b, Table 2.1). After additional warming, corals exposed to high nitrate eutrophication (HN + W) revealed 58 % higher N contents compared to controls (LN; pwc, Bonferroni adjustment, *t*-test, $p < 0.005$), 34 % higher N contents compared to colonies exposed to warming alone (LN + W; $p < 0.05$), and 30 % higher N contents compared to colonies exposed to medium nitrate eutrophication and warming (MN + W; $p < 0.05$).

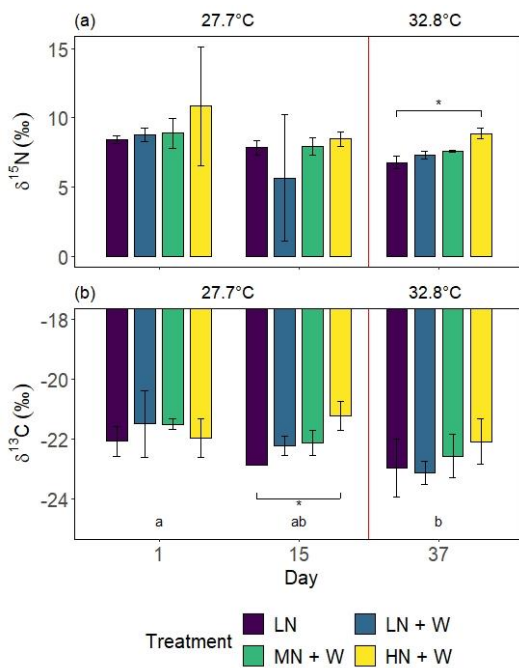
The effect of treatment on percent C contents of coral colonies varied between days of the experiment (2-way ANOVA, $F = 2.821$, $p < 0.05$). Coral colonies exposed to high nitrate eutrophication (HN + W) displayed 18 % lower C contents compared to controls (LN) after 15 days (Fig. 2.5c, Table 2.1; pwc, Bonferroni adjustment, *t*-test, $p < 0.05$), with no significant effects after additional warming.

Treatment and day of the experiment both significantly affected $\delta^{15}\text{N}$ values of coral colonies (2-way ANOVA, Treatment: $F = 3.28$, $p < 0.05$; Day: $F = 5.04$, $p < 0.05$). The $\delta^{15}\text{N}$ values were not affected after 15 days of nitrate eutrophication alone (Fig. 2.6a), averaging 8.4 ± 2.3 ‰. After additional warming, colonies exposed to high nitrate eutrophication (HN + W) exhibited 31 % higher $\delta^{15}\text{N}$ values than controls (LN; pwc, Bonferroni adjustment, Dunn's test, $p < 0.05$) and 21 % higher $\delta^{15}\text{N}$ values compared to colonies exposed to warming alone (LN + W; $p > 0.05$).

The overall treatment effect on $\delta^{13}\text{C}$ values was not significant. Colonies exposed to high nitrate eutrophication (HN + W) displayed 7 % higher $\delta^{13}\text{C}$ values compared to controls (LN) after 15 days (Fig. 2.6b; pwc, Bonferroni adjustment, *t*-test, $p < 0.05$). No significant treatment effect was observed after additional warming. The $\delta^{13}\text{C}$ values decreased over time, with day of the experiment significantly affecting $\delta^{13}\text{C}$ values (2-way ANOVA, $F = 5.557$, $p < 0.05$).



< **Figure 2.5** (a) Carbon to nitrogen ratio, (b) percent nitrogen and (c) percent carbon per dry weight of *Xenia umbellata* colonies from control tanks with low nitrate (LN, $\sim 0.6 \mu\text{M}$) and three treatments: LN + W = low nitrate ($\sim 0.6 \mu\text{M}$) + warming from day 17; MN + W = medium nitrate eutrophication ($\sim 6 \mu\text{M}$) + warming from day 17; HN + W = high nitrate eutrophication ($\sim 37 \mu\text{M}$) + warming from day 17. Error bars represent standard deviations of three replicates, with exceptions of two replicates for controls on day 15 (a & c) and the “warming” treatment on day 37 (a, b & c). Temperatures represent mean temperatures of the respective days, excluding controls. Asterisks indicate significant differences between treatments within days (pwc, Bonferroni adjustment, *t*-test, ** = *p* < 0.005, * = *p* < 0.05). Raw data is available in [Supplementary Table S2.3](#).



< **Figure 2.6** (a) Nitrogen and (b) carbon stable isotope ratios of *Xenia umbellata* colonies from control tanks with low nitrate (LN, $\sim 0.6 \mu\text{M}$) and three treatments: LN + W = low nitrate ($\sim 0.6 \mu\text{M}$) + warming from day 17; MN + W = medium nitrate eutrophication ($\sim 6 \mu\text{M}$) + warming from day 17; HN + W = high nitrate eutrophication ($\sim 37 \mu\text{M}$) + warming from day 17. Error bars represent standard deviations of three replicates, with exceptions of two replicates for controls on day 15 (b) and the “warming” treatment on day 37 (a & b). Temperatures represent mean temperatures of the respective days, excluding controls. Different letters in (b) indicate significant differences between days (pwc, Bonferroni adjustment, *t*-test, *p* < 0.05). Asterisks indicate significant differences between treatments within days (pwc, Bonferroni adjustment, (a) Dunn’s test, (b) *t*-test, * = *p* < 0.05). Raw data is available in [Supplementary Table S2.3](#).

2.4 Discussion

Nitrate eutrophication alone did not significantly affect pulsation rate, growth rate or survival

Pulsation rates were reduced by 34 % with high nitrate eutrophication after 15 days, though not significantly compared to controls. In pulsating soft corals, reduced pulsation rates can also lead to reduced photosynthesis, as pulsation normally enhances gas exchange, e.g. oxygen transport away from the coral's surface³³. Thus, reduced pulsation rates may have caused reduced P_{gross} with high nitrate eutrophication, or vice versa. Furthermore, reduced P_{gross} can lead to reduced transfer of photosynthates to the coral host¹⁵. Resulting energy depletion of the coral host could have caused a reduction of the energy demanding pulsation to conserve energy for more vital processes. The additionally observed increase in $\delta^{13}\text{C}$ values in colonies exposed to high nitrate eutrophication compared to controls on day 15 also indicates a shift in C metabolism. Increasing $\delta^{13}\text{C}$ values may arise from increasing photosynthesis³⁴, which was likely not the case in the present study, as P_{gross} declined while $\delta^{13}\text{C}$ increased. Zooplankton is generally depleted of the heavier ^{13}C isotope³⁴ and thus, Grottoli et al.³⁵ interpreted an increase in the $\delta^{13}\text{C}$ value of two bleached hard corals to be caused by reduced heterotrophy. This may also explain the results of the present study, as reduced pulsation rates may affect the coral's ability to filter feed³³. While coral host growth rate in the present study was not affected by nitrate eutrophication and no mortality was observed after 15 days at ambient temperatures, growth rates decreased significantly across all treatments and controls, from an initial five polyps d^{-1} to almost zero. In contrast, eutrophication often leads to declining coral growth rates in hard corals, especially with simultaneously declining photosynthesis¹². The decline of growth rates observed for all treatments could be explained by reduced food availability of *X. umbellata* colonies during the experiment compared to prior aquarium conditions, where they were kept with other invertebrates and reef fish, potentially resulting in higher input of organic matter into the water relative to experimental conditions.

High nitrate eutrophication enhanced coral pigmentation, while it reduced photosynthesis

Cellular chl *a* content was significantly enhanced under high nitrate eutrophication compared to controls after 15 days, while P_{gross} declined, and algal symbiont cell densities remained stable. These observations are contradictory to previous studies on hard corals, which found simultaneous increases of chl *a* and P_{gross} with N eutrophication^{36,37}, generally explained by a release from N limitation of algal symbionts^{8,15}. However, Ezzat et al.¹⁵ also found reduced P_{gross} with simultaneous increases in total chl *a* and algal symbiont cell densities in *Stylophora pistillata*, and explained this with the energy consuming process of nitrate reduction in the chloroplasts³⁸. An additional explanation could be a limitation of photosynthesis by dissolved inorganic carbon (DIC) with increasing cellular chl *a* contents³⁹. Release from N limitation can result in reduced energy supply to the coral host, as photosynthates are increasingly retained by the algal symbionts for their own growth^{6,8,15}. This could affect the energy demanding CO_2 -concentration mechanisms (CCMs) by the coral host³⁹. DIC limitation under continued irradiance can cause the production of ROS, and reduced photosynthetic rates even before algal

symbiont expulsion³⁹. Damage to chl *a* due to ROS could not be assessed, due to interference of chl *a* degradation products with the used method⁴⁰. Furthermore, the colour of *X. umbellata* colonies exposed to high nitrate eutrophication changed distinctly, with increasing green and blue values ([Supplementary Table S2.2](#)). Change of colour in corals is often associated with coral bleaching. However, bleaching describes paling of the tissue as a result of loss of algal pigmentation or loss of algal symbionts from the coral host^{3,4}, both of which were not observed in the present study. In contrast, tissue darkened while cellular chl *a* content increased.

The C:N ratios of *X. umbellata* tissue and algal symbionts remained above the canonical Redfield ratio of 6.625⁴¹ throughout the experiment (i.e., 6.72 and higher). In addition, phosphate starvation (e.g., caused by a high influx of N) may cause reduced photosynthesis under high environmental N:P ratios, especially with increasing algal symbiont populations^{9,13}. High concentrations of nitrate (37 μM), and subsequent N:P ratios (176:1, based on phosphate concentrations of $\leq 0.21 \mu\text{M}$, [Supplementary Table S2.1](#)) exceeding the Redfield ratio of 16:1, were accompanied with significantly reduced P_{gross} after 16 days while no effect on R was observed. However, in the present study, no effect was found on algal symbiont cell densities ([Fig. 2.4a](#)). Rather, algal symbiont cell densities remained stable and within the range expected for soft corals⁴², while cellular chl *a* content increased. This suggests a disturbance of photosynthesis rather than loss of algal symbionts to be the cause for reduced P_{gross} . Thus, together with the high C:N ratios found in the current study, N may have remained the limiting nutrient throughout this study or it is possible that *X. umbellata* has mechanisms in place to effectively deal with high environmental N availability and/or algal symbiont P starvation. Pupier et al.⁴³ found up to 10-fold lower dissolved nitrogen assimilation rates in soft corals compared to hard corals, highlighting their differences in nutritional strategies which may benefit soft corals in eutrophic environments. Further investigation is required to specify the underlying cause of the reduced photosynthesis under nitrate eutrophication observed in the present study, with studies simulating phosphate eutrophication, also in combination with an N-source, to potentially indicate if algal symbionts of *X. umbellata* are prone to phosphate starvation.

Bednarz et al.⁴⁴ found no effect on chl *a* content, P_{gross} or R in *Xenia spp.* after four weeks of ammonium eutrophication (20 μM), indicating potential different effects of ammonium and nitrate on xeniid corals. Nitrate reduction can act as an additional sink for reduction equivalents involved in photosynthesis, which was shown to reduce photosynthesis in *S. pistillata*, with ammonium having an opposite effect¹⁵. Furthermore, nitrate eutrophication in combination with warming caused increased oxidative stress and coral bleaching in *S. pistillata*, while ammonium eutrophication benefited the coral during warming²³. Similarly, the resistance of *Turbinaria reniformis* to warming was increased with ammonium eutrophication⁴⁵, but negatively affected by nitrate eutrophication without simultaneous P enrichment⁴⁶. Further studies comparing the effects of nitrate and ammonium eutrophication on the response of *X. umbellata* to warming may reveal if nitrate eutrophication has particularly negative

effects on the response of *X. umbellata* to warming, or if N eutrophication (and possibly P starvation) is responsible for the observed effects on thermal tolerance of the soft coral.

Nitrate eutrophication negatively affected the resistance of *X. umbellata* to warming

Pulsation stopped with combined nitrate eutrophication (both medium and high concentrations) and warming at the end of the experiment, with additional increased partial mortality and 26 % colony mortality with high nitrate eutrophication. In contrast, corals exposed to warming alone only exhibited a 45 % reduction in pulsation rates relative to controls (not significant), with stable growth rates and no mortality. This strongly indicates negative effects of nitrate eutrophication, even at medium concentrations, on the resistance of *X. umbellata* to warming, while photophysiological parameters (algal symbiont cell density, pigmentation, photosynthesis) were not negatively affected. N eutrophication can increase the susceptibility of hard corals to warming, due to P starvation^{9,15}, oxidative stress²³, or increased parasitism of algal symbionts²². All of these explanations presume a decrease in photophysiological parameters, but recently, Rådecker et al.⁶ found increased parasitism (i.e., reduced transfer of photosynthates to the coral host) in algal symbionts prior to loss of algal symbiont cells from the coral host. Thus, it may be possible that the coral-algae symbiosis of *X. umbellata* in the present study was disrupted at the end of the experiment. A future experiment with similar experimental N and warming treatments and additional phosphate eutrophication could reveal if P starvation affects the resistance of *X. umbellata* to warming. For hard corals, moderate combined N and P eutrophication may even be beneficial under future ocean conditions⁴⁷.

Warming did not affect photophysiological parameters regardless of nitrate eutrophication

Algal symbiont cell density increased by 36 %, although not significantly, under combined high nitrate eutrophication and warming compared to controls, whereas cell densities did not change in the warming treatment. Similarly, chl *a* content per algal symbiont cell and P_{gross} were not significantly affected by warming, regardless of nitrate eutrophication treatment. These results suggest that algal symbionts of *X. umbellata* were not negatively affected by the exposure to warming or combined warming and eutrophication.

Warming usually causes a loss of algal symbionts in *Xenia*^{48,49}. *Xenia sp.* from the GBR showed highest loss of algal symbionts at 30 °C after only two days⁴⁸ and *Xenia elongata* from the GBR was suggested as a biological indicator species for major bleaching events due to its high sensitivity to warming⁴⁹. The superior thermal tolerance of *X. umbellata* from the northern Red Sea in the present study over *Xenia spp.* from the GBR concurs with predictions of previous studies^{35,50-52}, that corals of the northern Red Sea have especially high thermal tolerances, making this region a potential thermal refuge for coral reefs. Studies comparing the thermal tolerance of *X. umbellata* along the north-south gradient of the Red Sea (e.g., as Sawall et al.⁵³) may reveal if the observed high thermal tolerance is caused by local adaptation or if it is a general trait of the species. Increasing algal symbiont cell densities

are a common response to N eutrophication in corals, as N is often the limiting factor for algal symbiont growth⁸. Enhanced %N content and $\delta^{15}\text{N}$ values of corals exposed to high nitrate eutrophication and warming at the end of the experiment suggest that nitrate was taken up, as dinitrogen fixation commonly leads to reduced $\delta^{15}\text{N}$ ⁵⁴ and thus, assimilation of anthropogenic N can be traced through increasing $\delta^{15}\text{N}$ ⁵⁵. Although %C values in the present study increased (not significantly) in the high eutrophication treatment after additional warming, possibly due to non-significant increases in algal symbiont cell densities, the C:N ratio was significantly reduced, further supporting *X. umbellata*'s incorporation of N from nitrate. Karcher et al.⁵⁶ found reduced C:N values for xeniids, but not for turf algae or hard corals exposed to inorganic fertilizer. They concluded that soft corals may be more strongly affected by poor water quality due to their "luxury consumption"⁵⁷ of N.

Coral tissue darkened with high nitrate eutrophication and warming, with no significant differences in algal symbiont cell density or chl *a* content. A similar observation was reported by Tilstra et al.⁵⁸, who observed changes in colouration of *S. pistillata* colonies exposed to warming, without simultaneous changes in algal symbiont cell density or chl *a* content. Variation in colouration can also be caused by changing concentrations of the accessory pigment peridinin⁵⁹, which can be affected by changing nutrient and temperature conditions in corals⁴⁵. Additionally, non-significant changes in chl *a* contents, and algal symbiont cell densities, as well as protective algal pigments, especially conversions in xanthophyll pools, likely contributed to the change in colour⁶⁰. Darkening of the tissue due to increases in algal symbiont cell densities after nitrate eutrophication has been observed for *S. pistillata*, which led to increased light absorbance⁶¹. Similarly, Fabricius⁶² found darker pigmentation of *Acropora millepora* in nutrient rich nearshore waters, and measured higher temperatures at their tissue surface, especially in areas with low water movement. Thus, darkening of corals in the present study could have caused increased water temperatures around the tissue surface through higher absorbance, potentially increasing thermal stress for *X. umbellata* with high nitrate eutrophication. The simultaneously reduced pulsation rate could have exacerbated this effect, as normal pulsation enhances mixing across the coral-water boundary layer³³. Studies on pulsating soft corals should therefore monitor effects of pigmentation and pulsation rates on the corals' surface temperatures.

Nitrate concentrations of 15 μM in combination with warming reduced P_{gross} significantly for the hard coral *Porites fave*, when normalized to chl *a* content and algal symbiont cell density⁶³. P_{gross} in the present study was standardized to surface area and non-significant increases in algal cell densities may have compensated for reduced per-cell photosynthesis, resulting in similar P_{gross} values to controls. This is especially likely considering the reduced P_{gross} observed before and shortly after the start of warming (day 16 and 22) with high nitrate eutrophication. Thus, P_{gross} was initially reduced by high nitrate eutrophication, but whole-colony photosynthesis was likely compensated by enhanced algal symbiont cell densities (though not significant) with additional warming. R remained stable between treatments throughout the study. In contrast, coral holobiont R increased with warming for *Orbicella faveolata*²² and *S. pistillata*, indicative for stress and increased energy demand⁶. Soft corals tend to have

a higher heterotrophic capacity compared to hard corals, which likely alleviates their dependency on algal symbionts for metabolism during bleaching⁸⁷⁻⁹⁰. However, R rates in the present study strongly correlated with P_{gross} , suggesting that photosynthates were the main organic C source for R, despite the supply of zooplankton-containing coral food. The importance of heterotrophy in *Xenia* is not fully understood. Lewis⁶⁴ found particulate matter in the coral's gastrovascular cavity and Vollstedt et al.¹⁹ found that *X. umbellata* fed with dissolved organic carbon (DOC) had higher thermal tolerance than starved colonies. Further investigation is needed to clarify if heterotrophic particle feeding similarly enhances thermal tolerance of *X. umbellata*.

Algal symbiont communities of the *X. umbellata* in the present study persisted despite potentially stressful conditions (as indicated by reduced pulsation rates, partial, and complete mortality) during high nitrate eutrophication and warming. Similar results were found for *X. elongata*, in which large numbers of algal symbiont cells were seen in necrotic tissue following exposure to a chemical dispersant⁶⁵. Interestingly, some pulsating soft coral species have been reported to display within-colony algal symbiont migration into the gastrovascular cavity upon thermal stress, and thereby mitigating the bleaching response⁶⁶. However, enhanced pigmentation measured in the tentacles of polyps in the present study is evidence against migration of algal symbionts into the gastrovascular cavity, as polyps of xeniids studied by Parrin et al.⁶⁷ visibly paled due to migrating algal symbionts. Future studies are recommended to employ further microscopic analyses of host tissue to account for algal cell movement (e.g., as Parrin et al.⁶⁶), as reuptake from the gastrovascular system could also provide insight into post-bleaching recovery and resilience⁶⁸.

Is *X. umbellata* more or less resistant to nitrate eutrophication and warming than hard corals?

Comparisons across eight similar experimental studies (all using nitrate as N source) on ten different hard coral species revealed that seven hard coral species were negatively affected by warming alone, whereas warming up to 32.8 °C over 22 days did not affect *X. umbellata* in the present study (Table 2.2). However, differences in temperature treatments, origins of the mother colonies, and other experimental conditions (e.g., feeding regime, P concentrations) between studies may have led to different outcomes. Nonetheless, *X. umbellata* appears to be less sensitive to warming than some reef building scleractinian corals, including *S. pistillata* from the northern Red Sea²³. Overall, seven species were more negatively affected by combined nitrate eutrophication and warming than by warming alone in at least one response parameter. All of these previous studies used lower nitrate concentrations than the present study (< 37 μM) and seven of them were conducted over shorter experimental time periods. Six of the studies revealed reductions in photophysiology (algal symbiont cell density, chlorophyll content, photosynthesis), which were not significantly reduced by warming or the combined treatment in the present study. Therefore, while results of this study indicate that nitrate eutrophication can affect the otherwise high resistance of *X. umbellata* to warming, these impacts appear to be less than observed for a range of scleractinian corals.

Table 2.2 Experimental studies on effects of combined nitrate eutrophication and warming on hard corals in comparison to the present study. Only parameters similar to the ones measured in the present study were summarized. NO₃ = Nitrate concentration, Warming = increase of temperature relative to controls, algal symbionts = algal symbiont cell density; Fv/Fm = maximum quantum efficiency of Photosystem II. % values are changes relative to controls (* changes of imbalanced relative to nutrient replete conditions), n. s. = no significant difference to controls. Effect: "+" = combined warming and nitrate eutrophication result in greater reduction than warming alone; "-" = combined warming and nitrate eutrophication result in lesser reduction than warming alone; "=" = combined nitrate eutrophication and warming have similar effects to warming alone; "0" = no effects detected.

Study	Time	Treatment	Coral species and origin	Parameter	Response	Effect
63	14 days	NO ₃ : 15 µM Warming: 2 °C	<i>Porites cylindrica</i> Philippines	Algal symbionts	n. s.	0
				P _{gross}	Warming: reduced by ~20 % Warming + NO ₃ : reduced by ~50 %	+
				R	n. s.	0
				Growth	n. s.	0
83	30 days	NO ₃ : 20 µM Warming: 5 °C	<i>Pocillopora damicornis</i> Gulf of Panama	Algal symbionts	Warming: n. s. Warming + NO ₃ : reduced by ~50 %	+
				Chl <i>a</i> content	Warming: n. s. Warming + NO ₃ : increase by ~100 %	-
			<i>Porites lobata</i> Gulf of Panama	Algal symbionts	Warming: reduced by ~30 % Warming + NO ₃ : reduced by ~30 %	=
				Chl <i>a</i> content	n. s.	0
84	One day	NO ₃ : 5 µM Warming: 6 °C	<i>Turbinaria mesenteria</i> Vietnam	P _{gross}	n. s.	0
				R	n. s.	0
				Mortality	Warming: 16.7 % Warming + NO ₃ : 33 %	+
20	90 days	NO ₃ : 4 µM Warming: 4 °C	<i>Acropora millepor</i> , Central Great Barrier Reef	Fv/Fm	n. s.	0
				Skeletal growth	Warming: reduced by 45 % Warming + NO ₃ : reduced by 45 %	=
				Mortality	n. s.	0
			<i>Montipora tuberculosa</i> Central Great Barrier Reef	Fv/Fm	n. s.	0
				Skeletal growth	n. s.	0
Mortality	n. s.	0				
9	10 days	NO ₃ : ~2.7 µM Warming: 6 °C + light stress	<i>Acropora polystoma</i>	Algal symbionts	Warming + light + NO ₃ + PO ₄ : n. s. Warming + light + NO ₃ : reduced by 60 %*	+
				Chl <i>a</i> content	n. s.	0
				Fv/Fm	Warming + light + NO ₃ + PO ₄ : dropped later below critical threshold Warming + light + NO ₃ : dropped earlier	+
20 days	NO ₃ : ~2.7 µM Warming: 9 °C + light stress	<i>Acropora micro-phthalma</i>	Mortality	Warming + light + NO ₃ + PO ₄ : 0 % Warming + light + NO ₃ : 100 %*	+	
85	Two days	NO ₃ : 10 µM Warming: 5 °C	<i>Pocillopora damicornis</i> Japan	Algal symbionts	Warming: reduced Warming + NO ₃ : reduced, higher increase after recovery	-
				Chlorophyll content	Warming: n. s. Warming + NO ₃ : reduced after recovery	+
				Fv/Fm	Warming: reduced Warming + NO ₃ : reduced, longer recovery period	+
86	Six days	NO ₃ : 10 µM Warming: 5 °C	<i>Montipora digitata</i> Japan	Algal symbionts	Warming: reduced by ~50 % after 6 days Warming + NO ₃ : reduced by ~50 % after 3 days	+
				Fv/Fm	Warming: reduced by ~30 % after 6 days Warming + NO ₃ : reduced by ~30 % after 6 days	=

23	35 days	NO ₃ : 3 µM Warming: 5 °C	<i>Stylophora pistillata</i> Northern Red Sea	Algal symbionts	Warming: reduced by 46 %	-
					Warming + NO ₃ : reduced by 33 %	
				Chlorophyll content	Warming: reduced by 36 %	-
					Warming + NO ₃ : reduced by 28 %	
				Fv/Fm	Warming: reduced by 31 %	+
					Warming + NO ₃ : reduced by 42 %	
				Growth (calcification)	Warming: reduced by 66 %	-
		Warming + NO ₃ : no effect				
Present study	37 days	NO ₃ : 6 µM / 37 µM Warming: 5 °C	<i>Xenia umbellata</i> Northern Red Sea	Algal symbionts	n. s.	0
				Chl <i>a</i> content	n. s.	0
				P _{gross}	n. s.	0
				R	n. s.	0
				Growth	Warming: n. s.	0 / +
					Warming + NO ₃ : n. s. / partial mortality	
				Mortality	Warming: 0 %	0 / +
	Warming + NO ₃ : 0 % / 26 %					

What are the implications for coastal management?

In the present study, tank microcosms were enriched daily to nitrate concentrations of 6 µM and 37 µM, but measurements conducted only two to three hours later indicated nitrate concentrations of the water column averaging 2 µM and 23 µM, respectively. Thus, nitrate concentrations used in the present study represent daily nitrate input and not average nitrate concentrations during the whole experiment. In contrast, *in situ* nitrate measurements represent only what is present in the water column at a specific point of time, and are therefore not equivalent to nitrate input into the system due to rapid assimilation, for example by phytoplankton⁶⁹. The finding of the present study that nitrate eutrophication as low as 2 - 6 µM can impact soft coral resistance to warming is relevant for the management of nearshore corals impacted by eutrophication. In the Red Sea for example, Ziegler et al.⁷⁰ observed that soft corals, particularly xeniids, dominated reefs along the highly developed Jeddah coastline and Peña-García et al.¹⁰ measured total nitrogen (TN) concentrations of > 6 µM at these exact locations and concentrations of up to 2000 µM TN within the city bay. Nitrate composed on average 41 % of TN in wastewater, making it the most common source of anthropogenic N at these sites. For the GBR, Gruber et al.⁷¹ reported highest nitrate + nitrite concentrations of 4.8 µM (300 µg L⁻¹) near river mouths and up to 2.4 µM (150 µg L⁻¹) at inshore reefs in the Tully region, with average nitrate + nitrite concentrations for the GBR below 1 µM. *Xenia* is one of the dominating soft coral genera on near shore reefs⁷² and upper mesophotic reefs⁷³ of the GBR and was the only soft coral genus observed during a recent study in the Red Sea (El-Khaled et al., in press.). Additionally, *Xenia* was involved in hard coral to soft coral community shifts after blast fishing³¹ and an outbreak of the corallivore *Acanthaster planci*⁷⁴. Moreover, Ziegler et al.⁷⁰ reported highest abundance of *Xenia* at sites impacted by sedimentation and sewage discharge in the Red Sea (~12-15 % vs. 0-3 % at other sites). Although soft corals provide less structural complexity than hard corals^{27,28}, they may still be a suitable habitat for many fish species²⁹. Results of the present study indicate that soft coral populations may be severely impacted by the effects of combined nitrate eutrophication (of ≥ 2 - 6 µM) and warming. This can potentially lead to further degradation of these ecosystems towards dominance of macro- and turf algae, which often benefit from

N eutrophication⁵⁶. Thus, the results presented here support the conservation approach of enhancing coral resistance to global threats by managing local factors like inorganic N eutrophication^{75,76} for soft coral conservation. However, soft corals may be more resistant to nitrate eutrophication and warming than some hard coral taxa, which may facilitate community shifts from hard coral to soft coral dominance.

2.5 Methods

Experimental design and conditions

X. umbellata specimens used for the present study were collected from the northern Red Sea and maintained under aquarium conditions (salinity ~ 35 ‰, temperature ~ 27 °C) for over three years prior to the start of this experiment. Mother colonies from the maintenance aquarium were fragmented with sterile scalpels and attached to coral plugs (AF Plug Rocks, Aquaforest, Poland) with rubber bands. All mother colonies originated from the same genotype to reduce genotype-associated variation in the response to the experimental conditions. During a two-week acclimation period under ambient conditions, colonies were able to heal and grow onto coral plugs within the experimental tanks. Prior to the start of the experiment, a total of 168 colonies were randomly distributed among twelve experimental tanks (each 60 L). The tanks were separated into a technical part with heater, pump, and temperature logger (HOBO pendant temp/light, Onset, USA) and the experimental part. The experimental part was laid out with approximately 10 cm of sand five months before the start of the experiment to create a microcosm with microbial activity. Tanks were filled with 43 L of artificial seawater, prepared in a barrel with demineralized water and aquarium sea salt (Zoo Mix, Tropic Marin, Switzerland) to dissolve and reach required temperatures. In total, 14 coral colonies were placed on grid plateaus in each tank. Two light-emitting diode (LED) lamps (one Royal Blue matrix module and one Ultra Blue White matrix module, WALTRON daytime® LED light, Germany) were adjusted above each tank to guarantee equal light intensities measured in photosynthetically active radiation (PAR, [Supplementary Table S2.1](#)) with the LI-1400 Data Logger (LI-COR Biosciences, Germany) and day:night cycles of 12:12 h PAR was chosen to be close to conditions in the maintenance aquarium (~100 $\mu\text{mol photons m}^{-2} \text{s}^{-1}$). The tanks were arranged in a three-level tower system with four tanks per level. The four treatments were distributed in an approximate latin square design, with each treatment in every level ([Fig. 2.1](#)). The coral colonies were fed with dried marine plankton (Reef-Roids, Polyp Lab, USA) at concentrations of 10 mg L⁻¹ twice a week throughout the experiment to keep conditions close to the previous maintenance aquarium. Pumps were turned off for 30 minutes during feeding. The twelve tanks were connected to form one system with continuous water through-flow, and separated on day one of the experiment to ensure equal water quality among treatments at the start of the experiment. During the experiment, oxygen, pH, salinity, and temperature were measured daily and salinity and temperatures were adjusted when necessary. Chemical water parameters for all tanks were maintained at equal conditions

(Supplementary Table S2.1) through regular water exchange of 10-20 %. Tanks were cleaned every one to two weeks to remove any biofouling.

Experimental nitrate and temperature treatments

Nitrate was adjusted to medium (6 μM) and high (37 μM) concentrations, which are comparable to previous nitrate eutrophication experiments with corals^{9,13,20} and *in situ* conditions around coastal metropolitan areas in the Red Sea¹⁰. Each treatment was replicated in three tanks while six other tanks were kept at low nitrate concentrations ($\sim 0.6 \mu\text{M}$). These were divided into three controls (LN) and three tanks with additional warming from day 17 (LN + W, Figure 1). Nitrate solutions were prepared from sodium nitrate (NaNO_3) and demineralized water before every addition. Nitrate concentrations were measured twice a week photometrically (Supplementary Fig. S2.2). Briefly, 100 mg zinc dust and 1 mL cadmium-sulphate solution ($\text{CdSO}_4 \times 8 \text{H}_2\text{O}$) were added to 10 mL water samples to reduce nitrate to nitrite. Subsequently, 0.05 mL sulphanilamide-solution ($\text{C}_6\text{H}_8\text{N}_2\text{O}_2\text{S}$) and 0.05 mL N-(1-naphthyl) ethylenediamine dihydrochloride) were added. The resulting change in colouration is linear to the nitrate concentration and was measured with a photometer after calibration (Trilogy, Turner Designs, USA). Nitrate was added once on day one and daily from day five of the experiment, as nitrate was taken up rapidly from the water column. For medium concentrations (6 μM), it was assumed that nitrate was reduced to ambient concentrations within a day, as concentrations in high treatment tanks were reduced by $24.6 \pm 9.1 \mu\text{M}$ per day. From day eleven, nitrate concentrations in the high eutrophication treatments were measured daily and adjusted to the aimed concentration. Temperatures fluctuated by $\sim 1^\circ\text{C}$ on a daily basis due to additional heat created by the LED lamps. Temperatures were equal among all tanks for the first 16 days, averaging $27.7 \pm 0.7^\circ\text{C}$ and fluctuating between 26.1°C and 29.3°C due to weather conditions affecting the indoor temperatures (Fig. 2.1). From day 17, temperatures in all but three control tanks (LN) were gradually increased and reached $32.8 \pm 0.3^\circ\text{C}$ on day 37. Control tanks (LN) were not experimentally warmed and stayed within the initial temperature range until day 35, when the temperature in one control tank increased to 30°C , and on day 37 to 30.7°C due to the heat coming from adjacent tanks.

Growth rate and survival measurement

The polyps of three marked coral colonies were counted by the same observer every five to eleven days and percent growth rates were calculated as the change in total number of polyps which were counted (p) standardized to the number of days (d) that have passed since the last measurement relative to the initial number of counted polyps (Formula 2.1).

$$\text{Growth rate} = \left(\frac{\left(\frac{p_{\text{end}} - p_{\text{start}}}{d} \right)}{p_{\text{start}}} \right) * 100 \quad (\text{Formula 2.1})$$

Negative growth rates were defined as partial mortality (i.e., mortality of some colony polyps), which is a characteristic of modular colonial organisms like corals, where parts of their living tissue can die

off without causing whole-colony mortality⁷⁷. Mean growth rates of three colonies were calculated per tank. *X. umbellata* colonies were individually placed into glass jars within the experimental tanks without exposing them to air, then the jars were removed from the tanks and kept in tempered water baths of the same temperature as the respective experimental tank to avoid stress from sudden temperature change prior to counting. Soft tweezers were used to spread and count the polyps. Colony survival of all *X. umbellata* colonies present in the experimental tanks was determined daily by checking for polyp movement. Corals that did not show movement were touched with soft tweezers to test for a reaction. Unresponsive colonies were defined as dead and removed from the tanks.

Pulsation rate measurement

Pulsation rate as a proxy for coral health was counted following the method developed by Vollstedt et al.¹⁹. Briefly, pulsation rates of three randomly selected polyps from three marked colonies per experimental tank were measured by the same observer at noon, before addition of coral food, and every six to eight days, starting on day one of the experiment. Mean rates were calculated for each colony and subsequently, for each tank, resulting in three replicate values per treatment. Pulsations were counted within a time frame of 30 seconds and standardized to one minute with one pulsation defined as one whole contraction of the polyp (open – fully closed – open). Incomplete contractions were not counted. Upon mortality of marked colonies, new colonies from the same tank were allocated to pulsation measurements.

Gross photosynthesis and respiration measurements

Every six to eight days, starting on day one of the experiment, one marked colony per tank (same colony measured each time point, $n = 3$) was placed into 160-mL gas tight jars submerged in the experimental tanks to avoid stress from air exposure. Jars were removed from the experimental tanks, closed without capturing air and incubated for 90 to 120 minutes in the light ($135 \pm 4 \mu\text{mol photons m}^{-2} \text{s}^{-1}$ PAR) and in darkness in tempered water baths of the same temperature as the respective experimental tank. Stirring bars in the jars ensured homogenous oxygen concentrations. Oxygen concentrations were measured with an optode sensor (HACH LDO, HACH HQ 40d, Hach Lange, Germany) before and after each incubation and the start concentration was subtracted from the end concentration to eventually calculate oxygen fluxes (*oxy*), which was defined as net photosynthesis (P_{net}) in the light, and R in the dark. Values were normalized to incubation time (*h*). Biofouling on the plug was carefully removed with a soft brush prior to being placed in the jars, though to account for any remaining biofilm, one blank plug was placed in every tank during the experiment and used for blank P_{net} and R measurements. For every measurement day, one to two tanks were randomly chosen for blank incubations and additional blank incubations were conducted on day 35. The average of all blank oxygen fluxes ($n = 24$, *blank*) standardized to time of incubation (*h*) was subtracted from the coral incubations for each, light and dark incubations, as there was no significant difference in blank fluxes between treatments (1-way ANOVA; Light: $F=0.445$, $p=0.775$; Dark: $F=2.029$, $P=0.131$). After the incubations, the number of polyps per colony (*p*) was

multiplied by the average surface area (s) of one *X. umbellata* polyp⁴⁴ to normalize oxygen fluxes to colony surface area. This method was established by Bednarz et al.⁴⁴ for *Xenia*. Measurements of the polyps were taken from pictures using the software ImageJ (1.53e, Wayne Rasband and contributors, National Institutes of Health, USA) to reduce stress on the corals and to avoid polyp retraction affecting the measurement. In this way, 80 random polyps from 18 colonies used in the experiment were measured. Finally, all values were normalized to the volume of the incubation jars (v , [Formula 2.2](#)).

$$P_{net (light)} \text{ or } R_{(dark)} = \frac{\left(\frac{(oxy_{(light \text{ or } dark)})}{h} - \frac{(blank_{(light \text{ or } dark)})}{h} \right)}{p*s*v} \quad (\text{Formula 2.2})$$

Gross photosynthesis (P_{gross}) was calculated with [Formula 2.3](#).

$$P_{gross} = P_{net} + |R| \quad (\text{Formula 2.3})$$

Sample processing for algal symbiont cell density and chlorophyll a measurement

Methods for soft coral sample processing and normalisation metrics were adopted as recommended by Pupier et al.⁴². Briefly, on day 1, 15, and 37, one colony per tank (i.e. three colonies per treatment) was removed from its coral plug, any biofouling was removed, and finally stored in plastic bags and frozen at -20 °C. All samples were then freeze-dried at -60 °C for 24 h and stored in the dark pending analysis. Dry weight (DW) of each sample was used as the normalisation metric for algal symbiont cell density. Samples were homogenised in distilled water, as Pupier et al.⁴² found no differences in algal symbiont cell densities when samples were prepared with distilled water or filtered seawater. The tissue slurry was used for algal cell density counts and chl a measurement.

To separate coral tissue and algal cells in the tissue slurry, subsamples were centrifuged for 10 minutes, supernatant discarded, pellet re-suspended in 2 mL distilled water, centrifuged again for 10 minutes and the supernatant discarded. The pellet was re-suspended in 2 mL distilled water, thoroughly mixed and transferred onto two grids of one haemocytometer (Improved Neubauer counting chamber, depth 0.1 mm) allowing for two replicate counts per sample. For algal symbiont counts, the standardized haemocytometer counting method described by LeGresley & McDermott⁷⁸ was used.

Subsamples for the chl a concentration measurement were rinsed twice by centrifugation as described previously. The remaining pellet was re-suspended in 2 mL 100 % acetone for chlorophyll extraction, and kept in darkness for 24 h at 4 °C. Under minimal light exposure, the extraction sample was centrifuged for five minutes and then transferred into two quartz cuvettes, allowing for two replicate readings per sample. Chl a concentration measurements were conducted using a UV-Spectrophotometer (GENESYS 150, Fisher Scientific, Germany), following the method for dinoflagellates described by Jeffrey & Humphrey⁷⁹. Resulting concentrations were standardized to host DW and subsequently, to algal symbiont cell density to calculate cellular chl a content.

Quantification of coral colouration

Photographs of three colonies per tank were taken over the course of the experiment. Documenting the same colonies was important for establishing changes over time. Photographs were taken under white light with an Olympus TG6 underwater camera with fixed manual settings (ISO 100, f/1.4, x4 magnification). A colour standard was used for later white balance adjustment in Adobe Photoshop CS6. One marked colony per high nitrate enriched tank was used to create colour reference cards similar to the method by Siebeck et al.⁵⁹, who identified brightness, saturation and hues that correlated with algal symbiont densities and chl *a* content of hard corals to monitor coral bleaching. Since *X. umbellata* lacks a calcium carbonate skeleton that can act as a white contrast when algal symbionts are removed from host tissue, red, green, and blue (RGB) pixel values were used in the present study to assess overall colouration change. Briefly, for each coral, five polyps were randomly selected and RGB values (25x25 pixel square) obtained from their tentacles. Previous studies have found algal densities frequently higher in tentacles and tentacle tips⁸⁰, thus these areas are likely prone to colouration change. The resulting range of RGB values (Supplementary Fig. S2.3) was used to identify five colour scores by #HEX colour codes (Supplementary Table S2.2) which represented the change in colouration from one (initial colour) to five (most darkened). Using these colour references, the colour score of three marked colonies per tank was identified by one observer from pictures taken as described above. Mean colour scores were calculated per tank, resulting in three replicates per treatment.

Carbon and nitrogen elemental, and stable isotope analysis

Colonies for elemental analysis were randomly chosen from each tank and removed from coral plugs, stored in plastic bags and frozen at -20 °C pending analysis. *X. umbellata* colonies were dried in an oven for 48 h at 40 °C until weight consistency was reached, then grinded with a mortar and pestle, and the tissue powder was transferred into tin cups. Carbon (C) and N quantities and stable isotope ratios were analysed as described in Karcher et al.⁵⁶. Isotopic ratios (*r*) are shown as the ratio of heavier:lighter isotope (¹³C:¹²C or ¹⁵N:¹⁴N) and notated as either δ¹³C or δ¹⁵N (‰) using Formula 2.4:

$$\delta X = \left(\frac{r_{sample}}{r_{reference}} - 1 \right) * 1,000 \quad \text{(Formula 2.4)}$$

where $r_{reference}$ is Vienna Pee Dee Belemnite for δ¹³C (0.01118) and atmospheric N for δ¹⁵N (0.00368).

Statistical analyses

All data was presented as means with error bars representing standard deviations, and the alpha levels for all statistical tests were set to $p = 0.05$. To test for significant effects of treatments over time for randomly collected data (Cell density, chl *a* & elemental stoichiometry), 2-way analyses of variance (ANOVA) were conducted, and non-normally distributed data (δ¹⁵N) were rank-transformed and analysed using non-parametric approaches (*ARTool* package), as proposed by Feys⁸¹. For data obtained

from the repeated measurements P_{gross} , R, and growth rate, a 2-way mixed-model ANOVA was conducted with 'day' as within-subject factor and 'treatment' as between-subject factor. Normality was tested with the Shapiro-Wilk test, homogeneity of variance was tested with the Levene's test, and no outliers were identified (*rstatix* package). Box's M-test was used to confirm homogeneity of covariance, and sphericity was tested with the Mauchly's test and corrected with the Greenhouse-Geisser sphericity correction when violated. For non-parametric data of repeated measurements (survival, pulsation rates, colour scores), non-parametric mixed-effects models were conducted using the R package *nparLD*⁸². For *post-hoc* analysis, pairwise comparisons (pwc) with Bonferroni adjustment were used, with *t*-test for parametric and Dunn's test for non-parametric data. No *post-hoc* test could be conducted for survival data, as there was no variance within most groups. Day one was excluded to enable *post-hoc* tests for colour score data, because all groups had identical values. Spearman's correlation was run to test for the relationship between P_{gross} and R.

2.6 Author contributions

B.M.T., A.T., S.D.M., F.B., L.Z., A.B.Y.S., A.K. and C.W. designed the experiment. B.M.T., F.B. and L.Z. carried out the experiment. D.G.B., K.S. and C.W. supervised the project. K.S. and U.S. contributed with resources and technical support. B.T. analysed the data and wrote the manuscript. All authors read and revised the manuscript.

2.7 References

1. Doney, S. C. *et al.* Climate change impacts on marine ecosystems. *Annu. Rev. Mar. Sci.* **4**, 11–37; 10.1146/annurev-marine-041911-111611 (2012).
2. Hoegh-Guldberg, O., Poloczanska, E. S., Skirving, W. & Dove, S. Coral reef ecosystems under climate change and ocean acidification. *Front. Mar. Sci.* **4**, 158; 10.3389/fmars.2017.00158 (2017).
3. Weis, V. M. Cellular mechanisms of Cnidarian bleaching: stress causes the collapse of symbiosis. *J. Exp. Biol.* **211**, 3059–3066; 10.1242/jeb.009597 (2008).
4. Fitt, W., Brown, B., Warner, M. & Dunne, R. Coral bleaching: interpretation of thermal tolerance limits and thermal thresholds in tropical corals. *Coral Reefs* **20**, 51–65; 10.1007/s003380100146 (2001).
5. Fujise, L., Yamashita, H., Suzuki, G. & Koike, K. Expulsion of zooxanthellae (*Symbiodinium*) from several species of scleractinian corals: comparison under non-stress conditions and thermal stress conditions. *Galaxea, JCRS* **15**, 29–36; 10.3755/galaxea.15.29 (2013).
6. Rådecker, N. *et al.* Heat stress destabilizes symbiotic nutrient cycling in corals. *PNAS USA* **118**; 10.1073/pnas.2022653118 (2021).

7. LaJeunesse, T. C. *et al.* Systematic revision of Symbiodiniaceae highlights the antiquity and diversity of coral endosymbionts. *Curr. Biol.* **28**, 2570-2580.e6; 10.1016/j.cub.2018.07.008 (2018).
8. Wooldridge, S. A. Breakdown of the coral-algae symbiosis. Towards formalising a linkage between warm-water bleaching thresholds and the growth rate of the intracellular zooxanthellae. *Biogeosciences* **10**, 1647–1658; 10.5194/bg-10-1647-2013 (2013).
9. Wiedenmann, J. *et al.* Nutrient enrichment can increase the susceptibility of reef corals to bleaching. *Nat. Clim. Change* **3**, 160–164; 10.1038/NCLIMATE1661 (2013).
10. Peña-García, D., Ladwig, N., Turki, A. J. & Mudarris, M. S. Input and dispersion of nutrients from the Jeddah Metropolitan Area, Red Sea. *Mar. Pollut. Bull.* **80**, 41–51; 10.1016/j.marpolbul.2014.01.052 (2014).
11. Morris, L. A., Voolstra, C. R., Quigley, K. M., Bourne, D. G. & Bay, L. K. Nutrient availability and metabolism affect the stability of coral–Symbiodiniaceae symbioses. *Trends Microbiol.* **27**, 678–689; 10.1016/j.tim.2019.03.004 (2019).
12. Ferrier-Pagès, C., Gattuso, J.-P., Dallot, S. & Jaubert, J. Effect of nutrient enrichment on growth and photosynthesis of the zooxanthellate coral *Stylophora pistillata*. *Coral Reefs* **19**, 103–113; 10.1007/s003380000078 (2000).
13. Rosset, S., Wiedenmann, J., Reed, A. J. & D'angelo, C. Phosphate deficiency promotes coral bleaching and is reflected by the ultrastructure of symbiotic dinoflagellates. *Mar. Pollut. Bull.* **118**, 180–187; 10.1016/j.marpolbul.2017.02.044 (2017).
14. Patterson, K. *et al.* Distinct signalling pathways and transcriptome response signatures differentiate ammonium- and nitrate-supplied plants. *Plant Cell Environ.* **33**, 1486–1501; 10.1111/j.1365-3040.2010.02158.x (2010).
15. Ezzat, L., Maguer, J.-F., Grover, R. & Ferrier-Pagès, C. New insights into carbon acquisition and exchanges within the coral–dinoflagellate symbiosis under NH₄⁺ and NO₃[–] supply. *Proc. R. Soc. B.* **282**, 20150610; 10.1098/rspb.2015.0610 (2015).
16. Guan, Y., Hohn, S., Wild, C. & Merico, A. Vulnerability of global coral reef habitat suitability to ocean warming, acidification and eutrophication. *Glob. Change Biol.* **26**, 5646–5660; 10.1111/gcb.15293 (2020).
17. Roff, G. & Mumby, P. J. Global disparity in the resilience of coral reefs. *Trends Ecol. Evol.* **27**, 404–413; 10.1016/j.tree.2012.04.007 (2012).
18. Knowlton, N. & Jackson, J. B. C. Shifting baselines, local impacts, and global change on coral reefs. *PLoS Biol.* **6**, e54; 10.1371/journal.pbio.0060054 (2008).
19. Vollstedt, S., Xiang, N., Simancas-Giraldo, S. M. & Wild, C. Organic eutrophication increases resistance of the pulsating soft coral *Xenia umbellata* to warming. *PeerJ* **8**, e9182; 10.7717/peerj.9182 (2020).

20. Fabricius, K. E., Cséke, S., Humphrey, C. & De'ath, G. Does trophic status enhance or reduce the thermal tolerance of scleractinian corals? A review, experiment and conceptual framework. *PloS one* **8**, e54399; 10.1371/journal.pone.0054399 (2013).
21. Cardini, U. *et al.* Functional significance of dinitrogen fixation in sustaining coral productivity under oligotrophic conditions. *Proc. Biol. Sci.* **282**, 20152257; 10.1098/rspb.2015.2257 (2015).
22. Baker, D. M., Freeman, C. J., Wong, J. C. Y., Fogel, M. L. & Knowlton, N. Climate change promotes parasitism in a coral symbiosis. *ISME J* **12**, 921–930; 10.1038/s41396-018-0046-8 (2018).
23. Fernandes de Barros Marangoni, L., Ferrier-Pagès, C., Rottier, C., Bianchini, A. & Grover, R. Unravelling the different causes of nitrate and ammonium effects on coral bleaching. *Sci. Rep.* **10**, 11975; 10.1038/s41598-020-68916-0 (2020).
24. Steinberg, R. K., Dafforn, K. A., Ainsworth, T. & Johnston, E. L. Know thy anemone. a review of threats to octocorals and anemones and opportunities for their restoration. *Front. Mar. Sci.* **7**, 590; 10.3389/fmars.2020.00590 (2020).
25. Norström, A. V., Nyström, M., Lokrantz, J. & Folke, C. Alternative states on coral reefs. Beyond coral–macroalgal phase shifts. *Mar. Ecol. Prog. Ser.* **376**, 295–306; 10.3354/meps07815 (2009).
26. van de Water, J. A. J. M., Allemand, D. & Ferrier-Pagès, C. Host-microbe interactions in octocoral holobionts - recent advances and perspectives. *Microbiome* **6**, 64; 10.1186/s40168-018-0431-6 (2018).
27. Syms, C. & Jones, G. P. Disturbance, habitat structure, and the dynamics of a coral-reef fish community. *Ecology* **81**, 2714–2729; 10.1890/0012-9658(2000)081[2714:DHSATD]2.0.CO;2 (2000).
28. Syms, C. & Jones, G. P. Soft corals exert no direct effects on coral reef fish assemblages. *Oecologia* **127**, 560–571; 10.1007/s004420000617 (2001).
29. Epstein, H. E. & Kingsford, M. J. Are soft coral habitats unfavourable? A closer look at the association between reef fishes and their habitat. *Environ. Biol. Fishes* **102**, 479–497; 10.1007/s10641-019-0845-4 (2019).
30. Janes, M. P. Distribution and diversity of the soft coral family Xenidiidae (Coelenterata: Octocorallia) in Lembah Strait, Indonesia. *Galaxea, JCRS* **15**, 195–200; 10.3755/galaxea.15.195 (2013).
31. Fox, H. E., Pet, J. S., Dahuri, R. & Caldwell, R. L. Recovery in rubble fields. Long-term impacts of blast fishing. *Mar. Pollut. Bull.* **46**, 1024–1031; 10.1016/S0025-326X(03)00246-7 (2003).
32. Al-Sofyani, A. A. & Niaz, G. R. A comparative study of the components of the hard coral *Seriatopora hystrix* and the soft coral *Xenia umbellata* along the Jeddah coast, Saudi Arabia. *Rev. Biol. Mar. Oceanogr.* **42**, 207–219 (2007).
33. Kremien, M., Shavit, U., Mass, T. & Genin, A. Benefit of pulsation in soft corals. *PNAS USA* **110**, 8978–8983; 10.1073/pnas.1301826110 (2013).

34. Swart, P. K., Saied, A. & Lamb, K. Temporal and spatial variation in the $\delta^{15}\text{N}$ and $\delta^{13}\text{C}$ of coral tissue and zooxanthellae in *Montastraea faveolata* collected from the Florida reef tract. *Limnol. Oceanogr.* **50**, 1049–1058; 10.4319/lo.2005.50.4.1049 (2005).
35. Grottoli, A. G., Tchernov, D. & Winters, G. Physiological and biogeochemical responses of super-corals to thermal stress from the northern gulf of Aqaba, Red Sea. *Front. Mar. Sci.* **4**, 215; 10.3389/fmars.2017.00215 (2017).
36. Tanaka, Y., Miyajima, T., Koike, I., Hayashibara, T. & Ogawa, H. Imbalanced coral growth between organic tissue and carbonate skeleton caused by nutrient enrichment. *Limnol. Oceanogr.* **52**, 1139–1146; 10.4319/lo.2007.52.3.1139 (2007).
37. Marubini, F. & Davies, P. S. Nitrate increases zooxanthellae population density and reduces skeletogenesis in corals. *Mar. Biol.* **127**, 319–328; 10.1007/BF00942117 (1996).
38. Dagenais-Bellefeuille, S. & Morse, D. Putting the N in dinoflagellates. *Frontiers in microbiology*, 369; 10.3389/fmicb.2013.00369 (2013).
39. Wooldridge, S. A. A new conceptual model for the warm-water breakdown of the coral - algae endosymbiosis. *Mar. Freshwater Res.* **60**, 483; 10.1071/MF08251 (2009).
40. Moed, J. R. & Hallegraeff, G. M. Some problems in the estimation of chlorophyll-*a* and phaeopigments from pre- and post-acidification spectrophotometric measurements. *Int. Revue ges. Hydrobiol. Hydrogr.* **63**, 787–800; 10.1002/iroh.19780630610 (1978).
41. Redfield, A. C. The biological control of chemical factors in the environment. *Am. Sci.* **46**, 230A-221 (1958).
42. Pupier, C. A., Bednarz, V. N. & Ferrier-Pagès, C. Studies with soft corals – recommendations on sample processing and normalization metrics. *Front. Mar. Sci.* **5**, 2620; 10.3389/fmars.2018.00348 (2018).
43. Pupier, C. A. *et al.* Dissolved nitrogen acquisition in the symbioses of soft and hard corals with Symbiodiniaceae: A key to understanding their different nutritional strategies? *Front. Microbiol.* **12**, 657759; 10.3389/fmicb.2021.657759 (2021).
44. Bednarz, V. N., Naumann, M. S., Niggel, W. & Wild, C. Inorganic nutrient availability affects organic matter fluxes and metabolic activity in the soft coral genus *Xenia*. *J. Exp. Biol.* **215**, 3672–3679; 10.1242/jeb.072884 (2012).
45. Béraud, E., Gevaert, F., Rottier, C. & Ferrier-Pagès, C. The response of the scleractinian coral *Turbinaria reniformis* to thermal stress depends on the nitrogen status of the coral holobiont. *J. Exp. Biol.* **216**, 2665–2674; 10.1242/jeb.085183 (2013).
46. Ezzat, L., Towle, E., Irisson, J.-O., Langdon, C. & Ferrier-Pagès, C. The relationship between heterotrophic feeding and inorganic nutrient availability in the scleractinian coral *T. reniformis* under a short-term temperature increase. *Limnol. Oceanogr.* **61**, 89–102; 10.1002/lno.10200 (2016).

47. Dobson, K. L. *et al.* Moderate nutrient concentrations are not detrimental to corals under future ocean conditions. *Mar. Biol.* **168**; 10.1007/s00227-021-03901-3 (2021).
48. Strychar, K. B., Coates, M., Sammarco, P. W., Piva, T. J. & Scott, P. T. Loss of *Symbiodinium* from bleached soft corals *Sarcophyton ehrenbergi*, *Simularia sp.* and *Xenia sp.* *J. Exp. Mar. Biol. Ecol.* **320**, 159–177; 10.1016/j.jembe.2004.12.039 (2005).
49. Sammarco, P. W. & Strychar, K. B. Responses to high seawater temperatures in zooxanthellate octocorals. *PloS one* **8**, e54989; 10.1371/journal.pone.0054989 (2013).
50. Osman, E. O. *et al.* Thermal refugia against coral bleaching throughout the northern Red Sea. *Glob. Change Biol.* **24**, e474-e484; 10.1111/gcb.13895 (2018).
51. Fine, M., Gildor, H. & Genin, A. A coral reef refuge in the Red Sea. *Glob. Change Biol.* **19**, 3640–3647; 10.1111/gcb.12356 (2013).
52. Evensen, N. R., Fine, M., Perna, G., Voolstra, C. R. & Barshis, D. J. Remarkably high and consistent tolerance of a Red Sea coral to acute and chronic thermal stress exposures. *Limnol. Oceanogr.* **66**, 1718–1729; 10.1002/lno.11715 (2021).
53. Sawall, Y. *et al.* Extensive phenotypic plasticity of a Red Sea coral over a strong latitudinal temperature gradient suggests limited acclimatization potential to warming. *Sci. Rep.* **5**, 8940; 10.1038/srep08940 (2015).
54. Carpenter, E. J., Harvey, H., Fry, B. & Capone, D. G. Biogeochemical tracers of the marine cyanobacterium *Trichodesmium*. *Deep-Sea Res. I: Oceanogr. Res. Pap.* **44**, 27–38; 10.1016/S0967-0637(96)00091-X (1997).
55. Kürten, B. *et al.* Influence of environmental gradients on C and N stable isotope ratios in coral reef biota of the Red Sea, Saudi Arabia. *J. Sea Res.* **85**, 379–394; 10.1016/j.seares.2013.07.008 (2014).
56. Karcher, D. B. *et al.* Nitrogen eutrophication particularly promotes turf algae in coral reefs of the central Red Sea. *PeerJ* **8**, e8737; 10.7717/peerj.8737 (2020).
57. Sterner, R. W. & Elser, J. J. *Ecological Stoichiometry. The Biology of Elements from Molecules to the Biosphere* (Princeton University Press, 2002).
58. Tilstra, A. *et al.* Light induced intraspecific variability in response to thermal stress in the hard coral *Stylophora pistillata*. *PeerJ* **5**, e3802; 10.7717/peerj.3802 (2017).
59. Siebeck, U. E., Marshall, N. J., Klüter, A. & Hoegh-Guldberg, O. Monitoring coral bleaching using a colour reference card. *Coral Reefs* **25**, 453–460; 10.1007/s00338-006-0123-8 (2006).
60. Venn, A. A., Wilson, M. A., Trapido-Rosenthal, H. G., Keely, B. J. & Douglas, A. E. The impact of coral bleaching on the pigment profile of the symbiotic alga, *Symbiodinium*. *Plant Cell Environ.* **29**, 2133–2142; 10.1111/j.1365-3040.2006.001587.x (2006).
61. Dubinsky, Z. V. Y. *et al.* The effect of external nutrient resources on the optical properties and photosynthetic efficiency of *Stylophora pistillata*. *Proc. R. Soc. B.: Biol. Sci.* **239**, 231–246; 10.1098/rspb.1990.0015 (1990).

62. Fabricius, K. E. Effects of irradiance, flow, and colony pigmentation on the temperature microenvironment around corals: Implications for coral bleaching? *Limnol. Oceanogr.* **51**, 30–37; 10.4319/lo.2006.51.1.0030 (2006).
63. Nordemar, I., Nyström, M. & Dizon, R. Effects of elevated seawater temperature and nitrate enrichment on the branching coral *Porites cylindrica* in the absence of particulate food. *Mar. Biol.* **142**, 669–677; 10.1007/s00227-002-0989-0 (2003).
64. Lewis, J. B. Feeding behaviour and feeding ecology of the Octocorallia (Coelenterata: Anthozoa). *J. Zool.* **196**, 371–384; 10.1111/j.1469-7998.1982.tb03509.x (1982).
65. Studivan, M. S., Hatch, W. I. & Mitchelmore, C. L. Responses of the soft coral *Xenia elongata* following acute exposure to a chemical dispersant. *SpringerPlus* **4**, 80; 10.1186/s40064-015-0844-7 (2015).
66. Parrin, A. P. *et al.* Symbiodinium migration mitigates bleaching in three octocoral species. *J. Exp. Mar. Biol. Ecol.* **474**, 73–80; 10.1016/j.jembe.2015.09.019 (2016).
67. Parrin, A. P. *et al.* Within-colony migration of symbionts during bleaching of octocorals. *Biol. Bull.* **223**, 245–256; 10.1086/BBLv223n2p245 (2012).
68. Bourne, D. G., Morrow, K. M. & Webster, N. S. Insights into the coral microbiome. Underpinning the health and resilience of reef ecosystems. *Annu. Rev. Microbiol.* **70**, 317–340; 10.1146/annurev-micro-102215-095440 (2016).
69. Furnas, M., Mitchell, A., Skuza, M. & Brodie, J. In the other 90%: phytoplankton responses to enhanced nutrient availability in the Great Barrier Reef Lagoon. *Mar. Pollut. Bull.* **51**, 253–265; 10.1016/j.marpolbul.2004.11.010 (2005).
70. Ziegler, M. *et al.* Coral microbial community dynamics in response to anthropogenic impacts near a major city in the central Red Sea. *Mar. Pollut. Bull.*, 629–640; 10.1016/j.marpolbul.2015.12.045 (2016).
71. Gruber, R. *et al.* Marine monitoring program: Annual report for inshore water quality monitoring 2018-19. Report for the Great Barrier Reef Marine Park Authority. *GBRMPA, Townsville* (2020).
72. Dinesen, Z. D. Patterns in the distribution of soft corals across the central Great Barrier Reef. *Coral Reefs* **1**, 229–236; 10.1007/BF00304420 (1983).
73. Benayahu, Y. *et al.* Octocorals of the Indo-Pacific. In *Mesophotic Coral Ecosystems*, edited by Y. Loya, K. A. Puglise & T. C. Bridge (Springer International Publishing, Cham, 2019), Vol. 12, pp. 709–728.
74. Tilot, V., Leujak, W., Ormond, R. F. G., Ashworth, J. A. & Mabrouk, A. Monitoring of South Sinai coral reefs: Influence of natural and anthropogenic factors. *Aquat. Conserv.* **18**, 1109–1126; 10.1002/aqc.942 (2008).

75. D'Angelo, C. & Wiedenmann, J. Impacts of nutrient enrichment on coral reefs. New perspectives and implications for coastal management and reef survival. *Curr. Opin. Environ. Sustain.* **7**, 82–93; 10.1016/j.cosust.2013.11.029 (2014).
76. Wooldridge, S. A. & Done, T. J. Improved water quality can ameliorate effects of climate change on corals. *Ecol. Appl.* **19**, 1492–1499; 10.1890/08-0963.1 (2009).
77. Nugues, M. M. & Roberts, C. M. Partial mortality in massive reef corals as an indicator of sediment stress on coral reefs. *Mar. Pollut. Bull.* **46**, 314–323; 10.1016/S0025-326X(02)00402-2 (2003).
78. LeGresley, M. & McDermott, G. Counting chamber methods for quantitative phytoplankton analysis - haemocytometer, Palmer-Maloney cell and Sedgewick-Rafter cell. In *Microscopic and Molecular Methods for Quantitative Phytoplankton Analysis*, edited by B. Karlson, C. Cusack & E. Bresnan (IOC UNESCO, Paris, France, 2010), pp. 25–30.
79. Jeffrey, S. W. & Humphrey, G. F. New spectrophotometric equations for determining chlorophylls *a*, *b*, *c1* and *c2* in higher plants, algae and natural phytoplankton. *Biochem. Physiol. Pflanz.* **167**, 191–194; 10.1016/s0015-3796(17)30778-3 (1975).
80. D'Angelo, C. *et al.* Blue light regulation of host pigment in reef-building corals. *Mar. Ecol. Prog. Ser.* **364**, 97–106; 10.3354/meps07588 (2008).
81. Feys, J. Nonparametric tests for the interaction in two-way factorial designs using R. *R J.* **8**, 367; 10.32614/RJ-2016-027 (2016).
82. Noguchi, K., Gel, Y. R., Brunner, E. & Konietzschke, F. nparLD. An R software package for the nonparametric analysis of longitudinal data in factorial experiments. *J. Stat. Soft.* **50**, 1–23; 10.18637/jss.v050.i12 (2012).
83. Schlöder, C. & D'Croz, L. Responses of massive and branching coral species to the combined effects of water temperature and nitrate enrichment. *J. Exp. Mar. Biol. Ecol.* **313**, 255–268; 10.1016/j.jembe.2004.08.012 (2004).
84. Faxneld, S., Jörgensen, T. L. & Tedengren, M. Effects of elevated water temperature, reduced salinity and nutrient enrichment on the metabolism of the coral *Turbinaria mesenterina*. *Estuar. Coast. Shelf Sci.* **88**, 482–487; 10.1016/j.ecss.2010.05.008 (2010).
85. Chumun, P. K. *et al.* High nitrate levels exacerbate thermal photo-physiological stress of zooxanthellae in the reef-building coral *Pocillopora damicornis*. *Eco-Engineering* **25**, 1–9 (2013).
86. Higuchi, T., Yuyama, I. & Nakamura, T. The combined effects of nitrate with high temperature and high light intensity on coral bleaching and antioxidant enzyme activities. *Reg. Stud. Mar. Sci.* **2**, 27–31; 10.1016/j.rsma.2015.08.012 (2015).
87. Tremblay *et al.* Heterotrophy promotes the re-establishment of photosynthate translocation in a symbiotic coral after heat stress. *Sci. Rep.* **6**, 38112; 10.1038/srep38112 (2016).

88. Ferrier-Pagès *et al.* Photophysiology and daily primary production of a temperate symbiotic gorgonian. *Photosyn. Res.* **123**, 95-104; 10.1007/s11120-014-0042-4 (2015).
89. Grottoli, A. G., Rodrigues, L. J., Palardy, J. E. Heterotrophic plasticity and resilience in bleached corals. *Nature* **440**, 1186-1189; 10.1038/nature04565 (2006)
90. Fabricius, K. & Klumpp, D. Widespread mixotrophy in reef-inhabiting soft corals: the influence of depth, and colony expansion and contraction on photosynthesis. *Mar. Ecol. Prog. Ser.* **125**, 195-204; 10.3354/meps125195 (1995).

Chapter 3 | Phosphate enrichment increases the resilience of the
pulsating soft coral *Xenia umbellata* to warming

Chapter 3 | Phosphate enrichment increases the resilience of the pulsating soft coral *Xenia umbellata* to warming

Annabell Klinke^{1,2*}, Selma Mezger², Bianca M. Thobor², Arjen Tilstra², Yusuf C. El-Khaled², Christian Wild²

¹Reef Systems Working Group, Leibniz Centre for Tropical Marine Research, Bremen, Germany

²Marine Ecology Department, Faculty of Biology and Chemistry, University of Bremen, Bremen, Germany

*Corresponding author: klinkeannabell@gmail.com

3.1 Abstract

Hard corals are in decline as a result of the simultaneous occurrence of global (e.g., ocean warming) and local (e.g., inorganic eutrophication) factors, facilitating phase shifts towards soft coral dominated reefs. Yet, related knowledge about soft coral responses to anthropogenic factors remains scarce. We thus investigated the ecophysiological response of the pulsating soft coral *Xenia umbellata* to individual and combined effects of phosphate enrichment (1, 2, and 8 μM) and ocean warming (26 to 32 °C) over 35 days. Throughout the experiment, we assessed pulsation, mortality, Symbiodiniaceae density, and cellular chlorophyll *a* content. Simulated ocean warming up to 30 °C led to a significant increase in polyp pulsation and by the end of the experiment to a significant increase in Symbiodiniaceae density, whereas cellular chlorophyll *a* content significantly decreased with warming, regardless of the phosphate treatment. The combination of phosphate enrichment and simulated ocean warming increased pulsation significantly by 41 – 44 %. Warming alone and phosphate enrichment alone did not affect any of the investigated response parameters. Overall, *X. umbellata* displayed a high resilience towards ocean warming with no mortality in all treatments. Phosphate enrichment enabled soft corals to significantly increase their pulsation under increasing temperatures which may enhance their resilience towards ocean warming. This, in turn, could further facilitate their dominance over hard corals on future reefs.

Keywords: multiple stressors, soft coral, global factor, local factor, ocean warming, eutrophication, phosphate, pulsation

An adapted version of this chapter has been published in *Frontiers in Marine Science* **9**, 1026321. <https://doi.org/10.3389/fmars.2022.1026321>

3.2 Introduction

Tropical coral reefs provide essential ecosystem services including food provision, carbon sequestration, and coastal protection^{1,2}. Yet, the simultaneous occurrence of global and local factors has contributed to the decline of live coral cover and the capacity of coral reefs to provide ecosystem services by half since the 1950s³. Specifically, the simultaneous occurrence of global ocean warming and local eutrophication exacerbates this alarming trend^{4,5}.

Both ocean warming and eutrophication have been linked to bleaching in hard corals⁶⁻⁸. In most cases, extensive coral bleaching has been attributed to elevated ocean temperatures⁹. Following bleaching, hard corals can return to pre-bleaching states if the stressful conditions are relatively mild and short-term^{9,10}. Nevertheless, mass coral bleaching events have increased in magnitude and frequency in response to steadily warming ocean temperatures, leaving reef-building corals with insufficient time to recover^{11,12}. In addition, reduced water quality can interact with ocean warming and exacerbate the thermal-induced bleaching response in hard corals^{8,13-15}. Inorganic eutrophication, especially in form of nitrate enrichment, can cause an increase in density in algal symbionts of the family Symbiodiniaceae in host corals, thereby possibly shifting Symbiodiniaceae from a nitrogen limited to a phosphate starved state^{15,16}. Eutrophication can also shift the mutualism between host corals and Symbiodiniaceae towards parasitism or increase oxidative stress in corals^{8,17}. Subsequently, corals are more susceptible to bleaching due to the destabilisation of the coral-algal symbiosis¹⁸.

Together, global and local anthropogenic factors lead to hard coral decline and thus facilitate phase shifts on coral reefs towards new, rather opportunistic benthic organisms¹⁹⁻²¹. These are often associated with shifts from hard coral dominated to macroalgae dominated communities, while shifts towards other benthic communities following a disturbance are also possible outcomes²²⁻²⁴. Several studies observed an increase in soft coral abundances or reefs shifting from a previously hard coral dominated to a soft coral dominated state²⁵⁻²⁸. Norström et al.²³ hypothesized that shifts from hard to soft coral dominated reefs are often related to changes in the dynamics of bottom-up factors such as eutrophication. Although soft corals are important constituents in coral reef ecosystems, influencing ecological and biochemical processes on coral reefs²⁹⁻³³, they do not provide the diverse ecosystem services of hard corals^{27,34,35}.

Soft corals are successful colonisers due to fast growth rates, high fecundity, multiple dispersal modes, and strong chemical defence mechanisms^{25,32,36}. These features help soft corals to dominate space, pre-empt settlement room, inhibit hard coral recruitment, or impede hard coral growth on reefs^{23,25}. This makes them strong competitors against hard corals, specifically under environmental pressures. Soft corals display a considerable resilience towards global factors such as ocean warming and acidification^{27,37,38}. In addition, some soft coral species benefit from active heterotrophy by helping them to sustain their metabolism requirements during thermal stress^{21,39}. Soft corals generally rely more on heterotrophic feeding because of their lower photosynthetic activity compared to hard corals^{40,41}.

Indeed, reefs dominated by zooxanthellate soft corals extract large quantities of suspended particulate matter from the water column due to high levels of heterotrophy³⁹. In particular, pulsating soft corals seem to cope better under ocean warming and eutrophication⁴². Recently, Vollstedt et al.⁴² observed that the pulsating soft coral *Xenia umbellata* benefits from organic eutrophication (in form of glucose), resulting in an increased resilience to warming. In contrast, inorganic eutrophication (in form of nitrate) decreased the resilience of *X. umbellata* to warming⁴³ supporting the finding of Wiedenmann et al.¹⁵: high nitrogen to phosphorus (N:P) ratios can decrease the resilience of corals to warming, possibly due to a destabilised symbiosis between the coral host and its Symbiodiniaceae following phosphate starvation. Phosphate (PO_4^{3-}) generally plays an important role during thermal stress in corals by maintaining Symbiodiniaceae density and photosynthetic rates⁴⁴.

In the last decades, the body of literature concerning multiple stressor effects on coral reefs is growing^{45–47}. Yet, there are notable gaps in the literature with respect to numerous interaction pairs including temperature as a global factor and eutrophication as a local factor⁴⁸. Additionally, previous studies concentrated on threats to hard corals with less attention on soft corals, despite their potentially important ecological roles and increasing occurrence on many coral reefs^{23,29,30}. Hence, understanding how the ecophysiology of soft corals is affected by anthropogenic factors and what drives shifts on coral reefs towards a soft coral dominated state is fundamental for predicting future scenarios and implementing management actions.

To improve our understanding of the combined effects of inorganic eutrophication and warming on soft corals, this study aims to answer the following research questions: (1) How does phosphate enrichment affect *X. umbellata*? and (2) How does phosphate enrichment affect the response of *X. umbellata* to warming? The pulsating soft coral *X. umbellata* was used as a study organism because it is a common species in the Indo-Pacific region^{25,40,49,50}. We hypothesise that phosphate, in contrast to nitrate, will increase the resilience of *X. umbellata* to warming because its Symbiodiniaceae will not suffer from phosphate starvation^{15,16,43}. We tested our hypothesis in a five-week laboratory experiment with two phases. First, corals were exposed to phosphate enrichment (1, 2, 8 μM PO_4^{3-} addition) under ambient temperature (26 °C) for two weeks. Second, ocean warming was simulated by a stepwise increase in water temperature from 26 to 32 °C over the course of three weeks. To assess coral health in response to phosphate enrichment and/or warming, we measured ecophysiological parameters such as pulsation, mortality, Symbiodiniaceae density and their cellular chlorophyll *a* (Chl. *a*) content. By answering the research questions, our study aims to fill the knowledge gaps regarding the interactive effects of global and local factors on the eco-physiology of soft corals. Addressing these knowledge gaps will help to better understand phase shift dynamics and to predict the resilience of coral reefs in the future of the Anthropocene.

3.3 Materials and methods

Experimental design and conditions

The study was conducted in the Marine Ecology Laboratory at the University of Bremen, Germany, in 2020. *Xenia umbellata* specimens used for the present study were collected in the northern Red Sea in 2017 and kept in a maintenance aquarium under controlled conditions. Prior to the experiment, clonal mother colonies were fragmented into 276 smaller colonies using a scalpel and attached to calcium carbonate plugs (AF Plug Rocks, Aquaforest, Poland) with rubber bands. After coral fragments healed and were firmly attached to the plugs, the rubber bands were removed. Colonies were transferred from the maintenance aquarium to a tower system, which consisted of 12 individual tanks (60 L). 23 colonies were placed onto grid plateaus in each tank. Three of the colonies per tank were allocated for the observational parameter pulsation. Three random colonies per tank were used to assess Symbiodiniaceae density and cellular Chl. *a* concentration by freezing one colony per tank at -20 °C, pending further analysis, at three time points (day 0, 14, and 35). All colonies were used to observe mortality.

The 12 individual tanks were arranged in a three-level tower system with four tanks per level. Each tank contained ~ 40 L artificial seawater prepared from demineralized (DM) water and artificial sea salt (Zoo Mix, Tropic Marin, Switzerland). The tanks were separated into a technical part and an experimental part. The technical part contained a thermostat (3613 aquarium heater. 75 W220–240 V; EHEIM GmbH and Co. KG, Germany), temperature controller (Schego Thermostat TRD 1000 Art.-Nr. 112), recirculation pump (EHEIM CompactOn 1000 pump; EHEIM GmbH and Co. KG, Germany), and a temperature logger (HOBO pendant temp/light, Onset, USA). The experimental part contained *X. umbellata* colonies on polycarbonate grid plateaus and a calcium carbonate sand layer of approx. 10 cm. The reef sand (grain size 0.5 – 1.2 mm) (Orbit-Aquaristik, Germany) was transferred into the tanks 5 weeks before the start of the experiment, so that a microcosm with microbial activity could develop. Two light emitting diode (LED) lights (Royal Blue—matrix module and Ultra Blue White 1:1—matrix module, WALTRON daytime LED light, Germany) were adjusted above each tank. LED lights operated with a light intensity of $109.8 \pm 12.1 \mu\text{mol quanta m}^{-2} \text{s}^{-1}$, which was measured in photosynthetically active radiation (PAR) using a LI-1400 Data Logger (LI-COR Biosciences, Germany), in a day-night rhythm of 12-12 h (Table 3.1).

During an acclimation phase of 14 days, experimental tanks stayed connected to the maintenance aquarium (~ 24 °C). Afterwards, the tower system was disconnected from the main system and tanks were separated at the start of the experiment (day 0) to ensure equal starting water conditions across treatments. Further, the temperature in each tank was increased to ~ 26 °C (1 °C per day) to commensurate experimental conditions of previous studies^{42,43}. 10 % of the artificial seawater was replaced daily to maintain a high water renewal rate in each tank. Temperature, salinity, pH, and dissolved oxygen were measured daily with a digital multimeter (Hach HQ40D portable multi meter, United States) and chemical water quality parameters were monitored twice a week (Table 3.1). PO₄³⁻

concentrations were measured daily using a photometer (Turner Designs Trilogy Laboratory Fluorometer). To this end, we adjusted the protocol of a commercially available phosphate test kit for salt water (TESTLAB MARIN, JBL, Germany) by quantifying weights and volumes of reagents and by creating a calibration curve ($R^2 = 0.97$). Phosphate concentrations were manually adjusted using a 1 M stock solution of disodium hydrogen phosphate (purity $\geq 98\%$, Sigma-Aldrich 71645). Coral colonies were fed ~ 0.1 g dried marine plankton ($150 - 200 \mu\text{M}$) (Reef-Roids, Polyp Lab, USA) per tank two times per week to sustain previous maintenance conditions and avoid stress due to starvation. Tanks and grid plateaus were cleaned once a week.

Table 3.1 Mean values (\pm SD) of water quality parameters maintained in the tower system throughout the experiment (excluding PO₄³⁻ concentrations and temperature).

Parameter	Mean Values (\pm SD)
PAR ($\mu\text{mol m}^{-2} \text{s}^{-1}$)	109.8 \pm 12.1
Salinity (‰)	36.0 \pm 0.4
pH	8.6 \pm 0.4
Dissolved oxygen (mg L^{-1})	9.2 \pm 0.8
Alkalinity ($^{\circ}\text{dH}$)	7.2 \pm 1.2
Calcium (mg L^{-1})	430.6 \pm 47.1
Magnesium (mg L^{-1})	1 493.4 \pm 144.7
Nitrite (mg L^{-1})	< 0.01
Nitrate (mg L^{-1})	< 0.5
Ammonia (mg L^{-1})	< 0.05

Experimental phosphate and temperature treatments

Xenia umbellata was exposed to three different phosphate treatments. Three tanks served as controls in which colonies were exposed to very low phosphate concentrations ($< 0.2 \mu\text{M}$), simulating natural phosphate loads in oligotrophic reefs^{13,51,52}. Further, three different phosphate enrichment treatments were maintained in three tanks each by daily additions of disodium hydrogen phosphate (purity $\geq 98\%$, Sigma-Aldrich 71645). Phosphate treatments were adjusted to low ($1 \mu\text{M}$), medium ($2 \mu\text{M}$), and high ($8 \mu\text{M}$) concentrations which are comparable to previous phosphate experiments with corals and human-induced *in situ* conditions in coastal waters^{13,21,53–58}.

Phosphate concentrations were measured daily in all tanks to maintain the different phosphate treatments as described before. A photometric o-phosphate determination method was applied by using JBL ProAqua Phosphat Test-Kits and the resulting change in colouration was measured with a calibrated photometer (Turner Designs Trilogy Laboratory Fluorometer). Subsequently, the amount of phosphate needed to be added to maintain phosphate treatments was adjusted. The first phosphate addition was carried out after the recording of baseline values (day 0). Afterwards, phosphate addition was administered every afternoon.

During the first experimental phase (day 1 – 14), the water temperature was kept stable at 26°C in all tanks. During the second experimental phase (day 15 – 35), the temperature was increased stepwise by 2°C over three days (1°C per day) and then kept stable for four days. This procedure was repeated until the final water temperature of 32°C was reached. The selected temperature treatment was based on the experimental design of previous studies investigating the combined effect of organic/inorganic eutrophication and ocean warming on *X. umbellata*^{42,43}.

Effects on pulsation and mortality

Pulsation and mortality of *X. umbellata* colonies were monitored once a week throughout the experiment. Pulsations of three randomly selected polyps from three marked colonies per experimental tank were counted following the method developed by Vollstedt et al.⁴². Polyp pulsations were assessed in the morning to avoid the effects of circadian rhythms and possible disturbances due to other measurements and before the addition of coral food. Pulsations were counted for 30 sec. and then standardized to one minute as a comparative unit (beats min⁻¹). Only whole tentacle contractions of a polyp (open – fully closed – open) passed as a pulsation and were counted. Mean rates were calculated for each colony and subsequently for each tank, resulting in three true replicates per treatment.

Mortality was assessed for all *X. umbellata* colonies by counting the number of colonies alive or dead in each tank. In case of uncertainty, colonies were observed for polyp pulsation or tissue necrosis. If no reaction of polyps in combination with tissue necrosis was observed, colonies were determined to be dead and removed from the tank.

Symbiodiniaceae analysis

Sample processing and normalization metrics for Symbiodiniaceae analysis in soft corals followed the methods recommended by Pupier et al.⁵⁹. One colony per tank was randomly selected at the start of the experiment (day 0) and the end of the first and second experimental phase (day 14, day 35), resulting in three temporal samples and replicates per treatment. Colonies were removed from their coral plugs, rinsed with DM water, and frozen at -20 °C until further analysis.

At the end of the five-week experiment, all samples were freeze-dried at -60 °C for 24 h and stored under dry and dark conditions. The dry weight (DW) of the colonies was measured and used as a normalization metric. All samples were then homogenized in 10 mL DM water by using a hand tissue grinder (10 mL glass Potter-Elvehjem). Afterwards, two subsamples were transferred into 2 mL Eppendorf cups to analyse Symbiodiniaceae densities and Chl. *a* concentrations within 24 h. Subsamples were centrifuged for 10 min, supernatants were discarded, and pellets were re-suspended in DM water. Subsamples were centrifuged again for 10 min and supernatants were discarded.

Pellets of the subsamples for the Symbiodiniaceae density counts were re-suspended in 2 mL DM water. After samples were thoroughly mixed, 10 µL of the sample was transferred onto two hemocytometers (Improved Neubauer counting chamber, depth 0.1 mm), allowing for two replicate counts per sample. To obtain Symbiodiniaceae densities, the hemocytometer counting method as described by LeGresley & McDermott⁶⁰ was applied. Consequently, counts were adjusted to the total initial sample volume of 10 mL to calculate the algal cell density of the colony. The mean algal cell density per tank, obtained from the two replicate counts, was then normalized to host DW. In total, three replicates per treatment were obtained.

Pellets of the Chl. *a* subsamples were re-suspended in 2 mL 100 % acetone to extract chlorophyll from Symbiodiniaceae, and stored in darkness for 24 h at 4 °C. Following this, samples were centrifuged for 5 min and then transferred into two quartz cuvettes, allowing for two replicate readings per sample. The determination of Chl. *a* concentrations followed the method described by Jeffrey & Humphrey⁶¹ which is used for the spectrophotometric determination of Chl. *a* in dinoflagellates. Chl. *a* concentrations were measured at two fixed wavelengths (663 nm and 630 nm) using a UV-Spectrophotometer (GENESYS 150, Fisher Scientific, Germany). Resulting concentrations were standardized to host DW and subsequently to Symbiodiniaceae density to calculate the mean cellular Chl. *a* concentration per algal cell. In total, three replicates per treatment were obtained. All Chl. *a* analysis steps were conducted under minimal light exposure.

Statistical analyses

The statistical analysis was carried out in R version 3.6.1 using the packages *tidyverse*, *ggplot2*, *ggpubr*, and *rstatix*^{62,63}. Parametric data obtained from repeated measurements (i.e., pulsation) was analyzed by using a 2-way mixed ANOVA to test for significant differences between “days” as within-subject factors and “treatments” as between-subject factor. To check assumptions, normality was tested with the Shapiro-Wilk test, homogeneity of variance was confirmed by the Levene’s test, homogeneity of covariance was tested with the Box’s M-test, and sphericity was assessed by the Mauchly’s test. Randomly collected parametric data (Symbiodiniaceae density counts and cellular Chl. *a* concentrations) was analyzed by using a two-way ANOVA. To check assumptions, normality was tested with the Shapiro-Wilk test and homogeneity of variance was confirmed by the Levene’s test. In order to normalize the cellular Chl. *a* data, a log10 transformation was applied. No outliers were identified using the *rstatix* package. For post-hoc analysis, pairwise comparisons ([pwc](#)) with Bonferroni adjustment were applied. A pairwise *t*-test was used for parametric data while for non-parametric data a paired Wilcoxon signed-rank test for within-subject factors and a Dunn’s test for between-subject factors was used. Results in text, figures, and tables were represented as means ± standard error of the mean ([SEM](#)) and differences were considered as statistically significant at $p < 0.05$.

3.4 Results

Effects of phosphate enrichment

During the first experimental phase, the two-week exposure to phosphate enrichment did not significantly affect any of the investigated ecophysiological parameters of *X. umbellata*. Colonies exposed to different phosphate treatments did not display significant differences in pulsation (two-way mixed ANOVA, $F_{(3, 8)} = 3.71$, $p = 0.06$) ([Fig. 3.1](#), [Supplementary Table S3.1](#)). Yet, regardless of the phosphate treatment, average pulsation significantly increased from 36 ± 1.3 on day 0 (baseline value) to 43 ± 2.0 beats min^{-1} on day 14. At the end of the first experimental phase, no mortality of *X. umbellata* colonies was observed. Further, there were no statistically significant differences in Symbiodiniaceae

densities (two-way ANOVA, $F_{(3,24)} = 0.860$, $p = 0.48$) (Fig. 3.2, Supplementary Table S3.1) and cellular Chl. *a* concentrations in *X. umbellata* colonies (two-way ANOVA, $F_{(3,24)} = 0.770$, $p = 0.52$) (Fig. 3.3, Supplementary Table S3.1).

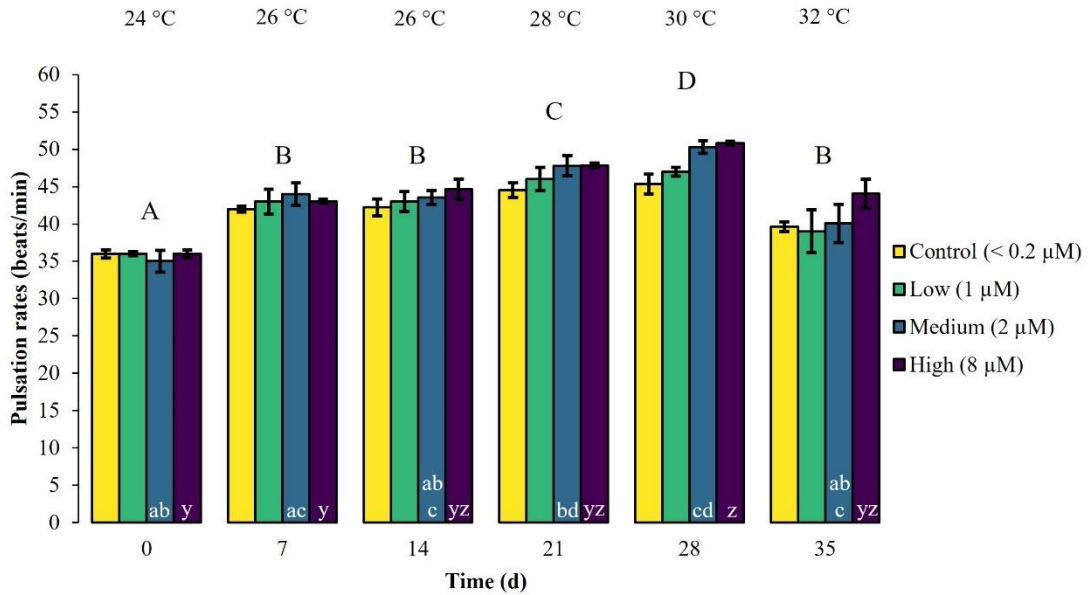


Figure 3.1 Pulsation rates \pm SEM of *Xenia umbellata* colonies ($n = 3$) kept at different phosphate concentrations (control $< 0.2 \mu\text{M}$; low $\sim 1 \mu\text{M}$; medium $\sim 2 \mu\text{M}$; high $\sim 8 \mu\text{M}$) and exposed to an artificially induced water temperature increase. Bars represent the mean of three replicates. Different capital letters above bars indicate significant differences between days and different letters within bars show significant differences within treatments over time (pwc, Bonferroni adjustment, pairwise t -test, $* = p < 0.05$). Raw data is available in Supplementary Table S3.1.

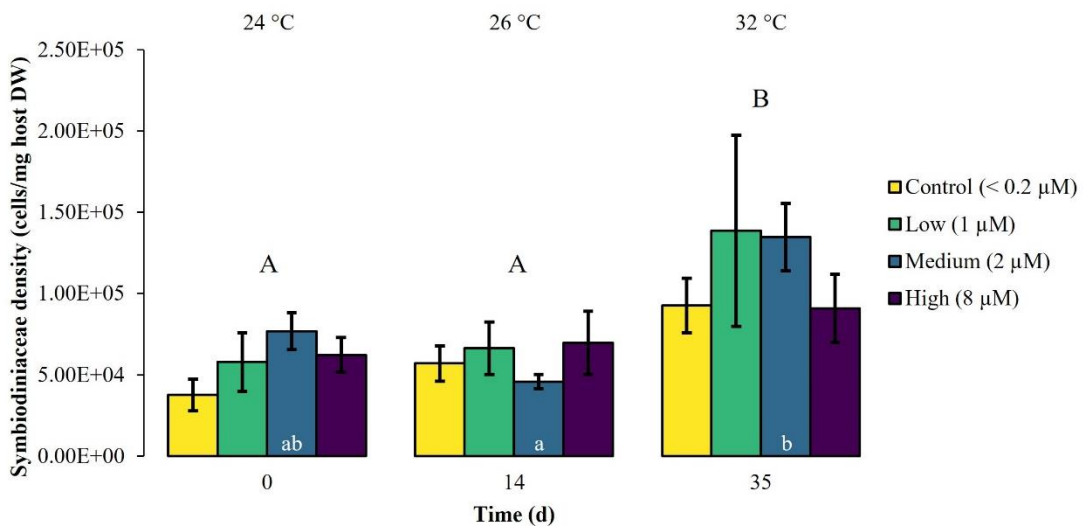


Figure 3.2 Symbiodiniaceae density \pm SEM of *Xenia umbellata* colonies ($n = 3$) kept at different phosphate concentrations (control $< 0.2 \mu\text{M}$; low $\sim 1 \mu\text{M}$; medium $\sim 2 \mu\text{M}$; high $\sim 8 \mu\text{M}$) and exposed to an artificially induced water temperature increase. Bars represent the mean of three replicates. Different capital letters above bars indicate significant differences between days and different letters within bars show significant differences within treatments over time (pwc, Bonferroni adjustment, t -test, $** = p < 0.01$). Raw data is available in Supplementary Table S3.1.

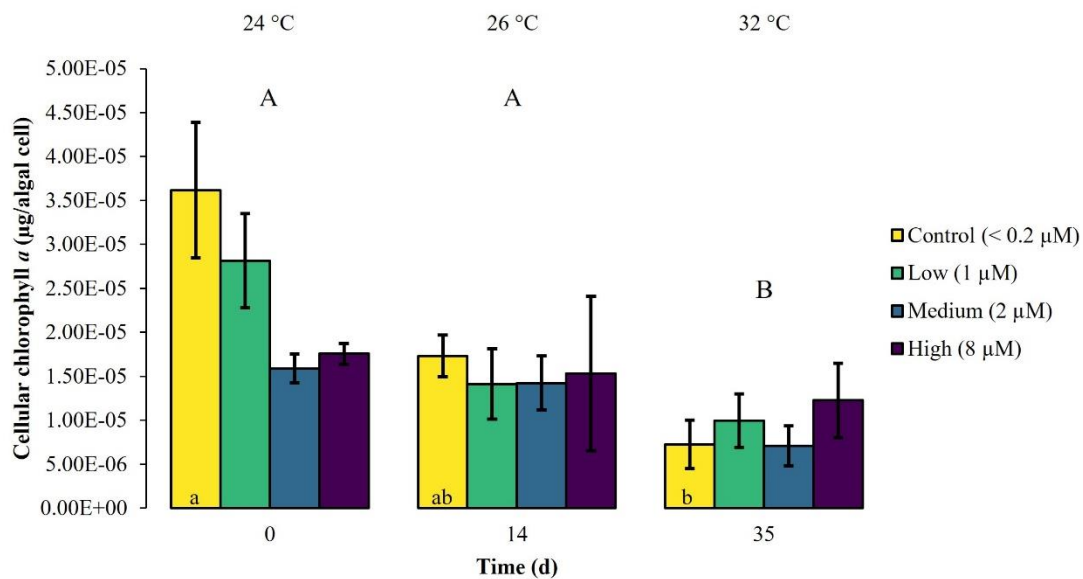


Figure 3.3 Cellular chlorophyll *a* ± SEM of *Xenia umbellata* colonies ($n = 3$) kept at different phosphate concentrations (control < 0.2 µM; low ~ 1 µM; medium ~ 2 µM; high ~ 8 µM) and exposed to an artificially induced water temperature increase. Bars represent the mean of three replicates. Different capital letters above bars indicate significant differences between days and different letters within bars show significant differences within treatments over time (pwc, Bonferroni adjustment, pairwise *t*-test, $* = p < 0.05$). Raw data is available in [Supplementary Table S3.1](#).

Effects of warming

Warming significantly affected pulsation of *X. umbellata* colonies (two-way mixed ANOVA, $F_{(5, 10)} = 49.464$, $p < 0.001$), regardless of the phosphate treatment, by increasing average pulsation up to 30 °C from day 0 to day 28 by 3.3% (pwc, Bonferroni adjustment, pairwise *t*-test, $p < 0.001$) (Fig. 3.1). Temperatures exceeding 30 °C led to a general significant decrease in pulsation in all treatments from day 28 to day 35 of 15% (pwc, Bonferroni adjustment, pairwise *t*-test, $p < 0.001$). Despite slight necrosis in some colonies (single polyp mortality), at the end of the experiment, all colonies survived. Warming caused a significant increase in average Symbiodiniaceae densities (two-way ANOVA, $F_{(2, 24)} = 7.996$, $p < 0.01$), regardless of the phosphate treatment (Fig. 3.2). Yet, the effect of warming alone was not significant in control colonies which showed an increase in Symbiodiniaceae densities by ~ 63%, possibly due to the low number of replicates ($n = 3$). Warming led to a general decrease in cellular Chl. *a* concentrations (two-way ANOVA, $F_{(2, 24)} = 12.927$, $p < 0.001$) within all treatments (Fig. 3.3). Nevertheless, at the end of the experiment, only Chl. *a* concentrations in control colonies exposed to warming alone significantly decreased by ~ 80% compared to baseline values (pwc, Bonferroni adjustment, *t*-test, $p < 0.01$).

Effects of combined phosphate enrichment and warming

Xenia umbellata colonies in the medium and high phosphate treatment significantly increased their pulsation rates when exposed to additional warming (Fig. 3.1). The colonies exposed to medium phosphate enrichment and warming showed a significant increase in their pulsation by ~ 10% from day

7 to day 21 and ~ 44 % from day 0 to day 28 (pwc, Bonferroni adjustment, pairwise *t*-test, $p < 0.05$). The colonies exposed to high phosphate enrichment and warming significantly increased their pulsation by ~ 18 % from day 7 to day 28 (pwc, Bonferroni adjustment, pairwise *t*-test, $p < 0.05$). Further, these colonies showed a significant increase in pulsation of ~ 41 % from day 0 to day 28 (pwc, Bonferroni adjustment, pairwise *t*-test, $p < 0.01$). Survival was not affected by the combined effect of phosphate enrichment and simulated ocean warming over a short period of three weeks. The Symbiodiniaceae density of colonies exposed to medium phosphate enrichment and warming was significantly increased by ~ 195 % (pwc, Bonferroni adjustment, *t*-test, $p < 0.01$) (Fig. 3.2). In contrast, warming from 26 °C to 32 °C caused an increase in Symbiodiniaceae densities of colonies exposed to low or high phosphate enrichment by ~ 109 %, and ~ 31 %, respectively. At the end of the experiment, Chl. *a* concentrations of colonies exposed to the combined factors of low, medium, and high phosphate enrichment and warming decreased by ~ 65 %, ~55 %, and ~30 %, respectively, compared to baseline values (Fig. 3.3).

3.5 Discussion

How does phosphate enrichment affect *X. umbellata*?

Phosphate enrichment did not significantly influence pulsation or survival

Inorganic phosphate enrichment alone did not affect polyp pulsation in *X. umbellata*. Similar, Vollstedt et al.⁴² found that organic eutrophication in form of glucose had no effect on pulsation in the same species. However, a significant increase in pulsation was observed during the first week of the experiment in the present study. While baseline values were measured shortly after the tower system was disconnected from the maintenance aquarium (~ 24 °C), the temperature in the tower system was increased to ~ 26 °C to commensurate experimental conditions of previous studies^{42,43}, possibly leading to the increase in pulsation. Pulsation in this study was comparable to observations in another laboratory experiment with *X. umbellata* at ambient temperatures of 26 – 28 °C⁴² and were similar to *in situ* pulsation rates of *Heteroxenia fuscescens*, another pulsating soft coral in the family *Xeniidae*, in the Red Sea^{64,65}. While inorganic phosphate enrichment does not suggest a disturbance of pulsation in *X. umbellata*, other studies discovered that exposure to excess concentrations of inorganic ions (potassium, sodium, magnesium, calcium), crude oil, or a chemical dispersant caused reduced pulsation or paralysis in xeniid soft corals^{64,66,67}. Horridge⁶⁷ suggested that the excess of certain inorganic ions caused alterations of the polarisation of excitable membranes in *Heteroxenia* affecting pulsation. Studivan et al.⁶⁶, in comparison, hypothesised that reduced pulsation in *Xenia elongata* after the exposure to a chemical dispersant may be related to reduced photosynthetic rates of Symbiodiniaceae or increased coral respiration. This, in turn, alleviates the necessity of pulsation behaviour to facilitate rapid oxygen diffusion on the coral surface.

Soft coral colonies did not show any signs of mortality in the present study due to inorganic phosphate enrichment at ambient temperatures. In contrast, phosphate enrichment can cause increased

mortality⁶⁸, reduced coral growth^{55,69}, and altered skeletogenesis^{13,70} in hard corals as a result of reduced light availability due to nutrient-stimulated phytoplankton growth, increased competition with macroalgae, and inhibited calcification. Yet, phosphate enrichment can also lead to enhanced hard coral growth at the cost of a significant reduction in skeletal density and an increased porosity, increasing the susceptibility of hard corals to breakage by natural events or colonisation by internal bioeroders^{13,56,71}. While soft corals lack a calcium carbonate skeleton, they do produce internal sclerites of calcium carbonate for the structural support of colonies and protection against predation^{72,73}. So far, only a single study by McCauley and Goulet⁷⁴ investigated the effect of phosphate enrichment (4 μM) on sclerites in two gorgonians, *Pseudoplexaura porosa* and *Eunicea tourneforti*, and found that sclerite content and their isotopic signatures were not affected. Considering that the effect of phosphate enrichment seems to be highly species specific in hard corals, it is sensible that future studies investigate the effect of phosphate enrichment on sclerites in pulsating Xeniidae and other soft coral species.

Phosphate enrichment did not affect symbiotic Symbiodiniaceae

After 14 days, phosphate enrichment alone did not cause significant differences in Symbiodiniaceae density and cellular Chl. *a* concentration, suggesting no disruption of the symbiotic relationship between Symbiodiniaceae and *X. umbellata*. In contrast, Bednarz et al.⁴¹ observed that Chl. *a* tissue content in *Xenia* sp. significantly increased after a 4-week exposure to phosphate enrichment (2 μM). Similar observations have been made in hard coral studies, where phosphate enrichment over time periods of 4 to 58 weeks resulted in significantly increased Symbiodiniaceae densities and Chl. *a* tissue contents^{75–77}. In comparison to the present study, these corals were exposed to phosphate enrichment over longer periods which could explain the different results, suggesting that phosphate may not have an immediate effect on Symbiodiniaceae. In addition, these studies measured Chl. *a* tissue content, not cellular Chl. *a* concentrations as in the present study. Another possibility could be that Symbiodiniaceae in the present study stored inorganic phosphate as a precaution measure in case of reduced heterotrophy rather than using it for population density growth or increasing cellular Chl. *a* concentrations. This is supported by previous studies that found Symbiodiniaceae acting as a sink of inorganic nutrients within the symbiotic association and actively controlling uptake rates depending on the organic and inorganic feeding history of the coral host^{78–80}. For instance, phosphate uptake rates by Symbiodiniaceae were significantly increased in starved corals and anemones^{79–81}.

How does phosphate enrichment affect the response of *X. umbellata* to warming?

*Phosphate enrichment increased the resilience of *X. umbellata* to warming*

Across all three phosphate treatments and controls, pulsation increased with warming up to a temperature of 30 °C. Specifically, colonies exposed to medium and high phosphate enrichment under warming significantly increased their pulsation by 44 % and 41 %, respectively, compared to their

baseline values. However, temperatures exceeding 30 °C led to an overall decrease in pulsation. These findings suggest that phosphate enrichment may support *X. umbellata* to increase its pulsation under warming to a certain thermal threshold. The continuous pulsation can benefit the coral in several ways by promoting water movement around the colony, fast removal of excess oxygen at the coral surface, and preventing the refiltration of water by neighbouring polyps^{65,82}. This, in turn, enhances the coral's photosynthesis and food supply with particulate and dissolved organic matter⁶⁵. The significantly increased pulsation observed in colonies exposed to phosphate enrichment under warming may enhance the heterotrophic feeding ability of *X. umbellata* and thus may support retaining necessary energy levels to withstand thermal stress. Further, increased pulsation rates may help to mitigate high water temperatures at the coral surface and may reduce their thermal bleaching susceptibility. In comparison, colonies exposed to organic eutrophication maintained but did not increase their pulsation under warming⁴². Overall, pulsating xeniid soft corals could be considered bioindicators by using pulsation rate as an easily detectable, non-invasive, and inexpensive early warning indicator for changes in water quality and ocean warming (sensu Vollstedt et al.⁴²).

Throughout the experiment, no mortality was observed in colonies exposed to phosphate enrichment and/or warming. Hence, *X. umbellata* generally displayed a high resistance towards ocean warming. However, previous work predicted *Xenia* spp. to be more susceptible to rising ocean temperatures than other Octocorallia in the Great Barrier Reef^{37,83}. One possible explanation for the high thermal tolerance of *X. umbellata* in our study could be their origination from the northern Red Sea. Studies discovered that hard corals are generally more thermal tolerant in the northern Red Sea^{84,85}, which may also apply to soft coral species. Another explanation could be the short exposure time (three weeks) of colonies to simulated ocean warming and thus may not be reflective of true thermal stress leading to colony mortality in this species. Yet, Vollstedt et al.⁴² observed a 30 % mortality rate of colonies with increasing temperatures up to 32 °C after three weeks that were not exposed to glucose enrichment (low (10 mg/L), medium (20 mg/L), high (40 mg/L)). As our study used a similar design to simulate ocean warming from 26 to 32 °C over the course of three weeks as Vollstedt et al.⁴², the finding of Vollstedt et al.⁴² is contradictory to the observation in the present phosphate enrichment experiment, where warming alone did not result in colony mortality. An explanation could be that corals exposed to warming alone in the present experiment were able to maintain survival due to supplemental feed as an additional energy resource. Vollstedt et al.⁴² hypothesised that *X. umbellata* can switch from photoautotrophy to mixotrophy, if necessary. Further, Hughes & Grottoli⁸⁶ hypothesised that heterotrophic compensation in corals could be a sign of resilience towards ocean warming. Heterotrophy could supply the coral holobiont with additional energy resources and may help the coral host to maintain functions, especially when experiencing autotrophic disruption^{87,88}. However, Ezzat et al.⁸⁹ points out that a shift towards greater heterotrophy under thermal stress requires a minimum of autotrophically acquired inorganic nutrients to be functional.

Regardless of phosphate treatment, Symbiodiniaceae density increased, while cellular Chl. a concentration decreased under warming

Warming significantly increased Symbiodiniaceae densities while cellular Chl. *a* contents were significantly decreased, regardless of the phosphate treatment. Increases in Symbiodiniaceae densities can be observed when Symbiodiniaceae are no longer nutrient restricted, especially when they are not nitrogen limited^{90,91}. While Symbiodiniaceae were not significantly affected by phosphate enrichment in the present study, higher Symbiodiniaceae densities could have been caused by increased dinitrogen fixation due to higher diazotroph activity because of warming^{6,16,92}. Lesser et al.⁹³ observed that Symbiodiniaceae are the primary users of the dinitrogen fixation products of diazotrophs, implying that this process is important for primary production. However, Rådecker et al.¹⁸ observed that heat stress reduces the contribution of diazotrophs to coral holobiont nitrogen cycling. They found that in the coral *Stylophora pistillata*, even though dinitrogen fixation rates were increased under warming, the additional fixed nitrogen was not assimilated by the coral tissue or the Symbiodiniaceae.

Phosphate plays a central role in the bleaching susceptibility of corals. Phosphate uptake rates can significantly increase while nitrate uptake rates significantly decrease in corals exposed to thermal stress^{44,94}. Corals required inorganic phosphate rather than nitrate during thermal stress to maintain their Symbiodiniaceae density and photosynthetic rate, as well as to enhance the translocation and retention of carbon within the host tissue⁴⁴. Therefore, phosphate starvation can destabilise the coral-algal symbioses, resulting in an increased bleaching susceptibility of corals^{15,52}. Wiedenmann et al.¹⁵, for instance, observed that corals previously incubated at high N:P ratios (< 5 weeks) displayed signs of bleaching within 10 days when exposed to a stepwise increase in heat (up to 30 °C) and light (up to 160 $\mu\text{mol m}^{-2} \text{s}^{-1}$) stress due to phosphate starvation. Supporting results were observed by Thobor et al.⁴³, who found a higher susceptibility of *X. umbellata* to ocean warming when previously exposed to nitrate enrichment (37 μM) for two weeks followed by a combined treatment of nitrate enrichment and a stepwise temperature increase from 26 to 32 °C in three weeks. However, *X. umbellata* colonies in the present study were not exposed to high N:P ratios and thus should not suffer from phosphate starvation.

The increase in Symbiodiniaceae density was accompanied by a reduction in cellular Chl. *a* content. Similar results have been reported by Hoegh-Guldberg & Smith⁹⁵, who observed that cellular Chl. *a* concentrations in Symbiodiniaceae of the coral *Seriatopora hystrix* decreased while Symbiodiniaceae population densities increased. They hypothesised that this was the result of reduced inorganic nitrogen availability to Symbiodiniaceae at high population densities. Reduced chlorophyll content due to reduced inorganic nitrogen availability has also previously been observed for marine algae⁹⁶⁻⁹⁸. In addition, Béraud et al.⁹⁹ showed that heat stress in combination with reduced nitrogen availability resulted in reduced cellular Chl. *a* concentrations in the scleractinian coral *Turbinaria reniformis*. Other studies observed that the chlorophyll content of the sea anemone *Aiptasia pallida* decreased as the host was starved¹⁰⁰. Hence, reduced cellular Chl. *a* contents in the present study could

be explained by either reduced inorganic nitrogen availability per algal cell, reduced heterotrophy, thermal stress of Symbiodiniaceae, or a combination of all these factors.

Overall, *X. umbellata* displayed a high resilience towards phosphate enrichment and/or ocean warming. This, in turn, could further increase their dominance over hard corals on future reefs. Soft corals, in general, have several competitive advantages against hard corals due to their high fecundity, multiple dispersal modes, chemical defence mechanisms, and their higher resistance to ocean warming and acidification^{25,27,36,82}. Shifts from hard to soft coral dominated reefs will have major implications for ecosystem functions as soft corals provide less structural complexity than hard corals, even though soft corals may still provide a suitable habitat for many fish species^{29,35}. Xeniids, for instance, were already associated with shifts from hard to soft coral dominated reefs after blast fishing events in the Komodo National Park in Indonesia and an outbreak of the corallivore *Acanthaster planci* in the South Sinai region of the Red Sea^{25,26}. In addition, *Xenia* displayed higher abundances at sites exposed to sedimentation and wastewater discharges compared to unimpacted sites in the Red Sea¹⁰¹.

Conclusion

Our findings suggest that inorganic phosphate enrichment enhanced the resilience of the pulsating soft coral *X. umbellata* towards ocean warming by enabling them to increase their pulsation. Although *X. umbellata* may be more resistant towards phosphate enrichment in a warming ocean compared to hard corals, they are still restricted in their capability to deal with eutrophication. Inorganic nitrate enrichment, for instance, reduced the resilience of *X. umbellata* towards ocean warming, causing reduced pulsation, darkening of colonies, and high rates of partial as well as whole-colony mortality⁴³. Considering that human activities will likely further increase nutrient levels in coastal ecosystems, a continued degradation of hard and soft coral communities under ocean warming is likely, shifting tropical reefs towards a macro- and turf algae dominated state, which often benefit from eutrophication^{20,102,103}. Thus, our findings support the conservation strategy of strengthening coral resilience towards climate change by addressing local factors such as inorganic eutrophication through regional management measures^{104–106}. It is of great importance to not only control nutrient inputs into coastal systems, but also to consider managing N:P ratios directly as imbalanced ratios have been found to be especially harmful to corals^{15,44,52}. A starting point to reach favourable N:P ratios is to focus on local nutrient profiles, adjusting agriculture and tertiary wastewater-treatment practices, and to evaluate whether the reduction of nitrate or phosphate or both nutrients is the most effective to promote reef resilience^{15,106,107}.

3.6 Author contributions

AK, SM, AT, BT, and CW conceptualized the study. AK and SM conducted the experiment. AK analyzed the samples and the data and wrote the manuscript. CW acquired the funding and supervised the study. All authors revised drafts of the manuscript.

3.7 Acknowledgments

We want to thank Daisy Ruhlmann for supporting us in daily marine aquaria maintenance activities during the experiment. The study was funded by resources of the Marine Ecology Department of University of Bremen, Germany, and the DFG grant Wi 2677/16-1.

3.8 References

1. Connell, J. H. Diversity in tropical rain forests and coral reefs. in *Foundations of Ecology II: Classic Papers with Commentaries* 114–122 (University of Chicago Press, Chicago, 1978). doi:10.7208/chicago/9780226125534-007.
2. Moberg, F. & Folke, C. Ecological goods and services of coral reef ecosystems. *Ecological Economics* **29**, 215–233 (1999).
3. Eddy, T. D. *et al.* Global decline in capacity of coral reefs to provide ecosystem services. *One Earth* **4**, 1278–1285 (2021).
4. Hall, E. R. *et al.* Eutrophication may compromise the resilience of the Red Sea coral *Stylophora pistillata* to global change. *Marine Pollution Bulletin* **131**, 701–711 (2018).
5. Zhao, H. *et al.* Impacts of nitrogen pollution on corals in the context of global climate change and potential strategies to conserve coral reefs. *Science of The Total Environment* **774**, 145017 (2021).
6. Pogoreutz, C. *et al.* Sugar enrichment provides evidence for a role of nitrogen fixation in coral bleaching. *Glob Change Biol* **23**, 3838–3848 (2017).
7. Cziesielski, M. J., Schmidt-Roach, S. & Aranda, M. The past, present, and future of coral heat stress studies. *Ecology and Evolution* **9**, 10055–10066 (2019).
8. Fernandes de Barros Marangoni, L., Ferrier-Pagès, C., Rottier, C., Bianchini, A. & Grover, R. Unravelling the different causes of nitrate and ammonium effects on coral bleaching. *Sci Rep* **10**, 11975 (2020).
9. Brown, B. E. Coral bleaching: causes and consequences. *Coral Reefs* **16**, S129–S138 (1997).
10. Fitt, W. K., Spero, H. J., Halas, J., White, M. W. & Porter, J. W. Recovery of the coral *Montastrea annularis* in the Florida Keys after the 1987 Caribbean “bleaching event”. *Coral Reefs* **12**, 57–64 (1993).
11. Hughes, T. P. *et al.* Coral reefs in the Anthropocene. *Nature* **546**, 82–90 (2017).
12. Hughes, T. P. *et al.* Global warming transforms coral reef assemblages. *Nature* **556**, 492–496 (2018).
13. Koop, K. *et al.* ENCORE: The effect of nutrient enrichment on coral reefs. synthesis of results and conclusions. *Marine Pollution Bulletin* **42**, 30 (2001).

14. Fabricius, K. E., Cséke, S., Humphrey, C. & De'ath, G. does trophic status enhance or reduce the thermal tolerance of scleractinian corals? A review, experiment and conceptual framework. *PLoS ONE* **8**, e54399 (2013).
15. Wiedenmann, J. *et al.* Nutrient enrichment can increase the susceptibility of reef corals to bleaching. *Nature Clim Change* **3**, 160–164 (2013).
16. Rådecker, N., Pogoreutz, C., Voolstra, C. R., Wiedenmann, J. & Wild, C. Nitrogen cycling in corals: the key to understanding holobiont functioning? *Trends in Microbiology* **23**, 490–497 (2015).
17. Baker, D. M., Freeman, C. J., Wong, J. C. Y., Fogel, M. L. & Knowlton, N. Climate change promotes parasitism in a coral symbiosis. *ISME J* **12**, 921–930 (2018).
18. Rådecker, N. *et al.* Heat stress destabilizes symbiotic nutrient cycling in corals. *Proc Natl Acad Sci USA* **118**, e2022653118 (2021).
19. Wild, C. *et al.* Climate change impedes scleractinian corals as primary reef ecosystem engineers. *Mar. Freshwater Res.* **62**, 205 (2011).
20. Naumann, M. S., Bednarz, V. N., Ferse, S. C. A., Niggel, W. & Wild, C. Monitoring of coastal coral reefs near Dahab (Gulf of Aqaba, Red Sea) indicates local eutrophication as potential cause for change in benthic communities. *Environ Monit Assess* **187**, 44 (2015).
21. Baum, G., Januar, I., Ferse, S. C. A., Wild, C. & Kunzmann, A. Abundance and physiology of dominant soft corals linked to water quality in Jakarta Bay, Indonesia. *PeerJ* **4**, e2625 (2016).
22. McManus, J. W. & Polsenberg, J. F. Coral–algal phase shifts on coral reefs: ecological and environmental aspects. *Progress in Oceanography* **60**, 263–279 (2004).
23. Norström, A., Nyström, M., Lokrantz, J. & Folke, C. Alternative states on coral reefs: beyond coral–macroalgal phase shifts. *Mar. Ecol. Prog. Ser.* **376**, 295–306 (2009).
24. McCook, L. J. Macroalgae, nutrients and phase shifts on coral reefs: scientific issues and management consequences for the Great Barrier Reef. *Coral Reefs* **18**, 357–367 (1999).
25. Fox, H. E., Pet, J. S., Dahuri, R. & Caldwell, R. L. Recovery in rubble fields: long-term impacts of blast fishing. *Marine Pollution Bulletin* **46**, 1024–1031 (2003).
26. Tilot, V., Leujak, W., Ormond, R. F. G., Ashworth, J. A. & Mabrouk, A. Monitoring of South Sinai coral reefs: influence of natural and anthropogenic factors. *Aquatic Conserv: Mar. Freshw. Ecosyst.* **18**, 1109–1126 (2008).
27. Inoue, S., Kayanne, H., Yamamoto, S. & Kurihara, H. Spatial community shift from hard to soft corals in acidified water. *Nature Clim Change* **3**, 683–687 (2013).
28. Spencer, T. *et al.* Coral recovery at Aldabra Atoll, Seychelles: five years after the 1998 bleaching event. *Philosophical Transactions of the Royal Society A: Mathematical, Physical and Engineering Sciences* **363**, 251–255 (2005).
29. Epstein, H. E. & Kingsford, M. J. Are soft coral habitats unfavourable? A closer look at the association between reef fishes and their habitat. *Environ Biol Fish* **102**, 479–497 (2019).

30. Steinberg, R. K., Dafforn, K. A., Ainsworth, T. & Johnston, E. L. Know thy anemone: a review of threats to octocorals and anemones and opportunities for their restoration. *Front. Mar. Sci.* **7**, 590 (2020).
31. El-Khaled, Y. C. *et al.* Nitrogen fixation and denitrification activity differ between coral- and algae-dominated Red Sea reefs. *Sci Rep* **11**, 11820 (2021).
32. Changyun, W. *et al.* Chemical defensive substances of soft corals and gorgonians. *Acta Ecologica Sinica* **28**, 2320–2328 (2008).
33. Jeng, M.-S., Huang, H.-D., Dai, C.-F., Hsiao, Y.-C. & Benayahu, Y. Sclerite calcification and reef-building in the fleshy octocoral genus *Sinularia* (Octocorallia: Alcyonacea). *Coral Reefs* **30**, 925–933 (2011).
34. Bednarz, V., Cardini, U., van Hoytema, N., Al-Rshaidat, M. & Wild, C. Seasonal variation in dinitrogen fixation and oxygen fluxes associated with two dominant zooxanthellate soft corals from the northern Red Sea. *Mar. Ecol. Prog. Ser.* **519**, 141–152 (2015).
35. Hall-Spencer, J. M. & Harvey, B. P. Ocean acidification impacts on coastal ecosystem services due to habitat degradation. *Emerging Topics in Life Sciences* **3**, 197–206 (2019).
36. Benayahu, Y. & Loya, Y. Settlement and recruitment of a soft coral: why is *Xenia macrospiculata* a successful colonizer? *Bull. Mar.Sci.* **36**, 12 (1985).
37. Sammarco, P. W. & Strychar, K. B. Responses to high seawater temperatures in zooxanthellate octocorals. *PLoS ONE* **8**, e54989 (2013).
38. Lopes, A. R. *et al.* Physiological resilience of a temperate soft coral to ocean warming and acidification. *Cell Stress and Chaperones* **23**, 1093–1100 (2018).
39. Fabricius, K. E. & Dommissé, M. Depletion of suspended particulate matter over coastal reef communities dominated by zooxanthellate soft corals. *Marine Ecology Progress Series* **196**, 157–167 (2000).
40. Fabricius, K. & Klumpp, D. Widespread mixotrophy in reef-inhabiting soft corals: the influence of depth, and colony expansion and contraction on photosynthesis. *Mar. Ecol. Prog. Ser.* **125**, 195–204 (1995).
41. Bednarz, V. N., Naumann, M. S., Niggel, W. & Wild, C. Inorganic nutrient availability affects organic matter fluxes and metabolic activity in the soft coral genus *Xenia*. *Journal of Experimental Biology* **215**, 3672–3679 (2012).
42. Vollstedt, S., Xiang, N., Simancas-Giraldo, S. M. & Wild, C. Organic eutrophication increases resistance of the pulsating soft coral *Xenia umbellata* to warming. *PeerJ* **8**, e9182 (2020).
43. Thobor, B. *et al.* The pulsating soft coral *Xenia umbellata* shows high resistance to warming when nitrate concentrations are low. *Sci Rep* **12**, 16788 (2022).
44. Ezzat, L., Maguer, J.-F., Grover, R. & Ferrier-Pagès, C. Limited phosphorus availability is the Achilles heel of tropical reef corals in a warming ocean. *Sci Rep* **6**, 31768 (2016).

45. Ellis, J. I. *et al.* Multiple stressor effects on coral reef ecosystems. *Glob Change Biol* **25**, 4131–4146 (2019).
46. Harborne, A. R., Rogers, A., Bozec, Y.-M. & Mumby, P. J. Multiple stressors and the functioning of coral reefs. *Annual Review of Marine Science* **9**, 445–468 (2017).
47. Cannon, S. E. *et al.* Coral reefs in the Gilbert Islands of Kiribati: resistance, resilience, and recovery after more than a decade of multiple stressors. *PLOS ONE* **16**, e0255304 (2021).
48. Ban, S. S., Graham, N. A. J. & Connolly, S. R. Evidence for multiple stressor interactions and effects on coral reefs. *Glob. Change Biol.* **20**, 681–697 (2014).
49. Benayahu, Y. Xenidiidae (Cnidaria: Octocorallia) from the Red Sea, with the description of a new species. *Zoologische mededelingen* **64**, 113–120 (1990).
50. Janes, M. P. Distribution and diversity of the soft coral family Xenidiidae (Coelenterata: Octocorallia) in Lembah Strait, Indonesia. *Galaxea, Journal of Coral Reef Studies* **15**, 195–200 (2013).
51. Crossland, C., Hatcher, B., Atkinson, M. & Smith, S. Dissolved nutrients of a high-latitude coral reef, Houtman Abrolhos Islands, Western Australia. *Mar. Ecol. Prog. Ser.* **14**, 159–163 (1984).
52. Rosset, S., Wiedenmann, J., Reed, A. J. & D’Angelo, C. Phosphate deficiency promotes coral bleaching and is reflected by the ultrastructure of symbiotic dinoflagellates. *Marine Pollution Bulletin* **118**, 180–187 (2017).
53. Ferrier-Pagès, C., Gattuso, J.-P., Dallot, S. & Jaubert, J. Effect of nutrient enrichment on growth and photosynthesis of the zooxanthellate coral *Stylophora pistillata*. *Coral Reefs* **19**, 103–113 (2000).
54. Cruz-Piñón, G., Carricart-Ganivet, J. P. & Espinoza-Avalos, J. Monthly skeletal extension rates of the hermatypic corals *Montastraea annularis* and *Montastraea faveolata*: biological and environmental controls. *Marine Biology* **143**, 491–500 (2003).
55. Renegar, D. A. & Riegl, B. M. Effect of nutrient enrichment and elevated CO₂ partial pressure on growth rate of Atlantic scleractinian coral *Acropora cervicornis*. *Marine Ecology Progress Series* **293**, 69–76 (2005).
56. Dunn, J. G., Sammarco, P. W. & LaFleur, G. Effects of phosphate on growth and skeletal density in the scleractinian coral *Acropora muricata*: a controlled experimental approach. *J. Exp. Mar. Biol. Ecol.* **411**, 34–44 (2012).
57. van der Wulp, S. A., Damar, A., Ladwig, N. & Hesse, K.-J. Numerical simulations of river discharges, nutrient flux and nutrient dispersal in Jakarta Bay, Indonesia. *Mar. Pollut. Bull.* **110**, 675–685 (2016).
58. Al-Farawati, R., El Sayed, M. A. K. & Rasul, N. M. A. Nitrogen, phosphorus and organic carbon in the Saudi Arabian Red Sea coastal waters: behaviour and human impact. in *Oceanographic and Biological Aspects of the Red Sea* (eds. Rasul, N. M. A. & Stewart, I. C. F.) 89–104 (Springer International Publishing, Cham, 2019).

59. Pupier, C. A., Bednarz, V. N. & Ferrier-Pagès, C. Studies with soft corals – recommendations on sample processing and normalization metrics. *Front. Mar. Sci.* **5**, 348 (2018).
60. LeGresley, M. & McDermott, G. Counting chamber methods for quantitative phytoplankton analysis - haemocytometer, Palmer-Maloney cell and Sedgewick-Rafter cell. *UNESCO (IOC Manuals and Guides)* 25–30 (2010).
61. Jeffrey, S. W. & Humphrey, G. F. New spectrophotometric equations for determining chlorophylls a, b, c1 and c2 in higher plants, algae and natural phytoplankton. *Biochemie und Physiologie der Pflanzen* **167**, 191–194 (1975).
62. Wickham, H. Data analysis. in *ggplot2: Elegant Graphics for Data Analysis* (ed. Wickham, H.) 189–201 (Springer International Publishing, Cham, 2016). doi:10.1007/978-3-319-24277-4_9.
63. Wickham, H. *et al.* Welcome to the tidyverse. *Journal of Open Source Software* **4**, 1686 (2019).
64. Cohen, Y., Nissenbaum, A. & Eisler, R. Effects of Iranian crude oil on the Red Sea octocoral *Heteroxenia fuscescens*. *Environ. Pollut. (1970)* **12**, 173–186 (1977).
65. Kremien, M., Shavit, U., Mass, T. & Genin, A. Benefit of pulsation in soft corals. *PNAS* **110**, 8978–8983 (2013).
66. Studivan, M. S., Hatch, W. I. & Mitchelmore, C. L. Responses of the soft coral *Xenia elongata* following acute exposure to a chemical dispersant. *SpringerPlus* **4**, 80 (2015).
67. Horridge, G. A. The responses of *Heteroxenia* (Alcyonaria) to stimulation and to some inorganic ions. *J. Exp. Biol.* **33**, 604–614 (1956).
68. Walker, D. I. & Ormond, R. F. G. Coral death from sewage and phosphate pollution at Aqaba, Red Sea. *Marine Pollution Bulletin* **13**, 21–25 (1982).
69. Kinsey, D. W. & Davies, P. J. Effects of elevated nitrogen and phosphorus on coral reef growth. *Limnol. Oceanogr.* **24**, 935–940 (1979).
70. Simkiss, K. Phosphates as crystal poisons of calcification. *Biological Reviews* **39**, 487–504 (1964).
71. Risk, M. J., Sammarco, P. W. & Edinger, E. N. Bioerosion in *Acropora* across the continental shelf of the Great Barrier Reef. *Coral Reefs* **14**, 79–86 (1995).
72. Van Alstyne, K. L., Wylie, C. R., Paul, V. J. & Meyer, K. Antipredator defenses in tropical pacific soft corals (Coelenterata: Alcyonacea). i. Sclerites as defenses against generalist carnivorous fishes. *Biol. Bull.* **182**, 231–240 (1992).
73. West, J. M. Plasticity in the sclerites of a gorgonian coral: tests of water motion, light level, and damage cues. *Biol. Bull.* **192**, 279–289 (1997).
74. McCauley, M. & Goulet, T. L. Caribbean gorgonian octocorals cope with nutrient enrichment. *Mar. Pollut. Bull.* **141**, 621–628 (2019).
75. Steven, A. D. L. & Broadbent, A. D. Growth and metabolic responses on *Acropora palifera* to long term nutrient enrichment. *Proc. 8th Int. Coral Reef Symp., 1997* **1**, 867–872 (1997).

76. Bucher, D. J. & Harrison, P. L. Growth response of the reef coral *Acropora longicyathus* to elevated inorganic nutrients: do responses to nutrients vary among coral taxa? *Proc. 9th Int. Coral Reef Symp.* (2000).
77. Godinot, C., Ferrier-Pagès, C., Montagna, P. & Grover, R. Tissue and skeletal changes in the scleractinian coral *Stylophora pistillata* Esper 1797 under phosphate enrichment. *Journal of Experimental Marine Biology and Ecology* **409**, 200–207 (2011).
78. Grover, R., Maguer, J.-F., Allemand, D. & Ferrier-Pagès, C. Nitrate uptake in the scleractinian coral *Stylophora pistillata*. *Limnol. Oceanogr.* **48**, 2266–2274 (2003).
79. Grover, R., Maguer, J.-F., Reynaud-Vaganay, S. & Ferrier-Pagès, C. Uptake of ammonium by the scleractinian coral *Stylophora pistillata*: effect of feeding, light, and ammonium concentrations. *Limnology and Oceanography* **47**, 782–790 (2002).
80. Godinot, C., Ferrier-Pagès, C. & Grover, R. Control of phosphate uptake by zooxanthellae and host cells in the scleractinian coral *Stylophora pistillata*. *Limnology and Oceanography* **54**, 1627–1633 (2009).
81. Muller-Parker, G., Cook, C. B. & D’Elia, C. F. Feeding affects phosphate fluxes in the symbiotic sea anemone *Aiptasia pallida*. *Mar. Ecol. Prog. Ser.* **60**, 283–290 (1990).
82. Wild, C. & Naumann, M. S. Effect of active water movement on energy and nutrient acquisition in coral reef-associated benthic organisms. *PNAS* **110**, 8767–8768 (2013).
83. Strychar, K. B., Coates, M., Sammarco, P. W., Piva, T. J. & Scott, P. T. Loss of *Symbiodinium* from bleached soft corals *Sarcophyton ehrenbergi*, *Sinularia* sp. and *Xenia* sp. *J. Exp. Mar. Biol. Ecol.* **320**, 159–177 (2005).
84. Fine, M., Gildor, H. & Genin, A. A coral reef refuge in the Red Sea. *Glob. Change Biol.* **19**, 3640–3647 (2013).
85. Osman, E. O. *et al.* Thermal refugia against coral bleaching throughout the northern Red Sea. *Glob. Change Biol.* **24**, e474–e484 (2018).
86. Hughes, A. D. & Grottoli, A. G. Heterotrophic compensation: a possible mechanism for resilience of coral reefs to global warming or a sign of prolonged stress? *PLOS ONE* **8**, e81172 (2013).
87. Borell, E. M. & Bischof, K. Feeding sustains photosynthetic quantum yield of a scleractinian coral during thermal stress. *Oecologia* **157**, 593–601 (2008).
88. Wooldridge, S. A. Breakdown of the coral-algae symbiosis: towards formalising a linkage between warm-water bleaching thresholds and the growth rate of the intracellular zooxanthellae. *Biogeosciences* **10**, 1647–1658 (2013).
89. Ezzat, L. *et al.* Nutrient starvation impairs the trophic plasticity of reef-building corals under ocean warming. *Funct. Ecol.* **33**, 643–653 (2019).

90. Ezzat, L., Maguer, J.-F., Grover, R. & Ferrier-Pagès, C. New insights into carbon acquisition and exchanges within the coral–dinoflagellate symbiosis under NH_4^+ and NO_3^- supply. *Proc. R. Soc. B.* **282**, 20150610 (2015).
91. Marubini, F. & Davies, P. S. Nitrate increases zooxanthellae population density and reduces skeletogenesis in corals. *Mar. Biol.* **127**, 319–328 (1996).
92. Tilstra, A. *et al.* Relative diazotroph abundance in symbiotic Red Sea corals decreases with water depth. *Front. Mar. Sci.* **6**, (2019).
93. Lesser, M. P. *et al.* Nitrogen fixation by symbiotic cyanobacteria provides a source of nitrogen for the scleractinian coral *Montastraea cavernosa*. *Mar. Ecol. Prog. Ser.* **346**, 143–152 (2007).
94. Godinot, C., Houlbrèque, F., Grover, R. & Ferrier-Pagès, C. Coral uptake of inorganic phosphorus and nitrogen negatively affected by simultaneous changes in temperature and pH. *PLoS ONE* **6**, e25024 (2011).
95. Hoegh-Guldberg, O. & Smith, G. J. Influence of the population density of zooxanthellae and supply of ammonium on the biomass and metabolic characteristics of the reef corals *Seriatopora hystrix* and *Stylophora pistillata*. *Mar. Ecol. Prog. Ser.* **57**, 173–186 (1989).
96. Falkowski, P. G. & Owens, T. G. Light-shade adaptation: Two strategies in marine phytoplankton. *Plant Physiol.* **66**, 592–595 (1980).
97. Dawes, C. J., Chen, C.-P., Jewett-Smith, J., Marsh, A. & Watts, S. A. Effect of phosphate and ammonium levels on photosynthetic and respiratory responses of the red alga *Gracilaria verrucosa*. *Mar. Biol.* **78**, 325–328 (1984).
98. Granéli, E. & Sundbäck, K. The response of planktonic and microbenthic algal assemblages to nutrient enrichment in shallow coastal waters, southwest Sweden. *J. Exp. Mar. Biol. Ecol.* **85**, 253–268 (1985).
99. Béraud, E., Gevaert, F., Rottier, C. & Ferrier-Pages, C. The response of the scleractinian coral *Turbinaria reniformis* to thermal stress depends on the nitrogen status of the coral holobiont. *J. Exp. Mar. Biol.* **216**, 2665–2674 (2013).
100. Cook, C. B., D’Elia, C. F. & Muller-Parker, G. Host feeding and nutrient sufficiency for zooxanthellae in the sea anemone *Aiptasia pallida*. *Mar. Biol.* **98**, 253–262 (1988).
101. Ziegler, M. *et al.* Coral microbial community dynamics in response to anthropogenic impacts near a major city in the central Red Sea. *Mar. Pollut. Bull.* **105**, 629–640 (2016).
102. Adam, T. C. *et al.* Landscape-scale patterns of nutrient enrichment in a coral reef ecosystem: implications for coral to algae phase shifts. *Ecol. Appl.* **31**, e2227 (2021).
103. Karcher, D. B. *et al.* Nitrogen eutrophication particularly promotes turf algae in coral reefs of the central Red Sea. *PeerJ* **8**, e8737 (2020).
104. Wooldridge, S. A. & Done, T. J. Improved water quality can ameliorate effects of climate change on corals. *Ecol. Appl.* **19**, 1492–1499 (2009).

105. Kuffner, I. B. & Paul, V. J. Effects of nitrate, phosphate and iron on the growth of macroalgae and benthic cyanobacteria from Cocos Lagoon, Guam. *Mar. Ecol. Prog. Ser.* **222**, 63–72 (2001).
106. D'Angelo, C. & Wiedenmann, J. Impacts of nutrient enrichment on coral reefs: new perspectives and implications for coastal management and reef survival. *Curr. Opin. Env. Sust.* **7**, 82–93 (2014).
107. Conley, D. J. *et al.* Controlling eutrophication: nitrogen and phosphorus. *Science* **323**, 1014–1015 (2009).

Chapter 4 | The widely distributed soft coral *Xenia umbellata* exhibits high resistance against phosphate enrichment and temperature increase

Chapter 4 | The widely distributed soft coral *Xenia umbellata* exhibits high resistance against phosphate enrichment and temperature increase

Selma D. Mezger^{*1}, Annabell Klinke^{1,2}, Arjen Tilstra¹, Yusuf C. El-Khaled¹, **Bianca M. Thobor**¹, Christian Wild¹

¹ University of Bremen, Faculty of Biology and Chemistry, Department of Marine Ecology, UFT Building, Leobener Str. 6, 28359 Bremen, Germany

² Leibniz Centre for Tropical Marine Research, Fahrenheitstraße 6, 28359 Bremen, Germany

*Corresponding author: mezger@uni-bremen.de

4.1 Abstract

Both global and local factors affect coral reefs worldwide, sometimes simultaneously. An interplay of these factors can lead to phase shifts from hard coral dominance to algae or other invertebrates, particularly soft corals. However, most studies have targeted the effects of single factors, leaving pronounced knowledge gaps regarding the effects of combined factors on soft corals. Here, we investigated the single and combined effects of phosphate enrichment (1, 2, and 8 μM) and seawater temperature increase (26 to 32 $^{\circ}\text{C}$) on the soft coral *Xenia umbellata* by quantifying oxygen fluxes, protein content, and stable isotope signatures in a 5-week laboratory experiment. Findings revealed no significant effects of temperature increase, phosphate enrichment, and the combination of both factors on oxygen fluxes. However, regardless of the phosphate treatment, total protein content and carbon stable isotope ratios decreased significantly by 62 % and 7 % under temperature increase, respectively, suggesting an increased assimilation of their energy reserves. Therefore, we hypothesize that heterotrophic feeding may be important for *X. umbellata* to sustain their energy reserves under temperature increase, highlighting the advantages of a mixotrophic strategy. Overall, *X. umbellata* shows a high tolerance towards changes in global and local factors, which may explain their competitive advantage observed at many Indo-Pacific reef locations.

Keywords: multiple stressors, global factor, local factor, ocean warming, isotopes, oxygen flux, mixotrophy

An adapted version of this chapter has been published in *Scientific Reports* **12**, 22135.

<https://doi.org/10.1038/s41598-022-26325-5>

4.2 Introduction

Coral reefs are highly diverse and complex ecosystems that play a crucial role for humankind as they provide a range of ecosystem services^{1,2}. Although coral reefs are ecologically and economically important, they are in decline due to several global and local anthropogenic factors^{2,3}. On a global scale, they are affected by increasing seawater temperatures⁴, ocean acidification⁵, and higher ultraviolet radiation⁶. While on a local scale, they may additionally experience factors such as eutrophication in coastal waters^{7,8}. This often results in substantial ecological shifts, also termed phase shifts, due to the decline in coral cover, loss of diversity on coral reefs⁹, and general reef degradation¹⁰. As these global and local factors can impact a coral reef simultaneously, it is important to understand which factors are the main drivers of ecological degradation and possible phase shifts, and how they interact with each other¹¹.

Over the last decades, many studies examined the effects of thermal stress¹² or nutrient enrichment^{9,13} on corals. However, their main focus was on single factors and their impacts on hard coral species. Thermal stress can lead to bleaching of the corals and subsequently reduced photosynthetic capacity¹⁴ but also a higher rate of mortality¹⁵, decreased growth¹⁶, and an increased susceptibility to diseases¹⁷. Experiments that examined hard corals under nutrient-enriched conditions showed widely varying results, ranging from somewhat positive effects¹⁸⁻²¹ to clear negative impacts²²⁻²⁴.

Recently, research is increasingly focussed on the combination of different potential stressors^{11,25}. Experiments with combined nutrient enrichment and thermal stress showed divergent results. Experiments by Wiedenmann et al.²⁶ showed that hard corals exposed to increased concentrations of dissolved inorganic nitrogen (DIN) were more susceptible to bleaching than corals exposed to low DIN concentrations. This increased bleaching susceptibility may ultimately be caused by a change in the holobionts' resource partitioning²⁷. The endosymbiotic algae of the family Symbiodiniaceae²⁸ may retain more photosynthates for its own growth as nitrogen (N) is no longer the limiting nutrient, which is essential for steady translocation of photosynthates from the Symbiodiniaceae to the coral host²⁹⁻³¹. Consequently, an increase in DIN leads to increasing numbers of algae, which results in phosphorous (P) starvation and in the end to alterations in the thylakoid membranes. This increases the susceptibility of the coral holobiont to thermal and light stress²⁶. As in this hypothesis P is the limiting factor, enriching the water with P can potentially prevent bleaching^{26,32}. This interruption of N limitation for the Symbiodiniaceae may also be induced by increasing water temperatures^{27,32}. As such, P may be of extreme importance for future coral reef health. Since the scientific focus was directed at hard corals, it remains primarily unknown how soft corals are affected by multiple stressors³³.

In general, soft corals are more resilient to ocean acidification and warming compared to hard corals^{34,35}. In addition, many soft corals can rapidly colonize new areas due to their high fecundity and different dispersal modes^{36,37}. Given the decrease in hard coral cover on many reefs and reported shifts in benthic reef communities towards non-hard coral taxa^{38,39}, it is crucial to understand the

ecophysiology of soft corals under different factors^{33,35}, and how they may alter the nutrient budgets on coral reefs^{40,41}. Particularly successful spreaders are soft corals that belong to the family of Xenidiidae. Xenidiids are recently being considered as strong invasive species that dominate alternative states on many reefs after phase shifts, like in the Caribbean Sea^{42,43}, Indonesia^{36,44}, or the southwest Atlantic^{45,46}. Few studies, conducted on the soft coral *Xenia umbellata*, showed that glucose enrichment^{47,48} increased, while nitrate enrichment⁴⁹ decreased the corals' tolerance to thermal stress. Yet, it remains unknown how phosphate (PO_4) enrichment affects its tolerance to warming.

Therefore, we conducted a five-week manipulative aquarium experiment to assess the effects of PO_4 enrichment and warming as single and combined factors on 1) oxygen fluxes, 2) protein content, and 3) elemental and stable isotope composition of the soft coral *X. umbellata*. For this, coral fragments were exposed to three different, ecologically relevant⁵⁰ concentrations of PO_4 (1, 2, and 8 μM) in combination with warming (26 to 32 °C). The response variables were assessed at different timepoints and finally we put the results in the context of *X. umbellata*'s metabolism and hypothesize what the ecological effects may be.

4.3 Material and methods

Experimental design

We conducted a five-week manipulative aquarium experiment in the Marine Ecology Lab in the Centre for Environmental Research and Sustainable Technology (UFT) at the University of Bremen in Bremen, Germany. The specimens of *X. umbellata* that were used in this experiment are originally from the Red Sea and have been in steady culture in the main holding tank for more than two years on a day-night rhythm of 12:12 hours (temperature ~ 27 °C, salinity ~ 35 ‰, light ~ 100 $\mu\text{mol photons m}^{-2} \text{ s}^{-1}$ photosynthetically active radiation (PAR)).

Clonal *Xenia* colonies from the main holding tank were fragmented into 260 smaller colonies of approximately 1–2 cm in width using a scalpel. All colony fragments, at the beginning of the experiment, were similarly sized and roughly contained between 20 and 60 polyps. We then attached these fragments to plugs made of calcium carbonate (AF Plug Rocks, Aquaforest, Poland) using rubber bands. For healing from the fragmentation process, colonies were kept under regular maintenance conditions for 2 weeks. After that, we evenly and randomly distributed the colonies among 12 individual tanks with each individual tank having a total volume of 60 L filled with 40 L of artificial seawater to let them acclimatize to the new environment for two weeks before the start of the experiment. Each tank consisted of 2 parts that were interconnected, i.e. a technical part and an experimental part. In the technical part we installed a heater (3613 aquarium heater; 75 W 220–240 V; EHEIM GmbH and Co. KG, Germany) and a recirculation pump (EHEIM CompactOn 1000 pump; EHEIM GmbH and Co. KG, Germany) to ensure constant temperatures and water flow. Each heater was connected to a separate temperature controller (TRD digital, SCHEGO GmbH and Co. KG, Germany) to allow for precise

control of the water temperature. Each tank was filled with artificial seawater (Zoo Mix, Tropic Marin, Switzerland) and a layer of CaCO₃ reef sand to ensure the development of healthy mesocosms. A HOBO Pendant Data Logger (HOBO pendant temp/light, Onset, USA) was placed at the bottom of the experimental part of the tank during the whole experiment to monitor temperature and light conditions (measurements were taken every hour). Coral fragments ($n = 20$ per tank) were then placed on a grid made from eggcrate. Above each experimental part of the tank, we placed two light-emitting diode (LED) lamps (one Royal Blue matrix module and one Ultra Blue White matrix module, WALTRON daytime LED light, Germany) so that light levels were similar to conditions in the maintenance aquarium ($\sim 100 \mu\text{mol photons m}^{-2} \text{ s}^{-1}$ PAR) on a day-night rhythm of 12:12 hours. Light intensities were tested twice a week with a LI-1400 Data Logger (LI-COR Biosciences GmbH, Germany) and adjusted when necessary.

To ensure stable conditions in the tanks, 10 % daily water exchanges were done to mimic the high renewal rate of seawater that can be found on coral reefs. Due to the daily water exchanges we did not install additional protein skimmers. Water parameters were maintained at the following levels (mean \pm SD): salinity 36.1 ± 0.3 ‰, nitrate $<0.5 \text{ mg L}^{-1}$, ammonium $<0.05 \text{ mg L}^{-1}$, nitrite $<0.01 \text{ mg L}^{-1}$, calcium $435 \pm 150 \text{ mg L}^{-1}$, alkalinity $7.3 \pm 2.5^\circ\text{dH}$, magnesium $1495 \pm 514 \text{ mg L}^{-1}$, and pH 8.6 ± 0.2 . These water parameters are equal to the ones the corals previously experienced over the last two years in the main holding tank filled with artificial seawater, with the elevated pH value likely caused by a high animal to water ratio. Coral plugs were cleaned from biofouling twice per week. Also, we fed the corals with 0.1 g of dried marine plankton (Reef-Roids, Polyp Lab, USA) per tank twice a week to avoid stress from starvation and to mimic conditions from the main holding tank. Yet, in the main holding tank corals lived in an ecosystem also containing fish and other organisms, hence in the holding tank they may have benefited also indirectly from the fish feed entering the water column which was missing in our experimental setup.

Experimental phosphate and temperature treatments

We created three different PO₄ enrichment treatments (1, 2, and 8 μM), which are comparable to previously conducted experiments with corals in the lab and the field^{23,24,51–54} and a control treatment without PO₄ addition ($n = 3$ tanks per treatment). For the first 14 days of the experiment, the corals were exposed to PO₄ enrichment only (Fig. 4.1). The length of the pure eutrophication treatment was chosen 1) as a previous study could already detect an effect of PO₄ and nitrate (NO₃) after two weeks⁵⁵, and 2) to allow for a better comparison due to similar experimental design of closely related studies conducted on *X. umbellata*^{47–49}. To keep the PO₄ enrichment treatments stable, we measured PO₄ concentrations every day after the water exchange with an adjusted protocol of a commercially available PO₄³⁻ test kit for salt water (TESTLAB MARIN, JBL, Germany) using a photometer (Turner Designs Trilogy Laboratory Fluorometer). For this we quantified weights and volumes of reagents and created a

calibration curve ($R^2 = 0.967$). Afterwards PO_4 concentrations were manually adjusted in each tank using a 1 M stock solution from sodium phosphate dibasic Dihydrate ($\text{Na}_2\text{HPO}_4 \times 2 \text{H}_2\text{O}$).

On day 15, we started the second part of the experiment with the stepwise ramping of the temperature up to 32 °C (Fig. 4.1). For this, the temperature was increased by 1 °C day⁻¹ on two consecutive days and then kept constant for five days. We conducted such a 7-day cycle three times until the temperature reached 32 °C. The temperature treatment in our laboratory experiment were synonymous to 2-degree heating weeks (DHW)⁵⁶ in the first, 6 DHW in the second, and 12 DHW in the third week of the 2nd phase of the experiment.

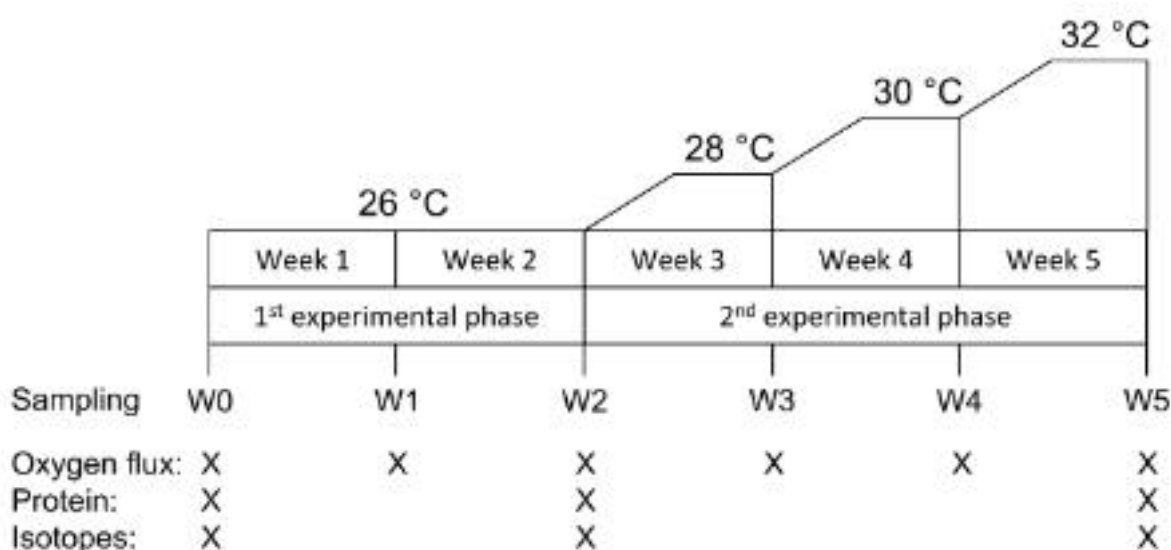


Figure 4.1. Experimental design with a 1st experimental phase of pure PO_4 enrichment, followed by a 2nd experimental phase during which temperature was increased stepwise from 26 to 32 °C. Sampling of oxygen fluxes took place after each week (W0-5), while corals for protein content as well as elemental and stable isotope analysis were collected at the beginning, and at the end of each experimental phase.

Oxygen flux measurements

One fragment per tank ($n = 3$ per treatment) was labeled and used throughout the experiment to determine the rates of oxygen consumption in the dark (dark respiration, R) and oxygen production in the light (net photosynthesis, P_{net}). The smallest colony tested for oxygen fluxes consisted of 28 polyps, while the biggest colony consisted of 70 polyps. To avoid stress, we transferred the colonies without air exposure to incubation chambers with a volume of 160 mL. We filled the incubation chambers with water from the respective tank and sealed them gas-tight without air bubbles inside. Then, we placed them in a temperature bath on a magnetic stirrer (Thermo Scientific, Variomag Poly) with 190 rotations per minute (rpm) for 1.5 to 2 h in the light and dark. The stirring bars allowed for mixing of the water column and ensured homogenous oxygen concentrations in the chambers throughout the measurement. The light used to measure oxygen production was emitted with approximately $100 \mu\text{mol photons m}^{-2} \text{s}^{-1}$ PAR by an LED light (Royal Blue—matrix module and Ultra Blue White 1:1—matrix module, WALTRON daytime LED light, Germany) to ensure equal light conditions as in the experimental tower.

We measured O₂ concentrations within each chamber before and after each incubation by an optode sensor (HACH LDO, HACH HQ 40d, Hach Lange, Germany). For later analysis, we calculated P_{net} in the light, and R in the dark, accounted for water background metabolism, and normalized the flux by incubation duration, chamber volume, and the corals' surface area (SA), to account for the differences in coral fragment size. This is common procedure when calculating oxygen fluxes and has been done in many studies beforehand⁵⁷⁻⁵⁹, with studies conducted on *X. umbellata*^{47,49} reporting oxygen fluxes in the unit of mg O₂ m⁻² h⁻¹. The calculations of the SA per polyp were based on the geometric method developed by Bednarz et al.⁵², multiplying the average polyp SA with the number of polyps. We additionally calculated gross photosynthesis (P_{gross}) rates, based on the assumption that respiration is constant during the day. Yet, as respiration rates may be significantly higher during active photosynthesis than in the dark⁶⁰, the calculated P_{gross} rates can be seen as conservative estimates based on dark respiration. Running a linear regression on the log-transformed data, we analysed that both P_{gross} and R were negatively allometric to the number of polyps with a slope of 0.34 and 0.50, respectively. This indicates that larger colonies produce and consume more oxygen, but relatively less oxygen is produced and consumed per polyp. Therefore, two hypotheses arise: 1) the ratio of coral base to polyp number of coral fragments with many polyps may be smaller than the ratio of colonies with fewer polyps, and is not accounted for by the method of Bednarz et al.⁵², and 2) self-shading in bigger colonies could also potentially cause non-isometric scaling.

Protein content measurements

For measuring the total protein quantification, we used the Bradford assay⁶¹ following the Coomassie Protein Assay Kit (Thermo Scientific). For this, we took one *X. umbellata* fragment out of each tank ($n = 3$ per treatment) randomly each week, rinsed it in distilled water to remove salt, and stored it in a plastic bag in the freezer at -20 °C until further processing. We lyophilized these colonies for 24 h at -60 °C and stored them under dark and dry conditions pending analysis. During lyophilization the samples get freeze-dried by sublimating all the liquid from the sample, leaving only the dry compounds of the animal, e.g., protein and carbohydrates, behind. After that, we then ground those dried samples using mortar and pestle and measured the dry weight (DW) of each colony to use as a normalization metric. The DW of the colonies ranged from 12 to 97 mg (see Supplementary Material). We used this to standardize the protein content of each colony. Using a linear regression on the log-transformed data of protein content and DW, we found a strong correlation between protein content and DW ($R^2 = 0.80$, see [Supplementary Fig. S4.3](#)). The slope above 1 indicates a positive allometry with protein content increasing faster than colony size.

After this, we homogenized the powder from every single sample in 5 mL of distilled water using a high-speed homogenizer (VEVOR, FSH-2A) for 2 min to extract the protein. For further quantification of the protein, we loaded 1 mL from each sample and mixed it with 1 mL of Bradford Dye Reagent 1x (Coomassie Brilliant Blue) in cuvettes. Lastly, we incubated the samples at room

temperature for 10 minutes and read the absorbance in the spectrophotometer under 595 nm wavelength. To gain the resulting concentration of protein in the water we calculated it via the measured absorbance, using a diluted Bovine Serum Albumin (BSA) calibration curve, and then standardized it to water volume and coral dry weight.

Carbon and nitrogen elemental, and stable isotope analysis

To assess carbon (C) and nitrogen (N) isotope signatures and C:N ratios of *X. umbellata*, we conducted an elemental and stable isotope analysis on the entire holobiont. Every week on the first day we randomly selected one fragment of each tank ($n = 3$ per treatment), counted polyps, removed the colony from the plug, washed it in distilled water to remove salt, stored it in a plastic bag, and froze the sample at $-20\text{ }^{\circ}\text{C}$ until further processing. Upon processing, *X. umbellata* colonies were dried in sterile glass petri dishes at $40\text{ }^{\circ}\text{C}$ until weight consistency was reached (~ 48 h). Then, we ground the dried colonies into a fine powder using mortar and pestle, weighed the tissue powder, and transferred 1-2 mg into tin cups. Samples were analysed for C and N quantities as well as stable isotope ratios as described in Karcher et al.⁴⁰. Isotopic ratios (r) are given as the ratio of the heavier to the lighter isotope ($^{15}\text{N}:^{14}\text{N}$ or $^{13}\text{C}:^{12}\text{C}$) and notated as either $\delta^{15}\text{N}$ or $\delta^{13}\text{C}$ (‰) using [Formula 4.1](#):

$$\delta X = \left(\frac{r_{\text{sample}}}{r_{\text{reference}}} - 1 \right) \cdot 1,000 \quad \text{(Formula 4.1)}$$

where $r_{\text{reference}}$ for $\delta^{15}\text{N}$ is atmospheric N (0.00368) and Vienna Pee Dee Belemnite (0.01118) for $\delta^{13}\text{C}$.

By analysing the corals' elemental and stable isotope composition, it is possible to infer the sources of C and N in the coral holobiont. While carbon stable isotope ratios ($\delta^{13}\text{C}$) are often used to understand the corals' C-metabolism⁵⁵, the N stable isotope composition ($\delta^{15}\text{N}$) can be used as a bioindicator to determine the N source of the holobiont⁶². This can be done as different sources for C and N result in different stable isotope ratios. While C fixed by the Symbiodiniaceae is mostly comprised out of dissolved inorganic carbon (DIC) from the surrounding seawater ($\delta^{13}\text{C}$ DIC = $0\text{ }‰$)^{63,64}, C acquired via heterotrophic feeding on plankton has a different $\delta^{13}\text{C}$ value (e.g. $\delta^{13}\text{C}$ zoop = $-19\text{ }‰$ or more negative^{65,66}). Therefore, $\delta^{13}\text{C}$ values vary proportionately to the contribution of either photosynthates or heterotrophic feeding as the main C source for the coral⁶⁷⁻⁷². The same applies to $\delta^{15}\text{N}$ values, which are used to determine whether the corals are getting their N mainly from dinitrogen (N_2) fixation of atmospheric N_2 ($\delta^{15}\text{N} = 0\text{ }‰$)⁷³, which decreases the values⁷⁴. Or if the coral is getting its N from other sources like sewage- and tourism-derived nutrient loading⁷⁵, which increases the value with increasing uptake of anthropogenic N^{62,76}.

Statistical analysis

We carried out the statistical analysis using RStudio (Version 1.4.1106)⁷⁷ with the packages *tidyverse*⁷⁸, *ggpubr*⁷⁹, and *rstatix*⁸⁰. As we used three separate tanks per treatment, we did not have a nested design and assume the tank effect to be zero for all statistical analyses. Additionally, all data was tested for

possible tank effects by inspecting it for significant differences between tanks in all measured water parameters, but none were detected. To test for significant effects of treatments over time in invasive parameters (protein content and elemental stoichiometry) we used the 2-way analyses of variance (ANOVA). Log-transformation of ratios was not conducted as the data was normally distributed. We tested repeated measurements (P_{gross} , and R) using a 2-way mixed ANOVA with 'Time' as within-subject factor and 'Treatment' as between-subject factor. First, we tested data sets for outliers and then tested normal distribution of the data using the Shapiro Wilk test and additionally qqplots for visual confirmation. We conducted 'Levene's test to test for homogeneity of variances, while we used 'Box's M-test for homogeneity of covariances. Thereby, sphericity was automatically tested with 'Mauchly's test and corrected when violated using the Greenhouse-Geisser sphericity correction. Lastly, we did a post-hoc analysis using pairwise comparison tests with Bonferroni adjustment with t -tests, and Dunn's test for non-parametric data. We considered results to be significant with a p -value lower than 0.05 ($p < 0.05$) and display them as mean \pm standard deviation.

4.4 Results

Effects on oxygen fluxes

Compared to baseline values both, P_{gross} values and R, remained stable under PO_4 enrichment and temperature increase, alone and combined. The growth of investigated coral colonies was around 0.14 – 0.30 polyps per day without any significant differences between treatments.

Under ambient conditions, *X. umbellata* colonies exhibited stable oxygen fluxes with P_{gross} and R values averaging 74 and -36 $\text{mg O}_2 \text{ m}^{-2} \text{ h}^{-1}$, respectively. Though the overall effect of PO_4 enrichment on P_{gross} values (Fig. 4.2) was not significant (2-way mixed ANOVA, $F_{(3, 8)} = 2.987$, $p = 0.096$), there was a significant difference between the P_{gross} values of colonies in the low and high PO_4 treatment in week 4 (pwc, Bonferroni adjustment, t -test, $p = 0.0386$). Additionally, P_{gross} values for all treatments varied significantly over time (2-way mixed ANOVA, $F_{(5, 40)} = 8.538$, $p < 0.001$) with highest values after 5 and lowest values after 2 weeks. When temperatures increased to 30 °C, colonies from the low PO_4 treatment had a P_{gross} rate 31 % higher than colonies from the high PO_4 treatment (91.5 and 63.2 $\text{mg O}_2 \text{ m}^{-2} \text{ h}^{-1}$, respectively). During the remaining days of the experiment, no significant treatment effects were observed, and all P_{gross} values were stable compared to baseline measurements throughout the experiment.

Respiration, just like P_{gross} values, was unaffected by PO_4 enrichment, as controls were not significantly different from PO_4 treated colonies, but showed significant differences over time (2-way mixed ANOVA, $F_{(1.34, 10.69)} = 9.308$, $p = 0.008$) with respiration rates being the lowest after two weeks of pure PO_4 enrichment (Fig. 4.2). However, while respiration increased during the stepwise temperature increase compared to values from week 2, with the highest values in weeks 4 and 5 (-38.215 and -38.899

mg O₂ m⁻² h⁻¹, respectively), it did not significantly change compared to baseline values (-37.648 mg O₂ m⁻² h⁻¹).

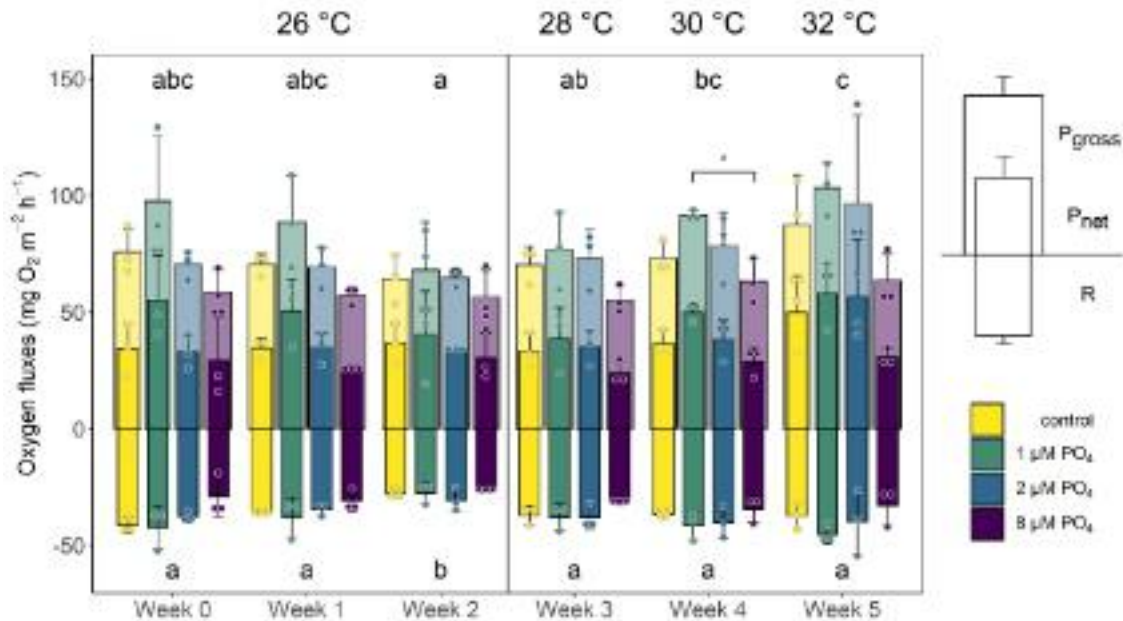


Figure 4.2. Gross- (P_{gross}), net photosynthesis (P_{net}), and respiration (R) of *Xenia umbellata* under experimental conditions: only temperature increase without PO_4 addition (control), 1 μM PO_4 + temperature increased from week 3 onwards (1 μM PO_4), 2 μM PO_4 + temperature increased (2 μM PO_4), and 8 μM PO_4 + temperature increased (8 μM PO_4). Letters indicate significant differences for P_{gross} and R between weeks and asterisks indicate significant differences between treatments per time ($p < 0.05$, pairwise comparison t -test, Bonferroni adjustment). Error bars represent standard deviations. Dots represent the individually measured data points. The vertical line indicates the start of the temperature treatment and the average temperature for all tanks for the different time points is given on top of the graph. Raw data is available in [Supplementary Table S4.2](#).

Effects on protein content

Protein content did not change between different PO_4 enrichment treatments but changed over time and with increasing temperatures.

Protein content in *X. umbellata* colonies (Fig. 4.3, [Supplementary Fig. S4.3](#)) changed significantly between PO_4 enrichment (2-way mixed ANOVA, $F_{(3,24)} = 3.076$, $p = 0.047$) and over time (2-way mixed ANOVA, $F_{(2,24)} = 174.187$, $p < 0.001$). The highest values were found in the baseline measurement with on average 20.2 μg protein g^{-1} coral DW. After two weeks of PO_4 enrichment alone, protein content significantly decreased by more than 50 % to 9.48 μg protein g^{-1} coral DW (pwc, Bonferroni adjustment, t -test, $p < 0.001$), and after the additional temperature increase, protein content dropped further down to 3.56 μg protein g^{-1} coral DW, which differed significantly from the two previous measurements (pwc, Bonferroni adjustment, t -test, $p < 0.001$). While there were no significant differences between PO_4 treatments at each time point, there were highly significant differences in each treatment over time, with the highest values always at the start and lowest values at the end of the experiment. Only the control and medium PO_4 treatment corals showed no further significant decline in protein content during the additional temperature increase in the last three weeks of the experiment.

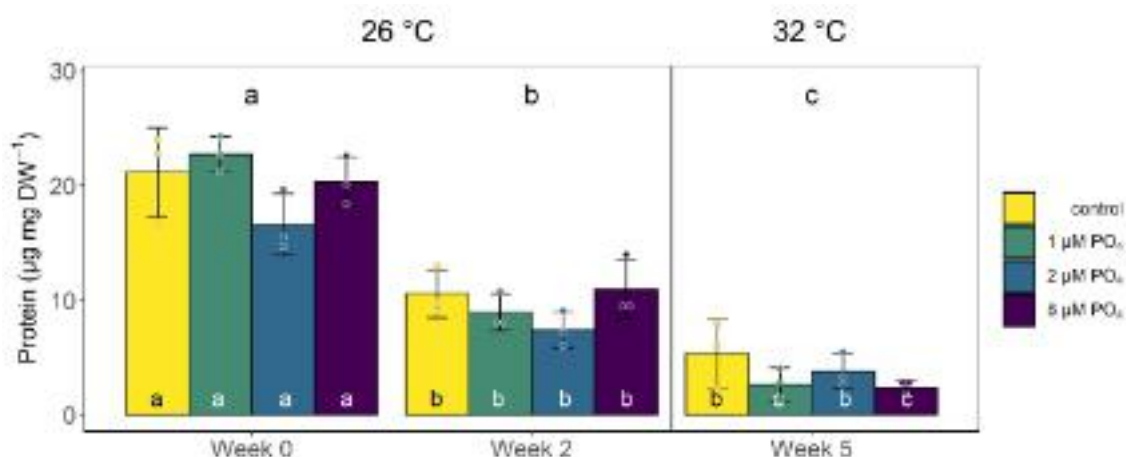


Figure 4.3. Protein content of *Xenia umbellata* colonies under experimental conditions: only temperature increase without PO₄ addition (control), 1 µM PO₄ + temperature increased from week 3 onwards (1 µM PO₄), 2 µM PO₄ + temperature increased (2 µM PO₄), and 8 µM PO₄ + temperature increased (8 µM PO₄). Letters above bars indicate significant differences between weeks and letters within bars indicate significant differences within the treatment over time ($p < 0.05$, pairwise comparison t -test, Bonferroni adjustment). Error bars represent standard deviations. Dots represent the individually measured data points. The vertical line indicates the start of the temperature treatment and the average temperature for all tanks for the different time points is given on top of the graph. Raw data is available in [Supplementary Table S4.2](#).

Effects on stable isotope signatures

All tested stable isotope signatures remained stable between different PO₄ enrichment treatments throughout the experiment and were only significantly affected by time and the stepwise temperature increase.

The $\delta^{15}\text{N}$, as well as $\delta^{13}\text{C}$ values, changed significantly over time (2-way ANOVA, $\delta^{15}\text{N}$: $F_{(2,24)} = 5.957, p = 0.008$; $\delta^{13}\text{C}$: $F_{(2,24)} = 18.212, p < 0.001$) (Fig. 4.4a & b). While $\delta^{15}\text{N}$ values (Fig. 4.4b) stayed constant at a level of 7.5 ‰ within the first two weeks of pure PO₄ enrichment, they decreased significantly by 10 ‰ over the stepwise temperature increase compared to the baseline (pwc, Bonferroni adjustment, Dunn's test, $p = 0.0112$). The $\delta^{13}\text{C}$ values (Fig. 4.4a) also decreased significantly during the temperature increase by 6.9 and 4.3 ‰ compared to baseline and the values after two weeks of PO₄ treatment ($p < 0.001$ and $p = 0.0018$, respectively).

The C content of the coral colonies showed no significant differences, while percent N content significantly changed over time (2-way ANOVA, $F_{(2,23)} = 11.212, p < 0.001$) (Fig. 4.4c & d). The values decreased by 14 ‰ within the first two weeks of the experiment compared to the baselines ($p < 0.001$) and returned close to starting values of 3.1 ‰ N again after the stepwise temperature increase. These differences in percent N content then lead to a significant difference in the total C:N ratio over time (2-way ANOVA, $F_{(2,24)} = 8.863, p = 0.001$) (Fig. 4.4e). The C:N ratio after two weeks of PO₄ enrichment was on average 6.9 ‰ higher and significantly different from the ratios at the start and end of the experiment ($p < 0.001$ and $p = 0.0137$, respectively).

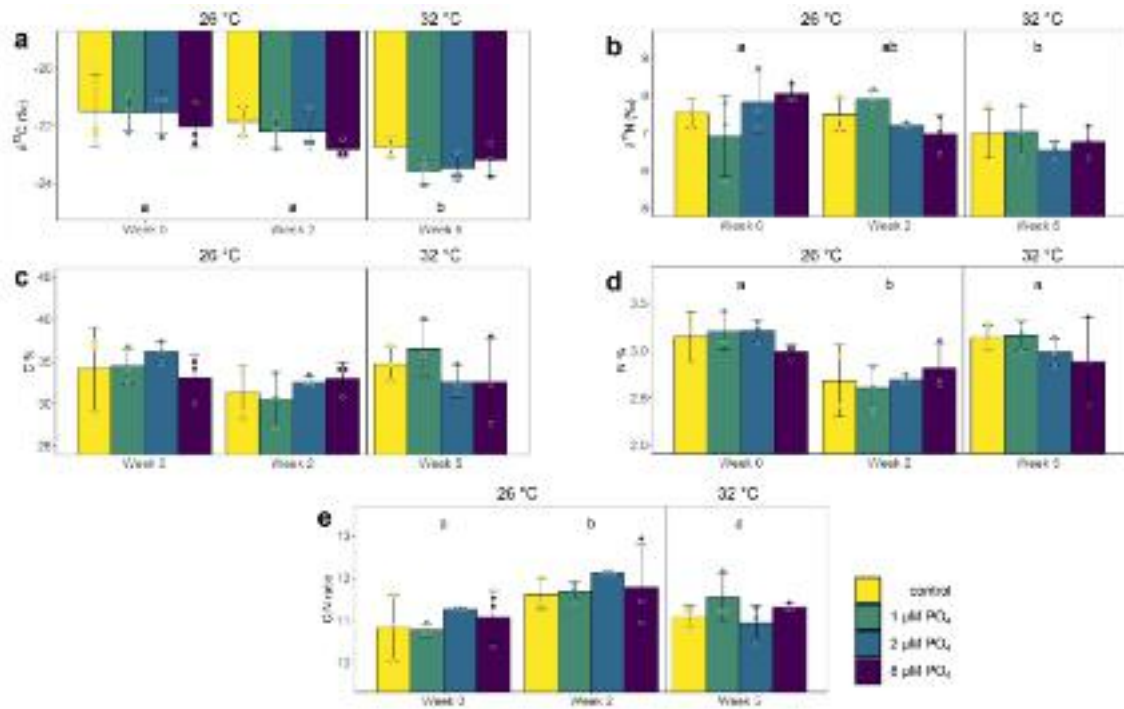


Figure 4.4. Carbon (a), and Nitrogen (b) stable isotope ratio, percent carbon (c), percent nitrogen (d), and carbon to nitrogen ratio (e) of *Xenia umbellata* colonies under experimental phosphate conditions: only temperature increase without PO_4 addition (control), $1 \mu\text{M PO}_4$ + temperature increased from week 3 onwards ($1 \mu\text{M PO}_4$), $2 \mu\text{M PO}_4$ + temperature increased ($2 \mu\text{M PO}_4$), and $8 \mu\text{M PO}_4$ + temperature increased ($8 \mu\text{M PO}_4$). Letters indicate significant differences between weeks ($p < 0.05$, pairwise comparison t -test, Bonferroni adjustment). Error bars represent standard errors. Dots represent the individually measured data points. The vertical line indicates the start of the temperature treatment and the average temperature for all tanks for the different time points is given on top of the graph. Raw data is available in [Supplementary Table S4.2](#).

4.5 Discussion

While hard coral cover decreases on reefs worldwide^{81–85}, a shift to other benthic organisms, such as soft corals, can be observed^{38,39}. As such, we tested the (combined) effects of two potentially stressful factors, i.e., PO_4 enrichment and warming, on the pulsating soft coral *X. umbellata*. Our results suggest a high tolerance of *X. umbellata* towards increasing temperatures, regardless of PO_4 enrichment.

How does PO_4 enrichment affect *X. umbellata*?

In general, no significant differences between *X. umbellata* in the control and PO_4 treatment groups were observed throughout the experiment, showing that PO_4 had no measurable effect on the coral in the observed parameters. Compared to hard corals, soft corals have lower photosynthetic productivity, observable in their respective $\text{P}_{\text{gross}}/\text{R}$ ratio of 1.0-1.3, while hard corals range within a $\text{P}_{\text{gross}}/\text{R}$ ratio of 2-4^{60,86}. Light intensity may have played a role, too. Mergner & Svoboda⁸⁶ measured oxygen fluxes of soft and hard corals from the same location, thereby reducing the effect of light intensity as far as possible. Also, Fabricius & Klumpp⁶⁰ acknowledged this possible limitation when comparing oxygen fluxes from different studies in their discussion. When comparing the absolute values for P_{gross} and R of studies on *X. umbellata*, P_{gross} values reach 22 up to $140 \text{ mg O}_2 \text{ m}^{-2} \text{ h}^{-1}$, while respiration ranges between

- 11 and - 60 mg O₂ m⁻² h⁻¹. Despite this range, with a P_{gross}/R ratio of around 2 measured in this study and previously^{47,49,52}, *X. umbellata* has higher photosynthetic productivity compared to other soft corals but is still at the lower edge of productivity compared to hard corals. The measured oxygen fluxes in our experiment remained stable under all added PO₄ concentrations. These results are in contrast with a study by Bednarz et al.⁵², which showed increased gross photosynthesis in xeniids under PO₄ enrichment, most likely due to increased chlorophyll *a* (chl *a*) concentrations. Our results also show that throughout the experiment the protein content significantly decreased in all colonies, regardless of PO₄ enrichment. Particularly the decrease in protein content over the first two weeks without warming was surprising, as the corals have not faced a specific stressor and did not show increased respiration rates, which would indicate an increased energy demand. While *X. umbellata* can live autotrophically⁸⁷, it is a heterotrophic suspension feeder⁸⁸. So, this reduction in protein content indicates that *X. umbellata* metabolised its protein energy reserves, probably as a result of reduced heterotrophy during the experiment, as they were only fed twice a week with dried zooplankton.

How does PO₄ enrichment affect the response of *X. umbellata* to a temperature increase?

*Warming does not disrupt oxygen fluxes in *X. umbellata**

While direct evidence showing that *X. umbellata* experiences PO₄ starvation under warming scenarios, as hypothesized for hard corals by Wiedenmann et al.²⁶, is missing in our study, we here show that PO₄ enrichment does not affect the corals tolerance towards warming. Overall, the measured oxygen fluxes in our experiment and respectively the P_{gross}/R ratio remained stable around 2 in response to warming, regardless of PO₄ enrichment. The P_{gross}/R ratio above 1 indicates that *X. umbellata* can sustain its energy needs via net autotrophy and does not necessarily rely on heterotrophic feeding to meet their daily metabolic demands⁸⁹. These results are surprising at first, as warming increases the respiration of hard corals as a sign of stress and increased energy demand^{27,90}. At the same time, a general decrease in photosynthesis was often observed when temperatures exceeded 31 °C, due to a damaged photosystem II during temperature stress^{14,91,92} or as a result of decreased Symbiodiniaceae density or their chl *a* concentrations⁹³. A possible explanation for the constant photosynthesis rates observed in the present study may be the special characteristic of *X. umbellata* being a pulsating coral⁹⁴. Pulsation is known to have a positive effect on the corals' photosynthetic activity, as it enhances gas exchange, leading to a greater efflux of oxygen from the coral tissues and increases the photosynthetic activity^{35,94}. Additionally, the constant water movement may alleviate the coral from high temperature stress as fresh seawater is constantly circulating around the polyps, avoiding the build-up of a heated boundary layer. This may have enabled the corals used in the present study to sustain their photosynthetic efficiency even under warming scenarios. An experiment observing the effects of NO₃ enrichment under warming on *X. umbellata*⁴⁹ found that NO₃ enrichment decreased P_{gross} rates, possibly due to the reduced pulsation of the polyps. Lastly, Simancas-Giraldo et al.⁴⁷ found that *X. umbellata* colonies exhibit both reduced

P_{gross} and R under warming, regardless of additional glucose enrichment. The authors argued that the reduced respiration rates may be a result of an explicit metabolic depression.

Warming leads to a significant decrease in protein content, $\delta^{15}\text{N}$, and $\delta^{13}\text{C}$

The protein content continued to significantly decrease over time with increasing temperature. This may contradict other studies, which showed that water temperature did not affect the protein content of the hard corals *Stylophora pistillata*⁹⁵ and *Turbinaria reniformis*⁹³. Yet, it could also be an effect of time and not temperature specifically, as protein content already significantly declined without increased temperatures, showing that *X. umbellata* metabolizes its energy reserves in the experimental setup. Additionally, total N content went back to baseline values under increased temperatures, regardless of PO_4 treatment. A possible explanation could be that the higher temperatures led to increased N_2 fixation, as shown in several studies on hard corals^{96–99}, and therefore higher N availability and incorporation of it in the tissue of the holobiont. This hypothesis is supported by the decrease in $\delta^{15}\text{N}$ as this could be a sign of increased N_2 fixation⁷⁴. Increased N_2 fixation may relieve the Symbiodiniaceae from N-limitation. In combination with retaining their photosynthates for themselves, these conditions may allow the Symbiodiniaceae to grow, leaving the host with less organic C, as demonstrated for the hard coral species *Stylophora pistillata*²⁷. This hypothesis is supported by the parallel study of Klinke et al. (unpublished)¹⁰⁰, who showed increased algal cell densities under higher temperatures. However, a recent study by Rådecker et al.¹⁰¹ shows that diazotrophs derived N may not be utilized by the Symbiodiniaceae under heat stress. Yet, as the coral is catabolizing its protein reserves, N is also released and becomes available. As *X. umbellata* seems to be rather tolerant toward increased temperatures, the alleviation from N-limitation may be due to N_2 fixation, or N from the proteins, or a combination of both.

In the present study, both $\delta^{15}\text{N}$ and $\delta^{13}\text{C}$ significantly decreased from the start of the experiment until the end after five weeks of PO_4 enrichment and additional warming, regardless of the PO_4 treatment. A decrease in $\delta^{13}\text{C}$ is often a sign that less photosynthates are shared with the host organism who then, in turn, relies more on heterotrophic feeding, as zooplankton is depleted of the heavier ^{13}C isotope^{102,103}. However, in our study, we did not observe a change in oxygen fluxes, therefore fewer photosynthates are unlikely to be the reason for this decrease. A possible explanation could be that 1) the corals preferentially catabolized isotopically heavier organic matter, therefore reducing the $\delta^{13}\text{C}$ value⁵⁵. For example, bleached corals have reduced photosynthesis and catabolize heavier-isotope lipids, which overall depletes the lipid $\delta^{13}\text{C}$ ⁷⁰. In the present study, the corals gradually lost their protein content, suggesting that at the same time isotopically heavier lipids may have been catabolized. Tanaka et al.⁵⁵ suggest the same pathway as an explanation for the depletion of $\delta^{13}\text{C}$ in their corals experiencing pure NO_3 enrichment, implying that corals under imbalanced N:P ratios consume more lipids than corals under balanced N:P ratios. Another possible explanation for a decrease in $\delta^{13}\text{C}$ may be 2) a net release of Symbiodiniaceae derived photosynthates into the water column, thereby shifting the $\delta^{13}\text{C}$ value.

While the results of measured total organic carbon (TOC) concentrations in the water during the incubation for oxygen fluxes were obscured by high standard deviation and background fluxes, a net release of TOC was observed for colonies under PO_4 enrichment (see [Supplementary Fig. S4.1](#)). Lastly, an alternative explanation could be 3) the metabolization of the added marine zooplankton (reef roids) in the tanks' sediment. Thereby, the reef roids may have altered the isotopic composition of the available CO_2 in the tank which was then used by the corals for photosynthesis thereby causing the more negative $\delta^{13}\text{C}$ through a secondary pathway.

Ecological implications

Despite soft corals' growing importance due to phase shifts and their increasing abundance on reefs worldwide, there is a knowledge gap on how the simultaneously occurring alterations in the seawater N:P ratio and ocean warming scenarios affect soft coral species. Since 64 % of all reefs are located near the shoreline of densely populated areas, they are more likely to be exposed to high inputs of inorganic nutrients in the water from human activities^{26,104,105}. Groundwater percolation and submarine groundwater discharge is likely a major source of nutrient input on reefs^{50,106,107}. Combined with ocean warming, this can have detrimental effects on hard corals^{26,108}.

Compared to studies conducted with hard corals looking at either nutrient enrichment or temperature increase ([Supplementary Table S4.1](#)), it becomes clear that *X. umbellata* is relatively unaffected by these factors. In [Supplementary Table S4.1](#) it is shown that warming above 2.5 °C led to lowered P_{gross} , increased R and consequently reduced P/R ratios in 85 % of species observed. Also, Fv/Fm, a proxy of photosynthetic activity, decreased in 6 of 7 observed species. Additionally, protein content was reduced in half of the observed species, indicating a need for using energy reserves under increased temperatures. While generally less studies focus on the effects of PO_4 enrichment compared to temperature increase, only two studies combined these two factors. One of these two studies showed that *Stylophora pistillata* had reduced Fv/Fm and P_{net} under temperature increase and nutrient enrichment, respectively, leaving the authors to hypothesize that eutrophication may compromise the corals resilience to global change¹⁰⁹. While the other study showed that *Pocillopora damicornis* had increased R under warming, even more pronounced when combined with PO_4 enrichment, and decreased P_{gross} rates⁵⁴.

With *X. umbellata* being able to live autotrophically⁸⁷, and not showing any changes in P_{gross} and R values under warming and PO_4 enriched conditions, this would imply their resistance towards these two factors, even under extended periods. Nevertheless, our study indicates that *X. umbellata* had to utilize its energy reserves during the course of the experiment. Thobor et al.⁴⁹ found a significant decrease in P_{gross} of *X. umbellata* under nitrate enrichment, but no significant changes under temperature increase. The combination of both factors led to severe declines in polyp pulsation, increased tissue loss, and mortality. This indicates that while *X. umbellata* is resistant towards warming, nitrate enrichment may reduce this resistance, potentially by disrupting the symbiosis between the coral host and its

Symbiodiniaceae, as was found for hard corals²⁶. This scenario would lead to a higher dependence of the coral on heterotrophic feeding.

While hard corals from the northern Red Sea show a net release of particulate organic matter (POM)¹¹⁰, *X. umbellata* showed net POM uptake⁵². Such coral-derived POM plays an essential role in the recycling of nutrients in reef ecosystems¹¹¹. With *X. umbellata* not contributing to POM release, but instead actively taking up the organic matter, this may have implications for reef C cycling under shifts towards soft coral dominance due to their invasiveness. But not only C cycling may change in soft coral dominated reefs, but also N cycling. In this context, a study of El-Khaled et al.⁴¹ speculated that soft corals, i.e. *Xenia* sp., can help alleviate reefs from excessive N, as they may play a key role in reef-wide denitrification. Future studies should therefore conduct further investigations into the metabolism of *X. umbellata* to help clarify under which scenarios this functional autotroph changes to a mixotrophic strategy, to what extent, and how this may affect overall energy and nutrient budgets on future reefs.

4.6 Author contributions

All authors conceived and designed the experiment. S.D.M. and A.K. conducted the experiment. S.D.M. processed samples, analysed and visualized the data, and wrote the manuscript with significant contributions of all authors. All authors read and approved the final manuscript.

4.7 Acknowledgments

We want to thank Ulrich Struck from the stable isotope facility at Free University of Berlin, Germany, for his sample preparation and analysis support. This study was supported by baseline funds of Marine Ecology Department of the University of Bremen, Germany, and DFG grant Wi 2677/16-1.

4.8 References

1. Moberg, F. & Folke, C. Ecological goods and services of coral reef ecosystems. *Ecol. Econ.* **29**, 215–233 (1999).
2. Woodhead, A. J., Hicks, C. C., Norström, A. V., Williams, G. J. & Graham, N. A. J. Coral reef ecosystem services in the Anthropocene. *Funct. Ecol.* **33**, 1023–1034 (2019).
3. Hughes, T. P. *et al.* Coral reefs in the Anthropocene. *Nature* **546**, (2017).
4. Hughes, T. P., Kerry, J. T. & Simpson, T. Large-scale bleaching of corals on the Great Barrier Reef. *Ecology* **99**, 501 (2017).
5. Anthony, K. R. N., Kline, D. I., Diaz-Pulido, G., Dove, S. & Hoegh-Guldberg, O. Ocean acidification causes bleaching and productivity loss in coral reef builders. *PNAS* **105**, 17442–17446 (2008).

6. Courtial, L., Roberty, S., Shick, J. M., Houlbrèque, F. & Ferrier-Pagès, C. Interactive effects of ultraviolet radiation and thermal stress on two reef-building corals. *Limnol. Oceanogr.* **62**, 1000–1013 (2017).
7. Jessen, C. *et al.* In-situ effects of eutrophication and overfishing on physiology and bacterial diversity of the Red Sea coral *Acropora hemprichii*. *PLoS One* **8**, (2013).
8. Jessen, C., Roder, C., Villa Lizcano, J. F., Voolstra, C. R. & Wild, C. In-situ effects of simulated overfishing and eutrophication on benthic coral reef algae growth, succession, and composition in the Central Red Sea. *PLoS One* **8**, (2013).
9. Fabricius, K. E. Effects of terrestrial runoff on the ecology of corals and coral reefs: review and synthesis. *Mar. Pollut. Bull.* **50**, 125–146 (2005).
10. Hughes, T. P. *et al.* Climate change, human impacts, and the resilience of coral reefs. *Science.* **301**, 929–933 (2003).
11. Fabricius, K. E., Cséke, S., Humphrey, C. & De'ath, G. Does trophic status enhance or reduce the thermal tolerance of scleractinian corals? A review, experiment and conceptual framework. *PLoS One* **8**, (2013).
12. McLachlan, R. H., Price, J. T., Solomon, S. L. & Grottoli, A. G. Thirty years of coral heat-stress experiments: a review of methods. *Coral Reefs 2020 394* **39**, 885–902 (2020).
13. Fabricius, K. E. Factors determining the resilience of coral reefs to eutrophication: a review and conceptual model. in *Coral Reefs: An Ecosystem in Transition* (eds. Dubinsky, Z. & Stambler, N.) (Springer, 2011).
14. Tilstra, A. *et al.* Light induced intraspecific variability in response to thermal stress in the hard coral *Stylophora pistillata*. *PeerJ* (2017).
15. Connolly, S. R., Lopez-Yglesias, M. A. & Anthony, K. R. N. Food availability promotes rapid recovery from thermal stress in a scleractinian coral. *Coral Reefs* **31**, 951–960 (2012).
16. Coles, S. L. & Brown, B. E. Coral bleaching - capacity for acclimatization and adaptation. advances in marine biology. *Adv. Mar. Biol.* **46**, 183-223 (2003).
17. Rosenberg, E., Koren, O., Reshef, L., Efrony, R. & Zilber-Rosenberg, I. The role of microorganisms in coral health, disease and evolution. *Nat. Rev. Microbiol.* **5**, 355–362 (2007).
18. Szmant, A. M. Nutrient enrichment on coral reefs: Is it a major cause of coral reef decline? *Estuaries* **25**, 743–766 (2002).
19. Atkinson, M. J., Carlson, B. & Crow, G. L. Coral growth in high-nutrient, low-pH seawater: a case study of corals cultured at the Waikiki Aquarium, Honolulu, Hawaii. *Coral Reefs* **14**, 215–223 (1995).
20. Bongiorno, L., Shafir, S., Angel, D. & Rinkevich, B. Survival, growth and gonad development of two hermatypic corals subjected to in situ fish-farm nutrient enrichment. *Mar. Ecol. Prog. Ser.* **253**, 137–144 (2003).

21. Grigg, R. W. Coral reefs in an urban embayment in Hawaii: a complex case history controlled by natural and anthropogenic stress. *Coral Reefs* **14**, 253–266 (1995).
22. Fabricius, K. E. & De'ath, G. Identifying ecological change and its causes: a case study on coral reefs. *Ecol. Appl.* **14**, 1448–1465 (2004).
23. Ferrier-Pagès, C., Gattuso, J. P., Dallot, S. & Jaubert, J. Effect of nutrient enrichment on growth and photosynthesis of the zooxanthellate coral *Stylophora pistillata*. *Coral Reefs* **19**, 103–113 (2000).
24. Rosset, S., Wiedenmann, J., Reed, A. J. & D'Angelo, C. Phosphate deficiency promotes coral bleaching and is reflected by the ultrastructure of symbiotic dinoflagellates. *Mar. Pollut. Bull.* **118**, 180–187 (2017).
25. Ban, S. S., Graham, N. A. J. & Connolly, S. R. Evidence for multiple stressor interactions and effects on coral reefs. *Glob. Chang. Biol.* **20**, 681–697 (2014).
26. Wiedenmann, J. *et al.* Nutrient enrichment can increase the susceptibility of reef corals to bleaching. *Nat. Clim. Chang.* **3**, 160–164 (2012).
27. Rådecker, N. *et al.* Heat stress destabilizes symbiotic nutrient cycling in corals. *PNAS* **118**, (2021).
28. LaJeunesse, T. C. *et al.* Systematic revision of symbiodiniaceae highlights the antiquity and diversity of coral endosymbionts. *Curr. Biol.* **28**, 2570–2580 (2018).
29. Falkowski, P. G., Dubinsky, Z., Muscatine, L. & McCloskey, L. Population control in symbiotic corals - ammonium ions and organic materials maintain the density of zooxanthellae. *Bioscience* **43**, 606–611 (1993).
30. Muscatine, L. & Pool, R. R. Regulation of numbers of intracellular algae. *Proc. R. Soc. London. Ser. B, Biol. Sci.* **204**, 131–139 (1979).
31. Muller-Parker, G., D'Elia, C. F. & Cook, C. B. Interactions between corals and their symbiotic algae. *Coral Reefs Anthr.* 99–116 (2015).
32. Rådecker, N., Pogoreutz, C., Voolstra, C. R., Wiedenmann, J. & Wild, C. Nitrogen cycling in corals: the key to understanding holobiont functioning? *Trends Microbiol.* **23**, 490–497 (2015).
33. Steinberg, R. K., Dafforn, K. A., Ainsworth, T. & Johnston, E. L. Know thy anemone: a review of threats to octocorals and anemones and opportunities for their restoration. *Front. Mar. Sci.* **7**, 590 (2020).
34. Inoue, S., Kayanne, H., Yamamoto, S. & Kurihara, H. Spatial community shift from hard to soft corals in acidified water. *Nat. Clim. Chang.* **3**, 683–687 (2013).
35. Wild, C. & Naumann, M. S. Effect of active water movement on energy and nutrient acquisition in coral reef-associated benthic organisms. *PNAS* **110**, 8767–8768 (2013).
36. Fox, H. E., Pet, J. S., Dahuri, R. & Caldwell, R. L. Recovery in rubble fields: long-term impacts of blast fishing. *Mar. Pollut. Bull.* **46**, 1024–1031 (2003).

37. Benayahu, Y. & Loya, Y. Settlement and recruitment of a soft coral : why is *Xenia macrospiculata* a successful colonizer? *Bull. Mar. Sci.* **36**, 177–188 (1985).
38. Norström, A. V., Nyström, M., Lokrantz, J. & Folke, C. Alternative states on coral reefs: beyond coral-macroalgal phase shifts. *Mar. Ecol. Prog. Ser.* **376**, 293–306 (2009).
39. Reverter, M., Helber, S. B., Rohde, S., De Goeij, J. M. & Schupp, P. J. Coral reef benthic community changes in the Anthropocene: biogeographic heterogeneity, overlooked configurations, and methodology. *Glob. Chang. Biol.* **28**, 1956–1971 (2022).
40. Karcher, D. B. *et al.* Nitrogen eutrophication particularly promotes turf algae in coral reefs of the central Red Sea. *PeerJ* **2020**, 1–25 (2020).
41. El-Khaled, Y. C. *et al.* Nitrogen fixation and denitrification activity differ between coral- and algae-dominated Red Sea reefs. *Sci. Reports 2021 III* **11**, 1–15 (2021).
42. Ruiz-Allais, J. P., Benayahu, Y. & Lasso-Alcalá, O. M. The invasive octocoral *Unomia stolonifera* (Alcyonacea, Xeniidae) is dominating the benthos in the Southeastern Caribbean Sea. *Mem. la Fund. La Salle Ciencias Nat.* **79**, 63–80 (2021).
43. Ruiz Allais, J. P., Amaro, M. E., McFadden, C. S., Halász, A. & Benayahu, Y. The first incidence of an alien soft coral of the family Xeniidae in the Caribbean, an invasion in eastern Venezuelan coral communities. *Coral Reefs* **33**, 287 (2014).
44. Baum, G., Januar, I., Ferse, S. C. A., Wild, C. & Kunzmann, A. Abundance and physiology of dominant soft corals linked to water quality in Jakarta Bay, Indonesia. *PeerJ* **2016**, 1–29 (2016).
45. Menezes, N. M. *et al.* New non-native ornamental octocorals threatening a South-west Atlantic reef. *J. Mar. Biol. Assoc. United Kingdom* 1–7 (2022).
46. Mantelatto, M. C., Silva, A. G. da, Louzada, T. dos S., McFadden, C. S. & Creed, J. C. Invasion of aquarium origin soft corals on a tropical rocky reef in the southwest Atlantic, Brazil. *Mar. Pollut. Bull.* **130**, 84–94 (2018).
47. Simancas-Giraldo, S. M. *et al.* Photosynthesis and respiration of the soft coral *Xenia umbellata* respond to warming but not to organic carbon eutrophication. *PeerJ* **9:e11663**, (2021).
48. Vollstedt, S., Xiang, N., Simancas-Giraldo, S. M. & Wild, C. Organic eutrophication increases resistance of the pulsating soft coral *Xenia umbellata* to warming. *PeerJ* **2020**, 1–16 (2020).
49. Thobor, B. *et al.* The pulsating soft coral *Xenia umbellata* shows high resistance to warming when nitrate concentrations are low. *Sci. Rep.* **12**, (2022).
50. Costa, O. S., Leão, Z. M. A. N., Nimmo, M. & Attrill, M. J. Nutrification impacts on coral reefs from northern Bahia, Brazil. *Hydrobiologia* **440**, 307–315 (2000).
51. Fleury, B. G., Coll, J. C., Tentori, E., Duquesne, S. & Figueiredo, L. Effect of nutrient enrichment on the complementary (secondary) metabolite composition of the soft coral *Sarcophyton ebrenbergi* (Cnidaria: Octocorallia: Alcyonaceae) of the Great Barrier Reef. *Mar. Biol.* **136**, 63–68 (2000).

52. Bednarz, V. N., Naumann, M. S., Niggel, W. & Wild, C. Inorganic nutrient availability affects organic matter fluxes and metabolic activity in the soft coral genus *Xenia*. *J. Exp. Biol.* **215**, 3672–3679 (2012).
53. Bruno, J. F., Petes, L. E., Harvell, C. D. & Hettinger, A. Nutrient enrichment can increase the severity of coral diseases. *Ecol. Lett.* **6**, 1056–1061 (2003).
54. Ezzat, L., Maguer, J.-F. F., Grover, R. & Ferrier-Pagès, C. Limited phosphorus availability is the Achilles heel of tropical reef corals in a warming ocean. *Sci. Rep.* **6**, 1–11 (2016).
55. Tanaka, Y., Grottoli, A. G., Matsui, Y., Suzuki, A. & Sakai, K. Effects of nitrate and phosphate availability on the tissues and carbonate skeleton of scleractinian corals. *Mar. Ecol. Prog. Ser.* **570**, 101–112 (2017).
56. Liu, G., Strong, A. E., Skirving, W. & Arzayus, L. F. Overview of NOAA coral reef watch program's near-real time satellite global coral bleaching monitoring activities. in *Proc. 10th Int. Coral Reef Symp.* 1783–1793 (2006).
57. Bellworthy, J. & Fine, M. Beyond peak summer temperatures, branching corals in the Gulf of Aqaba are resilient to thermal stress but sensitive to high light. *Coral Reefs* **36**, 1071–1082 (2017).
58. Rex, A., Montebon, F. & Yap, H. T. Metabolic responses of the scleractinian coral *Porites cylindrica* Dana to water motion. I. Oxygen flux studies. *J. Exp. Mar. Bio. Ecol.* **186**, 33–52 (1995).
59. Long, M. H., Berg, P., de Beer, D. & Zieman, J. C. *In situ* coral reef oxygen metabolism: an eddy correlation study. *PLoS One* **8**, e58581 (2013).
60. Fabricius, K. E. & Klumpp, D. W. Widespread mixotrophy in reef-inhabiting soft corals: the influence of depth, and colony expansion and contraction on photosynthesis. *Mar. Ecol. Prog. Ser.* **125**, 195–204 (1995).
61. Bradford, M. M. A rapid and sensitive method for the quantitation of microgram quantities of protein utilizing the principle of protein-dye binding. *Anal. Biochem.* **72**, 248–254 (1976).
62. Raimonet, M., Guillou, G., Mornet, F. & Richard, P. Macroalgae $\delta^{15}\text{N}$ values in well-mixed estuaries: indicator of anthropogenic nitrogen input or macroalgae metabolism? *Estuar. Coast. Shelf Sci.* **119**, 126–138 (2013).
63. Furla, P., Galgani, I., Durand, I. & Allemand, D. Sources and mechanisms of inorganic carbon transport for coral calcification and photosynthesis. *J. Exp. Biol.* **203**, 3445–3457 (2000).
64. Hughes, A. D., Grottoli, A. G., Pease, T. K. & Matsui, Y. Acquisition and assimilation of carbon in non-bleached and bleached corals. *Mar. Ecol. Prog. Ser.* **420**, 91–101 (2010).
65. Rau, G. H., Takahashi, T. & Des Marais, D. J. Latitudinal variations in plankton $\delta^{13}\text{C}$ - Implications for CO_2 and productivity in past oceans. *Nature* **341**, 516–518 (1989).
66. McMahon, K. W., Hamady, L. L. & Thorrold, S. R. A review of ecogeochemistry approaches to estimating movements of marine animals. *Limnol. Oceanogr.* **58**, 697–714 (2013).

67. Muscatine, L., Porter, J. W. & Kaplan, I. R. Resource partitioning by reef corals as determined from stable isotope composition. *Mar. Biol.* **100**, 185–193 (1989).
68. Swart, P. K. *et al.* The isotopic composition of respired carbon dioxide in scleractinian corals: Implications for cycling of organic carbon in corals. *Geochim. Cosmochim. Acta* **69**, 1495–1509 (2005).
69. Rodrigues, L. J. & Grottoli, A. G. Calcification rate and the stable carbon, oxygen, and nitrogen isotopes in the skeleton, host tissue, and zooxanthellae of bleached and recovering Hawaiian corals. *Geochim. Cosmochim. Acta* **70**, 2781–2789 (2006).
70. Grottoli, A. G. & Rodrigues, L. J. Bleached *Porites compressa* and *Montipora capitata* corals catabolize $\delta^{13}\text{C}$ -enriched lipids. *Coral Reefs* **30**, 687–692 (2011).
71. Levas, S. J., Grottoli, A. G., Hughes, A., Osburn, C. L. & Matsui, Y. Physiological and biogeochemical traits of bleaching and recovery in the mounding species of coral *Porites lobata*: implications for resilience in mounding corals. *PLoS One* **8**, 32–35 (2013).
72. Schoepf, V. *et al.* Annual coral bleaching and the long-term recovery capacity of coral. *Proc. R. Soc. B Biol. Sci.* **282**, (2015).
73. Lesser, M. P. *et al.* Nitrogen fixation by symbiotic cyanobacteria provides a source of nitrogen for the scleractinian coral *Montastraea cavernosa*. *Mar. Ecol. Prog. Ser.* **346**, 143–152 (2007).
74. Carpenter, E. J., Harvey, H. R., Brian, F. & Capone, D. G. Biogeochemical tracers of the marine cyanobacterium *Trichodesmium*. *Deep Sea Res. Part I Oceanogr. Res. Pap.* **44**, 27–38 (1997).
75. Lachs, L. *et al.* Effects of tourism-derived sewage on coral reefs: isotopic assessments identify effective bioindicators. *Mar. Pollut. Bull.* **148**, 85–96 (2019).
76. Kürten, B. *et al.* Influence of environmental gradients on C and N stable isotope ratios in coral reef biota of the Red Sea, Saudi Arabia. *J. Sea Res.* **85**, 379–394 (2014).
77. Core Team, R. R: A language and environment for statistical computing. R Foundation for Statistical Computing. (2020).
78. Wickham, H. *et al.* Welcome to the tidyverse. *J. Open Source Softw.* **4**, 1686 (2019).
79. Kassambara, A. ggpubr: ‘ggplot2’ based publication ready plots. R package version 0.4.0. (2020).
80. Kassambara, A. rstatix: pipe-friendly framework for basic statistical tests. R package version 0.7.0. (2021).
81. Contreras-Silva, A. I. *et al.* A meta-analysis to assess long-term spatiotemporal changes of benthic coral and macroalgae cover in the Mexican Caribbean. *Sci. Rep.* **10**, 1–12 (2020).
82. Ledlie, M. H. *et al.* Phase shifts and the role of herbivory in the resilience of coral reefs. *Coral Reefs* **26**, 641–653 (2007).
83. Kuffner, I. B. & Toth, L. T. A geological perspective on the degradation and conservation of western Atlantic coral reefs. *Conserv. Biol.* **30**, 706–715 (2016).

84. Hughes, T. P. Catastrophes, phase shifts, and large-scale degradation of a Caribbean coral reef. *Science* **265**, 1547–1551 (1994).
85. de Bakker, D. M., Meesters, E. H., Bak, R. P. M., Nieuwland, G. & van Duyl, F. C. Long-term shifts in coral communities on shallow to deep reef slopes of Curaçao and Bonaire: are there any winners? *Front. Mar. Sci.* **3**, 247 (2016).
86. Mergner, H. & Svoboda, A. Productivity and seasonal changes in selected reef areas in the Gulf of Aqaba (Red Sea). *Helgoländer Wissenschaftliche Meeresuntersuchungen* **30**, 383–399 (1977).
87. Schlichter, D., Svoboda, A. & Kremer, B. P. Functional autotrophy of *Heteroxenia fuscescens* (Anthozoa: Aleyonaria): carbon assimilation and translocation of photosynthates from symbionts to host. *Mar. Biol.* **78**, 29–38 (1983).
88. Al-Sofyani, A. A. & Niaz, G. R. A comparative study of the components of the hard coral *Seriatopora hystrix* and the soft coral *Xenia umbellata* along the Jeddah coast, Saudi Arabia. *Rev. Biol. Mar. Oceanogr.* **42**, 207–219 (2007).
89. McCloskey, L. R., Wethey, D. S. & Porter, J. W. Measurement and interpretation of photosynthesis and respiration in reef corals. in *Coral reefs: research methods*. (eds. Stoddart, D. R. & Johannes, R. E.) 379–396 (United Nations Educational, Scientific and Cultural Organization, 1978).
90. Baker, D. M., Freeman, C. J., Wong, J. C. Y., Fogel, M. L. & Knowlton, N. Climate change promotes parasitism in a coral symbiosis. *ISME J.* **12**, 921–930 (2018).
91. Hoegh-Guldberg, O. & Smith, G. J. The effect of sudden changes in temperature, light and salinity on the population density and export of zooxanthellae from the reef corals *Stylophora pistillata* Esper and *Seriatopora hystrix* Dana. *J. Exp. Mar. Bio. Ecol.* **129**, 279–303 (1989).
92. Iglesias-Prieto, R., Matta, J. L., Robins, W. A. & Trench, R. K. Photosynthetic response to elevated temperature in the symbiotic dinoflagellate *Symbiodinium microadriaticum* in culture. *Proc. Natl. Acad. Sci.* **89**, 10302–10305 (1992).
93. Béraud, E., Gevaert, F., Rottier, C. & Ferrier-Pagès, C. The response of the scleractinian coral *Turbinaria reniformis* to thermal stress depends on the nitrogen status of the coral holobiont. *J. Exp. Biol.* **216**, 2665–2674 (2013).
94. Kremien, M., Shavit, U., Mass, T. & Genin, A. Benefit of pulsation in soft corals. *Proc. Natl. Acad. Sci. U. S. A.* **110**, 8978–8983 (2013).
95. Grover, R. *et al.* Coral uptake of inorganic phosphorus and nitrogen negatively affected by simultaneous changes in temperature and pH. *PLoS One* **6**, 1–10 (2011).
96. Cardini, U. *et al.* Microbial dinitrogen fixation in coral holobionts exposed to thermal stress and bleaching. *Environ. Microbiol.* **18**, 2620–2633 (2016).
97. Cardini, U. *et al.* Functional significance of dinitrogen fixation in sustaining coral productivity under oligotrophic conditions. *Proc. R. Soc. B Biol. Sci.* **282**, (2015).

98. Santos, H. F. *et al.* Climate change affects key nitrogen-fixing bacterial populations on coral reefs. *ISME J.* **8**, 2272–2279 (2014).
99. Tilstra, A. *et al.* Relative diazotroph abundance in symbiotic Red Sea corals decreases with water depth. *Front. Mar. Sci.* **6**, 372 (2019).
100. Klinke, A. Impact of phosphate enrichment on the susceptibility of the pulsating soft coral *Xenia umbellata* to ocean warming. (2021).
101. Rådecker, N. *et al.* Heat stress reduces the contribution of diazotrophs to coral holobiont nitrogen cycling. *ISME J.* 1–9 (2021).
102. Swart, P. K., Saied, A. & Lamb, K. Temporal and spatial variation in the $\delta^{15}\text{N}$ and $\delta^{13}\text{C}$ of coral tissue and zooxanthellae in *Montastraea faveolata* collected from the Florida reef tract. *Limnol. Oceanogr.* **50**, 1049–1058 (2005).
103. Grottoli, A. G., Tchernov, D. & Winters, G. Physiological and biogeochemical responses of super-corals to thermal stress from the Northern Gulf of Aqaba, Red Sea. *Front. Mar. Sci.* **4**, (2017).
104. Dubinsky, Z. & Stambler, N. Marine pollution and coral reefs. *Glob. Chang. Biol.* **2**, 511–526 (1996).
105. Loya, Y., Lubinevsky, H., Rosenfeld, M. & Kramarsky-Winter, E. Nutrient enrichment caused by in situ fish farms at Eilat, Red Sea is detrimental to coral reproduction. *Mar. Pollut. Bull.* **49**, 344–353 (2004).
106. Costa, O. S., Nimmo, M. & Attrill, M. J. Coastal nutrification in Brazil: a review of the role of nutrient excess on coral reef demise. *J. South Am. Earth Sci.* **25**, 257–270 (2008).
107. Tait, D. R. *et al.* The influence of groundwater inputs and age on nutrient dynamics in a coral reef lagoon. *Mar. Chem.* **166**, 36–47 (2014).
108. Guan, Y., Hohn, S., Wild, C. & Merico, A. Vulnerability of global coral reef habitat suitability to ocean warming, acidification and eutrophication. *Glob. Chang. Biol.* **26**, 5646–5660 (2020).
109. Hall, E. R. *et al.* Eutrophication may compromise the resilience of the Red Sea coral *Stylophora pistillata* to global change. *Mar. Pollut. Bull.* **131**, 701–711 (2018).
110. Naumann, M. S. *et al.* Organic matter release by dominant hermatypic corals of the Northern Red Sea. *Coral Reefs* **29**, 649–659 (2010).
111. Wild, C. *et al.* Coral mucus functions as an energy carrier and particle trap in the reef ecosystem. *Nature* **428**, 66–70 (2004).

Chapter 5 | Short-term ocean acidification decreases pulsation and growth of the widespread soft coral *Xenia umbellata*

Chapter 5 | Short-term ocean acidification decreases pulsation and growth of the widespread soft coral *Xenia umbellata*

Arjen Tilstra^{1,*}, Lorena Braxator¹, **Bianca M. Thobor**¹, Selma D. Mezger¹, Claudia E.L. Hill¹, Yusuf C. El-Khaled^{1,#a}, Giulia Caporale¹, Sohyoung Kim^{1,#b}, Christian Wild¹

¹ Department of Marine Ecology, University of Bremen, Bremen, Germany

^{#a}Current Address: Marine Microbiomes Lab, King Abdullah University of Science and Technology (KAUST), Thuwal, Saudi Arabia

^{#b}Current Address: Department of Marine Biology and Ecology, University of Miami, Miami, Florida, United States of America

* Corresponding author: tilstra@uni-bremen.de

[#]These authors contributed equally to this work.

5.1 Abstract

Coral reefs may experience lower pH values as a result of ocean acidification (OA), which has negative consequences, particularly for calcifying organisms. Thus far, the effects of this global factor have been mainly investigated on hard corals, while the effects on soft corals remain relatively understudied. We therefore carried out a manipulative aquarium experiment for 21 days to study the response of the widespread pulsating soft coral *Xenia umbellata* to simulated OA conditions. We gradually decreased the pH from ambient (~8.3) to three consecutive 7-day long pH treatments of 8.0, 7.8, and 7.6, using a CO₂ dosing system. Monitored response variables included pulsation rate, specific growth rate, visual coloration, survival, Symbiodiniaceae cell densities and chlorophyll *a* content, photosynthesis and respiration, and finally stable isotopes of carbon (C) and nitrogen (N) as well as CN content. Pulsation decreased compared to controls with each consecutive lowering of the pH, i.e., 17 % at pH 8.0, 26 % at pH 7.8 and 32 % at pH 7.6, accompanied by an initial decrease in growth rates of ~60 % at pH 8.0, not decreasing further at lower pH. An 8.3 ‰ decrease of $\delta^{13}\text{C}$ confirmed that OA exposed colonies had a higher uptake and availability of atmospheric CO₂. Coral productivity, i.e., photosynthesis, was not affected by higher dissolved inorganic C availability and none of the remaining response variables showed any significant differences. Our findings suggest that pulsation is a phenotypically plastic mechanism for *X. umbellata* to adjust to different pH values, resulting in reduced growth rates only, while maintaining high productivity. Consequently, pulsation may allow *X. umbellata* to inhabit a broad pH range with minimal effects on its overall health. This resilience may contribute to the competitive advantage that soft corals, particularly *X. umbellata*, have over hard corals.

Keywords: soft coral, ocean acidification, global stressor, pulsation, phenotypic plasticity

An adapted version of this chapter has been published in *PLOS ONE* **18**, e0294470.

<https://doi.org/10.1371/journal.pone.0294470>

5.2 Introduction

Coral reefs are under threat from a variety of factors, including anthropogenically induced ocean acidification (OA)¹. Ocean acidification is characterized by a drop in pH caused by the increased dissolution of atmospheric CO₂ in ocean water². Since the start of industrialization and the subsequent increase of atmospheric CO₂ concentrations, the pH of the world's oceans has already decreased by 0.1 units and is currently at an average of 8.1^{3,4}. This value is expected to drop further by 0.3 to 0.4 units over the next 100 years^{5,6} if current CO₂ emissions persist. Simultaneously, because of the more acidic water, the aragonite saturation state decreases⁷, rendering calcifying organisms especially vulnerable⁸.

Scleractinian, or hard corals, i.e., the ecosystem engineers of coral reefs⁹, are an example of such. The effects of OA on hard corals are usually negative and can be direct, e.g., by reduced calcification rates^{10,11}, reduced sexual recruitment¹², reduced fixation of essential nitrogen by diazotrophs¹³, and increased macrobioerosion¹⁴, or indirect, e.g., from coral competition and (macro)algal interactions¹⁵. Some studies report high interspecific variability¹⁶ and severity¹⁷ in hard corals' responses, while others report short-term resistance¹⁸, or even positive effects by benefiting photophysiological measures¹⁹.

The focus of OA research has been primarily on hard corals while the second biggest taxon on coral reefs, i.e., soft corals, especially from tropical regions, are relatively overlooked. Soft corals may overtake reefs as the dominant taxon after die-offs of hard coral^{20–22, e.g., 23}. Despite the lower structural complexity that comes with soft coral dominance (compared to hard coral dominance), they may still provide important habitat to e.g., reef fishes^{24,25}. Some OA studies on tropical soft corals reported no negative effects on the corals' physiology^{26,27}, while others reported relatively minor negative effects^{28,29}. Gabay and colleagues^{26,27} suggested that the tissue of soft corals may act as a protective barrier against OA associated physiological and morphological change, i.e., the dissolution of calcium carbonate sclerites in their hydroskeleton. Ultimately, this may differentiate soft corals from hard corals in their response to OA.

Soft corals of the Xenidae family are particularly successful, both as native spreaders and non-native invaders^{30,31}. Because of their extensive vegetative reproduction with high growth rates, recruitment abilities, high fecundity, and extended annual planulation, these colony-forming soft corals often take over disturbed habitats^{32–34}. Like most hard corals, xeniids are photosymbiotic animals living in close association with endosymbiotic dinoflagellates of the family Symbiodiniaceae³⁵, which enables effective utilization and storage of nutrients and photosynthates (i.e., photosynthetically fixed carbon). Furthermore, the characteristic pulsating movement of some xeniid species effectively prevents refiltration by neighboring polyps through the induced upward movement of water³⁶, thereby increasing photosynthesis, heterotrophic feeding, and nutrient uptake³⁷. The pulsation of xeniids is not always consistent, however, and can change according to the environmental conditions the xeniid is exposed to^{38–40}. Pulsation may thus be used as a first indicator for environmental change.

The current study aimed to assess the effects of short-term OA on the physiology of the pulsating xeniid species *Xenia umbellata*. To do so, we investigated the ecological response of the coral holobiont based on pulsation rate, specific growth rate (SGR), visual coloration, survival, Symbiodiniaceae cell densities, chlorophyll *a* (chl. *a*) content, oxygen fluxes, carbon (C) and nitrogen (N) isotope signatures, and CN content. We hypothesized, based on previous research, that OA would increase the incorporation of lighter C isotopes due to higher atmospherically derived dissolved inorganic carbon (DIC) availability⁴¹, but that further response variables would remain unaffected^{e.g.,26}. However, in case C was the limiting factor for primary production, we hypothesized an increase in net photosynthesis and respiration⁴², followed by increased pulsation rates and holobiont C and N content.

5.3 Materials and Methods

Sample species, setup, and maintenance

Fragments of *X. umbellata* were taken from several mother colonies of the same genotype that have been cultured under stable conditions for several years in the aquarium facilities at the University of Bremen Marine Ecology department. This particular genotype was purchased at a retail shop in Germany and originally sampled in the Red Sea. Colonies from the main holding aquarium were fragmented following the plug mesh method by⁴³. In brief, colonies were cut into smaller 2 cm pieces and secured to a calcium carbonate plug (AF Plug Rocks, Aquaforest, Poland), creating a total of 132 fragments. Fragments were randomly distributed over 12 independent glass aquaria (60 L) on 40 x 20 cm plastic grids, with a minimum of 2 cm between each fragment, resulting in 11 fragments per aquarium.

Each aquarium was divided into 1) a technical part containing a heating element (EHEIM thermo control, 50W, EHEIM, Germany, accuracy ± 0.5 °C), which was sufficient to keep the water temperatures stable, a return pump for water circulation (EHEIM CompactOn 300 pump, EHEIM, Germany), and a pendant logger (HOBO pendant, Onset, USA, accuracy ± 0.5 °C) for constant measurements of temperature and light, and 2) an experimental part housing the corals. Both parts were separated by a glass wall with an overflow but had a consistent water exchange using the previously described return pump. The light was provided by LED lamps (Royal blue matrix module and ultra-white blue 1:3-matrix module WALTRON daytime) in a 12:12 h day-night cycle at a PAR intensity of ~ 100 $\mu\text{mol photons m}^{-2} \text{ s}^{-1}$. Tanks were filled with unfiltered artificial seawater, which was created by adding aquarium sea salt (Zoo Mix, Tropic Marin, Switzerland) in a barrel with demineralized water containing a heating element and circulation pump. Salinity and temperature were checked daily using a portable multimeter (HACH HQ40D portable multimeter, United States, accuracy ± 0.5). For salinity, a value of 35 ‰ was targeted, while temperature was kept at 25.7 ± 0.3 °C. Nitrate, nitrite, ammonium and phosphate were measured twice per week, calcium and magnesium were measured once per week, and alkalinity was tested daily using JBL TestLab Marin test kits. Water parameters (except for pH) of

all tanks were constantly maintained throughout the entire experiment (see Table 5.1). Biofouling on glass surfaces was removed regularly without physically disturbing the fragments.

Experimental design

The experiment was run for 21 days as previous research conducted with the same organisms resulted in reactions of response variables within this timeframe^{38,39}. Controls and OA treatments were each replicated in six aquaria ($n_{\text{treatment}} = 6$), randomly arranged in a three-level tower with four tanks per level to ensure equal representation.

Table 5.1 Mean \pm S.D. of water/environmental parameters maintained in all tanks. PAR = photosynthetically active radiation.

Parameter	Mean values (\pm SD)
Temperature	25.7 \pm 0.3 °C
Salinity	35.1 \pm 0.1 ‰
PAR	~100 $\mu\text{mol m}^{-2} \text{s}^{-1}$
Nitrate	< 0.5 ppm
Nitrite	< 0.01 ppm
Ammonium	< 0.05 ppm
Phosphate	< 0.02 ppm
Calcium	377 \pm 25 ppm
Magnesium	1327 \pm 72 ppm
Alkalinity	8 \pm 2 dKH

The acidification of the water took place in three stages by sequentially decreasing pH-levels from ambient, i.e., the pH of our holding tank: pH of $\sim 8.3 \pm 0.1$, to 8.0, 7.8, and finally to 7.6, each of which was maintained for a full week. According to the IPCC, pH 8.0 and 7.8 represent values that will be reached within the next decades under the RCP8.5 scenario⁶, while a pH of 7.6 is an even more extreme value than expected by IPCC scenarios.

The water within six aquaria was acidified using a CO₂ system (see Supplementary Figure S1) while maintaining stable alkalinity. A pH computer (NBS; pH computer set, Aqua Medic, accuracy 0.01 pH) was used to keep the pH stable. A CO₂ reactor (Aqua Medic) was used to dissolve CO₂ bubbles in the water. This reactor was connected via 4/6 mm tubing with fine needle valves and check valves to prevent backflow of water, a solenoid valve (M-valve Standard, Aqua Medic) for control, a CO₂ cylinder (Dupla), and a pressure reducer (Aqua Medic)⁴⁴.

Ecological assessments

To compare between treatments, pulsation, growth, coloration, survival, and oxygen fluxes were measured after each one-week period at a certain pH level, thus three times in total. Chlorophyll *a*, isotope signatures and CN content were only measured at the end of the experiment on day 21.

Pulsation rates

Polyp pulsation was counted for 30 seconds, and one pulsation was defined as the motion of a polyp from being fully closed to opened to closed again³⁹. The results were extrapolated to one minute to allow for comparisons with previous studies. For each tank, the pulsation of one polyp from three separate fragments, i.e., 36 fragments in total, the same fragments every week, was counted and averaged for further analysis. These three pseudo-replicates were averaged for statistical analyses, resulting in six tank replicates per treatment. The circulation pump of each respective tank was turned off 1 minute before the start of counting. Counting started approximately 10 minutes after the start of the light cycle in the morning to avoid differences due to circadian rhythms.

Specific growth rate

To estimate the SGR, all polyps of marked fragments were counted manually using tweezers while being submerged at all times to reduce further stress. Three colonies per aquarium were considered for SGR. These three pseudo-replicates were averaged for statistical analyses, resulting in six tank replicates per treatment. The SGR was calculated using [Formula 5.1](#)^{45,46}.

$$SGR(d^{-1}) = \frac{\ln P_t - \ln P_{t-1}}{\Delta t} \quad (\text{Formula 5.1})$$

P_t and P_{t-1} describe the final and the initial number of polyps, while Δt is the growth interval in days. The final growth rate unit is polyp polyp⁻¹ d⁻¹ which can be simplified to d⁻¹.

Visual coloration

A total of 12 colonies (one per tank) were examined weekly for visual coloration as an indicator of bleaching according to Thobor and colleagues³⁸. Briefly, photos were taken weekly with an Olympus TG6 underwater camera, with fixed manual settings (ISO 100, f/1.4, x4 magnification), and under identical light conditions. For correcting the white balance and obtaining red, green, and blue (RGB) pixel values, Adobe Photoshop 2020 was used. Color values from the tentacles of five randomly chosen polyps (25 x 25-pixel square) were averaged per colony. The RGB values were then averaged per treatment per day and the resulting #HEX color was reported visually. The use of one fragment per tank was representative of all fragments in their respective tanks (Tilstra, personal observation).

Survival

All colonies were monitored for survival throughout the experiment. Due to the high regeneration capacity of *X. umbellata*⁴⁷, colonies were only considered dead when they completely disappeared from the plug.

Symbiodiniaceae cell density and chlorophyll a content

On every measurement day, 12 colonies (one colony per tank) were randomly chosen and frozen at -20 °C until further processing. Upon processing, samples were thawed, 10 mL of demineralized water was added, and homogenized (MONIPA™ High Speed Homogenizer FSH-2A) into a slurry. To separate the coral tissue and the Symbiodiniaceae cells, the slurry was centrifuged for 10 mins at 6000 rpm. The supernatant was discarded, and the remaining pellet was resuspended in 2 mL distilled water and again centrifuged at 6000 rpm for another 10 mins in order to further separate the coral tissue and the Symbiodiniaceae cells. The supernatant was again discarded and the remaining pellet was resuspended in 2 mL of distilled water. To count the Symbiodiniaceae cells, 10 µL of resuspended cells were loaded on both grids of a counting chamber (Neubauer™ counting chamber, 0.1 mm depth). Cells were then counted using a microscope (DN-107T Digital Microscope, Xiamen Phio Scientific Instruments Co., Ltd). Cell counts from both grids were averaged for downstream analysis. Symbiodiniaceae cells were normalized to the surface area to obtain the cell density. For this purpose, photos were evaluated with

ImageJ, measuring the surface area of six polyps (three large polyps and three small polyps) each. The mean value and the number of polyps of the respective colony then produced the surface area, which led to the unit of “Symbiodiniaceae cells cm⁻²”.

Chlorophyll *a* was measured according to Jeffrey and Humprey⁴⁸ at the end of the experiment (day 21). Briefly, a pellet with known Symbiodiniaceae cell count was resuspended in 90 % acetone, vortexed and left in darkness for 24 h at 4 °C. After centrifugation, the supernatant was transferred to two 1 mL glass cuvettes. Chlorophyll *a* content was then measured in total darkness using a Trilogy Fluorometer (Turner Designs) fitted with a chl. *a* module against a pre-made calibration curve. Each sample was measured three times resulting in two times three measurements per treatment sample. Replicates were averaged and normalized per Symbiodiniaceae cell.

Oxygen fluxes

Net photosynthesis (P_{net}) and dark respiration (R_{dark}) rates were assessed by oxygen flow with light and dark incubations^{49,50}. The same colonies were used as for coloration in order to establish a potential connection. Briefly, the respective colony (one colony per tank) was placed in a 160 mL glass jar containing water from its respective tank. The jar was sealed airtight avoiding capture of air bubbles, and placed in a water bath with a constant temperature of 26 °C and ~100 $\mu\text{mol photons m}^{-2} \text{ s}^{-1}$ of light for P_{net} measurements using the same LED lights as the experimental tanks. Constant water mixing in the jars was ensured by using stirring plates with 190 rpm (Poly 15, Thermo Scientific VARIOMAG® Magnetic Stirrers) and a magnetic stirrer in each jar. The oxygen concentration was measured at the start, i.e., before closing the lid, as well as at the end of the incubation, i.e., after 1 h in the light for P_{net} and 1 h in total darkness for R_{dark} , using an optode sensor (Hach IntelliCAL/Optical Dissolved Oxygen Probe). Dark respiration is presented as a negative value. Gross photosynthesis (P_{gross}) was calculated using [Formula 5.2](#).

$$P_{\text{gross}} = P_{\text{net}} - R_{\text{dark}} \quad \text{(Formula 5.2)}$$

Oxygen measurements were normalized to the surface area to obtain oxygen fluxes. For this purpose, photos were evaluated with ImageJ, measuring the surface area of six polyps (three large polyps and three small polyps) each. The mean value and the number of polyps of the respective colony then produced the surface area, which led to the unit of “ $\mu\text{g O}_2 \text{ cm}^{-2} \text{ h}^{-1}$ ”.

Stable isotope signatures and CN content

To assess the effects of increased DIC on the isotope signatures and elemental composition of holobiont C and N, six samples from both treatments, i.e., one colony per tank, were taken at the end of the experiment (day 21) and prepared according to Mezger and colleagues⁵¹. Briefly, colonies were carefully detached from the plug and thoroughly rinsed with distilled water to eliminate any traces of salt. Subsequently, the colony was placed in a plastic bag and preserved by freezing it at a temperature of -20 °C. For subsequent processing, *X. umbellata* colonies were dried in sterile glass petri dishes at a

temperature of 40 °C, for a minimum of 48 h, and beyond if required, until they reached a consistent weight. Following this, the dried colonies were ground into a fine powder using a mortar and pestle. The resulting tissue powder was weighed, and 1–2 mg of the powder was then transferred into 5x9 mm tin cups (IVA Analysentechnik GmbH & Co. KG, Germany). Prepared samples were shipped to the Natural History Museum in Berlin and analyzed according to Karcher and colleagues⁵².

Statistical analysis

Statistical analyses were carried out using Sigmaplot v12.0 (Systat software). All data were normally distributed (Shapiro-Wilk normality test) with homogeneity of variances (Levene's test). Water parameters as well as pulsation rate, visual coloration, SGR, and oxygen flux data were analyzed via two-way repeated measures analysis of variance (2-way RM ANOVA) as data were obtained every week from the same colony. For this analysis, 'Day' and 'Treatment' were set as fixed factors, while tank number was used as subject. Symbiodiniaceae cell density data, which was collected from a different colony every week, was analyzed with a two-way analysis of variance (2-way ANOVA). For this analysis, 'Day' and 'Treatment' were set as fixed factors. Chlorophyll *a* content, isotope signatures, and CN content were analyzed via t-tests. Furthermore, all pairwise multiple comparison procedures were conducted to confirm the significant differences by carrying out Tukey's post hoc multiple comparison tests. Figures were generated with R (version 2023.03.0+386) and SigmaPlot v12.0 (Systat software). All data are presented as mean ± S.E. unless stated otherwise.

5.4 Results

Water parameters

Water parameters, except for pH, in all aquaria remained constant throughout the experiment (Table 5.1). There were no significant differences between aquaria for either parameter. The pH in the aquaria without acidification averaged 8.3 ± 0.1 . The pH of six OA tanks averaged at 8.0 ± 0.1 in the first week, 7.8 ± 0.1 in the week after, and 7.6 ± 0.1 in the last week.

Pulsation rate

In general, pulsation rates were lower in OA treatments compared to the control (Fig. 5.1). There was a significant interactive effect of Day and Treatment (2-way RM ANOVA, $F_{2,20} = 12.6$, $p < 0.001$). Pulsation rates of control fragments remained constant for the first two weeks (41 ± 1 and 40 ± 1 beats min^{-1} , respectively) and then decreased significantly to an average of 37 ± 1 beats min^{-1} in the final week (Fig. 5.1). For OA treatments, pulsation rates averaged at 34 ± 1 beats min^{-1} at pH 8.0, 30 ± 1 beats min^{-1} at pH 7.8, and 25 ± 1 beats min^{-1} at pH 7.6. All OA treatments differed significantly from the controls and each other (pairwise comparison, $p < 0.001$) (Fig. 5.1).

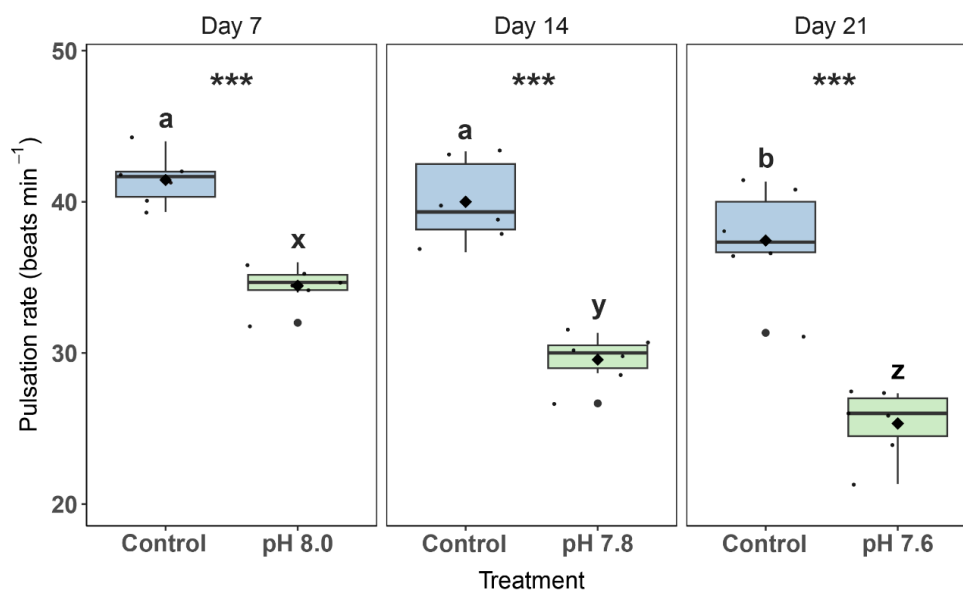


Figure 5.1. Pulsation rates of *Xenia umbellata* exposed to ocean acidification (OA). The black horizontal line in each boxplot represents the median, while the black diamond represents the mean. Blue boxplots are controls; green boxplots are the OA treatments. Small black circles represent data points ($n_{\text{treatment}} = 6$), and big black circles represent outliers. Significant differences ($p < 0.05$) within treatments between days are shown by different letters, while differences between treatments per day are shown by asterisks (***) ($p < 0.001$).

Specific growth rate

All colonies had a positive SGR during the experiment (Fig. 5.2). Colonies exposed to OA had significantly lower SGR compared to the control during all three weeks of the experiment (pairwise comparison, $p < 0.01$ for all significant comparisons). Significant main effects were found for Treatment (2-way RM ANOVA, $F_{1,20} = 67.6$, $p < 0.001$) and Day (2-way RM ANOVA, $F_{2,20} = 29.5$, $p < 0.001$). The SGR for both the control and OA treatments decreased significantly (pairwise comparison, $p < 0.01$ for all significant comparisons) after the first week and remained stable over the last two weeks (Fig. 5.2). Specific growth rates of control colonies decreased with 58 % at day 7 – day 14 and 54 % at day 14 – day 21 compared to day 0 – day 7, while SGR of OA exposed colonies with decreased with 58 % and 65 %, respectively (Fig. 5.2).

Visual coloration and survival

There were no significant differences between treatments for red, green, or blue coloration ($p = 0.656$, $p = 0.405$, $p = 0.218$, respectively). Overall, colors remained relatively consistent throughout the experiment and all coral fragments (100 %) survived the experiment (Fig. 5.2).

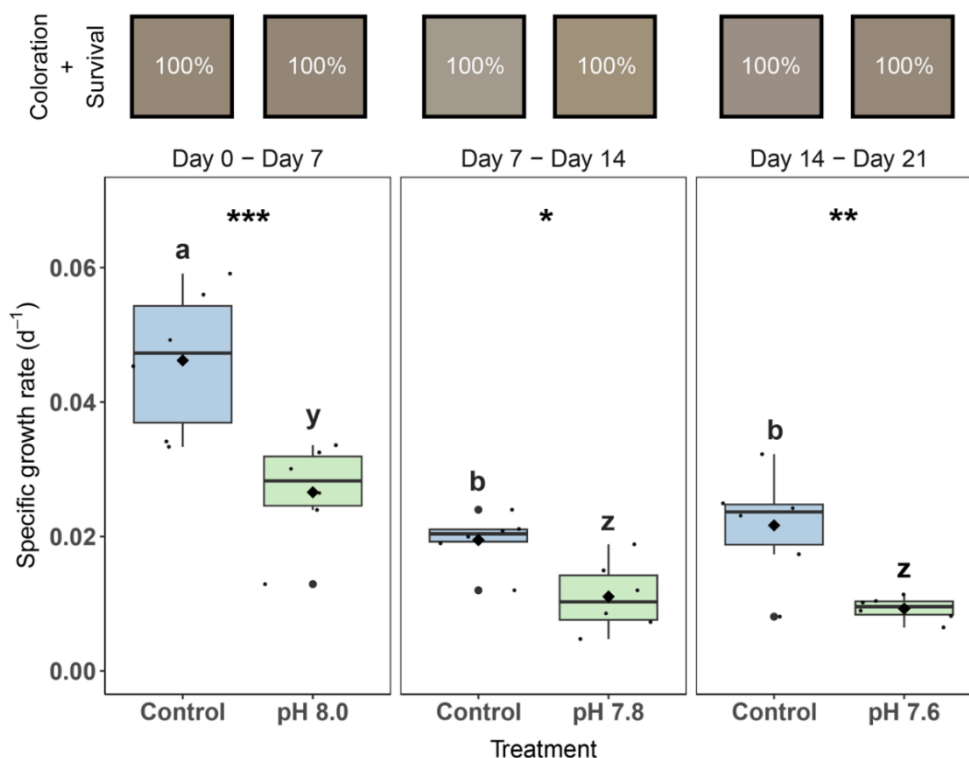


Figure 5.2. Specific growth rates, visual coloration, and survival of *Xenia umbellata* exposed to ocean acidification (OA). Color squares represent the average color of the colonies in its respective treatment (#HEX, based on Red, Green and Blue [RGB] values of photographs). Percentages inside the color squares refer to coral colonies that survived in every treatment; i.e., all colonies survived in every treatment. The black horizontal line in each boxplot represents the median, while the black diamond represents the mean. Blue boxplots are controls; green boxplots are the OA treatments. Small black circles represent data points ($n_{\text{treatment}} = 6$), and big black circles represent outliers. Significant differences ($p < 0.05$) within treatments between days are shown by different letters, while differences between treatments per day are shown by asterisks (* $p < 0.05$, ** $p < 0.01$, *** $p < 0.001$).

Symbiodiniaceae cell density and chlorophyll *a* content

In general, cell densities were always lower in the OA treatment compared to the control, but not significantly (Fig. 5.3A). Significant main effects were found for Treatment (2-way ANOVA, $F_{2,30} = 15.1$, $p < 0.001$) and Day (2-way ANOVA, $F_{1,30} = 7.6$, $p = 0.010$), but pairwise comparisons were only significant for changes in Symbiodiniaceae cell densities, and not between the control and the OA treatment. On day 7, cell densities for the control and OA treatment were 5.85 ± 0.46 and $5.03 \pm 0.72 \times 10^5$ cells cm^{-2} , respectively, which increased on day 14 by 35 % and 27 %, respectively, and decreased on day 21 by 40 % and 50 %, respectively, compared to day 14 (Fig. 5.3A). Chlorophyll *a* content was not significantly different between control (4.77 ± 0.73 $\mu\text{g cell}^{-1}$) and OA exposed colonies (6.56 ± 1.76 $\mu\text{g cell}^{-1}$) at the end of the experiment (t-test, $p = 0.371$) (Fig. 5.3B).

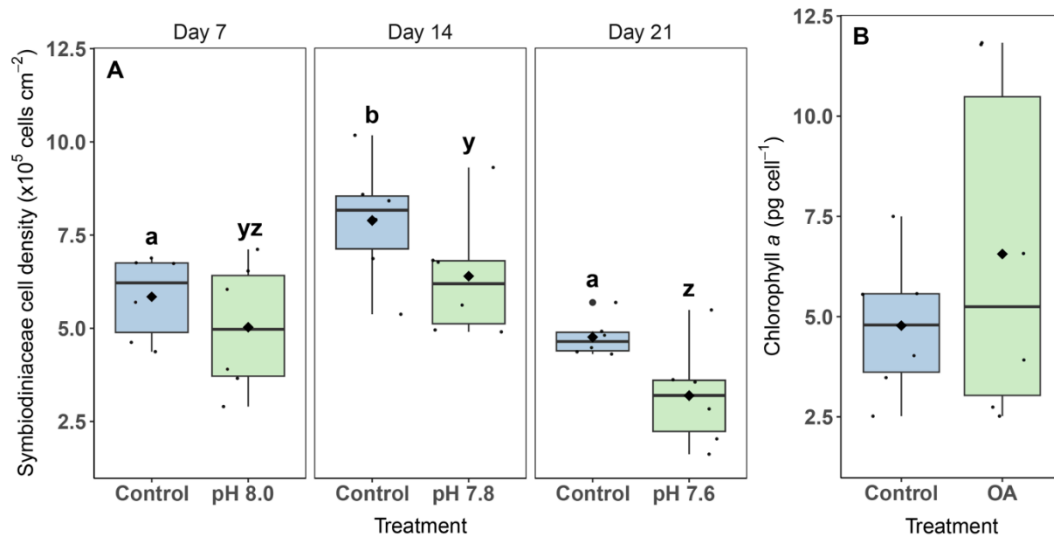


Figure 5.3. Symbiodiniaceae cell density (A) and chlorophyll *a* content (B) of *Xenia umbellata* exposed to ocean acidification (OA). The black horizontal line in each boxplot represents the median, while the black diamond represents the mean. Blue boxplots are controls; green boxplots are the OA treatments. Small black circles represent data points ($n_{\text{treatment}} = 6$), and big black circles represent outliers. For (A): Significant differences ($p < 0.05$) within treatments between days are shown by different letters, while no significant differences were found between treatments per day. For (B): No significant differences were found between treatments.

Oxygen fluxes

A significant main effect was found for Day for P_{net} (2-way RM ANOVA, $F_{2,20} = 8.5$, $p = 0.002$), P_{gross} (2-way RM ANOVA, $F_{2,20} = 8.8$, $p = 0.002$), and R_{dark} (2-way RM ANOVA, $F_{2,20} = 5.9$, $p < 0.009$), but not for Treatment nor was there an interaction of Day and Treatment. In general, P_{net} , P_{gross} , and R_{dark} decreased after Day 7 by $\sim 28\%$, $\sim 26\%$ and $\sim 19\%$, respectively, for Day 14 and 21 (Fig. 5.4). No significant difference between control and OA treatment was found for any day.

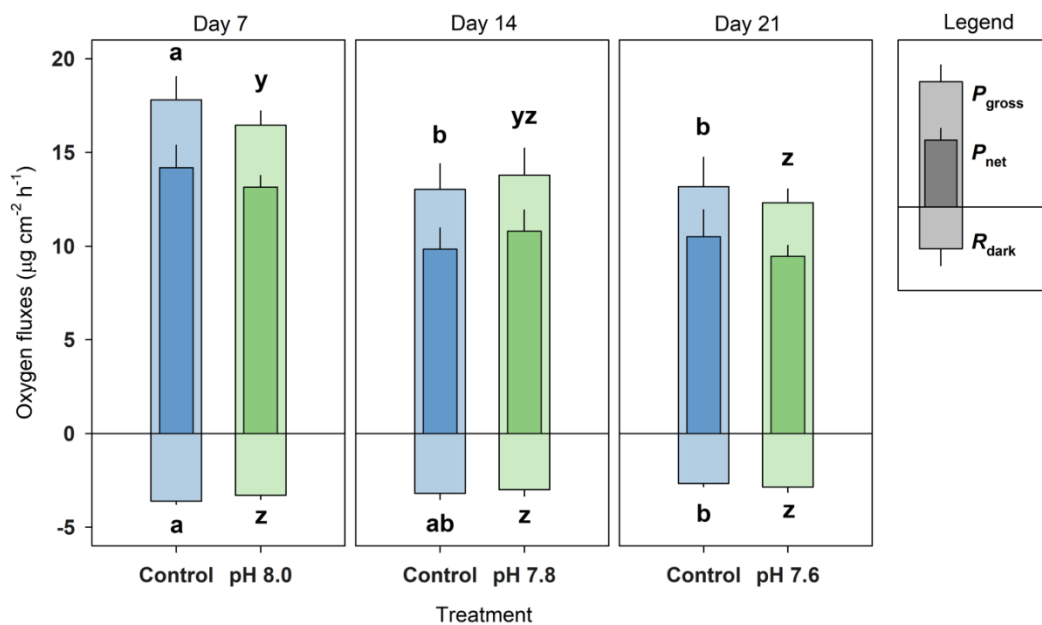


Figure 5.4. Oxygen fluxes of *Xenia umbellata* exposed to ocean acidification (OA). P_{gross} = gross photosynthesis, P_{net} = net photosynthesis, and R_{dark} = dark respiration. Blue bars represent the control; green bars represent the OA treatments. Bars are mean \pm standard error ($n_{\text{treatment}} = 6$). Significant differences ($p < 0.05$) within treatments between days are shown by different letters (P_{gross} and P_{net} share the same significance letters), while no significant differences were found between treatments per day.

Stable isotope signatures and CN content

The $\delta^{13}\text{C}$ of OA exposed colonies significantly decreased compared to the control (t -test, $p < 0.001$), on average by 8.3 ‰ (Fig. 5.5A). Colonies exposed to OA revealed a non-significant (t -test, $p = 0.09$) increase in %C compared to controls by ~ 3 ‰ (Fig. 5.5B). Nitrogen isotopes ($\delta^{15}\text{N}$) remained stable at 8.6 ± 0.1 ‰ and 8.7 ± 0.1 ‰ for the OA and control colonies, respectively (Fig. 5.5C). The percentage of N in the holobiont remained stable at 3.0 ± 0.1 for both treatments (Fig. 5.5D). The C:N ratio was higher in the OA treatment (10.0 ± 0.5), but not significantly (t -test, $p = 0.14$) compared to the control (9.0 ± 0.4) (Fig. 5.5E).

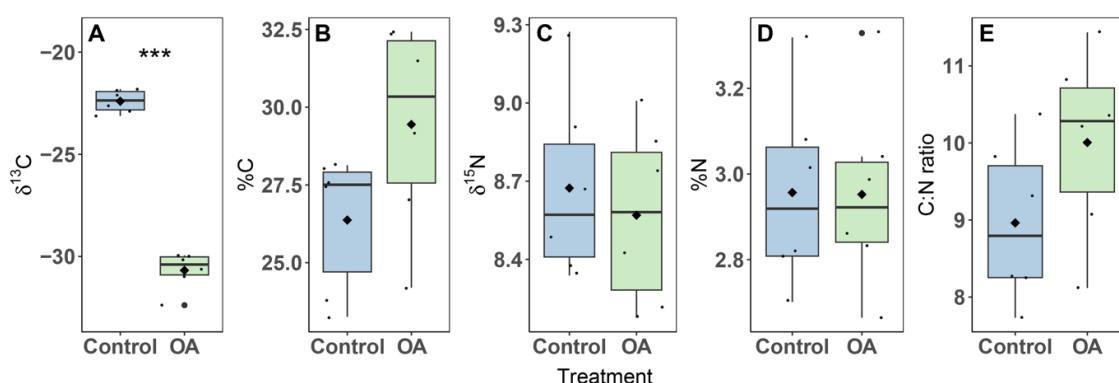


Figure 5.5. Stable isotope signature of carbon ($\delta^{13}\text{C}$) (A), elemental composition of carbon (%C) (B), stable isotope signature of nitrogen ($\delta^{15}\text{N}$) (C), elemental composition of nitrogen (%N) (D) and ratio of carbon and nitrogen (E) of the *Xenia umbellata* holobiont exposed to ocean acidification (OA) at day 21. The black horizontal line in each boxplot represents the median, while the black diamond represents the mean. Blue boxplots are controls; green boxplots are the OA treatments. Small black circles represent data points ($n_{\text{treatment}} = 6$), and big black circles represent outliers. Significant differences between treatments are shown by asterisks (***) ($p < 0.001$).

5.5 Discussion

Previous studies reported marginal effects of OA on soft coral health (Table 5.2), while none of these studies (except for one observation) reported altered physiology of xeniids in response to OA. In the present study, we found reduced pulsation and growth of the xeniid *X. umbellata* in response to OA. We posit that pulsation may be a very beneficial and phenotypically plastic trait for xeniids when exposed to higher $p\text{CO}_2$ concentrations. As a result, pulsating xeniids may become even more dominant under future climate change scenarios.

Acidification did not affect the photophysiology of *X. umbellata*

The $\delta^{13}\text{C}$ of the OA exposed colonies revealed a significant decrease compared to the control colonies, by ~ 8.3 ‰, indicating a higher uptake and incorporation of the lighter ^{12}C isotope from atmospheric CO_2 into the holobiont⁵³. Lighter C isotope signatures were also found in hard corals exposed to OA⁴¹, thus indicating similar responses between hard and soft corals. However, this increased incorporation, and ultimately availability, of DIC was not reflected in the C content or the C:N ratios, highlighting that C was likely not the limiting nutrient for coral productivity⁴². The higher availability and a subsequent alleviation of C limitation would have theoretically resulted in higher numbers of Symbiodiniaceae cells

through the use of before unused $N^{54,55}$. Though, in the present study, cell densities of Symbiodiniaceae, as well as chl. *a* content of Symbiodiniaceae, in OA exposed colonies were not significantly different from the controls. Concentrations of environmental dissolved inorganic N (DIN) also remained stable (Table 5.1). We can thus conclude that N was likely the limiting nutrient for primary production throughout the entire experiment. This was further evidenced by stable P_{net} , P_{gross} and R_{dark} between control and OA treatment. As pulsation and the fluxes of oxygen may be linked³⁷, we expected pulsation rates to remain stable as well²⁶.

Acidification affected pulsation and growth of *X. umbellata*

Even though the photophysiology of the holobiont remained unaffected, pulsation was significantly affected. Pulsation rates gradually decreased with every decrease in water pH compared to the control at the same stage, i.e., a decrease of 17 % at pH 8.0, 26 % at pH 7.8 and 32 % at pH 7.6. Previous studies have reported reductions of *Xenia* spp. pulsation rates in response to warming³⁹, heavy nitrate eutrophication³⁸, a lack of a heterotrophic food source (Hill et al., in review), and exposure to oil dispersants⁴⁰. The synchronous opening and contracting of the polyp tentacles, in a continuous rhythm, results in a water flow that enhances photosynthesis by rapidly removing excess oxygen while increasing CO_2 affinity of ribulose-1,5-bisphosphate carboxylase oxygenase (RuBisCO) and preventing refiltration of surrounding water by neighboring polyps^{36,37,56}. As such, a decrease in pulsation rates should theoretically have resulted in decreased photosynthesis, which remained unaffected. We therefore hypothesize that *X. umbellata* reduced its pulsation to compensate for the higher availability of DIC⁵⁷, thus reducing gas exchange to maintain stable productivity, which may have ultimately reduced the effects of OA on the corals' photophysiology.

As pulsation is an energy costly process³⁶, the reduction in pulsation rates could preserve energy for other vital processes such as growth. However, the observed reduction in pulsation rates associated with OA exposed colonies was accompanied with a decrease in SGR compared to controls. Growth rates in OA treatments decreased by 58 % and 65 %, respectively, during the second and third week compared to the first week of the experiment. Although growth rates in control tanks were also reduced in the second and third week (by 57 % and 53 %, respectively), this was less pronounced than the decline in OA treatments. We speculate that both treatments experienced an unknown factor affecting both treatments, e.g., a lower availability of (in)organic nutrients, not measurable by our analytic tests, that are available in the holding tank of the mother colonies^{sensu 51}. This lower availability of (in)organic nutrients may have been exacerbated by diminished pulsation rates associated with OA exposed colonies, though only at pH 7.6 in the third week. Indeed, lower pulsation rates and subsequent increased water refiltration by adjacent polyps may have reduced the uptake of particulate (e.g., detritus, small phyto- and zooplankton) and dissolved (e.g., small carbohydrates, amino and fatty acids) organic matter, as well as the supply of (in)organic N and phosphorus (P), which are essential for soft coral growth³⁷. In addition, the energy obtained from translocated photosynthates by the Symbiodiniaceae may have

been redirected to other processes, e.g., mucus production, in the holobiont rather than invested in growth. Translocation of photosynthates may even increase under OA as found for the hard coral *Stylophora pistillata*, though this was accompanied by reduced cell densities of the Symbiodiniaceae and their chl. *a* content⁶⁰. This is less likely to have happened in the present study as both remained stable. The opposite, i.e., a reduction in photosynthate translocation, would theoretically be possible, but could not be inferred with the reported response variables in our study. Future studies could shed light on resource acquiring/partitioning by separating the coral tissue and Symbiodiniaceae for isotope and elemental analyses, use labelled isotopes of C and N, and/or by performing nutrient uptake incubations. Taken together, our results suggest that *X. umbellata* had less nutrients and/or energy available for growth under OA conditions, which could have been induced by lower pulsation rates and/or altered use of translocated photosynthates.

Comparison to previous studies on octocorals

Previous studies have shown that xeniids could be protected from OA as their tissue may act as a protective barrier^{26,27}. Our results suggest that this is not necessarily the case for *X. umbellata* since pulsation- and growth rates in the present study were affected, thus partially contrasting²⁶ (Table 5.2). In their study, while exposing the pulsating xeniid *Ovabunda macrospiculata* to pH values of 7.6 and 7.3, pulsation and growth both persisted (though caution is needed as they quantified growth as “sclerite weight to polyp weight”). Hence, different species can show different responses to stressors, even if they belong to the same family and may therefore be more similar in physiology⁵⁸. To our knowledge, only one observation mentions flaccid and unhealthy-looking *Xenia* sp. with less coordinated pulsation in response to lower pH exposure (8.1 and lower)⁵⁹. In the present study, colonies remained visually healthy and continued to pulsate in a coordinated manner. In accordance with²⁶, Symbiodiniaceae cell density and chl. *a* content remained unaffected, while another study on hard corals found reductions in both response variables⁶⁰.

Table 5.2. Comparison of results of previous OA experiments/observations using soft corals. N = Nitrogen, C = Carbon, P_{net} = net photosynthesis, P_{gross} = gross photosynthesis, R_{dark} = dark respiration, Chl. *a* = Chlorophyll *a*, *Observation made by the book authors, not part of an empirical study

Soft coral species	Family	pH exposures	Exposure length	Affected response variables	Non-affected response variables	Reference
<i>Xenia umbellata</i>	Xeniidae	8.3, 8.0, 7.8, 7.6	7 days per OA treatment	Reduced pulsation rate, growth rate and $\delta^{13}\text{C}$	Visual coloration, survival, Symbiodiniaceae cell density, chl. <i>a</i> content, P_{net} , P_{gross} , R_{dark} , $\delta^{15}\text{N}$, %C, %N, C:N content	Present study
<i>Xenia</i> sp.	Xeniidae	< 8.1	Longer periods	Uncoordinated pulsation*	N/A	59
<i>Corallium rubrum</i>	Coralliidae	8.09, 7.88, 7.77	10 and 45 days	Reduced biocalcification, growth rates and feeding	-	61
<i>Corallium rubrum</i>	Coralliidae	8.1, 7.81	314 days	Spicule morphology, reduced growth rate	Carbohydrate, lipid, protein and fatty acid composition	62
<i>Ovabunda macrospiculata</i>	Xeniidae	8.2, 7.6, 7.3	30-90 days	-	Symbiodiniaceae cell density and chl. <i>a</i> content, sclerite weight; polyp	26

<i>Heteroxenia fuscescens</i> <i>Sarcophyton</i> sp.	Xeniidae Alcyoniidae	8.2, 7.6, 7.3 8.2, 7.6, 7.3	30-90 days ~150 days	- -	weight, pulsation rate, polyp weight Symbiodiniaceae cell density and chl. a content Symbiodiniaceae cell density and chl. a content	
<i>Ovabunda macrospiculata</i>	Xeniidae	8.2, 7.6, 7.3	42 days	-	Sclerite microstructure	27
<i>Eunicea fusca</i>	Plexautidae	8.1 – 7.1	28 days	Growth and calcification both decreased with decreasing pH	-	63
<i>Sarcophyton glaucum</i>	Alcyoniidae	8.2, 8.0, 7.8	3 days	Reduced cytotoxic compounds (only at pH 7.8)	Cytotoxic compounds (at pH 8.0)	28
<i>Veretillum cynomorium</i>	Veretillidae	8.0, 7.7	60 days	-	Antioxidant enzymes, lipid peroxidation, heat shock response	64
<i>Rhytisma fulvum</i>	Alcyoniidae	~8.1, ~7.9, ~7.7	49 days	Reduced maximum relative electron transport rate	Alpha, Fv/Fm, Ek, NPQmax	29

Ecological implications

In the present study, we found no effect of strong OA (pH 7.6) on the photophysiology of *X. umbellata*, while pulsation and growth rates were significantly impacted compared to controls. Octocorals that have been exposed to longer periods of ecologically relevant pH values (i.e., above ~7.8) have shown little to no negative effects (Table 5.2). In contrast, though in accordance with the present study, hard corals have shown reductions of 50 % in skeletal growth at similar pH ranges^{10,65}. Previous research on octocorals (Table 5.2) suggests that the calcium carbonate microstructures (i.e., the sclerites) of octocorals maintain their integrity under OA conditions^{26,27}. However, to better predict the success of *X. umbellata* under future OA scenario, future studies should assess the dissolution and production rates of the sclerites as well as their microstructure, i.e., morphology^{e.g.,27}. If the sclerites of *X. umbellata* also maintain their integrity under OA conditions, a reduction in growth is only a small price to pay to remain viable. Ocean acidification is a gradual process where pH will decrease mostly linearly over the next decades rather than abruptly within days. Therefore, the results obtained in the present short-term study may differ from long-term effects on *X. umbellata*. Additionally, differences in light intensities due to large depth ranges of xeniids⁶⁶, could potentially interact with acidification and further influence the physiological responses. Thus, caution is required in extrapolating data of the present study to imply natural ecological effects.

Xenia umbellata has been subject to experiments assessing the (combined) effects of global and/or local factors; e.g., dissolved organic carbon (DOC) eutrophication and warming^{39,67,68}, nitrate eutrophication and warming³⁸, phosphate eutrophication and warming^{51,69}, water flow and food availability (Hill et al., in review), and *in-situ* eutrophication^{52,70}. Future scenarios for corals will likely include multiple global and local factors, with ocean warming as the most urgent threat. In some of the previously mentioned studies, the addition of a local factor mitigated the effects of ocean warming^{39,51,69},

while others exacerbated the effects of ocean warming³⁸. Future studies should also investigate combined effects of multiple global factors that are expected to happen simultaneously, i.e., ocean warming and acidification^{e.g.,71}. When there are too many stress factors, shifts in community composition may happen, where for example, soft corals will replace hard corals⁷². Xenidiids in particular are rapid, opportunistic colonizers of disturbed habitats, especially coral relicts³⁴, which are relatively resistant to ocean warming^{38,39}. Their rapid clonal growth through a strategy of larval incubation and effective asexual reproduction, as well as the production of allelopathic substances that chemically inhibits the growth of other organisms, helps them spread widely³²⁻³⁴. This shift away from hard corals can have harmful effects because they provide complex three-dimensional habitats for other organisms^{9,73}. Therefore, a wide distribution of soft corals has consequences for the functioning of the whole reef.

In conclusion, we posit that *X. umbellata* may adjust to OA by altering its pulsation activity, highlighting the phenotypic plasticity of this trait. Whilst cautiously interpreting the results of the present study due to its short-term nature, this study provides further evidence for the competitive advantage that *X. umbellata* may have over hard corals under future climate change scenarios.

5.6 Acknowledgments

We thank Annabell Klinke for technical support throughout the experiment. A special thanks goes to Jutta Scheffing and Horst Schulte, who helped with the preparation and implementation of the experiment. We also thank two anonymous reviewers from a previous submission who helped improve the quality of the manuscript. We thank Charles Delbeek for providing additional information concerning a chapter in his and Julian Sprung's 1997 book (see references). Lastly, we thank Dr. Hans-Konrad Nettmann, who provided important equipment and scientific support when needed.

5.7 References

1. Hughes, T. P. *et al.* Coral reefs in the Anthropocene. *Nature* **546**, 82–90 (2017).
2. Cai, W.-J. *et al.* Acidification of subsurface coastal waters enhanced by eutrophication. *Nat Geosci* **4**, 766–770 (2011).
3. Horwitz, R., Hoogenboom, M. O. & Fine, M. Spatial competition dynamics between reef corals under ocean acidification. *Sci Rep* **7**, 40288 (2017).
4. Hoegh-Guldberg, O., Poloczanska, E. S., Skirving, W. & Dove, S. Coral reef ecosystems under climate change and ocean acidification. *Front Mar Sci* **4**, 158 (2017).
5. Hennige, S. J. *et al.* Hidden impacts of ocean acidification to live and dead coral framework. *Proc. Roy. Soc. B: Biol. Sci.* **282**, 20150990 (2015).
6. Hoegh-Guldberg, O. *et al.* The ocean. in *Climate Change 2014: Impacts, Adaptation, and Vulnerability. Part B: Regional Aspects. Contribution of Working Group II to the Fifth Assessment Report of the Intergovernmental Panel on Climate Change* (eds. Barros, V. R. *et al.*)

- 1655–1731 (Cambridge University Press, Cambridge, United Kingdom and New York, NY, USA, 2014).
7. Pelejero, C., Calvo, E. & Hoegh-Guldberg, O. Paleo-perspectives on ocean acidification. *Trends Ecol Evol* **25**, 332–344 (2010).
 8. Azevedo, L. B., De Schryver, A. M., Hendriks, A. J. & Huijbregts, M. A. J. Calcifying species sensitivity distributions for ocean acidification. *Environ. Sci. Technol.* **49**, 1495–1500 (2015).
 9. Wild, C. *et al.* Climate change impedes scleractinian corals as primary reef ecosystem engineers. *Mar. Freshw. Res.* **62**, 205–215 (2011).
 10. Langdon, C. & Atkinson, M. J. Effect of elevated $p\text{CO}_2$ on photosynthesis and calcification of corals and interactions with seasonal change in temperature/ irradiance and nutrient enrichment. *J. Geophys. Res. Oceans* **110**, C09S07 (2005).
 11. Kavousi, J., Everett, J., Takashi, P., Parkinson, J. E. & Nakamura, T. Combined ocean acidification and low temperature stressors cause coral mortality. *Coral Reefs* **35**, 903–907 (2016).
 12. Albright, R., Mason, B., Miller, M. & Langdon, C. Ocean acidification compromises recruitment success of the threatened Caribbean coral *Acropora palmata*. *PNAS* **107**, 20400–20404 (2010).
 13. Rådecker, N., Meyer, F. W., Bednarz, V. N., Cardini, U. & Wild, C. Ocean acidification rapidly reduces dinitrogen fixation associated with the hermatypic coral *Seriatopora hystrix*. *Mar. Ecol. Prog. Ser.* **511**, 297–302 (2014).
 14. DeCarlo, T. M. *et al.* Coral macrobioerosion is accelerated by ocean acidification and nutrients. *Geology* **43**, 7–10 (2015).
 15. Hill, T. S. & Hoogenboom, M. O. The indirect effects of ocean acidification on corals and coral communities. *Coral Reefs* **41**, 1557–1583 (2022).
 16. Martins, C. P. P. *et al.* Growth response of reef-building corals to ocean acidification is mediated by interplay of taxon-specific physiological parameters. *Front Mar Sci* **9**, 872631 (2022).
 17. Langdon, C., Albright, R., Baker, A. C. & Jones, P. Two threatened Caribbean coral species have contrasting responses to combined temperature and acidification stress. *Limnol. Oceanogr.* **63**, 2450–2464 (2018).
 18. Comeau, S., Carpenter, R. C. & Edmunds, P. J. Effects of feeding and light intensity on the response of the coral *Porites rus* to ocean acidification. *Mar Biol* **160**, 1127–1134 (2013).
 19. Noonan, S. H. C. & Fabricius, K. E. Ocean acidification affects productivity but not the severity of thermal bleaching in some tropical corals. *ICES J. Mar. Sci.* **73**, 715–726 (2016).
 20. Johnson, J. V. *et al.* The relative influence of sea surface temperature anomalies on the benthic composition of an Indo-Pacific and Caribbean coral reef over the last decade. *Ecol. Evol.* **12**, e9263 (2022).

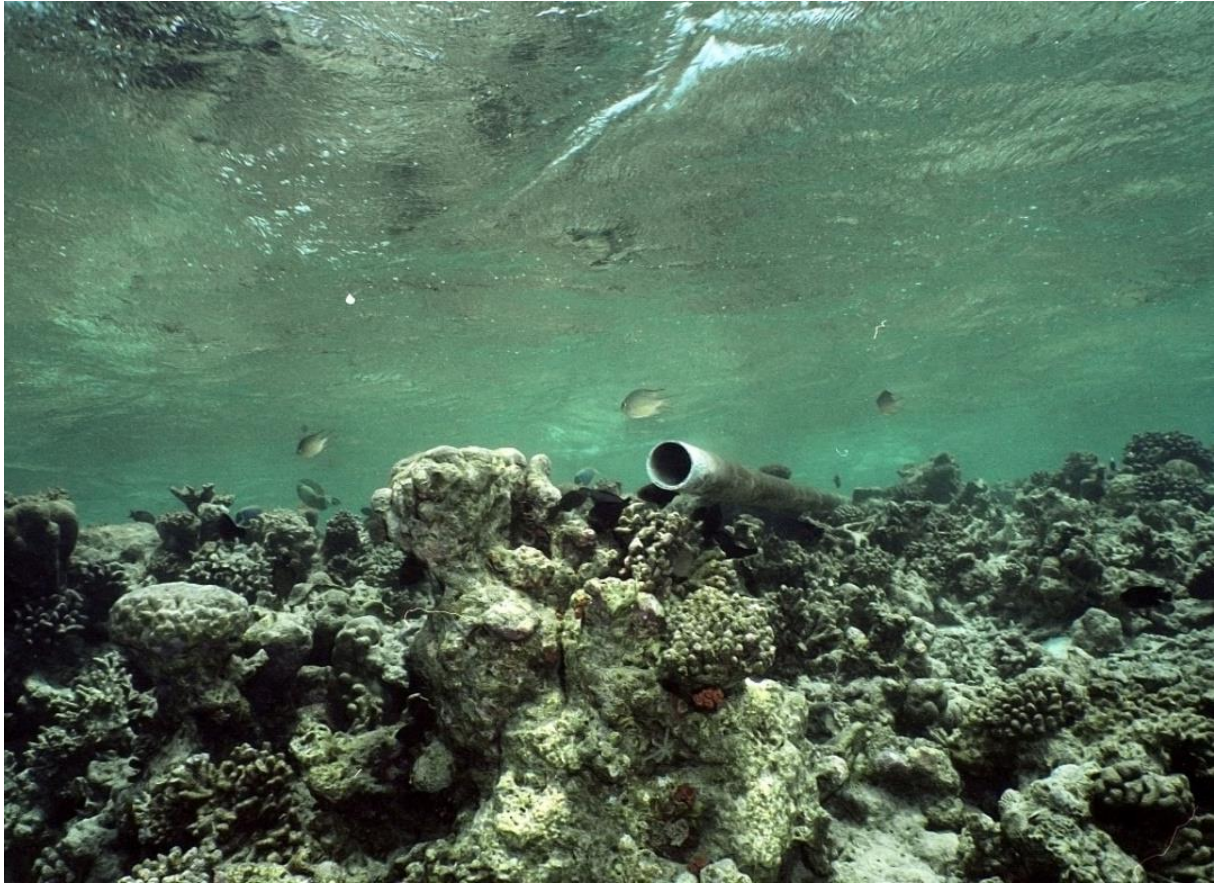
21. Stobart, B., Teleki, K., Buckley, R., Downing, N. & Callow, M. Coral recovery at Aldabra Atoll, Seychelles: five years after the 1998 bleaching event. *Philos. Trans. A Math. Phys. Eng. Sci.* **363**, 251–255 (2005).
22. Baum, G., Januar, I., Ferse, S. C. A., Wild, C. & Kunzmann, A. Abundance and physiology of dominant soft corals linked to water quality in Jakarta Bay, Indonesia. *PeerJ* **4**, e2625 (2016).
23. Endean, R., Cameron, A. & Devantier, L. *Acanthaster planci* predation on massive corals: the myth of rapid recovery of devastated reefs. In *Proc. 6th Int. Coral Reef Symp., Australia, Vol. 2* 143–148 (1988).
24. Moynihan, J. L., Hall, A. E. & Kingsford, M. J. Interrelationships between soft corals and reef-associated fishes on inshore-reefs of the Great Barrier Reef. *Mar. Ecol. Prog. Ser.* **698**, 15–28 (2022).
25. Epstein, H. E. & Kingsford, M. J. Are soft coral habitats unfavourable? A closer look at the association between reef fishes and their habitat. *Environ. Biol. Fishes* **102**, 479–497 (2019).
26. Gabay, Y., Benayahu, Y. & Fine, M. Does elevated $p\text{CO}_2$ affect reef octocorals? *Ecol. Evol.* **3**, 465–473 (2013).
27. Gabay, Y., Fine, M., Barkay, Z. & Benayahu, Y. Octocoral tissue provides protection from declining oceanic pH. *PLoS One* **9**, e91553 (2014).
28. Januar, H. I., Zamani, N. P., Soedarma, D. & Chasanah, E. Bioactive cembranoid composition in the soft coral of *Sarcophyton glaccum* on the response to changing pH. *Ilmu Kelaut* **22**, 25–30 (2017).
29. Liberman, R., Fine, M. & Benayahu, Y. Simulated climate change scenarios impact the reproduction and early life stages of a soft coral. *Mar. Environ. Res.* **163**, 105215 (2021).
30. Ruiz-Allais, J. P., Benayahu, Y. & Lasso-Alcalá, O. M. The invasive octocoral *Unomia stolonifera* (Alcyonacea, Xeniidae) is dominating the benthos in the Southeastern Caribbean Sea. *Memoria de la Fundación La Salle de Ciencias Naturales* **79**, 63–80 (2021).
31. Mantelatto, M. C., Silva, A. G. da, Louzada, T. dos S., McFadden, C. S. & Creed, J. C. Invasion of aquarium origin soft corals on a tropical rocky reef in the southwest Atlantic, Brazil. *Mar. Pollut. Bull.* **130**, 84–94 (2018).
32. Benayahu, Y. & Loya, Y. Settlement and recruitment of a soft coral: why is *Xenia macrospiculata* a successful colonizer? *Bull. Mar. Sci.* **36**, 177–188 (1985).
33. Kahng, S. E., Benayahu, Y. & Lasker, H. R. Sexual reproduction in octocorals. *Mar. Ecol. Prog. Ser.* **443**, 265–283 (2011).
34. Ziegler, M. *et al.* Coral microbial community dynamics in response to anthropogenic impacts near a major city in the central Red Sea. *Mar. Pollut. Bull.* **105**, 629–640 (2016).
35. LaJeunesse, T. C. *et al.* Systematic revision of Symbiodiniaceae highlights the antiquity and diversity of coral endosymbionts. *Curr. Biol.* **28**, 2570–2580.e6 (2018).

36. Kremien, M., Shavit, U., Mass, T. & Genin, A. Benefit of pulsation in soft corals. *PNAS* **110**, 8978–8983 (2013).
37. Wild, C. & Naumann, M. S. Effect of active water movement on energy and nutrient acquisition in coral reef-associated benthic organisms. *PNAS* **110**, 8767–8768 (2013).
38. Thobor, B. *et al.* The soft coral *Xenia umbellata* shows high resistance to warming when nitrate concentrations are low. *Sci. Rep.* **12**, 16788 (2022).
39. Vollstedt, S., Xiang, N., Simancas-Giraldo, S. M. & Wild, C. Organic eutrophication increases resistance of the pulsating soft coral *Xenia umbellata* to warming. *PeerJ* **8**, e9182 (2020).
40. Studivan, M. S., Hatch, W. I. & Mitchelmore, C. L. Responses of the soft coral *Xenia elongata* following acute exposure to a chemical dispersant. *Springerplus* **4**, 480 (2015).
41. Krief, S. *et al.* Physiological and isotopic responses of scleractinian corals to ocean acidification. *Geochim. Cosmochim. Acta* **74**, 4988–5001 (2010).
42. Rådecker, N., Pogoreutz, C., Wild, C. & Voolstra, C. R. Stimulated respiration and net photosynthesis in *Cassiopeia* sp. during glucose enrichment suggests *in hospite* CO₂ limitation of algal endosymbionts. *Front. Mar. Sci.* **4**, 267 (2017).
43. Kim, S., Wild, C. & Tilstra, A. Effective asexual reproduction of a widespread soft coral: comparative assessment of four different fragmentation methods. *PeerJ* **10**, e12589 (2022).
44. Watson, S.-A., Fabricius, K. E. & Munday, P. L. Quantifying pCO₂ in biological ocean acidification experiments: a comparison of four methods. *PLoS One* **12**, e0185469 (2017).
45. Tilstra, A. *et al.* Light induced intraspecific variability in response to thermal stress in the hard coral *Stylophora pistillata*. *PeerJ* **5**, e3802 (2017).
46. Wijgerde, T., Henkemans, P. & Osinga, R. Effects of irradiance and light spectrum on growth of the scleractinian coral *Galaxea fascicularis* - applicability of LEP and LED lighting to coral aquaculture. *Aquaculture* **344–349**, 188–193 (2012).
47. Nadir, E., Lotan, T. & Benayahu, Y. *Xenia umbellata* (Octocorallia): A novel model organism for studying octocoral regeneration ability. *Front. Mar. Sci.* **10**, 1021679 (2023).
48. Jeffrey, S. & Humphrey, G. New spectrophotometric equations for determining chlorophylls *a*, *b*, *c*₁ and *c*₂ in higher plants, algae and natural phytoplankton. *Biochemie und Physiologie der Pflanzen* **167**, 191–194 (1975).
49. Jantzen, C. *et al.* Benthic reef primary production in response to large amplitude internal waves at the Similan Islands (Andaman Sea, Thailand). *PLoS One* **8**, e81834 (2013).
50. Tilstra, A. *et al.* Denitrification aligns with N₂ fixation in Red Sea corals. *Sci Rep* **9**, 19460 (2019).
51. Mezger, S. D. *et al.* The widely distributed soft coral *Xenia umbellata* exhibits high resistance against phosphate enrichment and temperature increase. *Sci Rep* **12**, 22135 (2022).
52. Karcher, D. B. *et al.* Nitrogen eutrophication particularly promotes turf algae in coral reefs of the central Red Sea. *PeerJ* **8**, e8737 (2020).

53. Baker, D. M., Webster, K. L. & Kim, K. Caribbean octocorals record changing carbon and nitrogen sources from 1862 to 2005. *Glob. Chang. Biol.* **16**, 2701–2710 (2010).
54. Krueger, T. *et al.* Intracellular competition for nitrogen controls dinoflagellate population density in corals. *Proc. Roy. Soc. B* **287**, 20200049 (2020).
55. Cui, G. *et al.* Host-dependent nitrogen recycling as a mechanism of symbiont control in *Aiptasia*. *PLoS Genet* **15**, e1008189 (2019).
56. Mass, T., Genin, A., Shavit, U., Grinstein, M. & Tchernov, D. Flow enhances photosynthesis in marine benthic autotrophs by increasing the efflux of oxygen from the organism to the water. *Proc Natl Acad Sci U S A* **107**, 2527–2531 (2010).
57. Reynaud, S. *et al.* Interacting effects of CO₂ partial pressure and temperature on photosynthesis and calcification in a scleractinian coral. *Glob. Chang. Biol.* **9**, 1660–1668 (2003).
58. Janes, M. P. & Mary, A. G. Synopsis of the family Xenidae (Cnidaria: Octocorallia): status and trends. in *Proc. 12th Int. Coral Reef Symp.* (Cairns, Australia, 2012).
59. Sprung, J. & Delbeek, J. The reef aquarium, Vol. 2: A comprehensive guide to the identification and care of tropical marine invertebrates. in vol. 2 251–257 (Ricordea Publishing, Coconut Grove, Florida, 1997).
60. Tremblay, P., Fine, M., Maguer, J. F., Grover, R. & Ferrier-Pagès, C. Photosynthate translocation increases in response to low seawater pH in a coral-dinoflagellate symbiosis. *Biogeosciences* **10**, 3997–4007 (2013).
61. Cerrano, C. *et al.* Red coral extinction risk enhanced by ocean acidification. *Sci Rep* **3**, 1457 (2013).
62. Bramanti, L. *et al.* Detrimental effects of ocean acidification on the economically important Mediterranean red coral (*Corallium rubrum*). *Glob Chang Biol* **19**, 1897–1908 (2013).
63. Gómez, C. E. *et al.* Responses of the tropical gorgonian coral *Eunicea fusca* to ocean acidification conditions. *Coral Reefs* **34**, 451–460 (2015).
64. Lopes, A. R. *et al.* Physiological resilience of a temperate soft coral to ocean warming and acidification. *Cell Stress Chaperones* **23**, 1093–1100 (2018).
65. Schneider, K. & Erez, J. The effect of carbonate chemistry on calcification and photosynthesis in the hermatypic coral *Acropora eurystoma*. *Limnol. Oceanogr.* **51**, 1284–1293 (2006).
66. Janes, M. Distribution and diversity of the soft coral family Xenidae (Coelenterata: Octocorallia) in Lembah Strait, Indonesia. *Galaxea, J. Coral Reef Stud.* 195–200 (2013).
67. Simancas-Giraldo, S. M. *et al.* Photosynthesis and respiration of the soft coral *Xenia umbellata* respond to warming but not to organic carbon eutrophication. *PeerJ* **9**, e11663 (2021).
68. Xiang, N. *et al.* Contrasting microbiome dynamics of putative denitrifying bacteria in two octocoral species exposed to dissolved organic carbon (DOC) and warming. *Appl. Environ. Microbiol.* **88**, e01886-21 (2021).

69. Klinke, A. *et al.* Phosphate enrichment increases the resilience of the pulsating soft coral *Xenia umbellata* to warming. *Front. Mar. Sci.* **9**, 1026321 (2022).
70. El-Khaled, Y. *et al.* *In situ* eutrophication stimulates dinitrogen fixation, denitrification, and productivity in Red Sea coral reefs. *Mar. Ecol. Prog. Ser.* **645**, 55–66 (2020).
71. Li, J., Chai, G., Xiao, Y. & Li, Z. The impacts of ocean acidification, warming and their interactive effects on coral prokaryotic symbionts. *Environ. Microbiome* **18**, 49 (2023).
72. van de Water, J. A. J. M., Allemand, D. & Ferrier-Pagès, C. Host-microbe interactions in octocoral holobionts - recent advances and perspectives. *Microbiome* **6**, 64 (2018).
73. Inoue, S., Kayanne, H., Yamamoto, S. & Kurihara, H. Spatial community shift from hard to soft corals in acidified water. *Nat. Clim. Change* **3**, 683–687 (2013).

Chapter 6 | Microbial fuel cells in coral reef sediments as indicator tools for organic carbon eutrophication



Sewage pipe draining into a coral reef on Koh Tao, Thailand. Photo by Heinz Krimmer.

Chapter 6 | Microbial fuel cells in coral reef sediments as indicator tools for organic carbon eutrophication

Bianca M. Thobor^{1*}, Federica R. Schanz¹, Anna Förster⁴, Sven Kerzenmacher^{2,3}, and Christian Wild^{1,3}

¹Faculty of Biology and Chemistry, University of Bremen, 28359 Bremen, Germany

²Faculty of Production Engineering - Mechanical Engineering & Process Engineering, University of Bremen, 28359 Bremen, Germany

³Center for Environmental Research and Sustainable Technology (UFT), 28359 Bremen, Germany

⁴Faculty of Physics / Electrical Engineering, University of Bremen, 28359 Bremen, Germany

*Corresponding author: thobor@uni-bremen.de

6.1 Abstract

Eutrophication with organic carbon (OC) can be harmful for corals and their reefs due to its stimulating effects on associated and sedimentary microbes, leading to oxygen deficits. Mitigation measures require real-time monitoring of wastewater pulses close to coral reefs, where biogenic carbonate sands act as biocatalytic filters for OC. Microbial fuel cells (MFCs) where the anode is deployed in sediments and the cathode is in contact with the overlying water can directly generate electricity from the microbial degradation of OC in sediments, but their application in coral reefs has not yet been tested. During a laboratory experiment, we thus investigated if MFCs, vertically deployed in coral reef sands, can be used as indicator tools for eutrophication with artificial wastewater (AW, prepared from organic compounds and chemicals) at OC concentrations of 20, 40, or 52 mg C L⁻¹ higher than controls. AW pulses were repeated three times at every concentration, with five weeks between the first and second pulse, and six months between the second and third pulse. Results revealed significant increases in current densities in all AW treatments (means up to 11, 36, and 39 mV m⁻², respectively), while controls remained stable and low (-1 to 3 mV m⁻²). Current densities and OC concentrations correlated significantly ($r_{\text{rm}} = 0.64$), and the slope of the correlation increased with each consecutive AW pulse. This highlights the functionality of the MFC as a qualitative indicator tool for OC pulses even months after deployment. The response time of the MFCs was fast (< 1 day) compared to other indicators for water quality (e.g., coral colony- or community measures that take weeks to years to respond), and they successfully detected OC concentrations expected for wastewater effluents. Measurements can be automated for continuous monitoring, and no laboratory facilities are required (as for OC analysis), making MFC sensors a suitable tool for remote locations. Overall, these findings emphasize the high potential of these low-cost (< 20 € per MFC) MFCs as indicator tools for OC pulses in coral reef environments.

Keywords: biosensor, coastal management, monitoring, benthic metabolism, pollution, sewage

An adapted version of this chapter has been published in *Ecological Indicators* **153**, 110385. <https://doi.org/10.1016/j.ecolind.2023.110385>

6.2 Introduction

It is predicted that 83 % of coral reefs will be affected by local stressors¹ such as eutrophication through terrestrial run-off and sewage discharge^{2,3}. This results in pollution of coastal ecosystems with inorganic nutrients (inorganic eutrophication) which can alleviate nutrient limitations of autotrophs⁴, and eutrophication with organic substances, where the containing carbon can provide energy for heterotrophs². For hard corals, the main ecosystem engineers of coral reefs⁵, organic eutrophication can disrupt the symbiosis with their associated microbiome^{6,7} which can lead to coral bleaching⁶ and mortality⁸. Organic eutrophication stimulates the microbial oxygen consumption in reef sediment^{9,10}, and in the water column^{11,12}, which can lead to the formation of hypoxic zones and mass coral mortality¹¹. Furthermore, eutrophication can lead to phase shifts towards macroalgae, which release organic matter (OM) that exacerbates the degradation of reefs^{13,14}. Past research has focused on the effects of inorganic eutrophication on corals^{15,16} and reefs^{17,18}, but with this building evidence for severe OM effects, the importance of monitoring and regulating coastal OM input increases^{2,8}.

Nutrient concentrations in the water can be highly variable on temporal and spatial scales due to hydrodynamics and fast turnover¹⁹. Additionally, water parameters alone provide no information on ecological relevance¹⁹ and represent only the condition at the time of sampling, whereas specific features of organisms or communities (i.e. bioindicators) may represent a time-integrated response²⁰. In order to detect acute pollution events and prevent large-scale shifts in reef benthic community composition, changes in water quality should be detected early and fast, which requires high temporal resolution of measurements²⁰. Coral reef microbiome compositions are fast and informative bioindicators^{21,22}, and may vary in calcareous sediments according to water quality²³. However, no method yet exists for continuous monitoring of the benthic microbial response to eutrophication.

Coral reef carbonate sands harbor high densities of bacteria and function as biocatalytic filter systems²⁴. Oxygen penetrates only the first few millimeters of coral reef sediment when hydrodynamics are low²⁵, highlighting the importance of anaerobic processes. The oxygen- and redox gradient between seawater and sediment can be used to generate electricity with microbial fuel cells (MFCs), where the anode is buried in anaerobic sediment and the cathode is exposed to oxygen in the overlying water (see illustrated principle of MFC in Fig. 6.1)²⁶⁻²⁸. Electrochemically active microbes in the sediment (exoelectrogens) donate electrons from the anaerobic oxidation of OM to the anode, which are transported to the cathode through an external circuit, and finally react with oxygen to form water (Lovley, 2006; Tender et al., 2002). In addition to power supply, MFCs can be used as biosensors for a range of water properties reviewed by Cui et al.³⁰. One use of MFC biosensors is to measure the amount of biologically degradable OM in wastewater treatment plants, based on the limitation of the electron flow by availability of OM³¹⁻³³. Studies using sediment MFCs as biosensors are scarce, but the design may provide higher stability than floating MFCs for *in situ* sensing shown previously³⁴.

Thus, our study aims to answer the question if MFCs deployed in coral reef carbonate sediments can be used as indicator tools for OM eutrophication from wastewater pulses. Cooper et al.²⁰ proposed that a good bioindicator for water quality should display: (i) a high specificity, meaning that the indicator responds to the stressor of interest alone; (ii) a high monotonicity; which means that both the intensity and the duration of the stressor are accurately displayed by the indicator; and (iii) a low background variability. In addition, a good bioindicator should be (iv) ecologically relevant, and (v) practical²⁰. We aim to address all of these criteria with regards to the tested MFCs. To accomplish this, we conducted a laboratory experiment where we exposed MFCs, developed for deployment in coral reef sands, to three concentrations of artificial wastewater (AW; 20, 40, or 52 mg OC L⁻¹ higher than controls). AW pulses were repeated three times at every concentration, with five weeks between the first and second pulse, and six months between the second and third pulse. Voltage (transformed into current density) was measured daily, and organic carbon (OC) content of the water column was used as a proxy for OM concentration and was measured weekly. If successful, these MFCs could be deployed *in situ* to monitor anaerobic microbial degradation of OM and may be used as continuous-measurement indicator tools for wastewater/ OM eutrophication in the future.

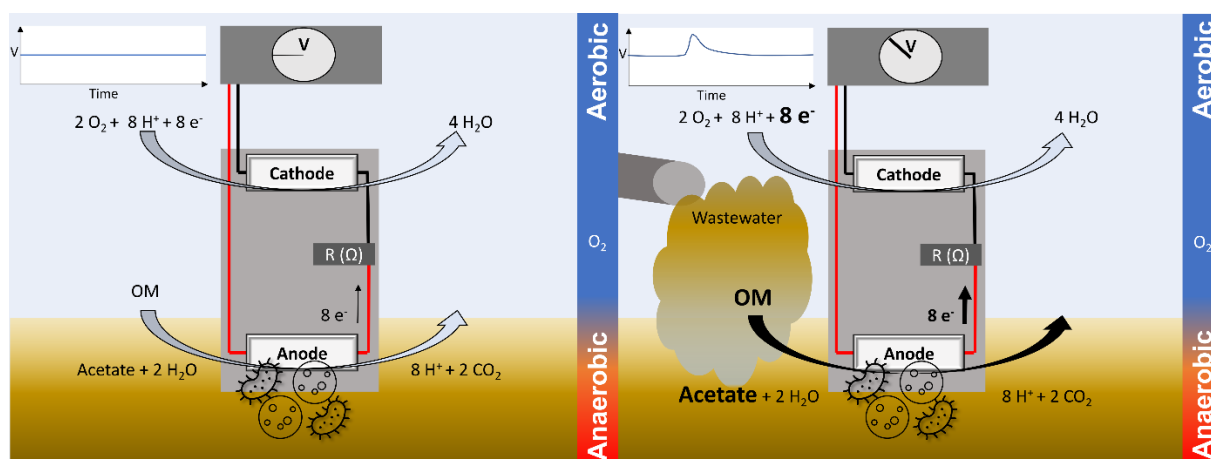


Figure 6.1. Simplified design and principle of microbial fuel cells (MFCs) where the anode is buried in anaerobic sediment and the cathode is in contact with oxygen in the water column. Organic matter (OM) fuels the donation of electrons (e-) to the anode, which are transported over an external resistor (R) to the cathode, where they react with oxygen to form water. This creates an electric potential difference which can be measured as voltage (V). When the concentration of OM increases due to wastewater input (right panel; bold black = stimulated), more e- are donated to the anode and the electric potential difference increases, which can be measured as a peak in V. Chemical reactions from Lovley (2006).

6.3 Material and methods

The microbial fuel cells

MFCs were constructed from polymethylmethacrylate (PMMA) frames which held electrodes and titanium wires (grade 1; $d = 0.2$ mm; AWG 32; Zivipf, Germany) in a vertical alignment, fixed with plastic screws (see simplified design in Fig. 6.1, and photographs of MFC in Fig. 6.2 a & c). The electrodes consisted of graphite felt (Sigracell® battery felt, SGL Carbon, Germany) with an active surface area of 4 cm² and a distance of 3 cm between anode and cathode. Anode and cathode were

connected over a 2 k Ω load resistor (MBB 0207-25; 0.1 %; Müttron, Germany), covered by a plastic box on top of the MFC. Wires extruding out of these boxes were connected to external luster terminals (2.5 mm²; 12 poles; 400 V; Bauhaus, Germany) for measurement of electrical potential difference (Volt) over the load resistor between anode and cathode.

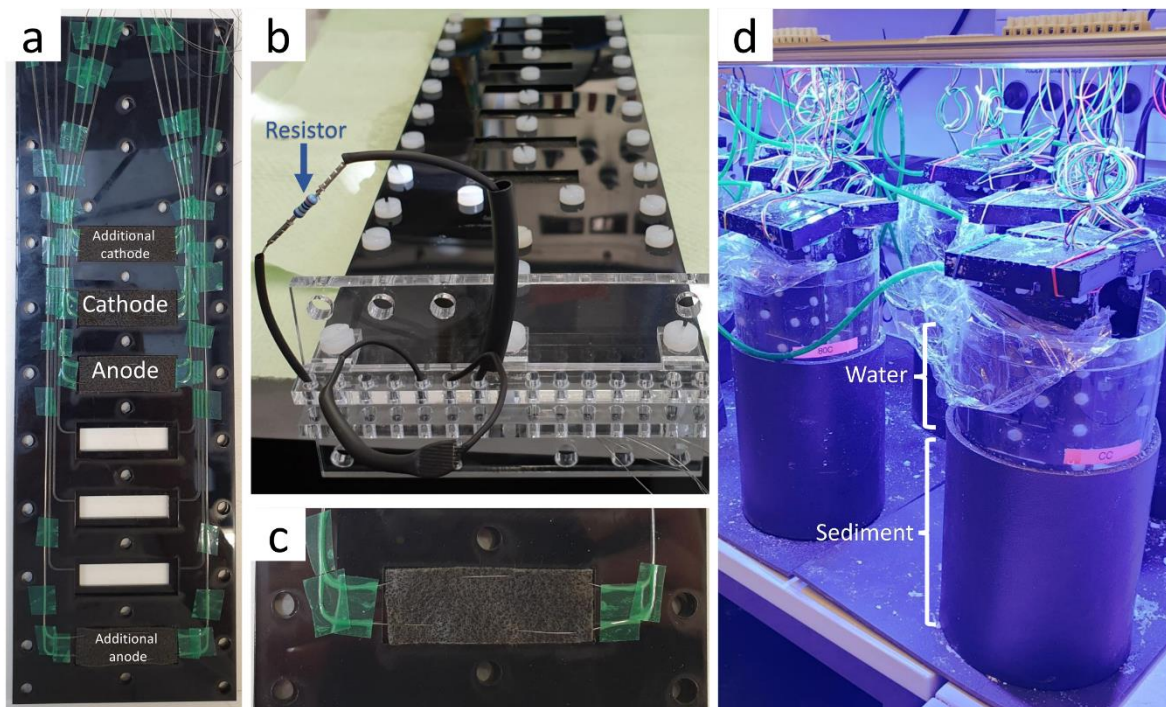


Figure 6.2. Construction of the microbial fuel cell (MFC, **a**, **b** & **c**) and deployment in tank microcosm (**d**). (**a**) Inside view of MFC with four electrodes (one additional set for comparisons between sediment depths, data not reported here). (**b**) Top view of closed MFC where one resistor is exposed (later covered by shrinking tube and plastic box). (**c**) Detailed view of one electrode made of graphite felt with two titanium wires woven through. (**d**) Experimental setup with two MFCs (one closed circuit and one open circuit) in every tank, filled with coral reef sediment to cover the anodes and artificial seawater to cover the cathodes.

Experimental conditions

Twelve tanks were filled with 1.85 L artificial seawater (deionized water with dissolved sea salt at ~ 34 %, ZooMix Sea Salt 10751, Tropic Marin, Switzerland) and natural coral reef sand (1-3 mm grain size) of 17 cm sediment depth (Fig. 6.2 d). The microbiome in experimental tanks developed from ambient microbes growing in the sediment and artificial seawater, and was selected for by coral reef-like conditions (i.e., natural coral reef sediment, artificial seawater). Black plastic wrappings on the outside ensured no sideways light penetration of the sands. MFCs were deployed vertically in the tanks, with the anode in the sand at a sediment depth of 2-3 cm, and the cathode in the overlying water column. A second, open circuit MFC was deployed in every tank to monitor open circuit electrode potentials of the cathode (Supplementary Fig. S6.1) and anode (results not displayed here) in relation to a saturated calomel electrode (SCE). To ensure aerobic conditions in the water column, air pumps (Eheim air100, Eheim GmbH & Co. KG, Germany) were active at all times. Light modules above each tank (Ultra Blue White, daytime LED; Waltron GmbH, Germany) simulated natural light:dark cycles of

12:12 h. Salinity and temperature were measured daily, and salinity was adjusted to approximately 34 ‰ if necessary (i. e., ranged between 33 and 35 ‰), while temperature was monitored only and ranged between 21.3 and 24.3 °C. Clinging wrap was used to cover the tanks to reduce evaporation. AW stock sub-solutions were prepared according to DIN 11733 (2004) for domestic wastewater by dissolving specific organic compounds and chemicals (listed in Table 6.1) in artificial seawater (ZooMix Sea Salt, Tropic Marin AG, Switzerland). Stock sub-solutions were stored for a maximum of two days at 4 °C in the dark. AW was prepared by mixing equal parts of stock sub-solutions A-E (Table 6.1), resulting in final OC concentrations of 109 mg OC L⁻¹ ± 3 SD. Three tanks were allocated to either control (no AW addition, 2 mg OC L⁻¹ ± 1 SD), low AW (peaks at 20 mg C L⁻¹ ± 4 SD), medium AW (peaks at 40 mg OC L⁻¹ ± 10 SD), and high AW (peaks at 52 mg OC L⁻¹ ± 6 SD) treatments. These concentrations of OC are within the range of wastewater treatment plant effluents³⁵. Electric potential differences (U) over the 2 kΩ load resistor (R) were measured daily and current (I) was calculated (Formula 6.1) and divided by the geometric surface area of the anode for current density.

$$I = \frac{U}{R} \quad \text{(Formula 6.1)}$$

The first 25 days after the initiation of the MFCs were not displayed, as microbial biofilms presumably formed, and electric potential differences increased until they reached a stable state. Afterwards, baseline values were recorded for 10 days, and the first AW pulse was initiated on day 36 in the evening after the daily measurement of electric potential differences. Treatment-specific OC concentrations were achieved by displacing calculated volumes of artificial seawater with the AW stock solution. The next measurement was conducted 12-15 h afterwards, to give the AW time to settle down and for the electric potential differences to stabilize. Five weeks after the first AW pulse, on day 71, a second AW pulse was initiated as described above. Afterwards, the electric potential differences were continuously measured without any AW addition, and no OC measurements were conducted for 6 months. On day 264, a third AW pulse was initiated as described above.

Table 6.1. Chemical composition of artificial wastewater (AW) stock sub-solutions to prepare AW according to the German Institute for Standardization (DIN) 11733 (2004) for domestic wastewater. All compounds were dissolved in artificial seawater.

Sub-solution	Compound	Chemical formula	Concentration (g L ⁻¹)	% (of g L ⁻¹)
A	Peptone from casein	-	2	27
B	Meat extract	-	1	13
C	Glucose monohydrate	C ₆ H ₁₂ O ₆ * H ₂ O	0.2	3
D	Ammonium chloride	NH ₄ Cl	0.21	3
	Potassium dihydrogen phosphate	KH ₂ PO ₄	0.04	< 1
	Disodium hydrogen phosphate dihydrate	Na ₂ HPO ₄ * 2H ₂ O	0.36	5
	Sodium hydrogen carbonate	NaHCO ₃	2.94	39
	Sodium chloride	NaCl	0.58	< 1
E	Iron (III) chloride hexahydrate	FeCl ₃ * 6H ₂ O	0.4	5

Organic carbon measurements

OC concentrations in the water column were measured weekly with high-temperature catalytic oxidation (TOC-L, Shimadzu, Germany). The first OC measurement after each AW pulse was done approximately

12 h after AW addition. Because the OC concentration measurements were conducted without acidification of the samples to a pH of 2-3³⁶, dissolved inorganic carbon (DIC) was not removed, resulting in very high measured concentrations of OC + DIC in control tanks (20 mg L⁻¹ ± 5 SD). From the measured OC + DIC, OC was estimated using Formula 6.2 for every measurement day. To calculate the % DIC content in the samples from control tanks, AW was first measured with the same method as used for the samples, and then acidified to pH < 2 and re-measured. This resulted in 89 % decrease of measured OC concentrations (from 20.6 to 2.2 mg L⁻¹). To estimate the amount of OC in the samples ($OC_{estimated}$), assuming constant DIC contents in all tanks, we calculated the mean amount of DIC of the three controls for every measurement day (i.e., 89 % of the mean measured value $OC + DIC_{controls}$) and subtracted this from all measured values ($OC + DIC_{all}$), including the tanks with elevated OC from AW. Thus, the relative differences between all tanks remained the same.

$$OC_{estimated} = OC + DIC_{all} - ((OC + DIC_{controls}) * 0.89) \quad (\text{Formula 6.2})$$

Statistical analyses

Outliers were excluded when voltage measurements indicated a malfunctioning of the MFC or of the measuring device (one replicate of: day 88, medium AW; day 105, high AW). The effect of AW pulses on electrical signals of the MFCs was tested with mixed-effects models of the R package *nparLD* for nonparametric analysis of longitudinal data, which provides the robust ANOVA-type statistic, and the classical Wald-type statistic³⁷. For this, the average current density of each MFC and experimental phase was used. “Treatment” was used as between- and “phase” as within-subjects factor. To investigate the effect of “phase” on each individual treatment, four separate tests with “phase” as single, within-subject factor were conducted, and the alpha level was Bonferroni adjusted. As *post-hoc* tests, Wilcoxon’s pairwise comparison tests were conducted with Bonferroni adjustment, and pooled data for every phase of the experiment (i.e., B1-B4, see Fig. 6.3). A similar method was used in a previous study to describe the development of MFC signals over time³⁸. *Post-hoc* tests were conducted separately for the first and second observation period (i.e., days 26 to 106 and 254 to 299) because values were generally higher during the second observation period (see different y axes for Fig. 6.3 a & b). To assess the relationship between current density of MFCs and OC concentration, temperature, and salinity, repeated measures correlation analyses were conducted with the R package *rmcorr*³⁹. For this, controls were excluded to enable parametric testing after transformation of current densities with the R package *LambertW* and the function *Gaussianize*. Afterwards, normal distribution and homogeneity of variance were tested visually, and no extreme outliers were detected (*rstatics* package). To compare the relationship of current density and OC concentration between the three AW pulses, spearman’s rank correlations were conducted for the first measurement day after every AW pulse.

6.4 Results

Response of current densities to three consecutive wastewater pulses

Current densities measured in control tanks without addition of AW were low, with daily averages ranging from $-1.3 (\pm 1.4 \text{ SD})$ to $2.9 (\pm 3.8 \text{ SD}) \text{ mA m}^{-2}$ (Fig. 6.3). Before the first eutrophication pulse (phase B1), current densities in all treatments were within the range of controls (-1.6 to 0.25 mA m^{-2}). The treatment effect on current densities varied significantly between phases of the experiment (Wald-Type Statistic = 209.87, $p < 0.001$; ANOVA-Type Statistic = 6.50, $p < 0.001$). All three AW treatments resulted in significant changes of current densities between phases of the experiment, while there was no significant change observed in controls (Table 6.2).

After the first AW pulse on day 36, current densities increased significantly to maximal values of 11.5 and 8.4 mA m^{-2} , in medium and high AW treatments, respectively (Fig. 6.3). Current densities in all AW treatments were significantly enhanced for the following 10 days (phase P1.2, Table 6.3). Two weeks after the first AW pulse (phase B2), current densities in the high AW treatment were similar to baseline values (B1) but remained significantly enhanced in the medium and low AW treatments until the initiation of the second eutrophication pulse five weeks after the first pulse (Fig. 6.3, Table 6.3).

After the second AW pulse on day 71, the medium and high AW treatments reached new maximal current densities of 38.1 and 31.6 mA m^{-2} , respectively (phase P2, Fig. 6.3) and were significantly enhanced compared to the previous phase B2 (Table 6.3). Current densities of all three treatments remained significantly enhanced compared to initial values (i.e., phase B1, Table 6.3) up to five weeks after the second pulse (phase B3).

Six months after the first observation period (phase B3.2), current densities in the medium and high AW treatments were still elevated compared to controls (Fig. 6.3, Table 6.3). The third wastewater pulse (phase P3) resulted in significant increases of current densities in all AW treatments, with new maximal current densities of 70.8 and 65.8 mA m^{-2} in the medium and high AW treatments (Fig. 6.3, Table 6.3). During the following five weeks, the medium AW treatment displayed a decline in current densities back to the range of values recorded before the third AW pulse (phase B3.2), while current densities in the high AW treatment (two of the three replicates) remained high over the next five weeks until the end of the experiment.

Table 6.2. Results of nonparametric analysis of longitudinal data (nparLD) with phase of the experiment as single, within-subjects factor for controls and three artificial wastewater (AW) treatments. Reported are the Wald-Type Statistic (WTS) and ANOVA-Type Statistic (ATS) with respective degrees of freedom (df) and p values. The alpha-level to identify a significant effect of “phase” (indicated by an asterisk) was set to $p = 0.0125$ (Bonferroni adjusted).

Treatment	WTS (df)	p (WTS)	ATS (df)	p (ATS)
Control	2.27 (2)	0.32	4.08 (1.6)	0.03
Low AW	2.56 (2)	0.28	7.92 (1.6)	< 0.001*
Medium AW	1.94 (2)	0.38	9.18 (1.4)	< 0.001*
High AW	66.97 (2)	< 0.001*	20.27 (1.0)	< 0.001*

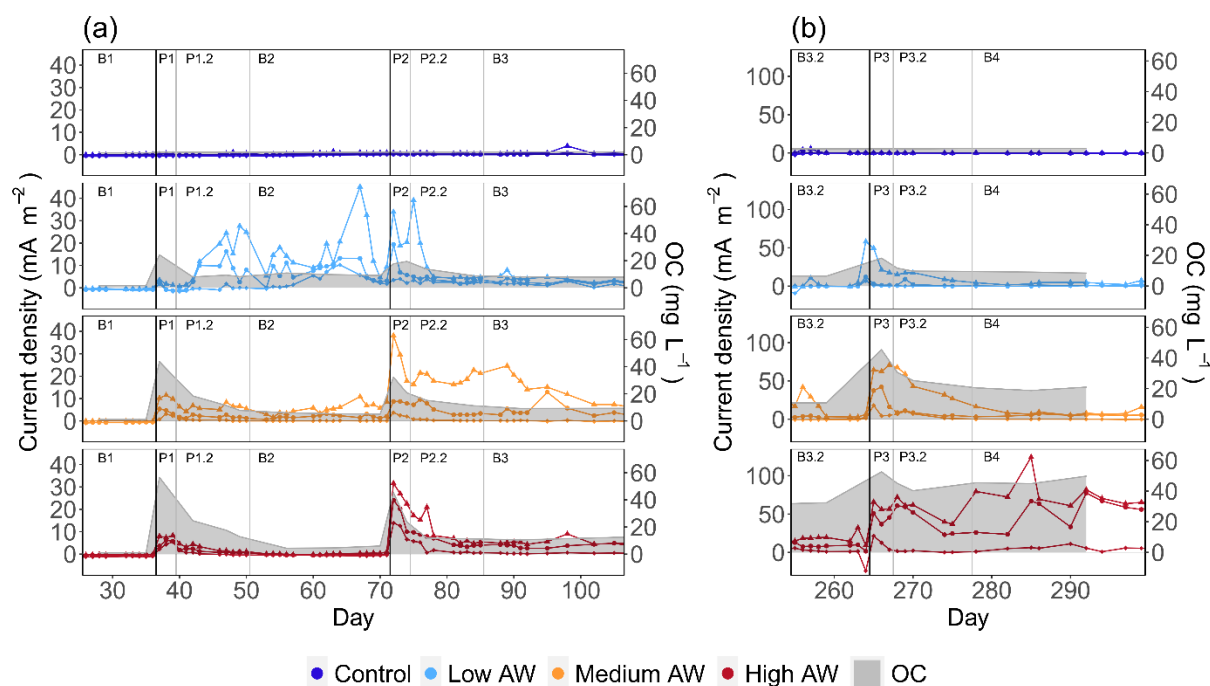


Figure 6.3. Current density (mA m^{-2}) of closed-circuit microbial fuel cells (MFCs) and mean organic carbon (OC) concentrations (mg L^{-1}) from days 26 to 106 (a) and days 254 to 299 (b) at three concentrations of artificial wastewater (AW) eutrophication (measured in mg OC L^{-1}) and controls. Black vertical lines indicate eutrophication pulse initiation on days 36, 71, and 264. Black and grey vertical lines indicate distinction of experimental phases. B1-B4: baseline; P1-P3: pulse (see statistical analysis results and mean current densities for every phase in Table 6.3). Each line represents one replicate MFC (distinguishable by different shapes). Grey area indicates mean OC concentration in three tanks of the respective treatment. Raw data to this figure is available online in supplementary data 2 (<https://doi.org/10.1016/j.ecolind.2023.110385>).

Table 6.3. Mean current density (CD) of microbial fuel cells (MFCs) for every treatment of artificial wastewater (AW) addition (Pulse = mean organic carbon concentration during phases P1, P2, and P3) and phase of the experiment. Sig. = Results of Wilcoxon's tests (when $nparLD$ was significant, see Table 6.2), different letters represent significant differences between phases (pooled data) within each treatment ($p < 0.05$; Bonferroni adjusted). Statistical tests were conducted separately for the first and second test period. Days 1 - 25 are not shown because they represent the initiation period of the MFC. Days = days since the initiation of the MFCs. MDs = measurement days, each with 3 replicates per treatment ($n = 3 \times \text{MDs}$). Phase = experimental phase, see Fig. 6.3.

Time		Control ~ 2 mg OC L^{-1}	Low AW Pulse: ~ 20 mg OC L^{-1}	Medium AW Pulse: ~ 40 mg OC L^{-1}	High AW Pulse: ~ 52 mg OC L^{-1}		
Phase	Days (MDs)	CD (mA m^{-2})	Sig. CD (mA m^{-2})	Sig. CD (mA m^{-2})	Sig. CD (mA m^{-2})		
B1	26-36 (9)	-0.32	A	-0.46	A	-0.56	
P1	37-39 (3)	-0.19	AB	0.78	BC	5.67	
P1.2	40-50 (8)	-0.15	BCD	6.23	B	2.86	
B2	51-71 (16)	0.18	D	9.05	B	2.47	
P2	72-74 (3)	0.29	D	12.75	C	13.25	
P2.2	75-85 (9)	0.30	CD	5.54	BC	8.17	
B3	86-106 (9)	0.41	BC	2.91	BC	6.29	
B3.2	254-264 (8)	0.21	A	3.23	A	5.61	
P3	265-267 (3)	-0.10	B	10.58	C	35.63	
P3.2	268-278 (6)	-0.11	B	4.61	BC	17.38	
B4	279-299 (8)	-0.26	B	1.65	AB	4.64	
						B	45.81

Relationship of current density with OC concentration, temperature, and salinity

A repeated measures correlation analysis of current densities and OC concentrations revealed a positive correlation ($r_{(179)} = 0.64$, 95 % CI = 0.54 - 0.72, $p < 0.001$, Fig. 6.4 a, Supplementary Fig. S6.2 a). From all current density measurements above 2.9 mA m^{-2} (the highest daily mean current density in controls), 95 % also displayed OC concentrations above 3.3 mg L^{-1} (the maximal OC concentration found in

controls). Values below 2.9 mA m^{-2} were not indicative for low OC concentrations, as 47 % were measured at OC concentrations above 3.3 mg L^{-1} . The percentage of measurements above the current density threshold for controls increased with increasing OC concentrations, from 6 % at OC concentrations below 3.3 mg L^{-1} to 81 % at OC concentrations above 40 mg L^{-1} (Fig. 6.4 a). Current density did not correlate with temperature (Fig. 6.4 b, Supplementary Fig. S6.2 b) or salinity (Fig. 6.4 c, Supplementary Fig. S6.2 c). Current densities from the day after each of the three AW pulses displayed significant positive Spearman's rank correlations with OC concentrations and increasing slopes over the course of the experiment (Fig. 6.5).

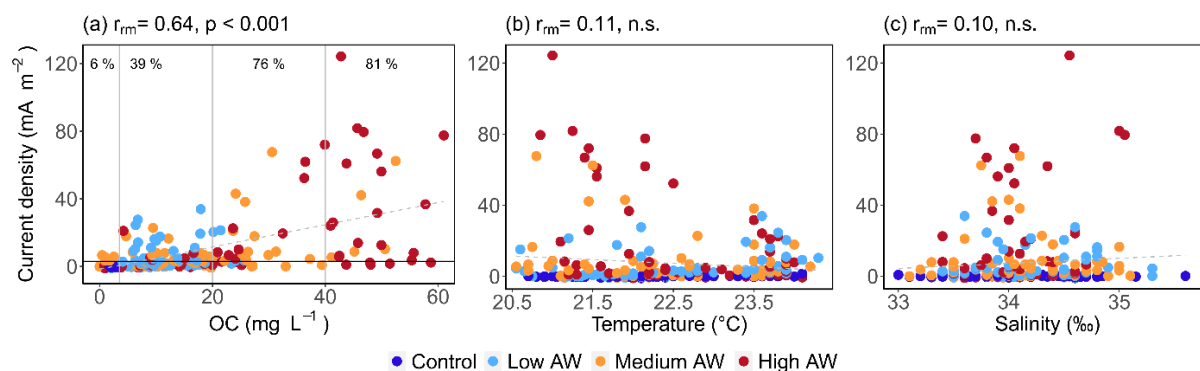


Figure 6.4. Current density of microbial fuel cells (MFCs) over (a) organic carbon (OC) concentration, (b) temperature, and (c) salinity, for three artificial wastewater (AW) treatments and controls, and all days with simultaneous measurements of all three parameters (21 days). To test for correlations, repeated measures correlation analysis (rmcorr) was conducted with transformed current density data (see Supplementary Fig. S6.2). Grey line represents linear regression and is dashed because data is non-parametric. Percentage values in (a) indicate the ratio of measurements above a current density of 2.9 mA m^{-2} (black horizontal line), separated into four groups of OC concentrations (grey vertical lines at 3.3, 20, and 40 mg L^{-1}). Raw data of this figure is available online in supplementary data 3 (<https://doi.org/10.1016/j.ecolind.2023.110385>).

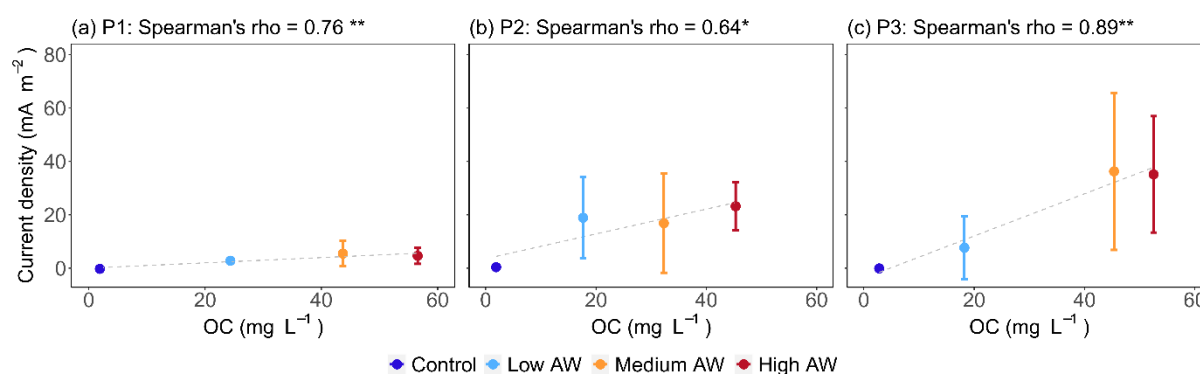


Figure 6.5. Current density over organic carbon (OC) concentration for the first measurement after each artificial wastewater (AW) pulse (P1-P3) for three AW treatments and controls. Spearman's rho was determined from current density and OC concentrations of the twelve experimental tanks, which are displayed as means with standard deviations per treatment ($n = 3$). Grey line represents linear regression and is dashed because data is non-parametric. Raw data of this figure is available online in supplementary data 3 (<https://doi.org/10.1016/j.ecolind.2023.110385>).

6.5 Discussion

To evaluate the performance of the presented MFCs in coral reef carbonate sediments as indicator tools for water quality, we will now discuss how they met each of the five criteria proposed by Cooper et al.²⁰.

Specificity

Without addition of AW (phases B1 and controls), mean daily current densities ranged between -1.6 and 2.9 mA m⁻², and after AW addition current densities increased by more than one order of magnitude in the high AW treatment (i.e., mean of 38.8 mA m⁻²). This is within the range detected by sediment MFCs in Tokyo Bay, an eutrophic coastal area⁴⁰. When using the maximal control values (current density of 2.9 mA m⁻²; OC concentration of 3.3 mg L⁻¹) as thresholds, higher current densities were almost always (95 %) indicative for elevated OC concentrations. The opposite could not be observed, as current densities below the threshold were equally common at low and elevated OC concentrations. Higher OC concentrations lead to increased chances of measuring current densities above the control threshold. Combined, these results indicate that the detection of OC eutrophication with the tested MFCs was conservative, and most reliable at OC concentrations above 40 mg L⁻¹. MFCs displayed a correlation coefficient of 0.64 with OC concentrations in the water. Previous studies on MFC biosensors for the detection of organic substances in water achieved higher correlation coefficients, but used certain microbial cultures^{32,33}, added only one type of substrate at a time^{32,41}, used membranes to separate the electrodes^{31-33,41}, and/or pumps to achieve stable substrate concentrations^{31,41}. However, these types of biosensors are less suitable for *in situ* deployment, and MFC electrodes in direct contact with the environment are affected by a variety of factors, resulting in higher variation of response signals³⁸. Another source of variation in the present study could be that the OC determination was based on values in the water column, although MFCs metabolize organic matter in the sediment²⁹, where OC may accumulate⁴². Future experiments should therefore measure sediment OC content in proximity to the anode. In addition, power generation of MFCs is limited by transfer of electrode reactants and/or products (i.e., OC or oxygen), and the threshold for this can be estimated with power density curves²⁶. In the present study, power density was limited at approximately 20 mA m⁻² (Supplementary Fig. S6.3) in the high AW treatment, likely caused by limitation of oxygen availability at the cathode. Future MFC designs could be improved by increasing the cathode to anode ratio⁴³.

Current densities did not correlate with temperatures, contrasting previous studies with MFCs^{31,38,44}. This could be explained by the relatively narrow temperature range in the present study (i.e., ~ 20 to 24 °C) compared to previous studies with MFCs where temperatures were changed by 10 to 30 °C^{38,44-46}. In general, temperature effects on MFC performance can be expected due to increased metabolic rates of microbes attached to the anodes³¹. However, Di Lorenzo et al.³¹ found only a 14 % increase in current produced by an MFC when increasing temperatures from 20 to 25 °C, while an increase from 25 to 30 °C resulted in an increase of 72 %, highlighting that the effect of temperatures is not linear and depends on the optimum for the microbial community. To avoid false interpretation due to compounding effects

of temperature fluctuations, temperature sensors should be included in *in situ* MFC designs. Changes in salinity in the range between 33 and 35 ‰ did not affect MFC current densities, supporting a previous MFC study with small variation in salinity³⁸. However, salt enhances water conductivity and can thus enhance MFC performance⁴⁵. In addition, saline water has a lower oxygen saturation value, which can reduce cathode performance⁴⁷. During flooding events, coral reefs can be exposed to salinities below 30 ‰⁴⁸, which could have short-term effects on MFC signal strength and should be considered during *in situ* studies.

MFCs can also be used to monitor oxygen concentrations through limitation of electron flow at the cathode⁴⁹⁻⁵¹, and this principle was proposed to detect eutrophication events when algal blooms increase oxygen concentrations^{49,50}. Wastewater eutrophication can enhance MFC current densities due to supply of OM, while it may also lead to reduced oxygen concentrations in the water column¹¹, reducing MFC current densities. In theory, these antagonistic effects could impede the detection of eutrophication with MFCs. However, as oxygen depletion generally starts close to the sediment-water interface¹¹, we propose to include several cathodes at different water depths into future MFC designs, as done by Song et al.⁵¹ in a lake. With this design, differences in current densities between cathodes can inform about oxygen stratification⁵¹, while the shared trends in current densities can inform about OM input. Depth of oxygen penetration in the sediment can also impact MFC performance when the anode gets exposed to oxygen, and is dependent on turbulence²⁵. Therefore, we suggest placing MFCs at locations protected from high turbulence and burying the anode below the maximal oxygen penetration depth. In addition, inorganic nutrients in wastewater can act as alternative electron acceptors in the anaerobic sediment^{52,53}. This likely impacted MFC performance in the present study but did not hinder the detection of AW pulses. MFC current densities can also be affected by the presence of toxins⁵⁴, which may occur in wastewater and can reduce microbial activity, thus working against the detection of OM⁵⁵. These interfering factors support that sediment MFCs should primarily be used as qualitative indicator tools for early warning of OM eutrophication⁵⁶, to be followed up with conventional measurements of water quality and coral reef community health (e.g.²⁰).

Monotonicity

Current densities of the tested MFCs displayed monotonicity of intensity to some extent, as they correlated significantly with OC concentrations in the water. The slope of the correlation increased over time with each consecutive AW pulse, which could be explained by a continuously growing microbial community on the anode, and changes in microbial community compositions towards dominance of exoelectrogens^{57,58}. High AW eutrophication could also have caused the formation of biogas bubbles from methanogens in the anaerobic sediment, which can lead to high variation in MFC electrical output⁵⁸. An additional explanation for variation with medium and high AW eutrophication could be that the cathodic biofilm, which catalyzes the oxygen reduction⁵⁹, became more anoxic due to increased respiration and the formation of an oxygen depleted boundary layer. Oxygen was not directly measured

in the present study, but open-circuit measurements of an additional cathode placed in the same experimental tanks revealed drops in the electrode potentials measured against an SCE after all AW pulses (Supplementary Fig. S6.1), indicating oxygen limitation³⁰. Thus, after AW pulses, the generation of electricity by the MFCs was limited by oxygen availability at the cathode (as final electron acceptor). This could be alleviated by increasing the flow rate of water across the cathode⁶⁰. As water flow in the experimental tanks was only stimulated by the aeration system and no pump was included, flow rates are expected to be higher *in situ*, possibly reducing the oxygen limitation.

The measured current densities also reflected the durations of elevated OC concentrations. Two weeks after the first high AW pulse (phase B2), OC was removed almost completely from the water column, while current densities returned to baseline values. After the second AW pulse, the OC concentrations remained elevated for six months, reflected by elevated current densities in two out of three MFCs previously exposed to high AW (phase B3.2). Sediment OM content close to anodic biofilms declines over time, and the OM composition changes towards more complex molecules because components with lower structural complexity and molecular size are more susceptible to microbial degradation⁶¹. Furthermore, microbial degradation of OM depends on the ability of the microbial community to metabolize them⁶². Thus, durations of MFC responses to OC pulses are influenced by the substrate composition and the microbial community composition of their biogenic anodes. The differences in current densities between treatments six months after the second AW pulse suggests that the tested MFCs can indicate not only acute eutrophication pulses through peaks in current densities, but also chronic exposure to OM through differences in baseline current densities to unpolluted control sites. Future research should therefore investigate if there is a general relationship between baseline current densities and OM content of sediment in coral reefs. Power output from MFCs in lake sediment can be higher when initial (naturally occurring) OM content is elevated, but the relationship also depends on the microbial community composition present in the sediment^{58,63}. In addition, power output of MFCs can be negatively affected by excessive organic content due to methane production⁵⁸. Thus, comparison of baseline current densities between MFCs in different locations could provide some information on the relative OM content but is likely also influenced by local microbial community composition.

Variability

The background variability in control tanks without AW addition was low compared to the detected responses to AW eutrophication. This was likely due to low OC concentrations in the sediment resulting in low microbial growth on the electrodes. A general explanation for stability of biofilms on MFC anodes with mixed microbial communities is the “exclusion-exfoliation theory”⁶⁴. Here, the anodic biofilm remains thin and not diffusion limited because the fastest growing layer is the innermost layer on the anode surface, dominated by exoelectrogens, which pushes outwards and constantly “washes away” other heterotrophs. Factors that may affect baseline values are biofouling of the cathodes by marine organisms⁴⁰, or clogging⁶⁵, which both reduces oxygen availability at the cathode, and prevention

of this should be considered for future MFC designs. Furthermore, *in situ* MFC current densities can fluctuate with the day-night cycle due to fluctuating environmental oxygen concentrations⁴⁰, which is why they should be measured either continuously, or at a constant time of day.

Ecological relevance

The content of OM in coral reef water is generally low ($> 1 \text{ mg L}^{-1}$)¹⁴, and carbonate sands filter OM from the water column, allowing coral reefs to be highly productive in oligotrophic environments⁶⁶. However, 58 % of coral reefs globally are exposed to wastewater³, through intentional or unintended direct discharge of untreated sewage, or entire lack of sanitation⁶⁷. OM is a major component of wastewater⁶⁸, and in addition to the direct OM input, inorganic nutrients in wastewater cause biomass production by micro- and macroalgae, which release dissolved OM (DOM) into the water column and contribute to settlement of detritus as particulate OM (POM)^{14,69,70}. The marine benthos is highly sensitive to eutrophication and pollution⁷¹, and elevated OM content in coral reef sediment can promote the formation of benthic cyanobacteria mats⁷², which contribute to reef degradation⁷³. Organic eutrophication can enhance sedimental oxygen consumption (SOC)¹⁰, sulphate reduction²⁵, and nitrogen fixation⁷⁴ in coral reef sediments, and elevated sediment OC content can lead to reduced microbial diversity⁷¹. Continuous monitoring with MFCs could provide detailed insights into these microbial processes which affect ecosystem-scale nutrient cycling. Metabolic measurements of the benthos are time-integrated (i.e., reflect the conditions of a longer time period), because particles sink and accumulate there¹⁰. In addition, micro- and meiobenthic indicators respond to changes in water quality faster than communities of larger organisms²⁰, and especially microbial communities have a high potential for indicating environmental change^{22,75}. However, sequencing methods to analyse microbial community compositions are cost intensive, impeding real-time assessment⁷⁵. MFCs in coral reef sediments could provide a solution for this, as their electrical output responds to changes in microbial metabolism. As MFCs select for specific microbes that are capable to donate electrons to the anode⁵⁷, microbial community compositions may differ between MFC electrodes and the environment. Therefore, we propose MFCs as tools to target sampling efforts for analysing environmental microbial community compositions. OM is often not included in coral reef monitoring programs^{2,8}, and the use of MFCs as OM indicator tools could increase the awareness of OM eutrophication and help to direct management efforts.

Practicality

For early warning of pollution events, bioindicators with short response times are needed, which require high intensities of sampling²⁰. Continuous, on-line monitoring with MFCs requires low sampling effort, as the unit of measurement is an electric signal. Response times of MFCs are defined as the time needed until electrical output reaches a steady state after the OM concentrations are changed, and generally vary between $< 1 \text{ min}$ and 10 h ⁵⁶. In the present study, electrical output of MFCs was only measured once a day and was stable $\sim 15 \text{ h}$ after the AW pulse initiation. Future studies with automated measurements

should include higher temporal resolution to identify the exact response time of MFCs to eutrophication pulses in coral reef sediments, which is likely < 15 h. Response times of < 1 day are rare among other bioindicators. Examples are gene expression, RNA/DNA ratio, and symbiont photophysiology²⁰, which all require laboratory facilities and thus are lacking in practicality compared to MFCs.

Due to the low maintenance requirements, MFCs are useful tools to charge remote sensors, which has been tested in lakes⁷⁶, rivers^{28,77–79}, and marine environments^{27,28,80}. The highest achieved power density in the present study during chronic high AW exposure was 11.7 mW m⁻² with an external resistance of 68 kΩ (Supplementary Fig. S6.3). MFCs with similar electrode types (graphite plate) achieved power densities of 12 mW m⁻²⁷⁹ and 16 mW m⁻²²⁸, and were able to power a wireless telecommunication system, and a meteorological buoy, respectively. The meteorological buoy was powered with 36 mW, with an electrode area of 2.2 m²²⁸. Increasing electrode surface areas can be achieved through multiple geometries and materials, for example through stacked graphite plates²⁸, or carbon fibre brushes⁸⁰. Thus, the electrode area in the current study could easily be increased to ~ 3.1 m² to achieve power densities of 36 mW. It remains to be tested if *in situ* coral reef sediments harbour sufficient organic matter to make MFC sensors self-powered.

Another aspect for practicality of bioindicators is cost efficiency²⁰, which should consider material costs as well as costs associated to data collection, -analysis and maintenance¹⁹. Sediment MFCs can be built of inexpensive materials, because they do not require cation exchange membranes⁸¹, and no catalyst is needed, because the naturally growing biofilm catalyses the cathodic reaction⁸². The here presented MFCs were built with materials for < 20 € per MFC, though the design did not include power management- and data transmission systems which are required for *in situ* on-line monitoring. Sediment MFCs need little to no maintenance because they do not rely on battery power, and oxygen and OM are constantly supplied through water flow and sedimentation²⁶. Due to their low material costs, the here presented MFCs are suitable for integration in wireless sensor networks (WSNs)⁸³. WSNs enable monitoring of an area through the distribution of many low-cost sensors which are connected in a network and send their monitoring data to a base station equipped with a transmission system⁸³. For underwater monitoring, an additional intermediate station on the surface (e.g., a buoy) should be connected to the underwater network of MFCs / sensors (e.g., acoustic transmission), and the base station on the shore (e.g., radio transmission)⁸⁴. However, incorporating MFCs into a WSN poses various additional challenges, such as ensuring connectivity and robustness of the whole system⁸³. Interdisciplinary collaboration among the fields of marine ecology, environmental process engineering, electrical engineering, and computer science is necessary to proceed the development of MFCs as sensors for on-line monitoring of OC eutrophication in coral reefs.

Conclusion

MFCs in the present study were reliable in detecting AW pulses, and current densities were indicative for OC concentrations. However, drawbacks of MFCs are their sensitivity to changes in environmental

parameters like temperature and oxygen concentrations (i.e., limited specificity and monotonicity), which is why they should be used primarily as qualitative indicators. MFCs in control tanks did not generate any peaks in current density throughout the experiment (i.e., low variability). In addition, their fast response times of less than one day enable early detection of eutrophication pulses in sensitive coral reef ecosystems, which may allow fast management action before higher trophic levels of the community are impacted (i.e., high ecological relevance). The greatest benefits of MFC indicator tools in comparison to already established indicators for organic eutrophication (summarized in [Supplementary Table S6.1](#)) are the possibility for continuous monitoring, fast response times, low maintenance and sampling effort once the device is deployed, and potential for self-sustainability, as well as low material costs (i.e., high practicality). The findings of the present study that MFCs in coral reef sediments can be used as indicator tools for OM eutrophication for more than 6 months are a first step towards designing MFC sensors that are adjusted to *in situ* conditions in coral reefs.

6.6 Author contributions

B.M.T. analyzed and visualized data and wrote the original draft. F.R.S, S.K., and C.W. designed the experiment and developed methods. F.R.S. carried out the experiment and curated the collected data. S.K. and C.W. supervised and administered the project and acquired funding and resources. All authors read and revised the manuscript.

6.7 Acknowledgements

We would like to thank Lennart Lüdtkke and Melanie Müller for their assistance in data collection and maintenance of the experimental setup. In addition, we want to thank Manuela Romero, Maximilian Pfeiffer, Leon Wedemeyer, and Jan Treumann for their preliminary technical work on the MFCs used in this study. For their support in building the MFCs, we want to thank Dipl.-Ing. Ralf Nieswandt and Noah Āuriš. This work was supported by baseline funds of the University of Bremen.

6.8 References

1. Guan, Y., Hohn, S., Wild, C. & Merico, A. Vulnerability of global coral reef habitat suitability to ocean warming, acidification and eutrophication. *Glob. Change Biol.* **26**, 5646–5660 (2020).
2. Deininger, A. & Frigstad, H. Reevaluating the role of organic matter sources for coastal eutrophication, oligotrophication, and ecosystem health. *Front. Mar. Sci.* **6**, 210 (2019).
3. Tuholske, C. *et al.* Mapping global inputs and impacts from of human sewage in coastal ecosystems. *PLOS ONE* **16**, e0258898 (2021).
4. Smith, V. H., Joye, S. B. & Howarth, R. W. Eutrophication of freshwater and marine ecosystems. *Limnol. Oceanogr.* **51**, 351–355 (2006).

5. Wild, C. *et al.* Climate change impedes scleractinian corals as primary reef ecosystem engineers. *Mar. Freshw. Res.* **62**, 205 (2011).
6. Pogoreutz, C. *et al.* Sugar enrichment provides evidence for a role of nitrogen fixation in coral bleaching. *Glob. Change Biol.* **23**, 3838–3848 (2017).
7. Allgeier, J. E. *et al.* Rewiring coral: Anthropogenic nutrients shift diverse coral–symbiont nutrient and carbon interactions toward symbiotic algal dominance. *Glob. Change Biol.* **26**, 5588–5601 (2020).
8. Kline, D., Kuntz, N., Breitbart, M., Knowlton, N. & Rohwer, F. Role of elevated organic carbon levels and microbial activity in coral mortality. *Mar. Ecol. Prog. Ser.* **314**, 119–125 (2006).
9. Bayraktarov, E. & Wild, C. Spatiotemporal variability of sedimentary organic matter supply and recycling processes in coral reefs of Tayrona National Natural Park, Colombian Caribbean. *Biogeosciences* **11**, 2977–2990 (2014).
10. Ford, A. K. *et al.* High sedimentary oxygen consumption indicates that sewage input from small islands drives benthic community shifts on overfished reefs. *Environ. Conserv.* **44**, 405–411 (2017).
11. Altieri, A. H. *et al.* Tropical dead zones and mass mortalities on coral reefs. *PNAS* **114**, 3660–3665 (2017).
12. Nelson, H. R. & Altieri, A. H. Oxygen: the universal currency on coral reefs. *Coral Reefs* **38**, 177–198 (2019).
13. Wild, C., Niggli, W., Naumann, M. & Haas, A. Organic matter release by Red Sea coral reef organisms—potential effects on microbial activity and *in situ* O₂ availability. *Mar. Ecol. Prog. Ser.* **411**, 61–71 (2010).
14. Haas, A. F. *et al.* Global microbialization of coral reefs. *Nat. Microbiol.* **1**, 16042 (2016).
15. Wiedenmann, J. *et al.* Nutrient enrichment can increase the susceptibility of reef corals to bleaching. *Nat. Clim. Change* **3**, 160–164 (2013).
16. Silbiger, N. J. *et al.* Nutrient pollution disrupts key ecosystem functions on coral reefs. *Proc. R. Soc. B Biol. Sci.* **285**, 20172718 (2018).
17. Littler, M. M., Littler, D. S. & Brooks, B. L. Harmful algae on tropical coral reefs: Bottom-up eutrophication and top-down herbivory. *Harmful Algae* **5**, 565–585 (2006).
18. D’Angelo, C. & Wiedenmann, J. Impacts of nutrient enrichment on coral reefs: new perspectives and implications for coastal management and reef survival. *Curr. Opin. Environ. Sustain.* **7**, 82–93 (2014).
19. Fabricius, K. E. *et al.* A bioindicator system for water quality on inshore coral reefs of the Great Barrier Reef. *Mar. Pollut. Bull.* **65**, 320–332 (2012).

20. Cooper, T. F., Gilmour, J. P. & Fabricius, K. E. Bioindicators of changes in water quality on coral reefs: Review and recommendations for monitoring programmes. *Coral Reefs* **28**, 589–606 (2009).
21. Glasl, B. *et al.* Microbial indicators of environmental perturbations in coral reef ecosystems. *Microbiome* **7**, 94 (2019).
22. Glasl, B., Webster, N. S. & Bourne, D. G. Microbial indicators as a diagnostic tool for assessing water quality and climate stress in coral reef ecosystems. *Mar. Biol.* **164**, 91 (2017).
23. Uthicke, S. & McGuire, K. Bacterial communities in Great Barrier Reef calcareous sediments: Contrasting 16S rDNA libraries from nearshore and outer shelf reefs. *Estuar. Coast. Shelf Sci.* **72**, 188–200 (2007).
24. Wild, C. *et al.* Benthic metabolism and degradation of natural particulate organic matter in carbonate and silicate reef sands of the northern Red Sea. *Mar. Ecol. Prog. Ser.* **298**, 69–78 (2005).
25. Werner, U. *et al.* Spatial patterns of aerobic and anaerobic mineralization rates and oxygen penetration dynamics in coral reef sediments. *Mar. Ecol. Prog. Ser.* **309**, 93–105 (2006).
26. Reimers, C. E., Tender, L. M., Fertig, S. & Wang, W. Harvesting energy from the marine sediment–water interface. *Environ. Sci. Technol.* **35**, 192–195 (2001).
27. Tender, L. M. *et al.* Harnessing microbially generated power on the seafloor. *Nat. Biotechnol.* **20**, 821–825 (2002).
28. Tender, L. M. *et al.* The first demonstration of a microbial fuel cell as a viable power supply: Powering a meteorological buoy. *J. Power Sources* **179**, 571–575 (2008).
29. Lovley, D. R. Microbial fuel cells: Novel microbial physiologies and engineering approaches. *Curr. Opin. Biotechnol.* **17**, 327–332 (2006).
30. Cui, Y., Lai, B. & Tang, X. Microbial fuel cell-based biosensors. *Biosensors* **9**, 92 (2019).
31. Di Lorenzo, M., Curtis, T. P., Head, I. M. & Scott, K. A single-chamber microbial fuel cell as a biosensor for wastewaters. *Water Res.* **43**, 3145–3154 (2009).
32. Hsieh, M.-C., Cheng, C.-Y., Liu, M.-H. & Chung, Y.-C. Effects of operating parameters on measurements of biochemical oxygen demand using a mediatorless microbial fuel cell biosensor. *Sensors* **16**, 35 (2016).
33. Alferov, S. V., Arlyapov, V. A., Alferov, V. A. & Reshetilov, A. N. Biofuel cell based on bacteria of the genus *Gluconobacter* as a sensor for express analysis of biochemical oxygen demand. *Appl. Biochem. Microbiol.* **54**, 689–694 (2018).
34. Olias, L. G. & Lorenzo, M. D. Microbial fuel cells for in-field water quality monitoring. *RSC Adv.* **11**, 16307–16317 (2021).

35. Ahmad, M., Bajahlan, A. S. & Hammad, W. S. Industrial effluent quality, pollution monitoring and environmental management. *Environ. Monit. Assess.* **147**, 297–306 (2008).
36. Spyles, G., Nimmo, M., Worsfold, P. J., Achterberg, E. P. & Miller, A. E. J. Determination of dissolved organic carbon in seawater using high temperature catalytic oxidation techniques. *TrAC Trends Anal. Chem.* **19**, 498–506 (2000).
37. Noguchi, K., Gel, Y. R., Brunner, E. & Konietzschke, F. *nparLD*: An R software package for the nonparametric analysis of longitudinal data in factorial experiments. *J. Stat. Softw.* **50**, (2012).
38. Velasquez-Orta, S. B., Werner, D., Varia, J. C. & Mgana, S. Microbial fuel cells for inexpensive continuous *in-situ* monitoring of groundwater quality. *Water Res.* **117**, 9–17 (2017).
39. Bakdash, J. Z. & Marusich, L. R. Repeated measures correlation. *Front. Psychol.* **8**, 456 (2017).
40. Kubota, K. *et al.* Operation of sediment microbial fuel cells in Tokyo Bay, an extremely eutrophicated coastal sea. *Bioresour. Technol. Rep.* **6**, 39–45 (2019).
41. Quek, S. B., Cheng, L. & Cord-Ruwisch, R. Microbial fuel cell biosensor for rapid assessment of assimilable organic carbon under marine conditions. *Water Res.* **77**, 64–71 (2015).
42. Wild, C. *et al.* Coral sand O₂ uptake and pelagic–benthic coupling in a subtropical fringing reef, Aqaba, Red Sea. *Aquat. Biol.* **6**, 133–142 (2009).
43. Corbella, C., Hartl, M., Fernandez-gatell, M. & Puigagut, J. MFC-based biosensor for domestic wastewater COD assessment in constructed wetlands. *Sci. Total Environ.* **660**, 218–226 (2019).
44. Larrosa-Guerrero, A. *et al.* Effect of temperature on the performance of microbial fuel cells. *Fuel* **89**, 3985–3994 (2010).
45. Liu, H., Cheng, S. & Logan, B. E. Power generation in fed-batch microbial fuel cells as a function of ionic strength, temperature, and reactor configuration. *Environ. Sci. Technol.* **39**, 5488–5493 (2005).
46. Tremouli, A., Martinos, M. & Lyberatos, G. The effects of salinity, pH and temperature on the performance of a microbial fuel cell. *Waste Biomass Valorization* **8**, 2037–2043 (2017).
47. Guo, F., Luo, H., Shi, Z., Wu, Y. & Liu, H. Substrate salinity: A critical factor regulating the performance of microbial fuel cells, a review. *Sci. Total Environ.* **763**, 143021 (2021).
48. Berkelmans, R., Jones, A. M. & Schaffelke, B. Salinity thresholds of *Acropora spp.* on the Great Barrier Reef. *Coral Reefs* **31**, 1103–1110 (2012).
49. Olias, L. G., Otero, A. R., Cameron, P. J. & Di Lorenzo, M. A soil microbial fuel cell-based biosensor for dissolved oxygen monitoring in water. *Electrochim. Acta* **362**, 137108 (2020).
50. Olias, L. G., Otero, A. R., Cameron, P. J. & Lorenzo, M. D. Ceramic soil microbial fuel cells sensors for early detection of eutrophication. *Proceedings* **60**, 64 (2020).

51. Song, N. *et al.* Development of a sediment microbial fuel cell-based biosensor for simultaneous online monitoring of dissolved oxygen concentrations along various depths in lake water. *Sci. Total Environ.* **673**, 272–280 (2019).
52. Guo, F. & Liu, H. Impact of heterotrophic denitrification on BOD detection of the nitrate-containing wastewater using microbial fuel cell-based biosensors. *Chem. Eng. J.* **394**, 125042 (2020).
53. Saito, T. *et al.* Effect of nitrogen addition on the performance of microbial fuel cell anodes. *Bioresour. Technol.* **102**, 395–398 (2011).
54. Adekunle, A., Raghavan, V. & Tartakovsky, B. On-line monitoring of heavy metals-related toxicity with a microbial fuel cell biosensor. *Biosens. Bioelectron.* **132**, 382–390 (2019).
55. Jiang, Y. *et al.* Enhancing signal output and avoiding BOD/toxicity combined shock interference by operating a microbial fuel cell sensor with an optimized background concentration of organic matter. *Int. J. Mol. Sci.* **17**, 1392 (2016).
56. Jiang, Y., Yang, X., Liang, P., Liu, P. & Huang, X. Microbial fuel cell sensors for water quality early warning systems: Fundamentals, signal resolution, optimization and future challenges. *Renew. Sustain. Energy Rev.* **81**, 292–305 (2018).
57. Obata, O. *et al.* Development of efficient electroactive biofilm in urine-fed microbial fuel cell cascades for bioelectricity generation. *J. Environ. Manage.* **258**, 109992 (2020).
58. Zhao, Q., Li, R., Ji, M. & Ren, Z. J. Organic content influences sediment microbial fuel cell performance and community structure. *Bioresour. Technol.* **220**, 549–556 (2016).
59. De Schampelaire, L., Rabaey, K., Boeckx, P., Boon, N. & Verstraete, W. Outlook for benefits of sediment microbial fuel cells with two bio-electrodes. *Microb. Biotechnol.* **1**, 446–462 (2008).
60. He, Z., Shao, H. & Angenent, L. T. Increased power production from a sediment microbial fuel cell with a rotating cathode. *Biosens. Bioelectron.* **22**, 3252–3255 (2007).
61. Hong, S. W., Kim, H. S. & Chung, T. H. Alteration of sediment organic matter in sediment microbial fuel cells. *Environ. Pollut.* **158**, 185–191 (2010).
62. Dittmar, T. *et al.* Enigmatic persistence of dissolved organic matter in the ocean. *Nat. Rev. Earth Environ.* **2**, 570–583 (2021).
63. Song, N. & Jiang, H.-L. Effects of initial sediment properties on start-up times for sediment microbial fuel cells. *Int. J. Hydrog. Energy* **43**, 10082–10093 (2018).
64. Greenman, J. *et al.* Microbial fuel cells and their electrified biofilms. *Biofilm* **3**, 100057 (2021).
65. Cristiani, P. *et al.* Long term feasibility study of in-field floating microbial fuel cells for monitoring anoxic wastewater and energy harvesting. *Front. Energy Res.* **7**, 119 (2019).

66. Wild, C. *et al.* Coral mucus functions as an energy carrier and particle trap in the reef ecosystem. *Nature* **428**, 66–70 (2004).
67. Wear, S. L. & Vega Thurber, R. Sewage pollution: Mitigation is key for coral reef stewardship. *Ann. N. Y. Acad. Sci.* **1355**, 15–30 (2015).
68. Huang, M., Li, Y. & Gu, G. Chemical composition of organic matters in domestic wastewater. *Desalination* **262**, 36–42 (2010).
69. El Sayed, M. A., Al Farawati, R. Kh., El Maradny, A. A., Shaban, Y. A. & Rifaat, A. E. Environmental status and nutrients and dissolved organic carbon budget of two Saudi Arabian Red Sea coastal inlets: A snapshot statement. *Environ. Earth Sci.* **74**, 7755–7767 (2015).
70. Furnas, M., Mitchell, A., Skuza, M. & Brodie, J. In the other 90%: phytoplankton responses to enhanced nutrient availability in the Great Barrier Reef Lagoon. *Mar. Pollut. Bull.* **51**, 253–265 (2005).
71. Hyland, J. *et al.* Organic carbon content of sediments as an indicator of stress in the marine benthos. *Mar. Ecol. Prog. Ser.* **295**, 91–103 (2005).
72. Brocke, H. J. *et al.* High dissolved organic carbon release by benthic cyanobacterial mats in a Caribbean reef ecosystem. *Sci. Rep.* **5**, 8852 (2015).
73. Ford, A. K. *et al.* Reefs under siege—the rise, putative drivers, and consequences of benthic cyanobacterial mats. *Front. Mar. Sci.* **5**, (2018).
74. El-Khaled, Y. *et al.* In situ eutrophication stimulates dinitrogen fixation, denitrification, and productivity in Red Sea coral reefs. *Mar. Ecol. Prog. Ser.* **645**, 55–66 (2020).
75. Glasl, B. *et al.* Establishing microbial baselines to identify indicators of coral reef health. *Microbiol. Aust.* **39**, 42–46 (2018).
76. Zhang, F., Tian, L. & He, Z. Powering a wireless temperature sensor using sediment microbial fuel cells with vertical arrangement of electrodes. *J. Power Sources* **196**, 9568–9573 (2011).
77. Donovan, C., Dewan, A., Heo, D., Lewandowski, Z. & Beyenal, H. Sediment microbial fuel cell powering a submersible ultrasonic receiver: New approach to remote monitoring. *J. Power Sources* **233**, 79–85 (2013).
78. Donovan, C., Dewan, A., Peng, H., Heo, D. & Beyenal, H. Power management system for a 2.5 W remote sensor powered by a sediment microbial fuel cell. *J. Power Sources* **196**, 1171–1177 (2011).
79. Donovan, C., Dewan, A., Heo, D. & Beyenal, H. Batteryless, wireless sensor powered by a sediment microbial fuel cell. *Environ. Sci. Technol.* **42**, 8591–8596 (2008).
80. Gong, Y. *et al.* Benthic microbial fuel cell as direct power source for an acoustic modem and seawater oxygen/temperature sensor system. *Environ. Sci. Technol.* **45**, 5047–5053 (2011).

81. Gajda, I., Greenman, J. & Ieropoulos, I. A. Recent advancements in real-world microbial fuel cell applications. *Curr. Opin. Electrochem.* **11**, 78–83 (2018).
82. He, Z. & Angenent, L. T. Application of bacterial biocathodes in microbial fuel cells. *Electroanalysis* **18**, 2009–2015 (2006).
83. Förster, A. *Introduction to wireless sensor networks*. (John Wiley & Sons, 2016).
84. Fattah, S., Gani, A., Ahmedy, I., Idris, M. Y. I. & Targio Hashem, I. A. A survey on underwater wireless sensor networks: Requirements, taxonomy, recent advances, and open research challenges. *Sensors* **20**, 5393 (2020).

Chapter 7 | Correlation between mucus carbohydrate composition and phylogeny suggests co-diversification within scleractinian corals



Mucus production in *Meandrina meandrites* when exposed to air. Photo by Bianca Thobor.

Chapter 7 | Correlation between mucus carbohydrate composition and phylogeny suggests co-diversification within scleractinian corals

Bianca M. Thobor^{1*}, Arjen Tilstra¹, Benjamin Mueller^{1,2,3}, Andreas Haas⁴, Jan-Hendrik Hehemann^{5,6}, and Christian Wild¹

¹Department of Marine Ecology, University of Bremen, Bremen, Germany

²Department of Freshwater and Marine Ecology, University of Amsterdam, Amsterdam, the Netherlands

³CARMABI Foundation, Willemstad, Curaçao

⁴Department of Microbiology & Biogeochemistry, NIOZ Royal Netherlands Institute for Sea Research, Texel, The Netherlands

⁵Department of Marine Glycobiology, Max Planck Institute for Marine Microbiology, Bremen, Germany

⁶MARUM Centre for Marine Environmental Sciences, University of Bremen, Bremen, Germany

*Corresponding author: thobor@uni-bremen.de

7.1 Abstract

The mucus surface layer serves vital functions for scleractinian corals and consists mainly of carbohydrates. Its carbohydrate composition has been suggested to be influenced by environmental conditions (e.g., temperature, nutrients) and microbial pressures (e.g., microbial degradation, microbial coral symbionts), yet to what extent the coral mucus composition is determined by phylogeny remains to be tested. To investigate the variation of mucus carbohydrate compositions among coral species, we analysed the composition of mucosal carbohydrate building blocks (i.e., monosaccharides) for five species of scleractinian corals, supplemented with previously reported data, to discern overall patterns using cluster analysis. Monosaccharide composition from a total of 23 species (belonging to 14 genera and 10 families) revealed significant differences between two phylogenetic clades that diverged early in the evolutionary history of scleractinian corals (i.e., complex and robust; $p = 0.001$, $R^2 = 0.20$), mainly driven by the absence of arabinose in the robust clade. Despite considerable differences in environmental conditions and sample analysis protocols applied, coral phylogeny significantly correlated with monosaccharide composition (Mantel test: $p < 0.001$, $R^2 = 0.70$). These results suggest that coral mucus carbohydrates co-diversify with scleractinian coral phylogeny and support their essential role in the functioning of corals.

An adapted version of this chapter is currently under review at *Scientific Reports*.

7.2 Introduction

The metazoan surface mucus layer (SML) is an outermost protective barrier of exposed tissues¹, and first evolved in Cnidarians and Ctenophores². Mucus consists largely of water (95 %) and mucin glycoproteins (~ 3 %), which have a high (50 – 90 %) carbohydrate content in the form of glycans (oligo- and polysaccharides) attached to a protein backbone³, giving mucus its viscoelastic properties². Traditionally, mucus has been considered to serve important functions in metazoan defense, feeding and locomotion⁴. Moreover, its role in controlling associated microbial communities is increasingly recognized². Constant renewal of the SML serves a physical antimicrobial function^{2,5}, and chemical defenses include adhesion (entrapment) or the prevention of adhesion (dispersal) of microbes to mucin glycans^{2,6}. Changes in mucin glycan structures can reduce antimicrobial functions of mucus^{7,8}, and may lead to disease⁹, highlighting the importance of mucosal carbohydrates for metazoan health.

Corals are considered model systems for metazoan evolution^{2,10,11}, and scleractinian corals in particular are ecologically important due to their role as ecosystem engineers of tropical as well as cold water coral reefs^{12,13}. Mucus serves especially diverse functions in corals compared to other invertebrates¹⁴, including protection against environmental stressors (e.g., desiccation, UV radiation, and sediment smothering), supplementation of calcification, and quenching of potentially harmful oxygen radicals (reviewed by Brown and Bythell¹⁴), as well as colonial integration through mucus-coordinated surface flows¹⁵. Despite these important functions of coral mucus, little is known about the composition of coral mucus glycans, nor their phylogenetic variation.

The structural analysis of glycans is challenging due to the lack of distinct spectroscopic signatures¹⁶, and mass spectra of mucin-type glycans are especially complex and notoriously difficult to interpret¹⁷. To our best knowledge, only two studies investigated the structure of coral mucus glycans in detail through mass spectrometry of oligosaccharides cleaved from the protein backbone of mucins^{18,19}. A less challenging and more commonly used method for total carbohydrate analysis is the measurement of monosaccharide building blocks after acid hydrolysis of glycans through chromatographic methods²⁰, which provides insight into the composition of carbohydrates at the cost of losing structural information¹⁶. Scleractinian corals from different geographic locations displayed common mucus monosaccharides²¹, and Wild et al.²² found conserved monosaccharide compositions of coral mucus glycans on the genus level in *Acropora* and *Fungia*.

Phylogenetic dependence (i.e., related species resemblance) is often low for carbohydrates^{23,24}, due to the constant selection pressure from co-evolving pathogens²⁵ and microbial degradation²⁶ (i.e., Red Queen effect / arms race). In addition, several factors can contribute to inter- and intraspecific variation in coral mucus. Firstly, coral mucus release rates and/or compositions can be influenced by environmental variables like water temperature^{27–29} and nutrient enrichment³⁰. Secondly, microbial communities associated with coral mucus can vary with environmental conditions³¹, potentially resulting in composition adaptations. Finally, endosymbiotic dinoflagellates of the family

Symbiodiniaceae³² are majorly involved in mucus production^{33–35}, and likely contribute to shaping mucus composition^{36,37}.

This raises the question whether the previously suggested phylogenetic dependence in coral mucus carbohydrate compositions is limited to the genus level²², or if it also applies to broader taxonomic groups. Scleractinian corals diverged into two main clades (i.e., “complex”, and “robust”) about 418 million years ago³⁸, which have few morphological differences, but can be discerned on a molecular level^{39,40}. We hypothesized that (1) mucus carbohydrate compositions are most different between the complex and robust clade and that (2) the phylogeny of scleractinian corals correlates with the composition of coral mucus carbohydrates, indicative for co-diversification. For the investigation, we analyzed the monosaccharide composition of hydrolyzed mucus glycans from five species of scleractinian corals (i.e., *Acropora cervicornis*, *Diploria labyrinthiformis*, *Meandrina meandrites*: collected *in situ* in the Caribbean; *Montipora digitata*, and *Montipora confusa*: grown *ex situ* in Bremen, Germany) and combined our results with reported literature data (total of 23 species from 14 genera and 10 families).

7.3 Results

Monosaccharide composition of mucosal carbohydrates

The monosaccharide compositions of mucosal carbohydrates of the five species analysed in the present study (i.e., *A. cervicornis*, *D. labyrinthiformis*, *M. meandrites*: collected *in situ* on Curaçao and maintained in ambient seawater; *M. confusa*, *M. digitata*: grown in aquarium facilities in Bremen, Germany) revealed a common presence of glucosamine (GlcN) in all analysed samples, and an absence of rhamnose (Rha), while all other monosaccharides (galactosamine, GalN; xylose, Xyl; galactose, Gal; fucose, Fuc; glucose, Glc; mannose, Man; arabinose, Ara) were only present in certain species (Table 7.1, Supplementary Table S7.1). The two Indo-Pacific sister species *M. confusa* and *M. digitata* had almost identical mucus carbohydrate compositions of GlcN (54.0 ± 1.6 and 56.9 ± 2.8 mole %) and Ara (46.0 ± 1.6 and 43.1 ± 2.8 mole %), while mucus carbohydrate compositions of *D. labyrinthiformis* and *M. meandrites* differed from *A. cervicornis*, due to high relative contribution of Fuc (47.8 ± 1.1 and 33.6 ± 7.1 vs. 2.0 ± 0.4 mole %) to total carbohydrates (Table 7.1). The total carbohydrate concentration of mucus from *A. cervicornis* was 9 to 16 times higher compared to the other species (ANOVA: $F_{(4, 9)} = 59.2$, $\eta^2 = 0.96$, $p < 0.001$; Tukey HSD: $p < 0.001$), which enabled the detection of monosaccharides with low relative abundance.

Table 7.1. Mean concentration (mg L^{-1}) \pm SD of monosaccharides and total carbohydrates in hydrolysed coral mucus of five coral species. Rhamnose was not detected (n.d.) in any sample. N = number of replicates, GalN = galactosamine, Xyl = xylose, Gal = galactose, Fuc = fucose, Glc = glucose, Man = mannose, Ara = arabinose, GlcN = glucosamine, Total = sum of all measured monosaccharides. Raw data is available in Supplementary Table S7.1. Origin: A = Collected *in situ* in the Caribbean (Curaçao); B = From Indo-Pacific, grown *ex situ* in Bremen, Germany.

Species	Origin	N	GalN	Xyl	Gal	Fuc	Glc	Man	Ara	GlcN	Total
<i>Acropora cervicornis</i>	A	3	1.53 ± 0.06	0.14 ± 0.25	2.68 ± 0.10	1.04 ± 0.08	n.d.	10.07 ± 3.65	22.80 ± 1.75	13.73 ± 2.82	51.98 ± 8.15
<i>Diploria labyrinthiformis</i>	A	3	0.02 ± 0.03	0.17 ± 0.30	n.d.	2.60 ± 2.68	0.03 ± 0.04	1.05 ± 1.36	n.d.	1.76 ± 1.69	5.62 ± 5.73
<i>Meandrina meandrites</i>	A	2	n.d.	n.d.	n.d.	1.14 ± 0.59	0.18 ± 0.25	0.38 ± 0.03	n.d.	1.79 ± 0.23	3.48 ± 1.10
<i>Montipora confusa</i>	B	3	n.d.	n.d.	n.d.	n.d.	n.d.	n.d.	1.39 ± 0.04	1.95 ± 0.13	3.34 ± 0.14
<i>Montipora digitata</i>	B	3	n.d.	n.d.	n.d.	n.d.	n.d.	n.d.	2.02 ± 0.55	3.15 ± 0.54	5.17 ± 1.18

Cluster analysis including literature data

Hierarchical cluster analysis including data from the present study (Table 7.1) and six previous studies (Supplementary Table S7.2) revealed three significantly different clusters (PERMANOVA: $F_{(2)} = 12.9$, $p = 0.001$; all pairwise comparisons: $p = 0.003$, Bonferroni adjusted; Fig. 1 & 2a) which explained 51 % of variance. Overall, the monosaccharides GlcN / N-acetyl glucosamine (GlcNAc), Ara, Man, and Glc were the most common, and GalN / N-acetyl galactosamine (GalNAc) and Rha were the least common components of coral mucus carbohydrates (Fig. 7.1). The difference between corals of the complex and robust clade alone was also significant and explained 20 % of the observed variance (PERMANOVA: $F_{(1)} = 7.9$, $p = 0.001$; Fig. 7.1 & 7.2b). Monosaccharide compositions did not differ between studies (PERMANOVA: $F_{(4)} = 3.2$, $p = 0.033$; all pairwise comparisons: $p > 0.05$; Fig. 7.2c), nor between geographic regions where the coral specimen originated from (PERMANOVA: $F_{(3)} = 2.5$, $p = 0.007$; all pairwise comparisons: $p > 0.05$; Fig. 7.2d).

The first cluster exclusively included coral species of the complex clade, covering three families and four genera, and all reported measurements of the family Acroporidae (Fig. 7.1). The cluster was characterized by significantly more Ara compared to the two other clusters ($p < 0.01$, Dunn's test, Bonferroni adjusted; see Fig. 7.3 for all Kruskal-Wallis test results), and significantly more GlcN compared to the third cluster ($p < 0.05$). The second cluster was only composed of corals from the robust clade, covering five families and six genera, including all three measurements of the family Fungiidae (Fig. 7.1). Mucus carbohydrates contained significantly more Fuc than the two other clusters ($p < 0.05$), and significantly more GlcN than the third cluster ($p < 0.001$; Fig. 7.3). The third cluster included all species of the family Pocilloporidae, as well as two other families of the robust clade, and *Galaxea fascicularis* of the complex clade (Fig. 7.1). Mucus carbohydrates contained significantly more Man ($p < 0.05$) and Glc ($p < 0.05$) than the other clusters (Fig. 7.3).

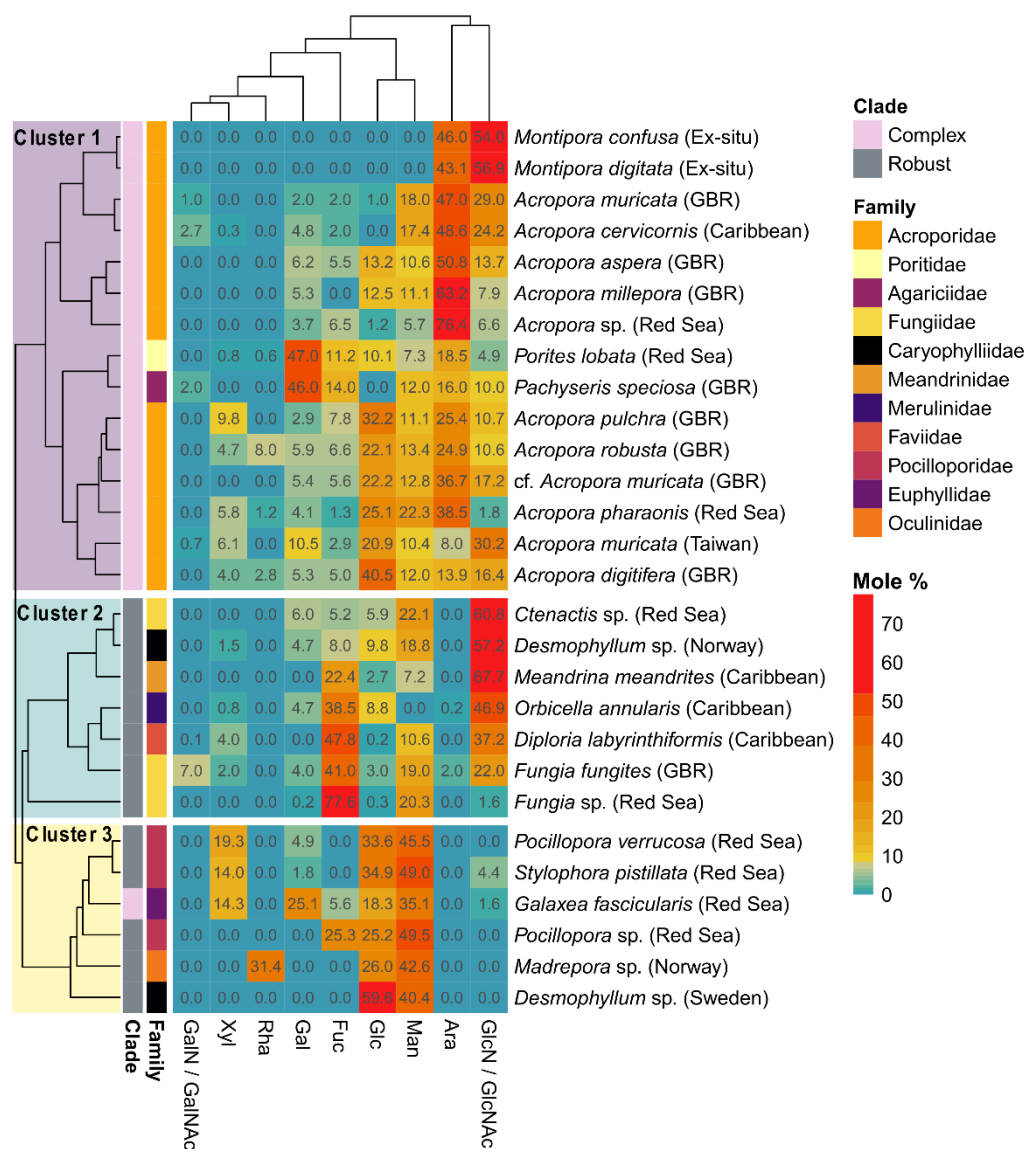


Figure 7.1. Coral mucus carbohydrate compositions form three significantly different clusters. Hierarchical cluster analysis and heatmap of relative monosaccharide compositions per coral species (mole % values are given in cells), measured in the present study and six previous studies (see [Supplementary Table S7.2](#) for more detail). Dendrogram is based on Euclidean distance. GalN/GalNAc = galactosamine / N-acetyl-galactosamine, Xyl = xylose, Rha = rhamnose, Gal = galactose, Fuc = fucose, Glc = glucose, Man = mannose, Ara = arabinose, GlcN/GlcNAc = glucosamine /N-acetyl-glucosamine.

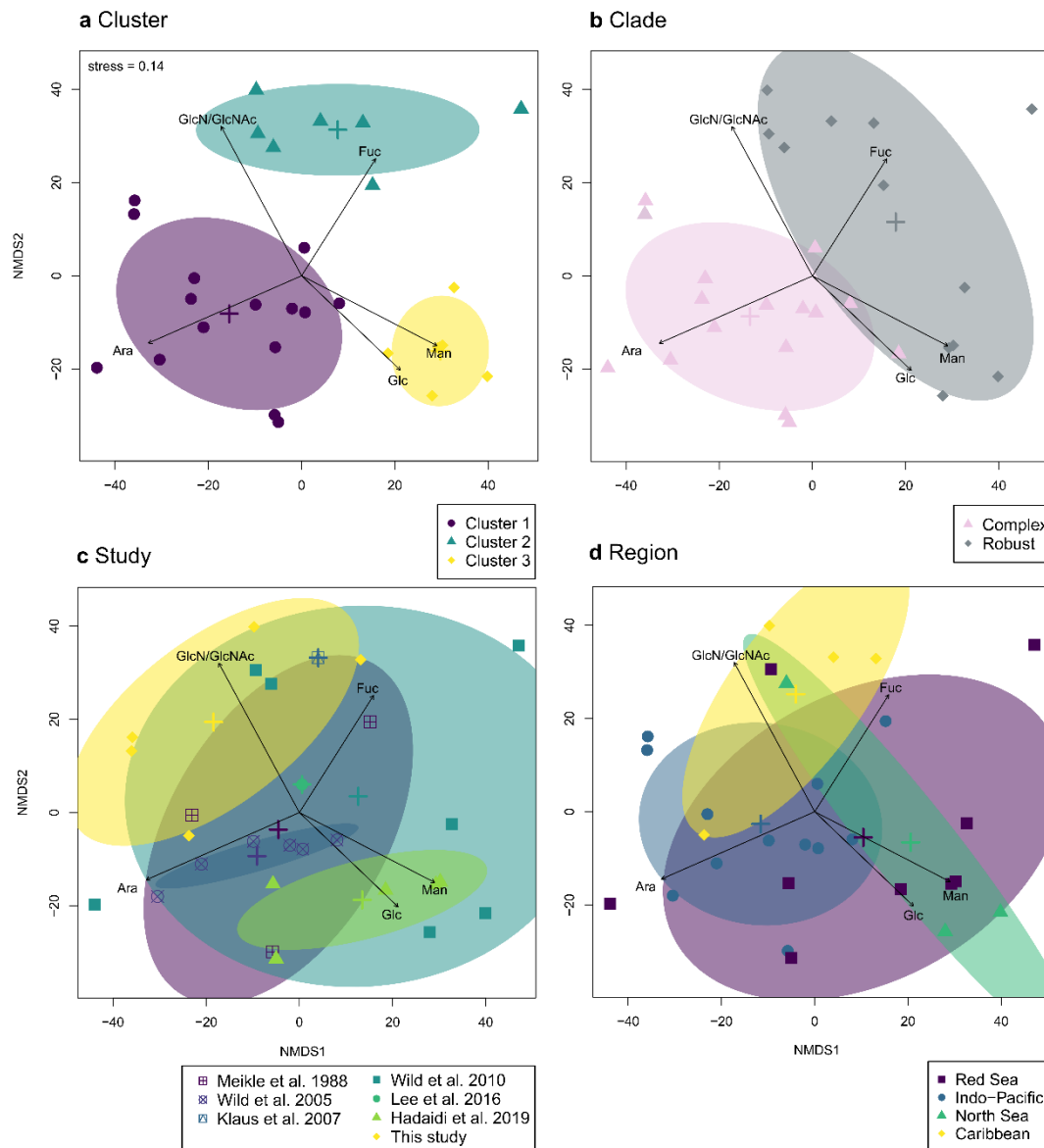


Figure 7.2. Non-metric multidimensional scaling of coral mucus carbohydrate compositions divided by (a) clusters established in hierarchical cluster analysis (see Fig. 7.1), (b) phylogenetic clade, (c) study where the data originated, and (d) geographic origin of specimen. Vectors for monosaccharides were only shown when significant ($p < 0.05$). All factors were significant in permutational multivariate analysis of variance, but only a and b revealed significant differences between groups in pairwise comparisons (*pairwiseAdonis*, $p < 0.05$). Plus-signs mark centroids of respective groups, and ellipses mark areas of 68 % confidence. Fuc = fucose, Glc = glucose, Man = mannose, Ara = arabinose, GlcN/GlcNAc = glucosamine /N-acetylglucosamine.

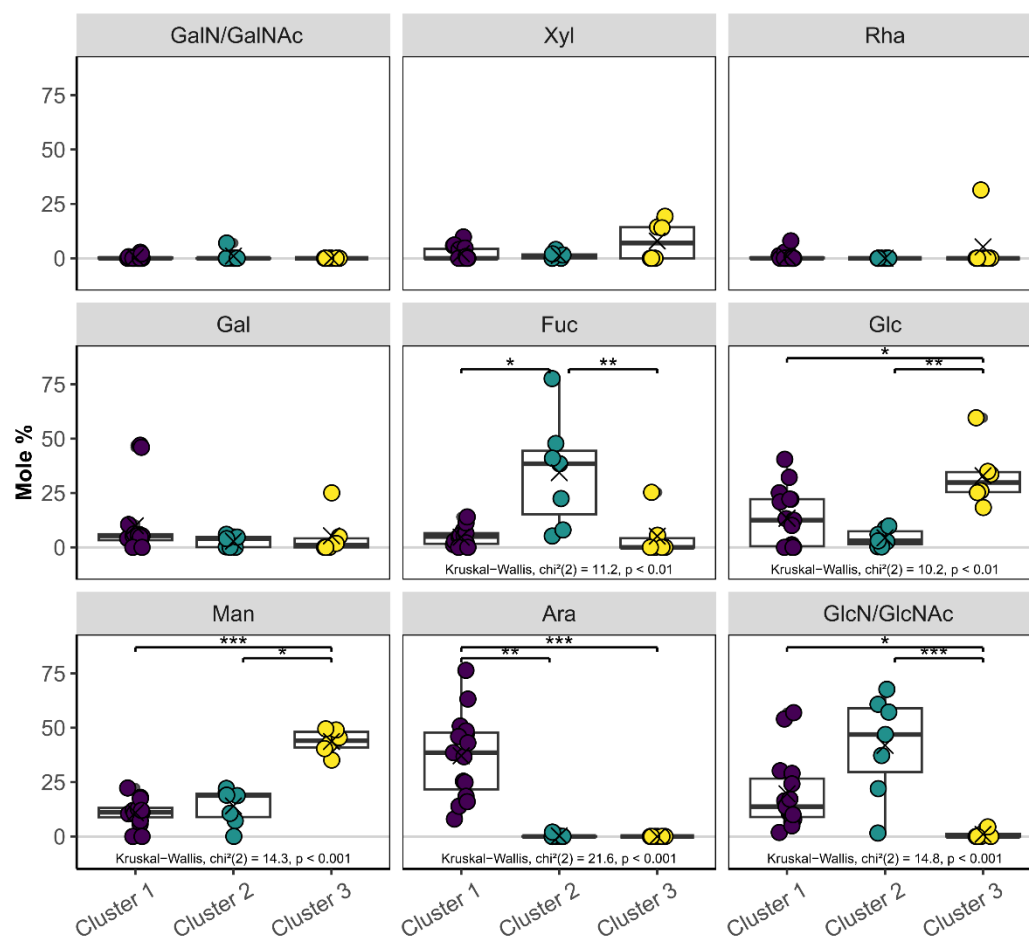


Figure 7.3. Characterization of the three clusters from hierarchical cluster analysis (Fig. 7.1). Comparison of relative monosaccharide contents among clusters. Asterisks indicate significant differences between clusters (* $p < 0.05$, ** $p < 0.01$, *** $p < 0.001$, Dunn's test, Bonferroni adjusted), where Kruskal Wallis tests were significant (results reported on the bottom of the respective panel). Boxes represent the interquartile range, with the horizontal black line indicating the median, and black crosses indicating the mean. GalN/GalNAc = galactosamine / N-acetyl-galactosamine, Xyl = xylose, Rha = rhamnose, Gal = galactose, Fuc = fucose, Glc = glucose, Man = mannose, Ara = arabinose, GlcN/GlcNAc = glucosamine /N-acetyl-glucosamine.

Correlation between coral mucus carbohydrate composition and coral phylogeny

To quantify the correlation of scleractinian coral phylogeny on coral mucus carbohydrate composition, we created a phylogenetic tree including the same species (or close sister species) used in the dendrogram for carbohydrate compositions (i.e., Fig. 7.1). Both dendrograms were connected with lines for visual comparison (Fig. 7.4), and a Mantel test was used to compare the two distance matrices, revealing a significant correlation ($R = 0.70$, $p = 0.001$, 999 permutations). The three clusters from the carbohydrate dendrogram were mostly reflected by the phylogenetic tree, with the exception of *Desmophyllum sp.* (Norway) and *G. fascicularis* (see grey dashed lines in Fig. 7.4).

For closely related species, relationships between phylogeny and mucus carbohydrate composition were more variable. *Orbicella annularis* and *D. labyrinthiformis*, *Stylophora pistillata* and *Pocillopora verrucosa*, as well as *M. digitata* and *M. confusa* were highly correlated (see bold connecting lines in Fig. 7.4). However, differences in mucus carbohydrate composition within the

genera *Desmophyllum*, *Fungia*, and *Pocillopora* were greater than differences between closely related families (i.e., Merulinidae and Faviidae). In addition, the three available carbohydrate measurements of mucus from *Acropora muricata* (from three different studies) displayed as much variation as was observed on the family level within the Acroporidae.

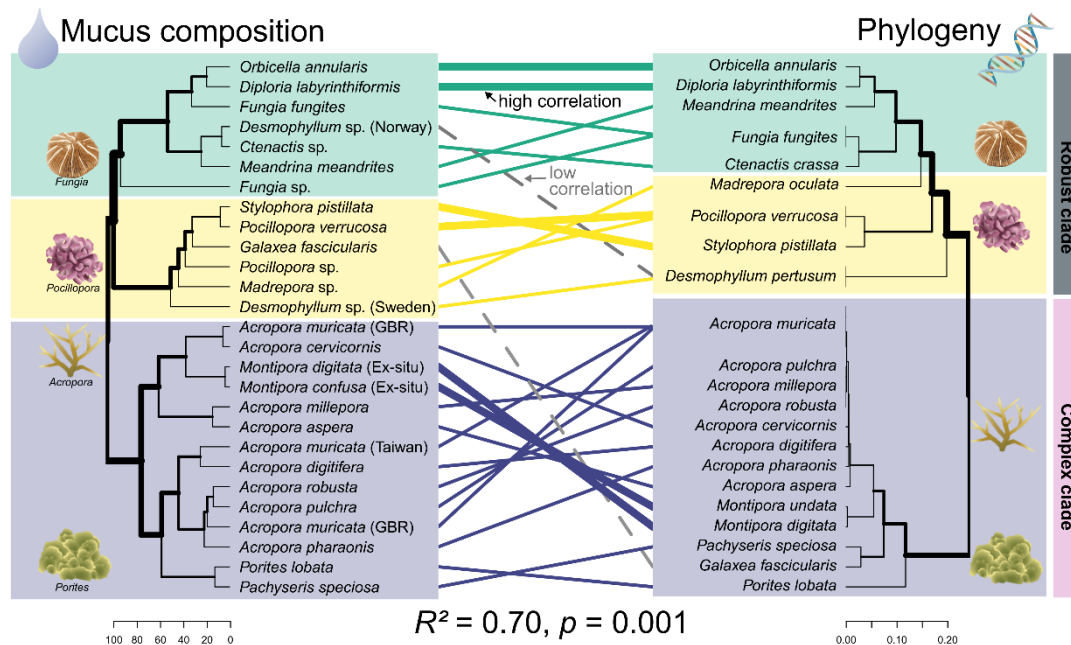


Figure 7.4. Mucus carbohydrate composition (left dendrogram, derived from Fig. 7.1) and phylogenetic tree (right dendrogram, based on cytochrome *c* oxidase subunit I (COI)) correlate significantly. Result of the Mantel test is given on the bottom, where the simulated *p* value is based on 999 permutations. Colours of connecting lines highlight the three main clusters of the left dendrogram. Bold lines indicate closely related species with high similarity in mucus compositions (i.e., high correlation). Grey dashed lines indicate species where the mucus carbohydrate composition reflects a different cluster compared to closely related species (i.e., low correlation). Symbols represent different scleractinian coral genera and are added for illustrational purposes. Symbol attribution: Integration and Application Network (ian.umces.edu/media-library).

7.4 Discussion

Hierarchical cluster analysis of the combined data on coral mucus carbohydrate compositions of 23 scleractinian coral species and 10 families revealed three significantly different clusters (Fig. 7.1 & 7.2a), due to differences in the monosaccharides Ara, Fuc, GlcN/GlcNAc, Glc, and Man (Fig. 7.3). The absence of Ara in the robust clade mainly contributed to a significant difference between complex and robust corals, while there was no significant difference between geographic regions where the specimen originated, nor between studies which first reported the data (Fig. 7.2). Finally, the dendrogram containing the three clusters correlated significantly with the phylogenetic tree of scleractinian corals (Fig. 7.4).

Coral mucus carbohydrate composition displays phylogenetic dependence

Results of the present study revealed a significant correlation between coral mucus carbohydrate composition and coral phylogeny, which indicates phylogenetic dependence of the mucosal

carbohydrate building blocks (i.e., monosaccharides). Phylogenetic dependence (or phylogenetic signal) is the trend of traits being more similar between more closely related species, and can be explained by genetic drift²⁵. Random mutations are suggested to lead to increasing differences in genes with increasing phylogenetic distance (i.e., the timespan since divergence of lineages)²³. Glycan structures and compositions usually do not reflect phylogenetic lineages, as glycans evolve rapidly to escape pathogens²³ and general microbial degradation²⁶ (i.e., Red Queen effect / arms race). For example, Tao et al.²⁴ proposed that rather than phylogeny, selective environmental and microbial pressures shape oligosaccharide compositions (carbohydrates composed of several monosaccharides) in primate milk.

The three mucus carbohydrate compositions of *A. muricata* used in this analysis originated from Taiwan²⁷ and the Great Barrier Reef (GBR) in Australia^{41,42} and revealed large differences. These differences could be explained by different environmental conditions. On the other hand, Klaus et al.⁴³ found no intra-specific variation across depth- and coastal pollution gradients in mucus carbohydrates of *M. annularis*⁴³. Thus, more research is needed to elucidate the species-specific effects of environmental factors on coral mucus carbohydrate compositions. Furthermore, changes in microbial communities due to environmental conditions³¹ and *ex situ* culturing^{44,45} (i.e., for *M. digitata* and *M. confusa* colonies in the present study) may influence coral mucus compositions, and thus should be included in future studies due to expected interaction of mucosal carbohydrates with associated microbes^{9,46}. Lastly, endosymbiotic Symbiodiniaceae likely influence coral mucus compositions^{36,37}. Arabinose is not common in animal cells^{41,47}, and may be delivered to the coral host by the endosymbiotic dinoflagellates^{22,41}. Arabinose characterized the mucus of corals from the complex clade, the only exception to this trend being *G. fascicularis*. The origin of Ara in the mucus of corals from the complex clade should be further investigated and studying the mucus Ara content in response to coral bleaching, or differences in dominant Symbiodiniaceae genera could reveal a link to Symbiodiniaceae metabolism.

Subsequently, it could be expected that these environmental and microbial pressures largely determine the variation in mucus carbohydrate composition and thereby overrule potential effects of phylogeny. Surprisingly, in the present study the opposite appears to be the case with coral phylogeny explaining 70 % of the observed variation on the level of monosaccharide building blocks in coral mucus glycans. Variation of host glycans is limited by the necessity to retain vital functions⁴⁸ such as successful interactions with microbial symbionts²³. Thus, phylogenetic dependence of carbohydrate compositions may contribute to conserving vital functions for scleractinian corals. However, monosaccharide compositions of hydrolysed glycans lack information on the overall glycan structure¹⁶, and future studies should aim to capture their full molecular variation (e.g., as proposed by Bligh et al.²⁶).

Meikle et al.¹⁹, one of the few studies that analysed the detailed glycan structure of coral mucus, revealed that mucins of *A. muricata* (then *A. formosa*⁴⁹) are highly glycosylated through O-glycosidic links, and glycan side chains rich in Ara, Man, and GlcNAc. These same monosaccharides (i.e., Ara,

Man, and GlcN/GlcNAc) were common in mucus of all *Acropora* species analysed in the present study (Fig. 7.1) and were thus likely parts of mucins. The protein backbone of mucins (encoded by MUC genes) dictates the position of O-glycans, which can only be attached to the hydroxyl groups of serine or threonine⁵⁰. The MUC genes differ between branches of the tree of life⁵¹, and evolutionary variation of the regions where glycosylation occurs can lead to structural and functional changes of mucins⁵². Thus, the correlation of coral mucus carbohydrate composition and coral phylogeny may indicate phylogenetic dependence in MUC genes and/or genes for enzymes involved in glycosylation (i.e. GT). This connection could be further investigated by studying the involved genes (i.e., MUC and GT) in scleractinian corals.

Potential caveats and limitations

Apart from the aforementioned potential effects of variations in environmental conditions, geographic locations, and *ex situ* vs *in situ* collections, the use of different sampling protocols and analytical methods have likely affected the mucus carbohydrate compositions reported in the different studies which were included in the cluster analysis (Supplementary Table S7.3). Coral mucus sampling was conducted either by drawing mucus from the corals' surface with low stress^{21,43}, or by removing the coral from water and catching the dripping mucus (i.e., "milking"; ^{22,27,42} and present study), which induces stress and may impact mucus compositions¹⁴. Additionally, carbohydrate analysis was conducted either by gas chromatography coupled with mass spectrometry (GC-MS)^{21,22,41,42}, high-performance liquid chromatography with MS detection (HPLC-MS)²⁷, or high-performance anion-exchange chromatography with pulsed amperometric detection (HPAEC-PAD; ⁴³ and present study). GC-MS requires chemical alteration of sugar molecules, while HPAEC-PAD does not require this step and has a lower detection range, making it more suitable for environmental samples⁵³. As coral mucus carbohydrate concentrations are generally high, the difference in detection limit between methods may be negligible, and differences in accuracy between methods are less relevant when comparing relative compositions (i.e., mole %). Furthermore, dialysis membranes used for desalination of mucus samples ranged in pore size between 0.1 and 50 kDa, and no dialysis was carried out in the present study where samples were diluted instead. The majority of carbohydrates in coral mucus are in the form of mucin glycoproteins and large heteropolysaccharides which have molecular sizes of 175 to 30,000 kDa^{18,54,55}. Thus, these molecules should have remained in the samples with any of the used pore sizes. Finally, we acknowledge the limited number of replicates for some of the analysed coral species, which was one for some of the early measurements⁴¹, and two to three for the here reported species (more detail in Supplementary Table S7.2). Despite the potential effects of these limitations, we would like to point out that there was no significant effect of study on the monosaccharide composition (Fig. 7.2c). In combination with the fact that 70 % of the observed variation in monosaccharide composition could be explained by coral phylogeny, this may indicate the dominating effect of phylogeny on the composition of monosaccharide building blocks in coral mucus carbohydrates.

Conclusion

The here analysed carbohydrate compositions of coral mucus from 23 species originated from seven different studies, and were thus likely influenced by i) differences in environmental conditions (including *in situ* vs *ex situ* growth), ii) associated microbiota, and iii) sample preparation- and measurement methods. Despite these factors which can induce variation, the mucus compositions from corals of the complex and robust clade were significantly different, and coral phylogeny explained 70 % of the variation. Therefore, the here presented results indicate that coral mucus carbohydrate composition co-diversifies (on the level of their monosaccharide building blocks) with coral phylogeny, suggesting important functions of mucosal carbohydrates for scleractinian corals.

7.5 Methods

Mucus collection

Fragments of the critically endangered coral species *A. cervicornis* (n = 3) were temporally provided by the coral restoration project Reef Renewal Curaçao to avoid any detrimental pressure on natural populations. Coral fragments were suspended on coral trees with strings and could therefore be removed and transported to the CARMABI research station without tissue damage. Colonies of *D. labyrinthiformis* (n = 3) and *M. meandrites* (n = 2) were collected from the reef in Piscadera Bay (12.121, -68.970) while avoiding injury to living tissue. All corals were kept and allowed to recover for one week at a suspended artificial structure at 10 m depth in front of the CARMABI research station. Colonies were brought to a seawater flow-through aquarium in the morning, incubated in an aquarium with 22 L of filtered seawater (0.2 µm pore size) for 6 h at ambient temperature and light conditions (29.0 °C ± 0.2 SD, 101 µmol photons m⁻² s⁻¹ ± 13 SD) as part of a different study, and then again placed in the flow-through aquarium for the night. Mucus was sampled the next morning by exposing the colonies to air, and collecting the dripping mucus for two minutes in a sterile falcon tube after discarding the first 30 seconds, according to Wild et al.⁴². This method is also called “milking” of corals, and may result in different biochemical compositions of mucus than what is present in the surface layer when undisturbed¹⁴. *Montipora digitata* (n = 3) and *M. confusa* (n = 3) colonies from the Indo-Pacific were grown in the aquarium facilities of the Marine Ecology department of the University of Bremen for six years under stable conditions (water temperature: ~ 26 °C; light: ~100 - 150 µmol photons m⁻² s⁻¹; salinity: ~35 ‰; sea salt: Zoo Mix, Tropic Marin, Switzerland). Although these two species are the only ones which were not collected *in situ*, we decided to include them in the analysis, as the aim of the study was to investigate phylogenetic effects on mucus composition. Mucus collection was done as described above, and colonies were placed back into the aquarium. All mucus samples were stored at -20 °C until further processing, as was done before for the analysis of carbohydrates in coral mucus samples^{22,27,56}.

Measurement of monosaccharide compositions

Mucus samples were hydrolysed at 100 °C for 24 h by adding 50 µL of 2 M HCl to 50 µL of mucus. Afterwards, mucus was diluted by a factor of 100 by adding 20 µL of the mucus-HCl mixture to 980 µL of ultrapure water (UW). Diluted mucus samples were vortexed, and then centrifuged (15 min at 21.100 x g), and 100 µL of the top layer were transferred into glass vials for measurement together with six calibration standards including all monosaccharides at concentrations ranging from 10 to 1000 µg L⁻¹. Monosaccharide concentrations of hydrolysed mucus were measured with a high-performance anion exchange chromatography system (Dionex ICS-5000⁺, Thermo Fisher Scientific), equipped with a PA10 column (2 x 250 mm) and PA10 guard column (both by Thermo Fisher Scientific). Monosaccharides were separated by an isocratic flow of 18 mM NaOH for 20 minutes. HPAEC was coupled with pulsed amperometric detection (HPAEC-PAD) as previously described²⁰.

Data preparation for hierarchical cluster analysis

Monosaccharide concentrations measured in the present study were converted to mole %, using the mean of two (*M. meandrites*) or three (all other species) replicates. Data of mucus carbohydrate compositions of 23 different scleractinian coral species, measured with varying numbers of replicates ranging from one to 36 (see [Supplementary Table S7.2](#) for more detail) were retrieved from six previous studies^{21,22,27,41-43}. Species or genera with several reported mucus compositions from different locations or studies (i.e., *A. muricata*, *Desmophyllum* sp.) were treated separately in analyses. Only studies which could detect the nine neutral and amino sugars Fuc, Rha, GalN/GalNAc, Ara, GlcN/GlcNAc, Gal, Glc, Man, and Xyl were included (see comparison of methods used in [Supplementary Table S7.3](#)). GlcN was pooled with its derivate GlcNAc, and GalN was pooled with GalNAc. Species names were changed to the currently accepted names, i.e., “*Montastrea annularis*” now *Orbicella annularis*⁵⁷, “*Acropora formosa*” now *A. muricata*⁴⁹, “*A. nobilis*” now *A. robusta*⁴⁹, and finally “*Lophelia* sp.” now *Desmophyllum* sp.⁵⁸. Three studies^{21,42,43} did not report the absence of GalN/GalNAc, but values were set to zero because the methods used ([Supplementary Table S7.3](#)) enable the detection of GalN/GalNAc (see Wild et al.²², where absence of GalNAc was reported). Similarly, absence of Rha was not reported in two studies^{27,41} although methods used ([Supplementary Table S7.3](#)) can detect Rha, and values were set to zero. Two studies^{21,43} reported the relative abundance of additional monosaccharides, and mole % values were adjusted accordingly for better comparison among studies. Mole % data of *Fungia* sp.²² was averaged from three measurements conducted in different seasons. Finally, *Stylophora* sp.²² was not included in the hierarchical cluster analysis of the present study, because only one monosaccharide (Glc) was detected. This was likely due to low carbohydrate concentrations in the mucus, leading to the sole detection of one monosaccharide, which was then over-estimated as contributing to 100 % of carbohydrates.

Phylogenetic tree construction

To be able to correlate the mucus carbohydrate dendrogram with coral phylogeny, a phylogenetic tree was constructed based on cytochrome *c* oxidase subunit I (COI). The COI sequences were downloaded from GenBank (see [Supplementary Table S7.4](#)). Sequences were loaded into Geneious Prime software (version 2023.0.3) and aligned using the Geneious Alignment tool. The phylogenetic tree was constructed based on unweighted pair group with arithmetic mean (UPGMA) with Hasegawa, Kishino, and Yano (HKY) genetic distances using the Geneious Tree Builder tool. The resulting distance matrix was exported and used to create the tanglegram (see statistical analyses section). For comparisons of unspecified genera or in case a COI sequence of a selected species was not available, COI sequences of sister species within the same genus were downloaded and used to construct the phylogenetic tree (*Genus species* mucus dendrogram vs. *Genus species* phylogeny), i.e., *Desmophyllum* sp. vs. *Desmophyllum pertusum*, *Ctenactis* sp. vs. *Ctenactis crassa*, *Fungia* sp. vs. *Fungia fungites*, *Pocillopora* sp. vs. *Pocillopora verrucosa*, *Madrepora* sp. vs. *Madrepora oculata*, and finally *Montipora confusa* vs. *Montipora undata*.

Statistical analyses

All statistical analyses were conducted with R version 4.3.0 and R Studio version 2023.03.1. Hierarchical clustering of mucus monosaccharide compositions was performed using the package *phreatmaps* and the “complete” clustering method (i.e., Euclidean distance). Permutational multivariate analysis of variance (PERMANOVA, *vegan* package, 999 permutations) was used to test for differences in Euclidean distance matrices of carbohydrate compositions between groups (i.e., clusters, clades, studies, geographic regions), and homogeneity of dispersion among groups was tested with permutational multivariate analysis of dispersion (PERMDISP, *vegan* package). Homogeneity of dispersion was not given for the factors *Clade* and *Study*, but PERMANOVA is robust to heterogeneity in dispersion for balanced designs⁵⁹ and sample sizes for *Clade* were nearly balanced ($n_2/n_1 = 1.33$). The two studies which only reported mucus compositions for one species^{27,43} were not included in PERMANOVA analysis for the factor *Study* to reduce the heterogeneity in dispersion. Distance matrices were additionally visualized with non-metric multidimensional scaling (NMDS, *vegan* package) to display the effects of *Cluster*, *Clade*, *Study*, and *Geographic region* on carbohydrate compositions. For post-hoc analysis, multiple pairwise comparisons were conducted with the R package *pairwiseAdonis*, Bonferroni adjustment, and 999 permutations. To test for differences in the relative abundance of single monosaccharides between the three main clusters, Kruskal-Wallis-Tests were performed, and when significant ($p < 0.05$), multiple pairwise comparisons were conducted using the Dunn’s test with Bonferroni adjustment. Correlation between the two distance matrices of the hierarchical cluster dendrogram and the phylogenetic tree was tested with a Mantel test (*ade4* package), which is frequently used to compare phylogenetic trees and test for cophylogeny^{60,61}. A tanglegram was created with the *dendextend* package⁶², combining the two distance matrices from mucus carbohydrate compositions and

phylogenetic information. The measurement for “*Acropora* sp. (Red Sea)” was removed from the carbohydrate dendrogram after clustering with the *prune* function, as it could not be connected to a species of the phylogenetic tree.

7.6 Author contributions

B.T. and A.T. analysed the data. J.-H.H. provided resources and technical support. B.T. collected the data, prepared the figures and wrote the main manuscript text. All authors conceptualized, read and revised the manuscript.

7.7 Acknowledgements

We want to thank Milou Arts for assisting with the collection of coral specimens which were later returned to the reef. We thank Bert Hoeksema and Christian Voolstra for their valuable input concerning the construction of the phylogenetic tree. We also thank Nicola Steinke, Silvia Vidal-Melgosa and Alek Bolte for their help and guidance with the HPAEC-PAD analyses of mucus samples.

7.8 References

1. Lai, S. K., Wang, Y.-Y., Wirtz, D. & Hanes, J. Micro- and macrorheology of mucus. *Adv. Drug Deliv. Rev.* **61**, 86–100 (2009).
2. Bakshani, C. R. *et al.* Evolutionary conservation of the antimicrobial function of mucus: a first defence against infection. *Npj Biofilms Microbiomes* **4**, 1–12 (2018).
3. Rose, M. C. & Voynow, J. A. Respiratory tract mucin genes and mucin glycoproteins in health and disease. *Physiol. Rev.* **86**, 245–278 (2006).
4. Denny, M. W. Invertebrate mucous secretions: functional alternatives to vertebrate paradigms. *Symp. Soc. Exp. Biol.* **43**, 337–366 (1989).
5. Wild, C. *et al.* Coral mucus functions as an energy carrier and particle trap in the reef ecosystem. *Nature* **428**, 66–70 (2004).
6. McLoughlin, K., Schluter, J., Rakoff-Nahoum, S., Smith, A. L. & Foster, K. R. Host selection of microbiota via differential adhesion. *Cell Host Microbe* **19**, 550–559 (2016).
7. Wheeler, K. M. *et al.* Mucin glycans attenuate the virulence of *Pseudomonas aeruginosa* in infection. *Nat. Microbiol.* **4**, 2146–2154 (2019).
8. Xia, B., Royall, J. A., Damera, G., Sachdev, G. P. & Cummings, R. D. Altered O-glycosylation and sulfation of airway mucins associated with cystic fibrosis. *Glycobiology* **15**, 747–775 (2005).
9. Belzer, C. Nutritional strategies for mucosal health: the interplay between microbes and mucin glycans. *Trends Microbiol.* **30**, 13–21 (2022).
10. Miller, D. J. & Ball, E. E. The coral *Acropora*: what it can contribute to our knowledge of metazoan evolution and the evolution of developmental processes. *BioEssays* **22**, 291–296 (2000).

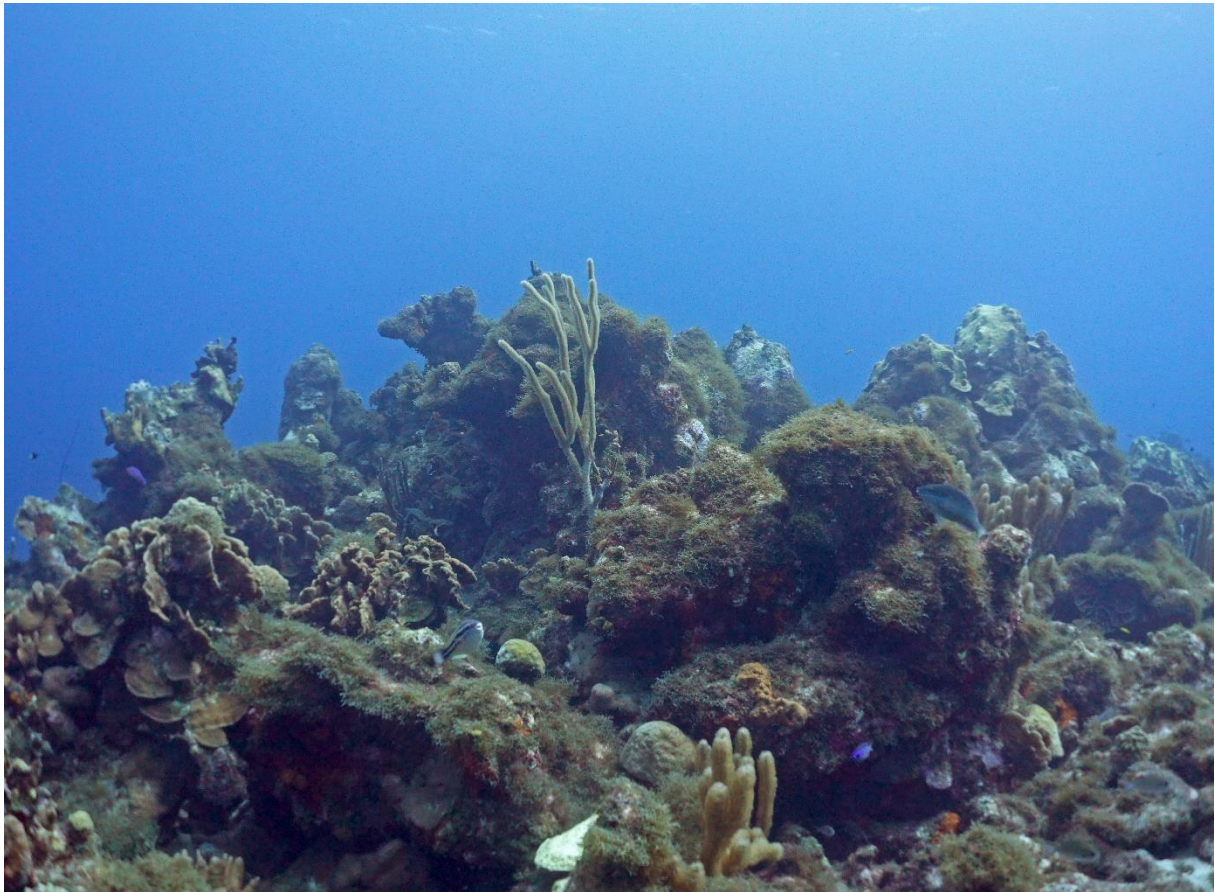
11. Technau, U. & Steele, R. E. Evolutionary crossroads in developmental biology: Cnidaria. *Development* **138**, 1447–1458 (2011).
12. Wild, C. *et al.* Climate change impedes scleractinian corals as primary reef ecosystem engineers. *Mar. Freshw. Res.* **62**, 205 (2011).
13. Woodhead, A. J., Hicks, C. C., Norström, A. V., Williams, G. J. & Graham, N. A. J. Coral reef ecosystem services in the Anthropocene. *Funct. Ecol.* **33**, 1023–1034 (2019).
14. Brown, B. E. & Bythell, J. C. Perspectives on mucus secretion in reef corals. *Mar. Ecol. Prog. Ser.* **296**, 291–309 (2005).
15. Boudierlique, T. *et al.* Surface flow for colonial integration in reef-building corals. *Curr. Biol.* (2022).
16. Arnosti, C. *et al.* The biogeochemistry of marine polysaccharides: sources, inventories, and bacterial drivers of the carbohydrate cycle. *Annu. Rev. Mar. Sci.* **13**, 81–108 (2021).
17. Grabarics, M. *et al.* Mass spectrometry-based techniques to elucidate the sugar code. *Chem. Rev.* **122**, 7840–7908 (2022).
18. Coddeville, B., Maes, E., Ferrier-Pagès, C. & Guerardel, Y. Glycan profiling of gel forming mucus layer from the scleractinian symbiotic coral *Oculina arbuscula*. *Biomacromolecules* **12**, 2064–2073 (2011).
19. Meikle, P., Richards, G. N. & Yellowlees, D. Structural determination of the oligosaccharide side chains from a glycoprotein isolated from the mucus of the coral *Acropora formosa*. *J. Biol. Chem.* **262**, 16941–16947 (1987).
20. Engel, A. & Händel, N. A novel protocol for determining the concentration and composition of sugars in particulate and in high molecular weight dissolved organic matter (HMW-DOM) in seawater. *Mar. Chem.* **127**, 180–191 (2011).
21. Hadaidi, G., Gegner, H. M., Ziegler, M. & Voolstra, C. R. Carbohydrate composition of mucus from scleractinian corals from the central Red Sea. *Coral Reefs* **38**, 21–27 (2019).
22. Wild, C., Naumann, M., Niggel, W. & Haas, A. Carbohydrate composition of mucus released by scleractinian warm- and cold-water reef corals. *Aquat. Biol.* **10**, 41–45 (2010).
23. Bishop, J. R. & Gagneux, P. Evolution of carbohydrate antigens—microbial forces shaping host glycomes? *Glycobiology* **17**, 23R–34R (2007).
24. Tao, N. *et al.* Evolutionary Glycomics: Characterization of milk oligosaccharides in primates. *J. Proteome Res.* **10**, 1548–1557 (2011).
25. Blomberg, S. P. & Garland Jr, T. Tempo and mode in evolution: phylogenetic inertia, adaptation and comparative methods. *J. Evol. Biol.* **15**, 899–910 (2002).
26. Bligh, M., Nguyen, N., Buck-Wiese, H., Vidal-Melgosa, S. & Hehemann, J.-H. Structures and functions of algal glycans shape their capacity to sequester carbon in the ocean. *Curr. Opin. Chem. Biol.* **71**, 102204 (2022).

27. Lee, S. T. M., Davy, S. K., Tang, S.-L. & Kench, P. S. Mucus sugar content shapes the bacterial community structure in thermally stressed *Acropora muricata*. *Front. Microbiol.* **7**, 371 (2016).
28. Niggli, W., Glas, M., Laforsch, C., Mayr, C. & Wild, C. First evidence of coral bleaching stimulating organic matter release by reef corals. *Proc. 11th Int. Coral Reef Symp.* 905–911 (2009).
29. Wright, R. M., Strader, M. E., Genuise, H. M. & Matz, M. Effects of thermal stress on amount, composition, and antibacterial properties of coral mucus. *PeerJ* **7**, e6849 (2019).
30. Quinlan, Z. A. *et al.* Fluorescent organic exudates of corals and algae in tropical reefs are compositionally distinct and increase with nutrient enrichment. *Limnol. Oceanogr. Lett.* **3**, 331–340 (2018).
31. Voolstra, C. R. & Ziegler, M. Adapting with microbial help: microbiome flexibility facilitates rapid responses to environmental change. *BioEssays* **42**, 2000004 (2020).
32. LaJeunesse, T. C. *et al.* Systematic revision of Symbiodiniaceae highlights the antiquity and diversity of coral endosymbionts. *Curr. Biol.* **28**, 2570-2580.e6 (2018).
33. Crossland, C. J. *In situ* release of mucus and DOC-lipid from the corals *Acropora variabilis* and *Stylophora pistillata* in different light regimes. *Coral Reefs* **6**, 35–42 (1987).
34. Crossland, C. J., Barnes, D. J. & Borowitzka, M. A. Diurnal lipid and mucus production in the staghorn coral *Acropora acuminata*. *Mar. Biol.* **60**, 81–90 (1980).
35. Davies, P. S. The role of zooxanthellae in the nutritional energy requirements of *Pocillopora eydouxi*. *Coral Reefs* **2**, 181–186 (1984).
36. Banin, E., Israely, T., Fine, M., Loya, Y. & Rosenberg, E. Role of endosymbiotic zooxanthellae and coral mucus in the adhesion of the coral-bleaching pathogen *Vibrio shiloi* to its host. *FEMS Microbiol. Lett.* **199**, 33–37 (2001).
37. Sivaguru, M. *et al.* Corals regulate the distribution and abundance of Symbiodiniaceae and biomolecules in response to changing water depth and sea surface temperature. *Sci. Rep.* **11**, 2230 (2021).
38. Arrigoni, R. *et al.* A new sequence data set of SSU rRNA gene for Scleractinia and its phylogenetic and ecological applications. *Mol. Ecol. Resour.* **17**, 1054–1071 (2017).
39. Kitahara, M. V. *et al.* The “naked coral” hypothesis revisited – evidence for and against scleractinian monophyly. *PLOS ONE* **9**, e94774 (2014).
40. Ying, H. *et al.* Comparative genomics reveals the distinct evolutionary trajectories of the robust and complex coral lineages. *Genome Biol.* **19**, 175 (2018).
41. Meikle, P., Richards, G. N. & Yellowlees, D. Structural investigations on the mucus from six species of coral. *Mar. Biol.* **99**, 187–193 (1988).
42. Wild, C., Woyt, H. & Huettel, M. Influence of coral mucus on nutrient fluxes in carbonate sands. *Mar. Ecol. Prog. Ser.* **287**, 87–98 (2005).

43. Klaus, J. S., Janse, I., Heikoop, J. M., Sanford, R. A. & Fouke, B. W. Coral microbial communities, zooxanthellae and mucus along gradients of seawater depth and coastal pollution. *Environ. Microbiol.* **9**, 1291–1305 (2007).
44. Kooperman, N., Ben-Dov, E., Kramarsky-Winter, E., Barak, Z. & Kushmaro, A. Coral mucus-associated bacterial communities from natural and aquarium environments. *FEMS Microbiol. Lett.* **276**, 106–113 (2007).
45. Pratte, Z. A., Richardson, L. L. & Mills, D. K. Microbiota shifts in the surface mucopolysaccharide layer of corals transferred from natural to aquaria settings. *J. Invertebr. Pathol.* **125**, 42–44 (2015).
46. Wu, C. M. *et al.* Mucin glycans drive oral microbial community composition and function. *Npj Biofilms Microbiomes* **9**, 1–14 (2023).
47. Mariette, A. *et al.* Not just a simple sugar: arabinose metabolism and function in plants. *Plant Cell Physiol.* **62**, 1791–1812 (2021).
48. Gagneux, P. & Varki, A. Evolutionary considerations in relating oligosaccharide diversity to biological function. *Glycobiology* **9**, 747–755 (1999).
49. Veron, J. E. N. *Corals of Australia and the Indo-Pacific*. (Angus & Robertson Publishers, 1986).
50. Corfield, A. P. & Berry, M. Glycan variation and evolution in the eukaryotes. *Trends Biochem. Sci.* **40**, 351–359 (2015).
51. Lang, T. *et al.* Searching the evolutionary origin of epithelial mucus protein components—mucins and FCGBP. *Mol. Biol. Evol.* **33**, 1921–1936 (2016).
52. Xu, D. *et al.* Recent evolution of the salivary mucin MUC7. *Sci. Rep.* **6**, 31791 (2016).
53. Panagiotopoulos, C. & Sempéré, R. Analytical methods for the determination of sugars in marine samples: a historical perspective and future directions. *Limnol. Oceanogr. Methods* **3**, 419–454 (2005).
54. Bythell, J. C. & Wild, C. Biology and ecology of coral mucus release. *J. Exp. Mar. Biol. Ecol.* **408**, 88–93 (2011).
55. Jatkar, A. A. *et al.* Coral mucus: the properties of its constituent mucins. *Biomacromolecules* **11**, 883–888 (2010).
56. Nelson, C. E. *et al.* Coral and macroalgal exudates vary in neutral sugar composition and differentially enrich reef bacterioplankton lineages. *ISME J.* **7**, 962–979 (2013).
57. Veron, J. E. N. *Corals of the World*. vols 1–3 (Australian Institute of Marine Science and CRR, Queensland, Australia, 2000).
58. Addamo, A. M. *et al.* Merging scleractinian genera: the overwhelming genetic similarity between solitary *Desmophyllum* and colonial *Lophelia*. *BMC Evol. Biol.* **16**, 108 (2016).
59. Anderson, M. J. & Walsh, D. C. I. PERMANOVA, ANOSIM, and the Mantel test in the face of heterogeneous dispersions: what null hypothesis are you testing? *Ecol. Monogr.* **83**, 557–574 (2013).

60. Mazel, F. *et al.* Is host filtering the main driver of phylosymbiosis across the tree of life? *mSystems* **3**, e00097-18 (2018).
61. Pollock, F. J. *et al.* Coral-associated bacteria demonstrate phylosymbiosis and cophylogeny. *Nat. Commun.* **9**, 4921 (2018).
62. Galili, T. *dendextend*: an R package for visualizing, adjusting and comparing trees of hierarchical clustering. *Bioinformatics* **31**, 3718–3720 (2015).

Chapter 8 | Coral exudates shape bacterioplankton community composition and function in an algae-dominated Caribbean reef



Algae-dominated reef of Piscadera Bay, Curaçao, Dutch Caribbean. Photo by Benjamin Mueller.

Chapter 8 | Coral exudates shape bacterioplankton community composition and function in an algae-dominated Caribbean reef

Bianca M. Thobor^{1*}, Andreas Haas², Christian Wild¹, Craig E. Nelson³, Linda Wegley Kelly⁴, Jan-Hendrik Hehemann^{5,6}, Milou G. I. Arts², Meine Boer², Hagen Buck-Wiese^{5,6}, Nguyen P. Nguyen^{5,6}, Inga Hellige^{5,6} and Benjamin Mueller^{1,7,8}

¹Department of Marine Ecology, University of Bremen, Bremen, Germany

²Department of Microbiology & Biogeochemistry, NIOZ Royal Netherlands Institute for Sea Research, Texel, The Netherlands

³Daniel K. Inouye Center for Microbial Oceanography: Research and Education, Department of Oceanography and Sea Grant College Program, University of Hawai'i at Mānoa, Honolulu, Hawai'i, USA

⁴Marine Biology Research Division, Scripps Institution of Oceanography, University of California, San Diego, California, USA

⁵MARUM Centre for Marine Environmental Sciences, University of Bremen, Bremen, Germany

⁶Department of Marine Glycobiology, Max Planck Institute for Marine Microbiology, Bremen, Germany

⁷Department of Freshwater and Marine Ecology, University of Amsterdam, Amsterdam, the Netherlands

⁸CARMABI Foundation, Willemstad, Curaçao

*Corresponding author: thobor@uni-bremen.de

8.1 Abstract

Marine dissolved organic matter (DOM), one of the most complex chemical mixtures on earth, constitutes the basis of the coral reef food web. Within this plethora of compounds high molecular weight (HMW, > 1 kDa) carbohydrates are the most abundant fraction exuded by benthic primary producers. Despite globally occurring shifts from coral- to algae-dominated reefs, not much is known about how their exuded carbohydrates shape coral reef community metabolism. Here we compared the monosaccharide composition of HMW carbohydrates in exudates from various hard corals against exudates from brown macroalgae, all collected on an algae-dominated reef off Curaçao, Dutch Caribbean. We further investigated the response of the ambient bacterioplankton community to the respective HMW fraction of exudates. Our results show that HMW coral exudates were compositionally distinct from the ambient, algae dominated reef waters and compositionally similar to coral mucus (mainly arabinose). The HMW exudate fraction selected for opportunistic microbial taxa commonly associated with corals (i.e., Rhodobacteraceae, Phycisphaeraceae, Vibrionaceae, Flavobacteriales). Additionally, coral exudates significantly increased the predicted energy-, amino acid-, and carbohydrate metabolism by 28 %, 44 %, and 111 %, respectively. In contrast, algae exudates were similar in HMW carbohydrate composition both to the reef water and to algal tissue extracts (mainly fucose) and did not significantly alter the composition and metabolism of the bacterioplankton community collected from the nearby reef. The strong effect of coral-derived HMW DOM on bacterioplankton communities of algae-dominated reefs is consistent with increasingly efficient trophic transfer (i.e., transformation of DOM into microbial biomass). In contrast, macroalgae-derived HMW DOM primarily supported microbial respiration (i.e., a shift from anabolism to catabolism), and/or resisted microbial degradation, both ultimately reducing trophic transfer. Increasing abundance of opportunistic microbes with coral HMW exudates further supports shifting DOM composition as one driver of the widespread microbialization of reefs.

A modified version of this manuscript will be submitted to *mSystems*.

8.2 Introduction

Corals are the main ecosystem engineers of tropical coral reefs, as they provide habitat and nutrients¹ to one of the most diverse and productive ecosystems on the planet^{2,3}. However, coral cover is declining on many reefs worldwide due to global and local human stressors⁴, often leading to the overgrowth by fleshy algae⁵⁻⁸. Particularly in the Caribbean widespread shifts towards stages of fleshy macroalgae dominance have been reported^{7,9,10} which may change coral reef community metabolism through exudation of dissolved organic matter (DOM), but the role of different DOM components in these interactions is poorly understood¹¹.

Algae usually exude more DOM than corals which increases the bacterioplankton abundance in reef water^{12,13}. In addition, algae DOM stimulates microbial respiration¹⁴ which can lead to deoxygenation of reefs¹⁵⁻¹⁷. Concomitantly, less energy is transformed into microbial biomass (i.e., a shift from biomass generation to respiration), reducing the transfer of energy to higher trophic levels^{18,19}. This shift in ecosystem-wide energy allocation from heterotrophic macrobes (e.g., fish and invertebrates) to foremost microbes was termed the microbialization of reefs, and was proposed to occur globally on degraded, algae-dominated reefs^{18,20}. Algae DOM also appears to select for putative opportunistic and pathogenic microbes^{18,21-23}. Combined, these indirect effects of algae DOM on the microbial community can lead to coral mortality through hypoxia and disease²⁴⁻²⁶. Coral mortality opens up space on the reef for algae growth, thus resulting in the DDAM positive feedback loop (DOC, disease, algae, microorganisms) which facilitates reef degradation^{27,28}.

These contrasting responses of microbial communities to coral- versus algae DOM suggest underlying differences in DOM composition. Indeed, liquid chromatography-tandem mass spectrometry (LC-MS/MS) has recently revealed the great diversity of coral and macroalgae exudates^{29,30}. However, this method is mostly limited to low molecular weight (LMW) components which efficiently elute from solid phase extraction columns^{31,32}, thus not capturing most carbohydrates. Carbohydrates are the most abundant biomolecules of high molecular weight (HMW; i.e., >1 nm or 1,000 Dalton) DOM in surface oceans^{33,34} and play a major role in shaping bacterioplankton communities^{35,36}. Only very few studies have investigated the carbohydrate composition of the coral reef DOM so far. Nelson et al.²³ found increased concentrations of fucose, galactose, and rhamnose in macroalgae-exuded dissolved combined neutral sugars, while the coral *Porites lobata* exuded DOM of a similar composition to ambient reef water, mainly consisting of glucose, mannose, and xylose. While coral DOM selected for oligotrophic microbes of the Alphaproteobacteria and exerted the smallest effect on the microbial community composition, macroalgae DOM selected for copiotrophs and putative pathogens of the Gammaproteobacteria and exerted the strongest effects on the natural bacterioplankton community²³.

Most carbohydrates exuded by corals³⁷ and macroalgae³⁸⁻⁴⁰ belong to the HMW size fraction (i.e., glycoproteins and polysaccharides, respectively), which can be extracted from seawater with ultrafiltration (UF, ~1 nm pore size)⁴¹. The HMW carbohydrates exuded by corals and macroalgae can

thus be concentrated using UF, and subsequently added to ambient seawater with minimal dilution of the bacterioplankton community, while at the same time keeping DOM concentrations within a natural range. The majority of studies investigating the effects of primary producer exudates on bacterioplankton apply dilution culture experiments⁴², where prefiltered exudate-enriched water is inoculated with unfiltered ambient reef water resulting in a reduction of microbial cell abundance by at least 40 %^{14,23,29,43}. This approach alleviates density-dependent effects and allows to determine exponential growth rates as a measure of substrate quality. However, dilution also influences the community composition of bacterioplankton^{44,45} and affects competitive outcomes^{46,47}. Differences in the amount of exuded DOM between corals and macroalgae in previous studies further resulted in higher starting concentrations for macroalgae- compared to coral DOM^{23,43}, which makes it difficult to untangle the effects of DOM concentration (i.e., quantity) and DOM composition (i.e., quality) on bacterioplankton communities. Thus, the question remains whether coral and macroalgae exudates, added at similar concentrations, also differentially influence an undiluted microbial community.

All in all, interaction of coral- and macroalgae-derived DOM with bacterioplankton received much attention over the last decades¹¹ due to increasing macroalgae dominance, especially in the Caribbean¹⁰, and global evidence that algae DOM supports reef microbialization¹⁸. However, there are considerable knowledge gaps concerning DOM-microbe interactions for algae-dominated, Caribbean reefs. It further remains unclear how much of the previously observed effects on bacterioplankton were due to differences in composition versus concentration of coral versus macroalgae-derived DOM²³. Finally, no study has yet assessed how the most reactive part of DOM, the HMW carbohydrate fraction, affects undiluted coral reef bacterioplankton communities.

To address these knowledge gaps we investigated the exudation of hydrolysable carbohydrates by corals and macroalgae, and how this particular DOM influences bacterioplankton communities from a Caribbean reef. We hypothesized that i) corals and macroalgae enrich HMW DOM in reef water with carbohydrates of different compositions, and ii) that the different exudates would enrich different taxa of the bacterioplankton community relative to seawater controls, with algae exudates exerting a stronger effect. We conducted a two-part experiment where we first incubated four hard coral species, two brown macroalgae genera, and seawater controls in aquaria to collect the exudates (see experimental design in [Fig. 8.1](#)). Subsequently, we concentrated HMW exudates from the incubation water, and analyzed the monosaccharide composition of hydrolysable carbohydrates. Finally, we added the concentrated HMW DOM to ambient seawater in four-day dark incubations to elucidate effects on the growth and community composition of the heterotrophic bacterioplankton community to coral and macroalgae HMW DOM. By investigating bacterioplankton dynamics from a macroalgae-dominated reef in response to primary producer-specific HMW DOM-carbohydrate compositions, our study may help to understand the functioning of changing reef communities from a microbial ecology perspective.

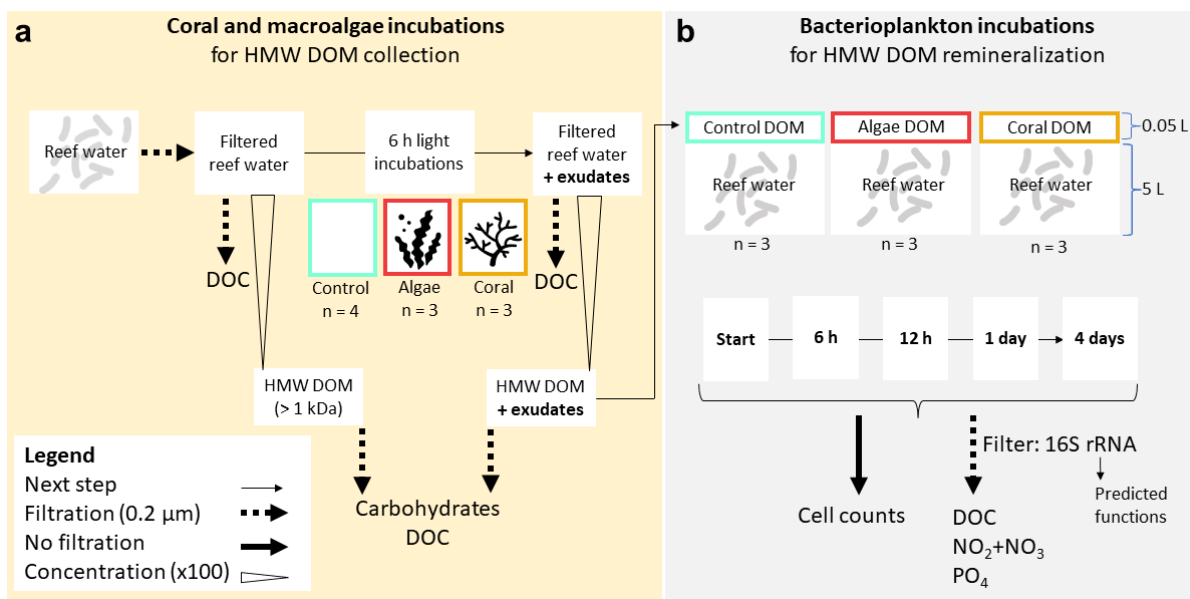


Figure 8.1. Experimental design divided into (a) coral and macroalgae incubations for exudate collection from corals and macroalgae and (b) bacterioplankton incubations for exudate remineralization by microbes from ambient reef water. DOC = dissolved organic carbon; HMW DOM = high molecular weight (> 1,000 Dalton) dissolved organic matter. Concentrated HMW DOM (concentration factor of 100) enriched with exudates from coral and macroalgae incubations was diluted with ambient reef water in dark incubations (dilution factor of 100).

8.3 Methods

The macroalgae and corals

The macroalgae *Dictyota* spp. and *Lobophora* spp., and three of the four coral species (i.e., *Diploria labyrinthiformis*, *Meandrina meandrites*, and *Madracis auretenra*) were collected from the reef of Piscadera Bay, Curaçao (12.121, -68.970) at 8-10 m depth. Additionally, fragments of *Acropora cervicornis* were provided by the coral restoration project Reef Renewal Curaçao and kept on a floating coral nursery (10 m depth) in front of the CARMABI research station until the experiment. All of the coral and algal species used here are abundant on Curaçaoan reefs and wide-spread through the Caribbean region⁴⁸⁻⁵¹. Algae were placed into plastic bags for transportation and carefully rinsed with fresh seawater to remove sediment or particles before placing them into the experimental tank. Coral colonies were carefully cleaned with tooth brushes to remove encrusting sponges from the underside of colonies and kept in the floating nursery to heal any small injuries for one week. After retrieving macroalgae and hard corals from the reef/nursery, the organisms were kept submerged in a flow-through aquarium until the start of the incubations on the same day. Following the completion of experiments in the present study, coral colonies were placed back on the reef or used for restoration activities (i.e., *A. cervicornis*). All collections and experimental work were carried out under the research permit (#2012/48584) issued by the Curaçaoan Ministry of Health, Environment and Nature (GMN) to the CARMABI foundation.

Coral and macroalgae incubations for exudate collection

To collect coral and macroalgae exudates, as well as DOM from unamended seawater controls, six-hour incubations were conducted in a glass tank (22 L, rinsed with 10 % hydrochloric acid, HCl) with seawater, which was filtered to remove particles and planktonic organisms (see details below and experimental design in Fig. 8.1a). Corals or macroalgae were placed into the tank with sterile gloves (nitrile, powder free), covering about one third (corals) or half (algae) of the aquarium floor (see photographs in Supplementary Fig. S8.1), which approximates the relative benthic cover at, respectively, coral- or algae-dominated reefs in the Caribbean⁵². The same experimental setup was used for all incubations (three of each treatment, and four seawater controls), which were done on different days between the 8th and 23rd of November 2021. Seawater from Piscadera Bay, collected the previous day through a pipe leading from the reef (5 m depth) into the aquarium facilities, was run over filters with decreasing pore sizes to remove particles (50, 20, 5, 0.5 μm), and microbes (0.2 μm , 12 cm diameter, polycarbonate, pre-flushed with 1 L seawater), for 4 hours. Filtered seawater was collected and stored in closed HDPE buckets (rinsed with 10 % HCl, ultrapure water, UW, and filtered seawater) in an air-conditioned room (29 °C) in the dark until the next day. The tank was placed in a flow-through water bath with fresh seawater to keep temperatures close to *in situ* conditions (measured every five minutes with HOBO Pendant; Table 8.1). Salinity remained stable throughout the incubations (Table 8.1). A recirculating pump (UW-rinsed) was used to provide water movement in the incubation tank, and the top of the tank was left open to allow gas exchange. Oxygen concentrations did not change in controls throughout the incubations, but increased for both treatments during the incubations to 195 % air saturation (Table 8.1). These oxygen concentrations can be observed in coral reefs in diffusive boundary layers (DBL), at the coral-algal interface, and on the reef scale⁵³. Artificial light was provided throughout the incubations (CoralCare, Philips Lighting, 190-W-LED fixture). Light intensities for the experimental setup were measured on the 9th of November 2021 in photosynthetically active radiation (PAR, Table 8.1) and were within the range of light intensities on the reef at 10 m depth in November (i.e. up to $\sim 500 \mu\text{mol photons m}^{-2} \text{s}^{-1}$ ¹³).

Table 8.1. Environmental parameters of incubations with seawater controls, corals, and macroalgae. Ambient values measured on the reef at 10 m depth (temperature, light) or at the start of the incubations (salinity, oxygen: n = 10). Values are presented as means with standard deviations. 100 % air saturation corresponds to $170 \mu\text{mol O}_2 \text{L}^{-1}$ (or 6.8mg L^{-1}). Temperature was measured every five minutes throughout the incubations, and salinity and oxygen were measured at the start (ambient) and end of the incubations. Light was measured once on the 9th of November 2021 for the experimental setup which was constant during the whole experiment.

Variable	Ambient	Control	Coral	Algae
Temperature (°C)	29.1 ± 0.1	29.0 ± 0.3	29.0 ± 0.2	29.0 ± 0.1
Light (PAR, $\mu\text{mol photons m}^{-2} \text{s}^{-1}$)	-	448 ± 6	448 ± 6	448 ± 6
Salinity (‰)	36.6 ± 0.2	36.7 ± 0.3	36.7 ± 0.1	36.9 ± 0.1
Oxygen ($\mu\text{mol L}^{-1}$ / % Air saturation)	196 ± 4 / 115 ± 2	196 ± 4 / 115 ± 3	332 ± 23 / 195 ± 14	332 ± 23 / 195 ± 14
Replicates (n)	3 / 10	4	3	3

Concentration of high molecular weight dissolved organic matter

Water samples (~ 20 L) from the six-hour aquarium incubations (start and end) were collected into HDPE buckets with a silicone tube (both 10 % HCl and sample-rinsed). Corals and algae were removed with sterile gloves (nitrile, powder free) before air exposure could lead to a stress response which may affect the incubation water. From the bucket, water was filtered with pre-flushed (200 mL) polyethersulfone filters (0.2 µm pore size, Millipore Sterivex) for 2 hours using a peristaltic pump (Masterflex L/S) and sample-rinsed platinum-cured silicone tubes (Masterflex, 96410-15). Dissolved nutrient samples (i.e., DOC, inorganic nutrients) were collected from the filtrate. All remaining water was concentrated with tangential flow-filtration (TFF) by a factor of 100 and a molecular weight cut-off of 1,000 Dalton (UFP-1-C-5, Cytiva). The TFF cartridge was cleaned according to the manufacturer manual, with 0.5 N NaOH and ultrapure water. Trans-membrane pressure was set to 2-3 bar during sample concentrations. From the concentrated water (i.e., 14 L concentrated to 140 mL), samples for dissolved organic carbon (DOC) measurements were collected (i.e., HMW DOC). The remaining concentrated water was stored at -20 °C for the microbial degradation experiment and carbohydrate analyses.

Bacterioplankton incubations for exudate remineralization

To test the effects of HMW exudates from macroalgae and corals on bacterioplankton communities in reef water, we conducted four days-long dark incubations (see experimental design in Fig. 8.1b). Fresh seawater was collected from the reef of Piscadera Bay on the 1st of December 2021 between 9:30 and 10:45 am at a depth of 6.8 m, 0.5 m above the benthos, with low current. Water was collected in four 20 L PE bottles (10 % HCl and seawater rinsed) while facing the opening of the bottles away from the diver and towards the current. Water bottles were stored at 29 °C in the dark for ~7 h until the start of the experiment. Equal parts of every bottle were used for the nine incubation containers (three per treatment or control, 5 L, PP) to ensure equal water quality and microbial community compositions. Extracts from coral and macroalgae incubations and seawater controls were thawed and pooled by treatment (i.e., extracts from three replicate exudation incubations per treatment were mixed). Subsequently, 50 mL of the respective extract were added to 5 L of fresh seawater. All incubation containers were placed in dark Styrofoam boxes where HOBO loggers recorded light intensities (always 0 Lux) and temperatures (26.7 °C ± 0.3 sd). Samples for all parameters were collected at five timepoints: shortly after the start of the incubations (ca. 30 minutes after exudate addition), after six and 12 hours, and after one and four days. Samples for DOC and inorganic nutrients were filtered with a peristaltic pump at a flow rate of 26 mL min⁻¹ (Masterflex L/S) through pre-flushed (200 mL) polyethersulfone filters (0.2 µm pore size, Millipore Sterivex) attached to sample-rinsed platinum-cured silicone tubes (Masterflex L/S Precision Pump Tubing, Tygon). Samples were collected from the bottom of each incubation container after gentle shaking.

Coral mucus and macroalgae tissue extraction

Data on coral mucus carbohydrate compositions of *A. cervicornis*, *D. labyrinthiformis*, and *M. meandrites* was already reported in a previous study (Thobor et al., submitted; [chapter 7](#)), where coral mucus collection and analyses are described in detail. Briefly, on the day after the coral and algae exudation experiment, coral colonies were exposed to air for three minutes. Dripping mucus was collected into sterile vials for two minutes after disposing mucus for the first minute, as done in previous studies⁵⁴, and stored at -20 °C until analysis of carbohydrate compositions. Macroalgae from the experimental tanks were rinsed with UW and then oven-dried (40 °C, 48 h) and stored in sterile PP tubes (Falcon, 50 mL, Thermo Fisher Scientific) at room temperature in the dark. Dried algae tissue was pulverized with a mortar and pestle, and alcohol insoluble residue (AIR) and subsequently the water-soluble fraction were prepared as described by Vidal-Melgosa et al.⁵⁵. Dried powder was suspended in pure ethanol (volume ratio 6:1 of solvent:pellet), vortexed, rotated for ten minutes, and then centrifuged (21.100 x g for 15 minutes at 15 °C). The pellet was then washed in a 1:1 Chloroform:Methanol solution until the supernatant was clear. The pellet was then washed in pure acetone, and air dried at room temperature. Subsequently, 10 mg of this AIR-washed powder were re-suspended in 300 µL of autoclaved UW, shaken for 2 h at 15 °C, centrifuged (6,000 x g for 15 minutes at 15 °C), and the supernatant collected. The supernatant containing the water-soluble fraction was stored at -20 °C until carbohydrate analysis.

Carbohydrate analysis

For carbohydrate analysis of HMW DOM, 200 µL of 2 M HCl were added to 200 µL of samples and acid hydrolyzed at 100 °C for 24 h in pre-combusted (400 °C, 4 h) glass ampules. After hydrolysis, samples were dried down with an acid-resistant vacuum concentrator (Martin Christ Gefriertrocknungsanlagen GmbH, Germany) together with calibration standards which were prepared in 1 M HCl. Standards and samples were then resuspended in 200 µL UW and transferred to sterile HPAEC vials for measurement. Coral mucus samples and algae tissue extracts were hydrolyzed as described above, and then diluted with UW by a factor of 100 (coral mucus) and 50 (algae tissue extracts), centrifuged (21.100 x g for 15 minutes at 15 °C), and 100 µL of the top layer was transferred to HPAEC vials for measurement with calibration standards. Monosaccharide concentrations of hydrolyzed carbohydrates were measured on a high performance anion exchange chromatography (Dionex ICS-5000⁺ system with CarboPac PA10 guard column (2 x 50 mm) and analytical column (2 x 250 mm, Thermo Fisher Scientific), coupled with pulsed amperometric detection (HPAEC-PAD), as previously described^{55,56}. Separation of neutral and amino sugars was achieved with an isocratic flow of 18mM NaOH, followed by a separation of acidic monosaccharides with a gradient reaching up to 200 mM NaCH₃COO. Concentrations were calculated from peak areas of six co-measured standard mixes with concentrations ranging from 10 to 1000 µg L⁻¹ per monosaccharide using Chromeleon (Thermo Fisher Scientific).

Dissolved organic carbon and inorganic nutrient analysis

DOC samples (20 mL) were collected in pre-combusted (4 h at 450 °C), sample-rinsed glass vials closed with teflon-lined lids (10 % HCl acid washed and sample-rinsed), acidified with 5 drops of 12N HCl to a pH < 2, and stored at 4 °C until measurement. Concentrations of DOC were measured with high-temperature catalytic oxidation (TOC-L CPN, Shimadzu), calibrated with a standard curve of potassium hydrogen phthalate (0; 25; 50; 100; 200; 400 $\mu\text{mol C L}^{-1}$). Every sample was injected 5-7 times, resulting in an analytical variation of 2.3 %. Measurement accuracy was tested by including consensus reference material (CRM: Batch 21, Lot: 04-21, DOC: $44.7 \mu\text{mol L}^{-1} \pm 0.8 \text{ sd}$, D.A. Hansell, University of Miami) into every measurement run, which was on average 8 % below the reported concentration. Two samples (i.e., algae 2 and coral 2) had to be collected ~1.5 h after the other samples due to practical constraints, affecting DOC concentrations which were thus excluded from analyses.

Dissolved inorganic nutrient samples (5 mL) were collected in sample-rinsed HDPE vials (Midivial, PerkinElmer; Waltham, MA, USA) and stored at -20 °C until measurement on a Gas Segmented Continuous Flow Analyzer (QuAatro / TRAACS, SEAL Analytical). Calibration standards were prepared in low nutrient seawater (LNSW) with the same ionic strength as analyzed samples (salinity ~ 35 ‰). For the analysis of nitrite (NO_2) + nitrate (NO_3), NO_3 was first reduced to NO_2 at pH 7.5 by a copperized cadmium column. The resulting NO_2 was then turned into a pink complex through addition of sulphonylamide and naphthyl ethylene-diamine and measured at 550 nm⁵⁷. Phosphate (PO_4) was first turned into a yellow phosphate-molybdenum complex at pH 1.0 with potassium antimonyl tartrate acting as a catalyst. The complex was then reduced into a blue molybdophosphate-complex with ascorbic acid and measured at 889 nm⁵⁸. Two samples from dark incubations had to be excluded (i.e.: control 2, Start; coral 1, 1 day) due to high salinity (an artifact from overflowing sample vials while freezing).

Microbial cell counts

Samples for microbial cell counts (1 mL) were taken with sterile pipette tips directly from the incubation containers, immediately fixed with 20 μL glutaraldehyde (15 min at 4 °C) and stored at -80 °C until analysis with flow cytometry (FACSCalibur, BD Biosciences, New Jersey, USA). Samples were 1:5 diluted with pre-filtered (0.2 μm) Tris-EDTA (TE) buffer, stained with 2 % SYBR Green, and stored in the dark for > 15 minutes prior to measurements. The output was analyzed with FCS Express 5 (DeNovo), and values from blanks (TE only) were subtracted from results.

DNA extraction

DNA was extracted from frozen (-20 °C) polyethersulfone filters (0.2 μm pore size, Millipore Sterivex) which were used for nutrient sample collection (filtered volume: 0.2 – 1.2 L) as described in Haas et al.⁵⁹. All extractions were done with sterile utensils in a UV cabinet (UVT-S-AR, BioSan). We used the NucleoSpin Tissue (Macherey-Nalgel, 250 preps) DNA extraction kit following manufacturer instructions with some adjustments. Filters were thawed at room temperature, air-dried with a Luer lock

syringe, and closed on one end. Subsequently, 410 μL of proteinase K (50 μL) and buffer T1 (360 μL) solution was pipetted into the Luer lock opening of the filter, which was then closed and rotated overnight (~ 18 h) at 55 $^{\circ}\text{C}$ in a hybridization oven (Compact Line OV4, Biometra). On the next day, 400 μL of Buffer B3 was added to the filters, and filters were rotated at 70 $^{\circ}\text{C}$ for 15 min. Subsequently, the liquid (500-750 μL) was removed from the filters with 3 mL Luer lock syringes and placed into a microtube. Samples were diluted with pure ethanol in a volume ratio of 1:2 ethanol:sample and vortexed. The solution was then added to the column and centrifuged for 1 min at $11,000 \times g$. After washing the column with 500 μL of BW and 600 μL of B5 buffers, the silica membrane containing the extracted DNA was dried for 2 min at $11,000 \times g$. Pure DNA was then eluted into a microtube with 100 μL BE buffer which was incubated for 10 min at room temperature, and spun down for 1 min at $11,000 \times g$. Extracted DNA was stored at -20 $^{\circ}\text{C}$, and then transported on ice to the University of Hawai'i at Mānoa for amplification.

Amplicon library sequencing and bioinformatics

The V4 region of the small subunit (16S) ribosomal RNA gene was amplified from each genomic DNA template using forward-indexed primers 515F-Parada: GTGYCAGCMGCCGCGGTAA and 806R-Apprill: GGACTACNVGGGTWTCTAAT⁶⁰ following the protocols of the Earth Microbiome Project⁶¹, with the following minor changes: we did not pool triplicate reactions, and we used 1 μL of genomic template. Amplicons were cleaned and normalized to equimolar concentrations using the SequelPrep kit (Thermo Fisher Scientific) and then pooled and sequenced on the Illumina MiSeq platform (600 cycle V3 chemistry). Sequences were demultiplexed using a custom probabilistic script and microbiome profiling was implemented in the MetaFlow|omics pipeline⁶² following the specific settings presented by Jani et al.⁶³: sequences were assembled, denoised and quality trimmed using DADA2⁶⁴, globally aligned with mothur⁶⁵ to the Silva (v132) global SSU rRNA alignment database⁶⁶, bayesian consensus classified (70 %) to the Genus level⁶⁷, and clustered into 99 % sequence identity operational taxonomic units using vsearch⁶⁸ refined to reduce intragenomic taxonomic splitting errors using LULU⁶⁹. Sequences that could not be classified at the Domain level or were classified as chloroplast or mitochondrial 16S were discarded and sequencing depth was subsequently standardized to 10,000 random reads per sample. All bioinformatics were deployed on the C-MAIKI gateway⁷⁰ at the University of Hawai'i at Mānoa by the Center for Microbial Oceanography: Research and Education.

We used MicFunPred⁷¹ to predict metabolic pathway abundance from 16S rRNA data. The tool normalized our OTU abundance table to library size, assigned taxonomy down to genus level and then used the MetaCyc database to predict core gene contents. The output is a product of normalized taxonomic abundance and core gene content. We acknowledge the limitations of using 16S rRNA data to infer metabolic functions. Firstly, the accuracy of predicting metabolic functions based on 16S rRNA amplicon sequencing depends on the quality and size of the reference database and may be limited for rare pathways and specific environments^{71,72}. Secondly, pathways specific to certain strains are not

included because 16S rRNA amplicons do not allow identification down to the microbial strain⁷². MicFunPred addresses the second limitation, as it predicts the functional potential based on a set of core genes (i.e., genes present in $\geq 50\%$ of genomes in the genus), which minimizes the false-positive results and uses MinPath to estimate the minimal set of pathways for pathway prediction⁷¹.

Statistical analyses

All statistical analyses were conducted using R Studio (R version 4.3.0, R Studio version 2023.06.2). Before conducting parametric tests, we checked for outliers (*rstatix* package), normal distribution (Shapiro-Wilk test), and homogeneity of variance (Levene test) across and within groups. The effect of treatments on DOC- and carbohydrate concentrations in light incubations was tested with one-way analysis of variance (ANOVA; data was square root-transformed if necessary to achieve normal distribution), and Tukey's HSD test for *post-hoc* analyses. One monosaccharide (rhamnose) was analyzed using non-parametric tests (Kruskal-Wallis and pairwise Dunn's tests with Bonferroni adjustment) because one group contained two zero values. We used false discovery rate (fdr) correction to control the family-wise error rate across different monosaccharides. Hierarchical cluster analysis of HMW exudate-, coral mucus- and algae tissue composition was conducted using Euclidean distance and the R package *ComplexHeatmap*⁷³; Simprof analysis (*clustsig* package) was used to test for significant differences between clusters. Differences of microbial cell densities among timepoints (within-subjects factor) and treatments (between-subjects factor) were analyzed using two-way mixed ANOVA and pairwise *t*-tests with Bonferroni adjustment. For mixed ANOVA, we additionally tested for homogeneity of covariance (Box's M-test). Some outliers had to be excluded from DOC concentrations (i.e., $n = 2$ for algae and coral treatments) and inorganic nutrient concentrations (i.e., $n = 2$ for controls at the start and coral treatments after one day) and were thus analyzed with non-parametric tests (Kruskal-Wallis and Friedmann), followed by pairwise Dunn's tests with Bonferroni adjustment.

To compare microbial community composition and predicted metabolic pathway abundances among treatments we used two-way permutational multivariate ANOVA (PERMANOVA) to test for the single and combined effects of time and treatment, and five one-way PERMANOVAs with fdr-correction to test for treatment effects at every time point. For visualization of the microbial community composition, we used a non-metric multidimensional scaling (NMDS) plot (*vegan* package) with Bray-Curtis dissimilarity between square root transformed relative abundances of microbial genera. We used hierarchical cluster analysis of the Euclidean distance (*ComplexHeatmap* package) between Z-score scaled (across samples) relative abundances of microbial genera ($> 0.5\%$ relative abundance), and predicted metabolic pathway abundance. For the two timepoints with significant treatment effects on the microbial community composition (i.e., one and four days), permutational supervised classification random forest (RF) analysis was performed (*rfPermute* package, 5000 trees, 100 permutations), as done previously to assess differences in microbial community compositions between pre-defined groups^{16,74}.

Diagnostic plots confirmed that enough trees were grown. In addition, we used differential expression analysis (*DESeq2* package⁷⁵) to contrast microbial community composition and metabolic pathway abundance of both treatments with control communities. A consensus approach of RF and *DESeq2* analyses was used to identify genera which were most important for characterizing treatments⁷⁶. Metabolic pathways were annotated by pathway class (i.e. super pathway, MetaCyc database) and pathway type (i.e., sub-groups of super pathways), and the abundance of each pathway class throughout the experiment was analyzed with mixed model ANOVAs (fdr-corrected). For metabolic classes with significant interaction terms, five one-way ANOVAs were conducted (one at each timepoint, Bonferroni-adjusted), and fdr-corrected for multiple testing across pathway classes.

8.4 Results

Dissolved organic carbon- and carbohydrate exudation by corals and macroalgae

DOC concentrations were significantly enriched after six hour exudation incubations with corals and macroalgae compared to starting concentrations by 13 % and 11 %, respectively (ANOVA, $F_{(3,15)} = 10.5$, $p < 0.001$, $\eta^2_G = 0.68$, HSD test; Fig. 8.2a). HMW DOC contributed on average 3.2 % (± 0.7 sd) to total DOC and was not significantly affected by treatments (Fig. 8.2b). Combined HMW carbohydrate concentrations were significantly enriched by 168 % in macroalgae incubations compared to controls and starting concentrations (ANOVA, $F_{(3,9)} = 6.5$, $p < 0.05$, $\eta^2_G = 0.68$, HSD test; Fig. 8.2c). Percent carbohydrate content of HMW DOC in macroalgae- and coral incubations was significantly enriched compared to controls and starting concentrations by 134 % and 110 %, respectively (ANOVA, $F_{(3,8)} = 13.0$, $p < 0.01$, $\eta^2_G = 0.83$, HSD test; Fig. 8.2d).

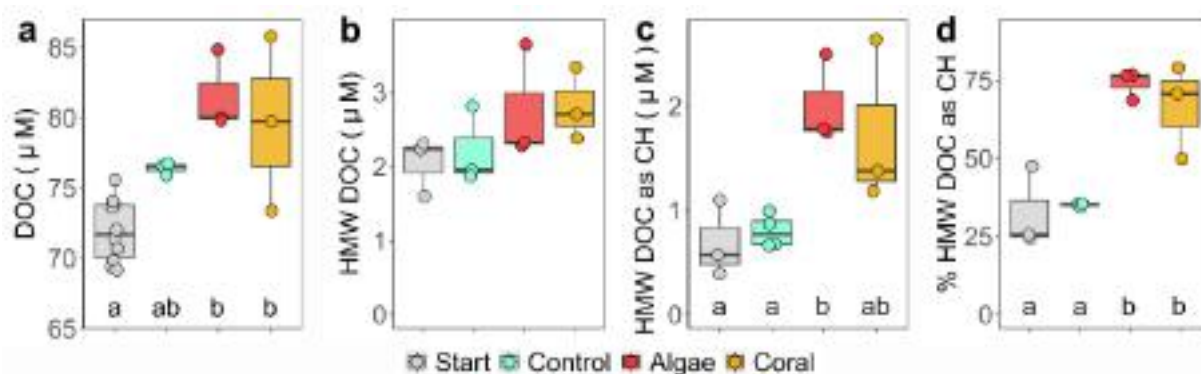


Figure 8.2. Change during 6h exudation incubations with corals and macroalgae in (a) dissolved organic carbon (DOC) concentrations, (b) high molecular weight (HMW) DOC concentrations, (c) HMW carbohydrate concentrations (as carbon equivalents), and (d) percentage of HMW DOC as carbohydrates (CH). Values in c and d were calculated based on carbon contents of neutral-, amino- and acidic monosaccharides measured after acid hydrolysis of HMW DOM (see Fig. 8.3). Boxes represent median \pm 95 % confidence intervals, and points represent replicates. Different letters indicate significant differences between treatments (HSD test; $p < 0.05$). Raw data to this figure is available in [Supplementary Table S8.3](#).

Hydrolysable monosaccharide composition of HMW coral- and macroalgae-exudates

In exudation incubations with macroalgae concentrations of fucose, galactose, and galacturonic acid significantly increased by 388 %, 252 %, and 128 %, respectively, compared to seawater controls and

starting concentrations ($p < 0.01$, HSD test, Fig. 8.3, all ANOVA results in Table 8.2). Rhamnose concentrations increased significantly by 932 % compared to starting concentrations ($p < 0.05$, pairwise Dunn's test, Bonferroni adjusted). The mole percent contribution of fucose to total carbohydrates increased significantly compared to seawater controls and starting concentrations ($p < 0.001$, HSD test, Supplementary Fig. S8.2). All other monosaccharides were not significantly affected by macroalgae exudation.

In exudation incubations with corals, concentrations of arabinose and glucosamine significantly increased by 812 % and 360 % compared to seawater controls and starting concentrations ($p < 0.01$, HSD test, Fig. 8.3). Galactosamine concentration increased by 125 % compared to starting concentrations ($p < 0.05$). The mole percent contribution to total carbohydrates increased significantly compared to seawater controls and starting concentrations for arabinose ($p < 0.0001$), glucosamine ($p < 0.01$), and mannose ($p < 0.05$) by 248 %, 59 %, and 21 %, respectively (HSD test, Supplementary Fig. S8.2). All other monosaccharides were not significantly affected by coral exudation and none of the monosaccharides within the HMW DOM pool increased in seawater control incubations compared to starting concentrations (Fig. 8.3).

Table 8.2. Statistical test results for differences in concentrations and mole percent compositions of HMW carbohydrates between treatments for all analyzed monosaccharides. DF_n = 3, DF_d = 9 for all tests. Test: AOV = analysis of variance; sqrt = analysis of variance of square root transformed data; KW: Kruskal-Wallis test. Bold values indicate significant fdr-corrected p values.

Monosaccharide	Test	F or H	Concentration			Test	F or H	Mole %		
			η^2	p	p (fdr)			η^2	p	p (fdr)
Fucose	AOV	30.1	0.91	< 0.0001	< 0.001	AOV	30.0	0.91	< 0.0001	< 0.001
Galactose	AOV	13.2	0.81	0.001	< 0.01	AOV	5.9	0.66	0.017	< 0.05
Galacturonic acid	AOV	17.8	0.86	< 0.0001	< 0.01	AOV	1.4	0.32	0.311	n. s.
Rhamnose	KW	9.2	0.69	0.027	< 0.05	KW	8.1	0.57	0.043	n. s.
Arabinose	Sqrt	12.3	0.80	0.002	< 0.01	AOV	54.3	0.95	< 0.0001	< 0.0001
Mannose	AOV	4.4	0.60	0.036	n. s.	AOV	7.7	0.72	0.007	< 0.05
Glucosamine	Sqrt	11.0	0.79	0.002	< 0.01	AOV	25.1	0.89	0.0001	< 0.001
Galactosamine	Sqrt	5.6	0.65	0.019	< 0.05	Sqrt	6.8	0.69	0.011	< 0.05
Xylose	AOV	2.9	0.49	0.093	n. s.	AOV	2.9	0.50	0.092	n. s.
Glucose	Sqrt	1.3	0.31	0.326	n. s.	Sqrt	8.7	0.74	0.005	< 0.05
Muramic acid	AOV	0.4	0.12	0.395	n. s.	AOV	9.8	0.77	0.003	< 0.01
Gluconic acid	AOV	0.7	0.18	0.596	n. s.	Sqrt	0.8	0.21	0.517	n. s.

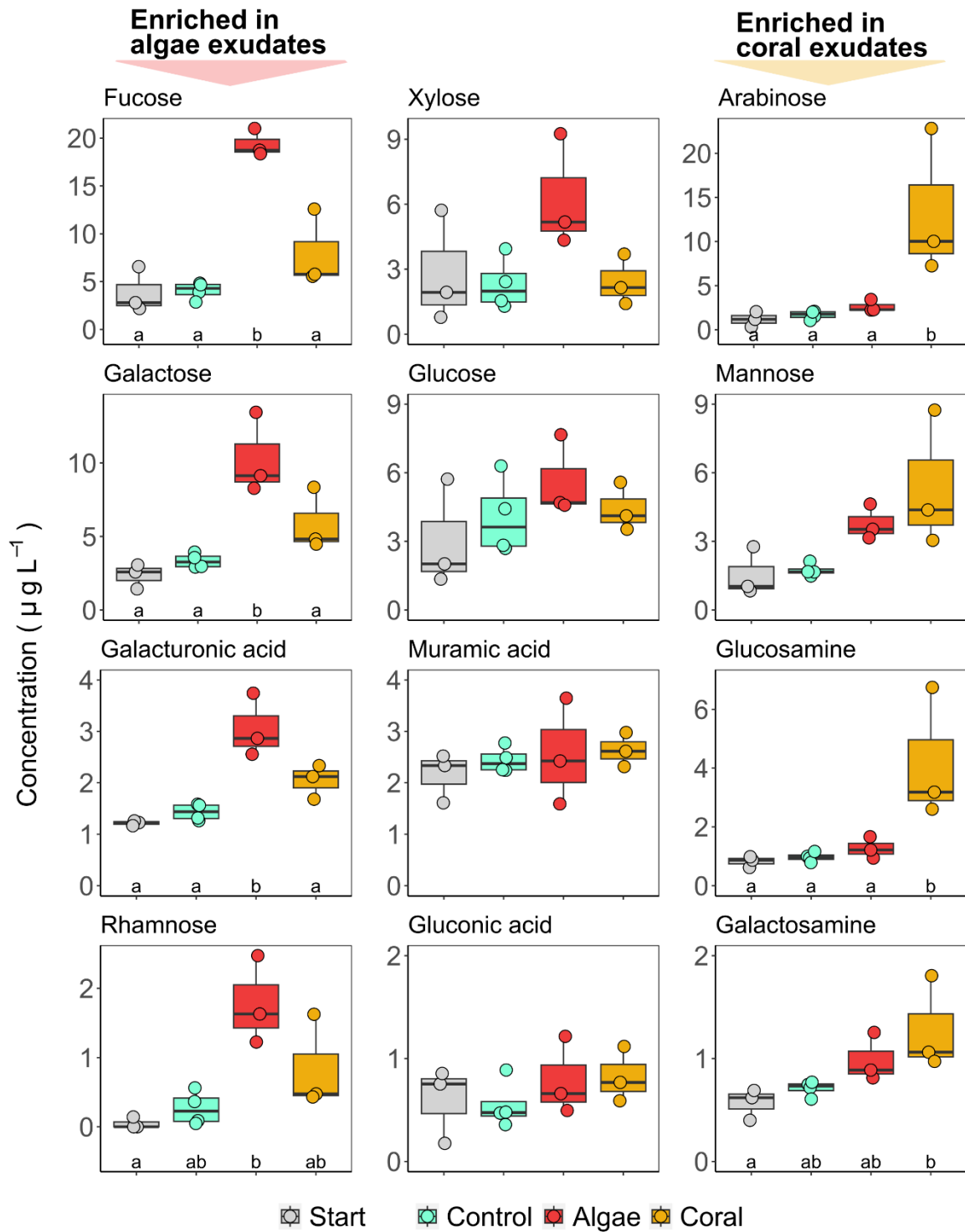
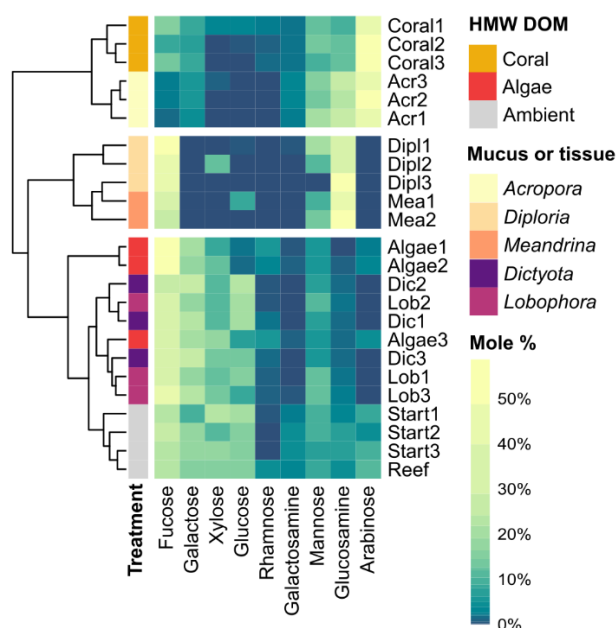


Figure 8.3. Carbohydrates released by corals and macroalgae. Boxes display concentrations of monosaccharides after hydrolysis of carbohydrates, in the high molecular weight (HMW) fraction of dissolved organic matter (DOM). Boxes represent median \pm 95% confidence intervals, and points represent replicates. Letters indicate significant differences between treatments (HSD test; $p < 0.05$). Only rhamnose had to be analyzed with non-parametric statistical tests (Dunn's test with Bonferroni adjustment). See further results of statistical tests in [Table 8.2](#). Raw data to this figure is available in [Supplementary Table S8.4](#).

Comparison of exudate compositions to coral mucus, macroalgae tissue, and ambient reef water

Coral exudate compositions clustered with coral mucus compositions of *A. cervicornis* (n = 3; SIMPROF, $p < 0.0001$; Fig. 8.4), which was characterized by high relative contents of arabinose (49 % \pm 4; always stated as mean \pm sd), glucosamine (24 % \pm 1), and mannose (17 % \pm 4). Mucus compositions of *D. labyrinthiformis* (n = 3) and *M. meandrites* (n = 2) were significantly different from coral exudates (SIMPROF, $p < 0.0001$), with high relative contents of glucosamine (37 % \pm 13 sd and 52 % \pm 10 sd, respectively), fucose (48 % \pm 1 and 34 % \pm 7, respectively), and mannose (11 % \pm 11 and 11 % \pm 3, respectively). No monosaccharides could be detected in the hydrolyzed mucus of *M. auretenra*. Ambient reef water from the start of the exudation incubations (“Start”, n = 3) and directly collected from the reef (“Reef”, n = 1) clustered with algae tissue extracts and algae exudates (SIMPROF, $p < 0.0001$; Fig. 4), and was characterized by high relative contents of fucose (24 % \pm 3), xylose (17 % \pm 5), glucose (16 % \pm 2), and galactose (15 % \pm 4). The tissue extracts of *Dictyota* spp. (n = 3) and *Lobophora* spp. (n = 3) were not separated into individual clusters and were characterized by high relative contents of fucose (34 % \pm 4), galactose (22 % \pm 4), glucose (17 % \pm 6), xylose (12 % \pm 1), and mannose (9 % \pm 3).



◀ **Figure 8.4.** Monosaccharide compositions of hydrolyzed coral and macroalgae HMW exudates (mole % composition of control-corrected fluxes) and ambient reef water HMW DOM in comparison to coral mucus and macroalgae tissue extracts. Coral mucus was collected from *Acropora cervicornis*, *Diploria labyrinthiformis*, and *Meandrina meandrites*, and macroalgae tissue was extracted from dried *Lobophora* spp. and *Dictyota* spp. thalli. The dendrogram represents Euclidean distance between samples. Only neutral- and amino-sugars were used for the comparative cluster analysis. White spaces in heatmap separate clusters of samples which were significantly different in SIMPROF analysis ($p < 0.0001$). Raw data to this figure is available in [Supplementary Table S8.5](#).

Microbial cell densities and dissolved nutrient concentrations in bacterioplankton incubations

Microbes in bacterioplankton incubations grew in all treatments within the first day, with a mean growth rate of 401,837 cells mL⁻¹d⁻¹ (\pm 105,708). Microbial cell densities did not differ between treatments and controls throughout the experiment. Only time had a significant effect on microbial cell densities (2-way mixed ANOVA: $F_{(2,9)} = 24.2$, $p < 0.001$, $\eta^2_G = 0.75$), with significantly increased densities by 46 %, 61 %, and 22 % after 12 hours, one day, and four days compared to starting conditions, respectively ($p < 0.05$, pairwise t -tests, Bonferroni adjusted, Fig. 8.5a). The estimated addition of HMW DOC for controls (i.e., the background material) was \sim 2.2 μ M C, while the added HMW DOC from coral- and macroalgae incubations was \sim 2.8 μ M C (i.e., mean HMW DOC concentrations, Fig. 8.2b). The

difference in DOC concentration between treatments and controls ($\sim 0.6 \mu\text{M C}$) was thus likely insufficient to elicit a measurable differential growth response. Dissolved nutrient concentrations (Fig. 8.5b-d) averaged $87.7 \mu\text{M DOC} (\pm 1.5)$, $0.5 \mu\text{M NO}_2 + \text{NO}_3 (\pm 0.1)$, and $0.013 \mu\text{M PO}_4 (\pm 0.002)$ at the start of the incubations, were not affected by treatments at any time throughout the experiment ($p > 0.05$, multiple Kruskal-Wallis tests), and declined over time (Friedmann tests; DOC: $\chi^2_{(4)} = 15.9$, $p < 0.01$; $\text{NO}_2 + \text{NO}_3$: $\chi^2_{(4)} = 15.4$, $p < 0.01$; PO_4 : $\chi^2_{(4)} = 17.9$, $p < 0.01$). After four days of dark incubation, DOC, $\text{NO}_2 + \text{NO}_3$, and PO_4 concentrations were reduced by 10 %, 68 %, and 26 % compared to starting concentrations, respectively.

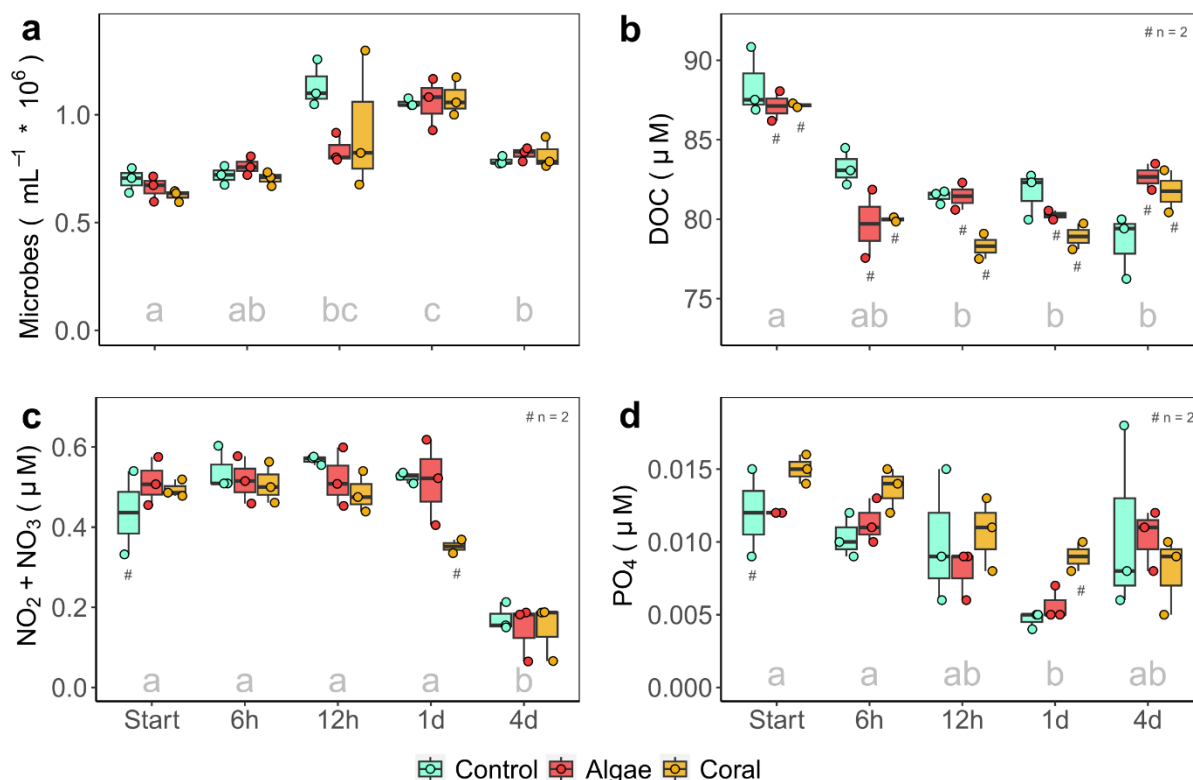


Figure 8.5. Development of (a) microbial cell densities, and (b-d) dissolved nutrient concentrations during dark incubations with corals and macroalgae HMW exudates and background HMW DOM (controls). DOC = Dissolved organic carbon, $\text{NO}_2 + \text{NO}_3$ = combined dissolved nitrite and nitrate, PO_4 = dissolved phosphate. Different letters indicate significant differences between times ($p < 0.05$, pairwise t -tests (a) or Dunn's tests (b-d), Bonferroni adjusted). Hashtags (in b-d) indicate groups where one sample had to be excluded due to sampling or measurement errors (i.e., $n = 2$). Raw data to this figure is available in [Supplementary Table S8.6](#).

Microbial community compositions in bacterioplankton incubations

The microbial community composition was significantly influenced by the interaction of time and treatment (PERMANOVA, $F_{(8)} = 2.0$, $R^2 = 0.03$, $p < 0.05$), with treatment only revealing significant effects after one and four days, explaining 52 % and 51 % of variation, respectively (Table 8.3, Fig. 8.6a). Both single factors were significant, with time and treatment alone explaining 88 % and 2 % of variation, respectively (PERMANOVA; Time: $F_{(4)} = 101.9$, $R^2 = 0.88$, $p = 0.0001$; Treatment: $F_{(2)} = 4.6$, $R^2 = 0.02$, $p < 0.01$).

The initial microbial community was dominated by Oxyphotobacteria of the Synechococcales order and Alphaproteobacteria of the SAR11 order (Fig. 8.6b). After one day, Oxyphotobacteria declined in relative abundance and were mainly replaced by Gammaproteobacteria of the Alteromonadales order. The change from day one to day four of the experiment was mainly due to increased relative abundance of Alphaproteobacteria of the SAR11 and Rhodobacterales orders (Fig. 8.6b).

Hierarchical cluster analysis of the genus-level microbial community (genera with a maximum in any one sample greater than 0.5 % rel. abundance, Z-score) revealed separation of coral exudate enriched samples from controls after one day (Fig. 8.6c), and a separate cluster of coral samples from controls and algae exudate enriched samples after four days (Fig. 8.6d), albeit clustering was not significant (SIMPROF: $p > 0.05$). To identify the most important genera for classification of treatments, we used permutational RF classification models and found 11 and 16 genera which significantly ($PFpermute: p < 0.05$) contributed to the classification of coral exudate treatments after one and four days, respectively, while only one genus at each timepoint was significant for the classification of algae exudate enriched communities (see green bars in Fig. 8.7; Supplementary Fig. S8.3 & S8.4). All coral exudate communities were successfully classified by the RF model at both timepoints, while algae exudate samples could not be distinguished from controls, and one algae sample was classified as coral sample after one day (Supplementary Table S8.1). In coral exudate treatments, six (one day) and 17 (four days) genera were significantly different from controls ($DESeq2: p < 0.05$, fdr -corrected, Fig. 8.7), while algae exudate treatments did not reveal any significant differences to controls. The consensus of both methods (RF and $DESeq2$) revealed four (one day) and eight (four days) genera (see black genus names in Fig. 8.7) which characterized coral exudate treatments.

Microbial genera significantly enriched in coral exudate treatments compared to controls (based on the consensus of RF and $DESeq2$) belonged to the Gammaproteobacteria (Vibrionaceae, Thiotrichaceae), Bacteroidia (Flavobacteriales, Saprospiraceae), Alphaproteobacteria (Rhodobacteraceae), and Planctomycetes (Phycisphaeraceae, OM190 class) (see black genus names in Fig. 8.7). Significant enrichment in coral treatments compared to controls after both one and four days occurred for genera of the three families Rhodobacteraceae, Vibrionaceae, and Phycisphaeraceae, and for unclassified Flavobacteriales (see bold names in Fig. 8.7). After one day, the most abundant member of the coral-enriched microbial community was the genus *Oleiphilus* of the Oleiphilaceae (mean rel. abundance: Coral = 2.8 %, Control = 1.1 %, Algae = 1.8 %), followed by unclassified Flavobacteriales (Coral = 1.1 %, Control = 0.2 %, Algae = 0.3 %), while all other coral exudate-enriched genera were still rare (< 1%). After four days of dark incubation, the most abundant member of the coral-enriched microbial community was an unclassified genus of the Rhodobacteraceae (Coral = 9.0 %, Control = 4.2 %, Algae = 4.7 %), followed by Planctomycetes of the uncultured class OM190 (Coral = 1.7 %, Control = 0.5 %, Algae = 0.6 %), and the genus *CL500-3* of the Phycisphaeraceae (Coral = 1.2 %, Control = 0.9 %, Algae = 0.8 %). All other coral exudate-enriched genera were still rare (< 1 %).

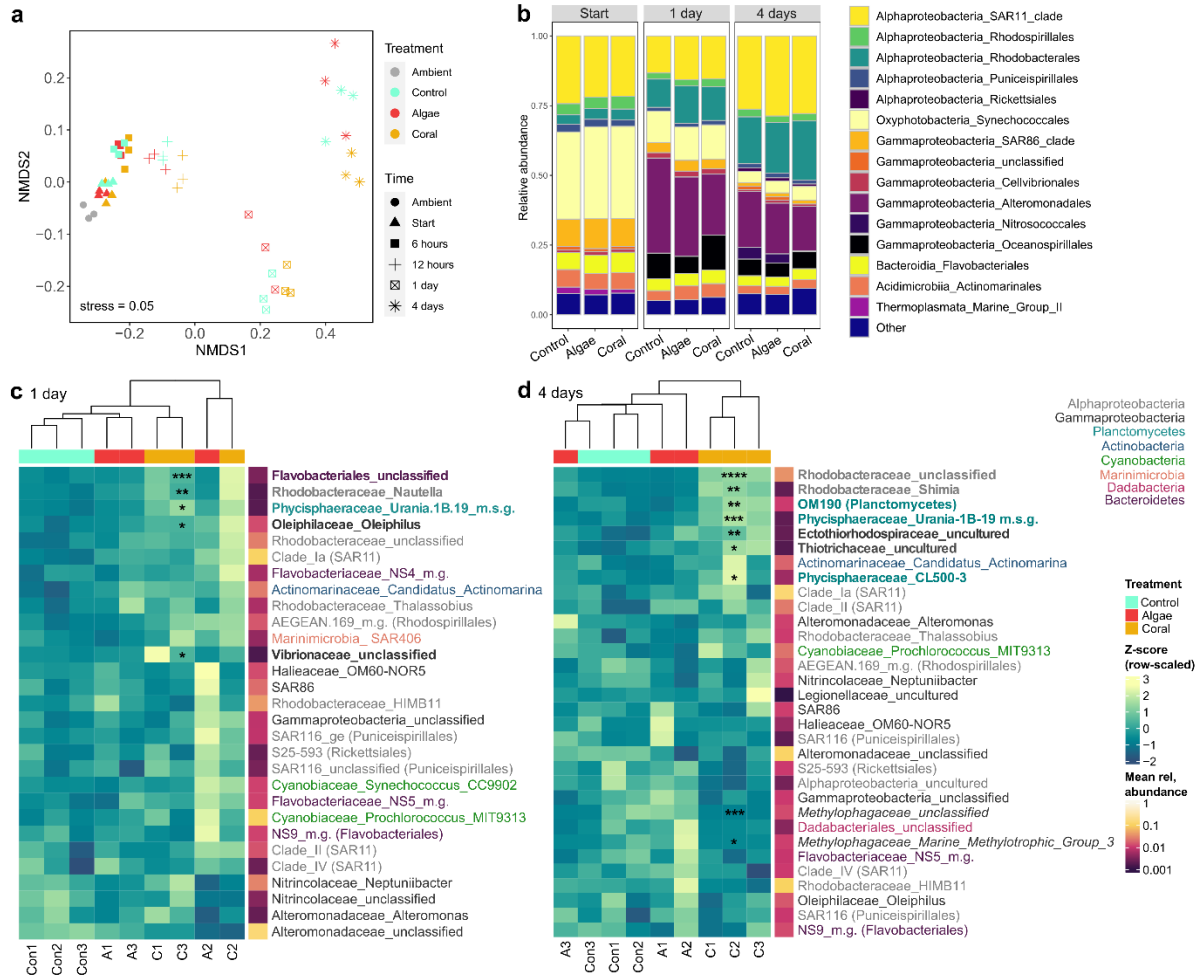


Figure 8.6. Microbial community composition in bacterioplankton incubations of reef water with addition of HMW DOM of macroalgae and coral exudates and seawater controls, displayed (a) through non-metric multidimensional scaling (NMDS), (b) as mean relative abundance of dominant orders, and (c & d) as row-scaled abundance (z-score) of genera (> 0.5 % mean relative abundance in any one sample) in hierarchical clustering heatmap for the two timepoints with significant treatment effects ($p < 0.05$, PERMANOVA, Table 8.3). NMDS plot (a) is based on square root transformed Bray-Curtis dissimilarity matrix from genus-level microbial community compositions. Dendrograms (c & d) represent Euclidean distance. Samples A2 and C2 (see column names in c & d) were collected about 1.5 hours later than the rest, which may explain close clustering after one day (c). Asterisks (in c & d) indicate significant coral treatment effect versus controls (**** $p < 0.0001$, *** $p < 0.001$, ** $p < 0.01$, * $p < 0.05$, *DESeq2*, *fdr*-corrected). Bold lineage names indicate an increase, and italicised names a decrease with coral exudates compared to controls.

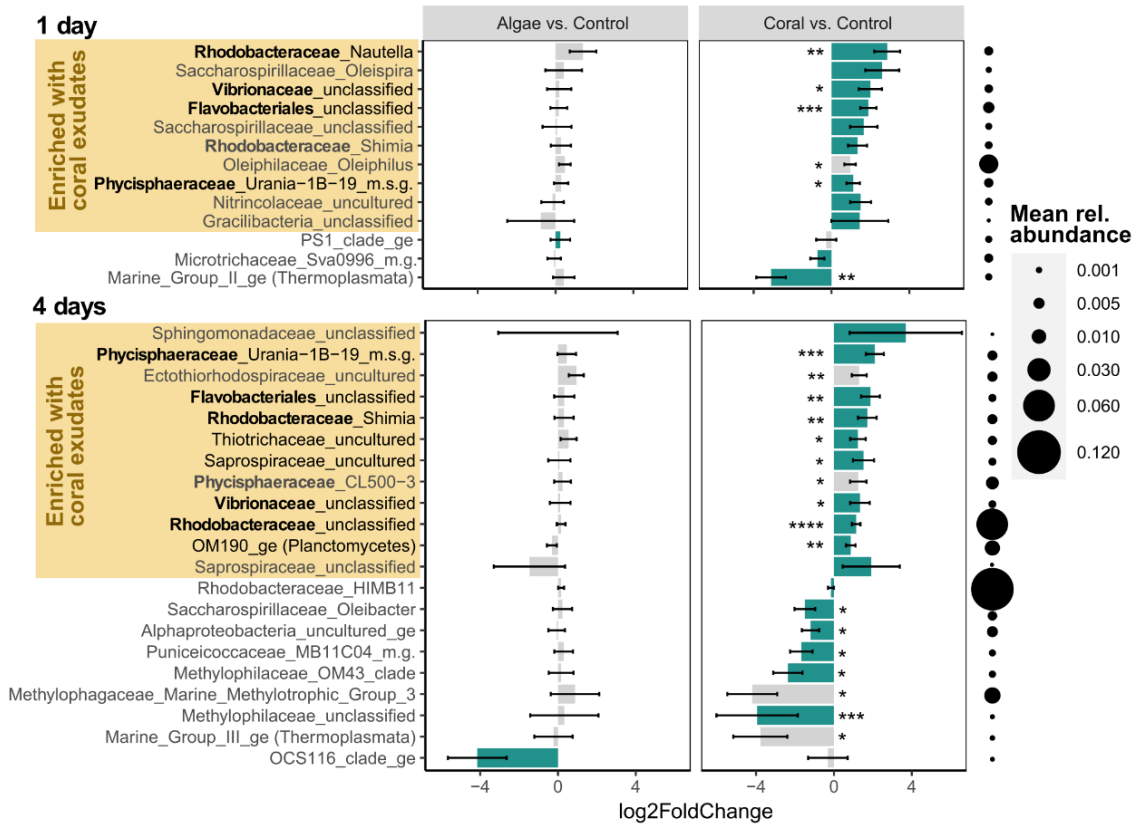


Figure 8.7. Log₂ fold change (*DESeq2*) of both treatments versus controls. Error bars represent standard error (lfcSE of *DESeq2* output). Asterisks indicate genera which were significant (fdr-corrected $p < 0.05$) in *DESeq2* analysis, and green bars indicate genera which were significant ($p < 0.05$, importance score > 5) in random forest model for classifying algae or coral treatments. Bold family names indicate families which were enriched with coral exudates at both times. Black genera names indicate genera which were significantly enriched in coral treatments vs controls in both, random forest- and *DESeq2* analysis (i.e., consensus). Only genera which were significant in *DESeq2* analysis and / or significantly contributed to classification of macroalgae or coral treatments in random forest classification model are shown. M.g. = marine group; m.s.g. = marine sediment group. Raw data to this figure is available in [Supplementary Table S8.7](#).

Table 8.3. PERMANOVA results of treatment effects on the microbial community composition (genus level) and predicted metabolic functions at five times during bacterioplankton incubations, using 9999 permutations. Df = 2 for all tests, fdr = false discovery rate. Significant fdr-corrected p values are bold.

Timepoint	Microbial community composition				Predicted metabolic functions (MicFunPred)			
	<i>F</i>	<i>R</i> ²	<i>p</i>	<i>p</i> (fdr)	<i>F</i>	<i>R</i> ²	<i>p</i>	<i>p</i> (fdr)
Start	0.67	0.18	0.73	0.73	0.5	0.15	0.91	0.91
6 hours	0.91	0.23	0.51	0.64	2.1	0.41	0.14	0.18
12 hours	1.33	0.30	0.23	0.38	4.0	0.57	0.05	0.13
1 day	3.28	0.52	0.018	0.045	2.2	0.42	0.12	0.18
4 days	3.09	0.51	0.014	0.045	13.3	0.82	0.02	0.11

Predicted metabolic functions

Predicted metabolic functions of the microbial communities (using MicFunPred) were significantly affected by the interaction of time and treatment (PERMANOVA, $F_{(8)} = 3.5$, $R^2 = 0.02$, $p < 0.01$) with the strongest treatment effect after four days, albeit not significant after p value correction (Table 8.3). Metabolic class abundance was significantly affected by the interaction of time and treatment for eight out of 13 classes, and seven of these increased significantly in coral treatments compared to controls and algae treatments after four days (Table 8.4, Fig. 8.8a). Hierarchical cluster analysis of the Z-score adjusted pathway type abundance revealed a separate cluster of coral samples from all other samples after four days (SIMPROF; $p < 0.0001$, Fig. 8.8b).

Energy metabolism in HMW coral DOM incubations increased by 28 % ($p < 0.001$, pairwise t -tests, Bonferroni adjusted, Fig. 8.8a), with significant increases in six out of ten pathway types, including glycolysis, Entner Duodoroff- and pentose phosphate pathways ($p < 0.001$, *DESeq2*, *fdr*-corrected, Fig. 8.8b). Amino acid metabolism increased by 44 % ($p < 0.001$), both in biosynthesis and degradation pathways, though not significantly for a specific pathway type. Carbohydrate metabolism increased by 111 % ($p < 0.0001$), with significant increases in seven out of 12 pathway types, including both degradation and biosynthesis pathways ($p < 0.001$). Fatty acid and lipid metabolism increased by 24 % ($p < 0.05$), with a significant increase in fatty acid degradation (i.e., one out of nine pathway types, $p < 0.001$). Secondary metabolism increased by 63 % ($p < 0.01$), with significant increases in terpenoid- and polyketide biosynthesis (i.e., two out of six pathway types, $p < 0.001$). Other degradation pathways increased by 22 % and other biosynthesis pathways by 9 % (see Supplementary Fig. S8.5 for more detail).

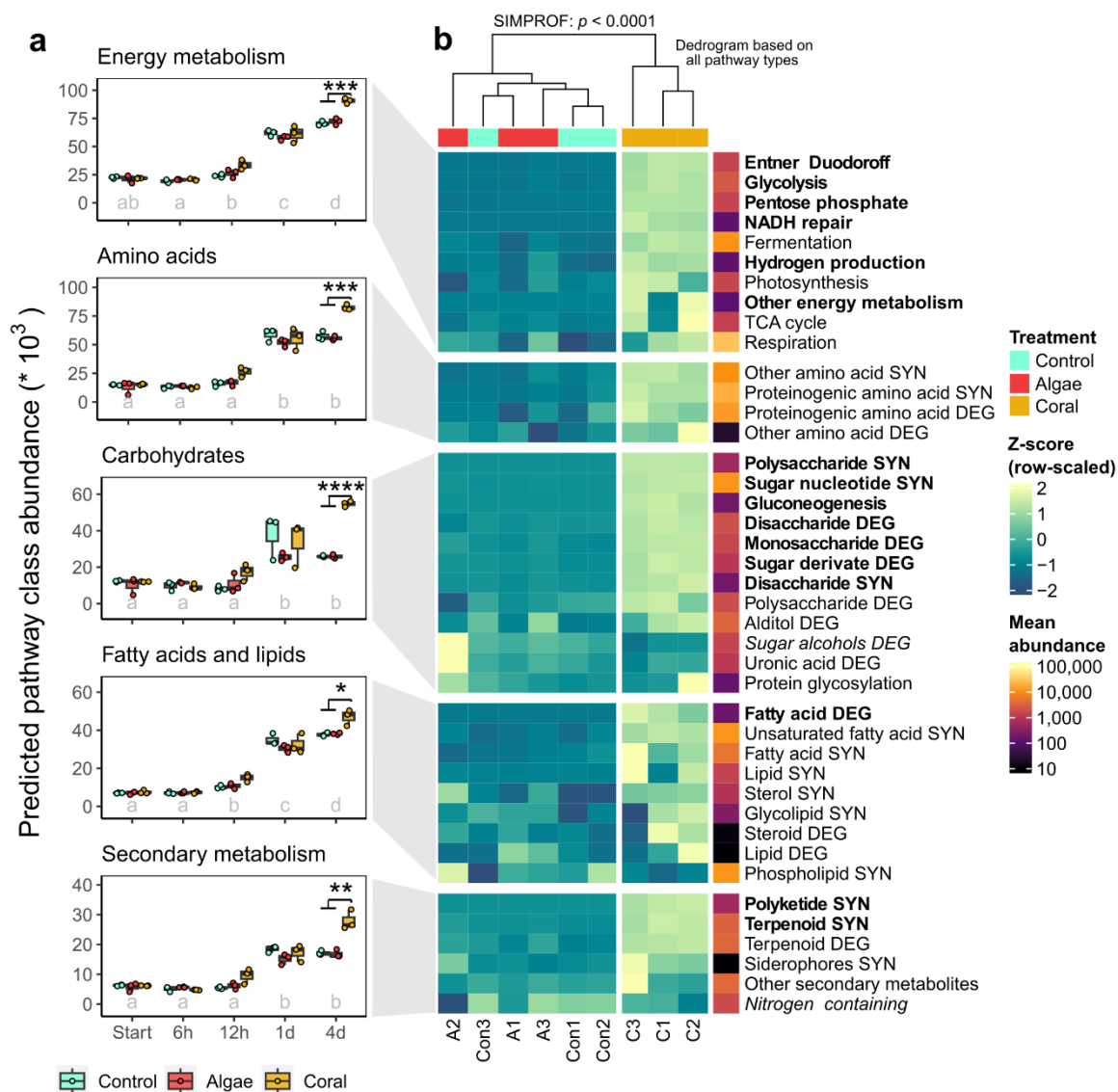


Figure 8.8. (a) Development of predicted metabolic pathway class abundances during bacterioplankton incubations with HMW coral- and macroalgal-DOM and background HMW DOM (controls). Different letters indicate significant differences between times ($p < 0.05$, pairwise t -tests, Bonferroni adjusted). Asterisks indicate significant differences between treatments (* $p < 0.05$, *** $p < 0.001$, **** $p < 0.0001$,

pairwise *t*-tests, Bonferroni adjusted). Predictions are based on the MicFunPred analysis tool, using the MetaCyc database. (b) Predicted pathway abundance by type for the significantly enriched classes as Z-scores after four days of dark incubation. The dendrogram on the top represents the Euclidean distance between samples including all pathway types of all classes. SYN = biosynthesis, DEG = degradation. Bold pathway types in (b) indicate a significant increase in coral treatments compared to controls (fdr-corrected $p < 0.001$, log2 fold change > 0.5 , *DESeq2* on all pathway types), and italicized types a significant decrease. Raw data to panel a of this figure is available in [Supplementary Table S8.8](#).

Table 8.4. Statistical test results for treatment and time interaction effect (DFn = 8, DFd = 24) of mixed model ANOVA, and treatment effect (DFn = 2, DFd = 6) after four days of bacterioplankton incubation for all metabolic classes with significant interaction effects. *p* (BF) = Bonferroni-adjusted *p*-values for multiple one-way ANOVAS (i.e., one at each timepoint, only the result for four days is reported). % of total pathways = percent contribution of mean pathway abundance per class to the sum of all pathways after four days; % coral effect size = percent increase with coral exudates compared to controls after four days.

Metabolic class	Mixed ANOVA: Treatment x Time				ANOVA: Treatment after 4 days				% of total pathways	% coral effect size
	<i>F</i>	η^2	<i>p</i>	<i>p</i> (fdr)	<i>F</i>	η^2	<i>p</i> (BF)	<i>p</i> (fdr)		
Energy metabolism	7.3	0.68	0.007	0.015	59.8	0.95	0.001	0.001	14	28
Amino acids	7.6	0.70	0.000	0.000	83.2	0.97	0.000	0.001	12	44
Carbohydrates	6.2	0.65	0.016	0.026	640	0.99	0.000	0.000	6	111
Fatty acids & lipids	4.3	0.53	0.003	0.008	12.9	0.80	0.035	0.040	7	24
Secondary metabolites	8.7	0.73	0.000	0.000	26.8	0.90	0.005	0.007	4	63
Other degradation	11.8	0.78	0.000	0.000	27.2	0.90	0.005	0.007	9	22
Other biosynthesis	3.1	0.48	0.014	0.026	27.1	0.90	0.005	0.007	11	9
Inorganic nutrients	4.4	0.55	0.002	0.007	5.4	0.64	0.230	0.230	7	-
Detoxification	2.3	0.39	0.054	0.078	-	-	-	-	4	-
Cofactors, carriers, vitamins	2.1	0.39	0.077	0.100	-	-	-	-	12	-
Cell structure biosynthesis	2.0	0.35	0.186	0.213	-	-	-	-	1	-
Nucleosides & nucleotides	2.0	0.38	0.197	0.213	-	-	-	-	11	-
Pigments	0.6	0.14	0.677	0.677	-	-	-	-	1	-

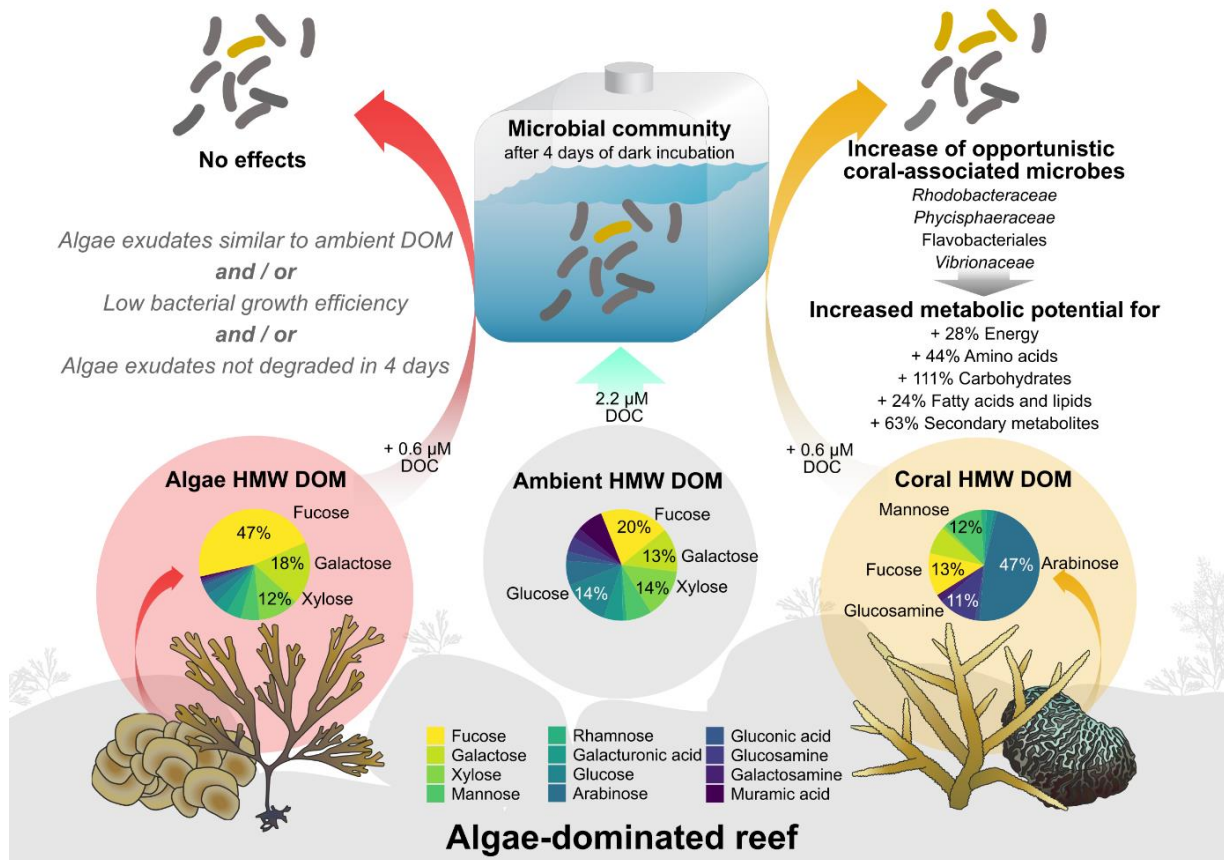


Figure 8.9. Summary of compositions of coral and macroalgae exudates and microbial community responses. Pie charts display mean mole percent compositions of control-corrected fluxes or ambient

seawater composition. Values > 10 % are shown in the figure. Gray italics indicate possible explanations for the lack of a microbial response to algae HMW exudates. HMW DOM = high molecular weight dissolved organic matter; DOC = dissolved organic carbon. Icon attribution: Integration and Application Network (ian.umces.edu/media-library).

8.5 Discussion

Our results (summarized in Fig. 8.9) revealed that brown macroalgae and scleractinian corals significantly enrich the HMW DOM fraction with carbohydrates (Fig. 8.2d) of different composition (Fig. 8.3). The compositional differences in exuded HMW DOM, added at low concentrations (~ 3 % of ambient DOC), had no effect on the overall bacterioplankton cell density or dissolved nutrient concentrations (Fig. 8.5). However, coral HMW DOM significantly affected the bacterioplankton community composition (Fig. 8.6 & 8.7) and increased the predicted potential for specific metabolic functions (Fig. 8.8). In contrast, algae HMW DOM addition induced no significant differences compared to seawater controls. These results could have three not mutually exclusive explanations which are discussed below: i) a greater alteration in HMW DOM composition through coral- compared to algal exudates, ii) a higher bacterial growth efficiency on coral- compared to algal HMW exudates, and iii) resistance of algal HMW exudates to microbial degradation.

Coral exudates reflected HMW carbohydrate composition of coral mucus and enriched opportunistic coral-associated microbes

The HMW carbohydrates released by corals were enriched in arabinose, glucosamine, mannose, and galactosamine (Fig. 8.3), and mostly reflected the monosaccharide composition of hydrolyzed mucus from *A. cervicornis* (Fig. 8.4). The main carbohydrate-containing macromolecules in coral mucus are mucin glycoproteins (i.e., 0.5-50 mDa)⁷⁷, and carbohydrate side chains of mucins isolated from *Acropora formosa* were rich in arabinose, glucosamine, and mannose⁷⁸, supporting the presence of mucins in HMW coral-DOM. Furthermore, the increase in predicted carbohydrate-, amino acid-, and fatty acid and lipid metabolism (Fig. 8.8) is consistent with degradation of coral mucus, which mainly consists of carbohydrates, proteins, and lipids^{79,80}. Thus, changes in the metabolic potential were consistent with microbial degradation of coral mucus components.

The minor addition of HMW coral DOM (~0.6 μM C; < 1 % of DOC) to an ambient bacterioplankton community significantly increased the relative abundance of several genera belonging to the Alphaproteobacteria (Rhodobacterales), Planctomycetes (Phycisphaerales, OM190 class), Gammaproteobacteria (Oceanospirillales, Vibrionales, Thiotrichales, Chromatiales) and Bacteroidetes (Flavobacteriales) (Fig. 8.7). However, the change in microbial cell densities over time was similar to those observed in HMW macroalgae- and seawater control DOM (Fig. 8.5). Bacterioplankton growth kinetics in dilution cultures usually include an exponential growth phase followed by a stationary phase⁴², where the stationary abundance at least partially depends on the amount of substrate added (e.g.,^{23,81}). As we only diluted the microbial community by ~1 % and added low and similar amounts of

substrate for treatments (2.8 μM DOC) and controls (2.2 μM DOC), we did not expect differences in final microbial cell abundances. Rhodobacterales, Oceanospirillales, Thiotrichales, Vibrionales, Flavobacteriales, and OM190 have been previously reported in coral mucus^{82–86} and/or increased in seawater when coral mucus^{87–89} or coral exudates^{23,29} were added (Supplementary Table S8.2). *Phycisphaeraceae* were previously found in *Acropora hyacinthus*⁹⁰, deep sea corals⁹¹, and in association with cultured *Symbiodiniaceae*⁹². *Ectothiorhodospiraceae* (purple sulfur bacteria of the order Chromatiales) have been previously found in *D. labyrinthiformis*⁹³. Thus, HMW coral-DOM enriched bacterioplankton taxa commonly associated with corals.

Rhodobacterales, Vibrionales, and Flavobacteriales were previously found to increase with macroalgae DOM addition and are considered to be opportunistic heterotrophic bacteria adapted to fast growth on DOM²³. Furthermore, they can increase in coral holobionts under stress^{94,95} and disease^{96,97} and were therefore suggested as indicators for poor reef health⁹⁸. Additionally, *Thiotrichaceae*⁹⁹ and *Phycisphaeraceae*^{90,100} can be associated with coral disease, and OM190 increased in bacterioplankton during a marine heatwave¹⁰¹. Thus, HMW coral DOM mostly selected for coral-associated microbes with the ability for opportunistic growth, which is also supported by the increase in predicted carbohydrate-, amino acid-, and fatty acid metabolism (Fig. 8.8)¹⁰².

Algae exudates reflected algae tissue- and ambient reef water HMW carbohydrate composition and did not affect the bacterioplankton community composition

HMW carbohydrates released by the two brown macroalgae *Dictyota* spp. and *Lobophora* spp. were enriched in fucose, galactose, galacturonic acid, and rhamnose (Fig. 8.3), and were similar in composition to tissue extracts from both species (Fig. 8.4). Furthermore, the HMW carbohydrate composition of ambient reef water mostly reflected algae exudate compositions (Fig. 8.4 & 8.9). In contrast, previously reported carbohydrate composition of ambient reef water from Moorea in the central Pacific was most similar to that of coral exudates²³. This suggests that the composition of HMW DOM in the reef may depend on the community of benthic primary producers fueling and shaping the local DOM pool^{18,103}. Indeed, our study site is characterized by high algae (i.e., 17 % macroalgae, 13 % turf algae) and low coral (i.e., 7 %) cover¹⁰⁴, with *Dictyota* and *Lobophora* being both highly abundant and releasing substantial amounts of DOM^{12,13,105}. On the other hand, the DOM pool of the rapidly flushed backreef of Moorea appears to be at least partly fueled by dense coral communities on the outer reefs^{23,106,107}.

Microbial communities growing on HMW macroalgae DOM did not reveal any differences to seawater control incubations, thus not confirming the hypothesis that algae HMW exudates exert stronger effects on bacterioplankton communities. However, our addition of DOM was different from previous studies in several ways: We enriched the microbial community exclusively with HMW DOM and thus removed any molecules < 1 kDa from the exuded fraction. Fresh primary producer exudates

can contain LMW DOM with high bioavailability like free monosaccharides and amino acids, which are taken up rapidly by microbes¹⁰⁸ and could have contributed to the microbial response in previous studies. Furthermore, the DOC addition in the present study (~ 2-3 μM DOC) is more than one order of magnitude lower compared to previous studies (~40-100 μM DOC^{23,43}). These comparable high DOC additions allowed for high DOC uptake rates to compensate for low bacterial growth efficiencies (i.e., increased respiration at the expense of biomass formation) of algal-DOM, resulting in higher microbial growth rates on algal- vs coral-DOM^{20,23,43}. In the present study, there were neither differences in initial DOC concentrations between coral and macroalgae exudates (Fig. 8.2a & b), nor differences in microbial growth rates (Fig. 8.5a). Our approach thereby allowed a decoupling of concentration-dependent from composition-dependent effects, which suggests that the increased DOC concentration component at least partly explained previously reported differences in bacterial growth rates between coral and algae DOM.

HMW macroalgae DOM could have also resisted microbial degradation throughout the four-day incubations. Brown macroalgae can secrete large quantities of fucoidan³⁹, a complex fucose-rich polysaccharide which forms an extracellular matrix and prevents desiccation of algal thalli^{109,110}. Fucose was the most abundant monosaccharide in HMW DOM of the brown macroalgae in the present study, as well as for the brown algae *Turbinaria* on reefs in French Polynesia²³. Using monoclonal antibodies (see supplementary methods), we detected three epitopes present in sulphated fucan (BAM1, BAM3, and BAM4) in macroalgae tissue (Supplementary Fig. S8.6a), which is consistent with previous findings of fucoidan in the tissue of both genera^{109,111}. Additionally, relative proportions of fucose, galactose, xylose, and mannose were similar in fucoidan extracted from *Dictyota* spp. and *Lobophora* spp. compared to macroalgae exudates (Supplementary Fig. S8.6b), suggesting that fucoidan contributed to macroalgae HMW DOM. Microbial degradation of brown algae fucoidans is energetically costly because it can require hundreds of different enzymes to degrade its complex structure¹¹². This could also explain why bacterioplankton growing on brown macroalgae exudates incorporate less carbon and have higher respiratory costs compared to green algae exudates^{23,43}, as green algae do not contain fucoidan in their cell walls¹¹³. Similarly, the high contribution of fucose, galactose, xylose and mannose in ambient reef water (combined making up 54 % of HMW carbohydrates, Fig. 8.4 & 8.9) suggests a considerable abundance of fucoidan in the HMW fraction of reef water, which supports the high resistance of brown macroalgae HMW DOM to microbial degradation.

Ecological implications

Previous studies were mainly conducted on coral-dominated reefs and found that coral exudates support a diverse oligotrophic bacterioplankton community, while algae exudates promote opportunistic microbial taxa²³ and less energy efficient nutrient cycling¹⁸. A shift towards macroalgae dominance can thus reduce ecosystem productivity by enhancing microbial respiration^{14,114} and reducing the transfer of energy to higher trophic levels^{18,19}. The here observed strong effects of a small addition of coral exudates

on the bacterioplankton community composition support the energy efficient transformation of coral exudates into microbial biomass^{14,18}. However, the increase in mainly opportunistic microbial taxa with coral exudates seems to contradict previous results. A change in carbon substrates can act as a disturbance on microbial communities¹¹⁵. Thus, the addition of coral exudates to a microbial community from a reef with macroalgae DOM dominating the local DOM pool could be considered a disturbance of the alternative stable state (i.e., the algae-dominance¹¹⁶). A common ecosystem response to stress is a shift towards opportunists which are less specialized, but respond rapidly to perturbations by adapting to new environmental conditions^{117,118}. Thus, the increase of some opportunistic microbial taxa on reefs may not be a direct response to the exudates of a specific primary producer, but rather to a disturbance in the form of a change in the availability of DOM producer-specific carbon substrates.

Brown macroalgae HMW DOM did not appear to support microbial growth, which could be explained by increased respiration instead of biomass production^{14,18,20}. An additional explanation could be that resistant HMW molecules from brown macroalgae such as fucoidan defied degradation during the four days of dark incubations. Previous studies revealed resistance of brown algae exudates to microbial degradation for up to five months, which leads to a net export of DOM from brown macroalgae beds^{119–122}. Water residence times of fringing reefs can range from hours to days^{123,124}. Thus, brown algae exudates could be exported from coral reefs. Release of refractory DOM by brown macroalgae which replace corals on many reefs could thus be an additional pathway by which the transfer of energy to higher trophic levels declines on degraded reefs. This hypothesis could be tested by measuring fucose concentrations at gradients away from algae-dominated reefs, as fucose can function as a biomarker for brown algae origin¹²⁵.

Effects of changing DOM compositions beyond coral reefs

Our results indicate that opportunistic microbial taxa increase in bacterioplankton communities of coral reefs following a change in the main DOM substrates (here induced by addition of coral DOM to macroalgae DOM-dominated ambient reef water, Fig. 8.9). This hypothesis is based on the *r*- and *K*-selection framework, where copiotrophic *r*-strategists can grow faster on new carbon sources, thus outcompeting the oligotrophic *K*-strategists¹¹⁷. Changes in the main benthic DOM producer are not exclusive to coral reefs, and have been reported for coastal ecosystems worldwide, including macroalgae beds¹²⁶, kelp forests¹²⁷, and seagrass meadows¹²⁸. These macrophytes release significant amounts of their photosynthetically fixed carbon as DOM^{39,129,130}. Changes in benthic composition and resulting alterations of the local DOM pool may disrupt the stable microbial community states, inducing the rise of opportunistic heterotrophic microbes until a new equilibrium has been reached following the perturbation.

Conclusion

Coral HMW DOM was compositionally distinct from ambient reef water and enriched opportunistic microbial taxa commonly associated with corals, significantly increasing the predicted metabolic potential for energy-, amino acid-, carbohydrate-, fatty acid and lipid-, and secondary metabolism (Fig. 8.9). In contrast, brown macroalgae HMW DOM was similar to ambient reef water, and did not induce any effects on the bacterioplankton community composition. These results indicate that whether coral or macroalgae DOM exerts stronger effects on the bacterioplankton community composition depends on local DOM- and bacterioplankton characteristics which are at least partly shaped by the local (benthic) DOM producing community. We hypothesize that a change in DOM away from the ambient composition acts as a disturbance, thus resulting in the dominance of opportunistic microbes which are able to adapt fast to environmental change. Furthermore, the strong effects of a small addition of coral HMW DOM to the bacterioplankton community suggest an efficient transformation of coral HMW DOM into microbial biomass, an important characteristic of nutrient cycles in healthy coral reefs. Brown macroalgae HMW exudate addition revealed no effects on the bacterioplankton community, indicating a low bacterial growth efficiency on algae exudates (i.e., more respiration), and/or resistance of brown algae HMW exudates to microbial degradation (i.e., reduced bioavailability). Both processes would ultimately lead to a reduced transfer of energy and nutrients stored in algae DOM to higher trophic levels, supporting the proposed microbialization of reefs.

8.6 Acknowledgements

We thank Dr Nicola Steinke and Dr Silvia Vidal-Melgosa for advice on methodology and assistance with monosaccharide analysis, and thank Tina Trautmann for conducting microarray analyses and sample preparations. We also thank Sven Pont for support with flow cytometry measurements, and Karel Bakker for analyzing our inorganic nutrient samples. B.M. received funding from the European Union's Horizon 2020 research and innovation program under the Marie Skłodowska-Curie grant (agreement No 894645).

8.7 References

1. Wild, C. *et al.* Climate change impedes scleractinian corals as primary reef ecosystem engineers. *Mar. Freshw. Res.* **62**, 205 (2011).
2. Fisher, R. *et al.* Species richness on coral reefs and the pursuit of convergent global estimates. *Curr. Biol.* **25**, 500–505 (2015).
3. Odum, H. T. & Odum, E. P. Trophic structure and productivity of a windward coral reef community on Eniwetok Atoll. *Ecol. Monogr.* **25**, 291–320 (1955).
4. Hughes, T. P. *et al.* Coral reefs in the Anthropocene. *Nature* **546**, 82–90 (2017).
5. Adam, T. C. *et al.* Landscape-scale patterns of nutrient enrichment in a coral reef ecosystem: implications for coral to algae phase shifts. *Ecol. Appl.* **31**, e2227 (2021).

6. Arif, S., Graham, N. A. J., Wilson, S. & MacNeil, M. A. Causal drivers of climate-mediated coral reef regime shifts. *Ecosphere* **13**, e3956 (2022).
7. Cruz, I. C. S., Waters, L. G., Kikuchi, R. K. P., Leão, Z. M. A. N. & Turra, A. Marginal coral reefs show high susceptibility to phase shift. *Mar. Pollut. Bull.* **135**, 551–561 (2018).
8. Hughes, T. P. *et al.* Phase shifts, herbivory, and the resilience of coral reefs to climate change. *Curr. Biol.* **17**, 360–365 (2007).
9. Reverter, M., Helber, S. B., Rohde, S., De Goeij, J. M. & Schupp, P. J. Coral reef benthic community changes in the Anthropocene: biogeographic heterogeneity, overlooked configurations, and methodology. *Glob. Change Biol.* **28**, 1956–1971 (2022).
10. Tebbett, S. B., Connolly, S. R. & Bellwood, D. R. Benthic composition changes on coral reefs at global scales. *Nat. Ecol. Evol.* **7**, 71–81 (2023).
11. Nelson, C. E., Wegley Kelly, L. & Haas, A. F. Microbial interactions with dissolved organic matter are central to coral reef ecosystem function and resilience. *Annu. Rev. Mar. Sci.* **15**, null (2023).
12. Haas, A., Jantzen, C., Naumann, M., Iglesias-Prieto, R. & Wild, C. Organic matter release by the dominant primary producers in a Caribbean reef lagoon: implication for in situ O₂ availability. *Mar. Ecol. Prog. Ser.* **409**, 27–39 (2010).
13. Mueller, B. *et al.* Effect of light availability on dissolved organic carbon release by Caribbean reef algae and corals. *Bull. Mar. Sci.* **90**, 875–893 (2014).
14. Haas, A. F. *et al.* Influence of coral and algal exudates on microbially mediated reef metabolism. *PeerJ* **1**, e108 (2013).
15. Candy, A. S. *et al.* Small-scale oxygen distribution patterns in a coral reef. *Front. Mar. Sci.* **10**, (2023).
16. Silveira, C. B. *et al.* Biophysical and physiological processes causing oxygen loss from coral reefs. *eLife* **8**, e49114 (2019).
17. Wild, C., Niggli, W., Naumann, M. & Haas, A. Organic matter release by Red Sea coral reef organisms—potential effects on microbial activity and *in situ* O₂ availability. *Mar. Ecol. Prog. Ser.* **411**, 61–71 (2010).
18. Haas, A. F. *et al.* Global microbialization of coral reefs. *Nat. Microbiol.* **1**, 16042 (2016).
19. McDole, T. *et al.* Assessing coral reefs on a pacific-wide scale using the microbialization score. *PLoS ONE* **7**, e43233 (2012).
20. Mueller, B. *et al.* Nocturnal dissolved organic matter release by turf algae and its role in the microbialization of reefs. *Funct. Ecol.* **36**, 2104–2118 (2022).
21. Cárdenas, A. *et al.* Excess labile carbon promotes the expression of virulence factors in coral reef bacterioplankton. *ISME J.* **12**, 59–76 (2018).
22. Dinsdale, E. A. *et al.* Microbial ecology of four coral atolls in the Northern Line Islands. *PLOS ONE* **3**, e1584 (2008).

23. Nelson, C. E. *et al.* Coral and macroalgal exudates vary in neutral sugar composition and differentially enrich reef bacterioplankton lineages. *ISME J.* **7**, 962–979 (2013).
24. Kline, D., Kuntz, N., Breitbart, M., Knowlton, N. & Rohwer, F. Role of elevated organic carbon levels and microbial activity in coral mortality. *Mar. Ecol. Prog. Ser.* **314**, 119–125 (2006).
25. Kuntz, N. M., Kline, D. I., Sandin, S. A. & Rohwer, F. Pathologies and mortality rates caused by organic carbon and nutrient stressors in three Caribbean coral species. *Mar. Ecol. Prog. Ser.* **294**, 173–180 (2005).
26. Smith, J. E. *et al.* Indirect effects of algae on coral: algae-mediated, microbe-induced coral mortality. *Ecol. Lett.* **9**, 835–845 (2006).
27. Barott, K. L. & Rohwer, F. L. Unseen players shape benthic competition on coral reefs. *Trends Microbiol.* **20**, 621–628 (2012).
28. Dinsdale, E. A. & Rohwer, F. Fish or germs? Microbial dynamics associated with changing trophic structures on coral reefs. in *Coral Reefs: An Ecosystem in Transition* (eds. Dubinsky, Z. & Stambler, N.) 231–240 (Springer Netherlands, Dordrecht, 2011).
29. Weber, L. *et al.* Benthic exometabolites and their ecological significance on threatened Caribbean coral reefs. *ISME Commun.* **2**, 1–13 (2022).
30. Wegley Kelly, L. *et al.* Distinguishing the molecular diversity, nutrient content, and energetic potential of exometabolites produced by macroalgae and reef-building corals. *Proc. Natl. Acad. Sci.* **119**, e2110283119 (2022).
31. Petras, D. *et al.* High-resolution liquid chromatography tandem mass spectrometry enables large scale molecular characterization of dissolved organic matter. *Front. Mar. Sci.* **4**, 405 (2017).
32. Raeke, J., J. Lechtenfeld, O., Wagner, M., Herzsprung, P. & Reemtsma, T. Selectivity of solid phase extraction of freshwater dissolved organic matter and its effect on ultrahigh resolution mass spectra. *Environ. Sci. Process. Impacts* **18**, 918–927 (2016).
33. Kaiser, K. & Benner, R. Biochemical composition and size distribution of organic matter at the Pacific and Atlantic time-series stations. *Mar. Chem.* **113**, 63–77 (2009).
34. McCarthy, M., Hedges, J. & Benner, R. Major biochemical composition of dissolved high molecular weight organic matter in seawater. *Mar. Chem.* **55**, 281–297 (1996).
35. Arnosti, C. *et al.* The biogeochemistry of marine polysaccharides: sources, inventories, and bacterial drivers of the carbohydrate cycle. *Annu. Rev. Mar. Sci.* **13**, 81–108 (2021).
36. Teeling, H. *et al.* Recurring patterns in bacterioplankton dynamics during coastal spring algae blooms. *eLife* **5**, e11888 (2016).
37. Bythell, J. C. & Wild, C. Biology and ecology of coral mucus release. *J. Exp. Mar. Biol. Ecol.* **408**, 88–93 (2011).
38. Abdullah, M. I. & Fredriksen, S. Production, respiration and exudation of dissolved organic matter by the kelp *Laminaria hyperborea* along the west coast of Norway. *J. Mar. Biol. Assoc. U.K.* **84**, 887–894 (2004).

39. Buck-Wiese, H. *et al.* Furoid brown algae inject fucoidan carbon into the ocean. *Proc. Natl. Acad. Sci.* **120**, e2210561119 (2022).
40. Haas, A. & Wild, C. Composition analysis of organic matter released by cosmopolitan coral reef-associated green algae. *Aquat. Biol.* **10**, 131–138 (2010).
41. Verdugo, P. *et al.* The oceanic gel phase: a bridge in the DOM–POM continuum. *Mar. Chem.* **92**, 67–85 (2004).
42. Ammerman, J., Fuhrman, J., Hagström, Å. & Azam, F. Bacterioplankton growth in seawater: I. Growth kinetics and cellular characteristics in seawater cultures. *Mar. Ecol. Prog. Ser.* **18**, 31–39 (1984).
43. Haas, A. F. *et al.* Effects of coral reef benthic primary producers on dissolved organic carbon and microbial activity. *PLoS ONE* **6**, e27973 (2011).
44. Agis, M., Granda, A. & Dolan, J. R. A cautionary note: examples of possible microbial community dynamics in dilution grazing experiments. *J. Exp. Mar. Biol. Ecol.* **341**, 176–183 (2007).
45. Fuchs, B. M., Zubkov, M. V., Sahm, K., Burkill, P. H. & Amann, R. Changes in community composition during dilution cultures of marine bacterioplankton as assessed by flow cytometric and molecular biological techniques. *Environ. Microbiol.* **2**, 191–201 (2000).
46. Abreu, C. I., Woltz, V. L. A., Friedman, J. & Gore, J. Microbial communities display alternative stable states in a fluctuating environment. *PLOS Comput. Biol.* **16**, e1007934 (2020).
47. Abreu, C. I., Friedman, J., Andersen Woltz, V. L. & Gore, J. Mortality causes universal changes in microbial community composition. *Nat. Commun.* **10**, 2120 (2019).
48. De Bakker, D. M. *et al.* 40 Years of benthic community change on the Caribbean reefs of Curaçao and Bonaire: the rise of slimy cyanobacterial mats. *Coral Reefs* **36**, 355–367 (2017).
49. De Bakker, D. M., Meesters, E. H., Bak, R. P. M., Nieuwland, G. & Van Duyl, F. C. Long-term shifts in coral communities on shallow to deep reef slopes of Curaçao and Bonaire: are there any winners? *Front. Mar. Sci.* **3**, (2016).
50. Diaz-Pulido, G. & Garzón-Ferreira, J. Seasonality in algal assemblages on upwelling-influenced coral reefs in the Colombian Caribbean. *Bot. Mar.* **45**, 284–292 (2002).
51. Waitt Institute. *Marine Science Assessment: The State of Curaçao's Coral Reefs.* (2017).
52. Quezada-Perez, F., Mena, S., Fernández-García, C. & Alvarado, J. J. Status of coral reef communities on the Caribbean coast of Costa Rica: are we talking about corals or macroalgae reefs? *Oceans* **4**, 315–330 (2023).
53. Nelson, H. R. & Altieri, A. H. Oxygen: The universal currency on coral reefs. *Coral Reefs* **38**, 177–198 (2019).
54. Wild, C., Naumann, M., Niggel, W. & Haas, A. Carbohydrate composition of mucus released by scleractinian warm- and cold-water reef corals. *Aquat. Biol.* **10**, 41–45 (2010).

55. Vidal-Melgosa, S. *et al.* Diatom fucan polysaccharide precipitates carbon during algal blooms. *Nat. Commun.* **12**, 1150 (2021).
56. Engel, A. & Händel, N. A novel protocol for determining the concentration and composition of sugars in particulate and in high molecular weight dissolved organic matter (HMW-DOM) in seawater. *Mar. Chem.* **127**, 180–191 (2011).
57. Grasshoff, K., Ehrhardt, M. & Kremling, K. *Methods of seawater analysis* Weinheim: Verlag Chemie. (1983).
58. Murphy, J. & Riley, J. P. A modified single solution method for the determination of phosphate in natural waters. *Anal. Chim. Acta* **27**, 31–36 (1962).
59. Haas, A. F. *et al.* Unraveling the unseen players in the ocean - a field guide to water chemistry and marine microbiology. *J. Vis. Exp.* 52131 (2014) doi:10.3791/52131.
60. Walters, W. *et al.* Improved bacterial 16S rRNA gene (V4 and V4-5) and fungal internal transcribed spacer marker gene primers for microbial community surveys. *mSystems* **1**, 10.1128/msystems.00009-15 (2015).
61. Caporaso, J. G. *et al.* EMP 16S illumina amplicon protocol. (2018).
62. Arisdakessian, C., Cleveland, S. B. & Belcaid, M. MetaFlow|mics: scalable and reproducible nextflow pipelines for the analysis of microbiome marker data. in *Practice and Experience in Advanced Research Computing* 120–124 (Association for Computing Machinery, New York, NY, USA, 2020). doi:10.1145/3311790.3396664.
63. Jani, A. J. *et al.* The amphibian microbiome exhibits poor resilience following pathogen-induced disturbance. *ISME J.* **15**, 1628–1640 (2021).
64. Callahan, B. J. *et al.* DADA2: High-resolution sample inference from Illumina amplicon data. *Nat. Methods* **13**, 581–583 (2016).
65. Schloss, P. D. *et al.* Introducing mothur: open-source, platform-independent, community-supported software for describing and comparing microbial communities. *Appl. Environ. Microbiol.* **75**, 7537–7541 (2009).
66. Yilmaz, P. *et al.* The SILVA and “All-species Living Tree Project (LTP)” taxonomic frameworks. *Nucleic Acids Res.* **42**, D643–D648 (2014).
67. Wang, Q., Garrity, G. M., Tiedje, J. M. & Cole, J. R. Naïve bayesian classifier for rapid assignment of rRNA sequences into the new bacterial taxonomy. *Appl. Environ. Microbiol.* **73**, 5261–5267 (2007).
68. Rognes, T., Flouri, T., Nichols, B., Quince, C. & Mahé, F. VSEARCH: a versatile open source tool for metagenomics. *PeerJ* **4**, e2584 (2016).
69. Frøslev, T. G. *et al.* Algorithm for post-clustering curation of DNA amplicon data yields reliable biodiversity estimates. *Nat. Commun.* **8**, 1188 (2017).

70. Cleveland, S. *et al.* The C-Māiki Gateway: a modern science platform for analyzing microbiome data. in *Practice and Experience in Advanced Research Computing* 1–7 (Association for Computing Machinery, New York, NY, USA, 2022). doi:10.1145/3491418.3530291.
71. Mongad, D. S. *et al.* MicFunPred: A conserved approach to predict functional profiles from 16S rRNA gene sequence data. *Genomics* **113**, 3635–3643 (2021).
72. Douglas, G. M. *et al.* PICRUSt2 for prediction of metagenome functions. *Nat. Biotechnol.* **38**, 685–688 (2020).
73. Gu, Z., Eils, R. & Schlesner, M. Complex heatmaps reveal patterns and correlations in multidimensional genomic data. *Bioinformatics* **32**, 2847–2849 (2016).
74. Silveira, C. B. *et al.* Viral predation pressure on coral reefs. *BMC Biol.* **21**, 77 (2023).
75. Love, M. I., Huber, W. & Anders, S. Moderated estimation of fold change and dispersion for RNA-seq data with DESeq2. *Genome Biol.* **15**, 550 (2014).
76. Nearing, J. T. *et al.* Microbiome differential abundance methods produce different results across 38 datasets. *Nat. Commun.* **13**, 342 (2022).
77. Bansil, R. & Turner, B. S. Mucin structure, aggregation, physiological functions and biomedical applications. *Curr. Opin. Colloid Interface Sci.* **11**, 164–170 (2006).
78. Meikle, P., Richards, G. N. & Yellowlees, D. Structural determination of the oligosaccharide side chains from a glycoprotein isolated from the mucus of the coral *Acropora formosa*. *J. Biol. Chem.* **262**, 16941–16947 (1987).
79. Crossland, C. J. *In situ* release of mucus and DOC-lipid from the corals *Acropora variabilis* and *Stylophora pistillata* in different light regimes. *Coral Reefs* **6**, 35–42 (1987).
80. Ducklow, H. W. & Mitchell, R. Composition of mucus released by coral reef coelenterates. *Limnol. Oceanogr.* **24**, 706–714 (1979).
81. Wright, R. T. A model for short-term control of the bacterioplankton by substrate and grazing. *Hydrobiologia* **159**, 111–117 (1988).
82. Apprill, A., Weber, L. G. & Santoro, A. E. Distinguishing between microbial habitats unravels ecological complexity in coral microbiomes. *mSystems* **1**, e00143-16 (2016).
83. Lee, S. T. M., Davy, S. K., Tang, S.-L., Fan, T.-Y. & Kench, P. S. Successive shifts in the microbial community of the surface mucus layer and tissues of the coral *Acropora muricata* under thermal stress. *FEMS Microbiol. Ecol.* **91**, fiv142 (2015).
84. Lima, L. F. O. *et al.* Coral and seawater metagenomes reveal key microbial functions to coral health and ecosystem functioning shaped at reef scale. *Microb. Ecol.* **86**, 392–407 (2023).
85. Marchioro, G. M. *et al.* Microbiome dynamics in the tissue and mucus of acroporid corals differ in relation to host and environmental parameters. *PeerJ* **8**, e9644 (2020).
86. Zou, Y., Chen, Y., Wang, L., Zhang, S. & Li, J. Differential responses of bacterial communities in coral tissue and mucus to bleaching. *Coral Reefs* **41**, 951–960 (2022).

87. Allers, E., Niesner, C., Wild, C. & Pernthaler, J. Microbes enriched in seawater after addition of coral mucus. *Appl. Environ. Microbiol.* **74**, 3274–3278 (2008).
88. Taniguchi, A., Kuroyanagi, Y., Aoki, R. & Eguchi, M. Community structure and predicted functions of actively growing bacteria responsive to released coral mucus in surrounding seawater. *Microbes Environ.* **38**, ME23024 (2023).
89. Taniguchi, A., Yoshida, T., Hibino, K. & Eguchi, M. Community structures of actively growing bacteria stimulated by coral mucus. *J. Exp. Mar. Biol. Ecol.* **469**, 105–112 (2015).
90. Ziegler, M., Seneca, F. O., Yum, L. K., Palumbi, S. R. & Voolstra, C. R. Bacterial community dynamics are linked to patterns of coral heat tolerance. *Nat. Commun.* **8**, 14213 (2017).
91. Kellogg, C. A. Microbiomes of stony and soft deep-sea corals share rare core bacteria. *Microbiome* **7**, 90 (2019).
92. Díaz-Almeyda, E. M. *et al.* Thermal stress has minimal effects on bacterial communities of thermotolerant *Symbiodinium* cultures. *Front. Ecol. Evol.* **10**, (2022).
93. Pratte, Z. A. & Richardson, L. L. Microbiome dynamics of two differentially resilient corals. *Dis. Aquat. Organ.* **131**, 213–226 (2018).
94. McDevitt-Irwin, J. M., Baum, J. K., Garren, M. & Vega Thurber, R. L. Responses of coral-associated bacterial communities to local and global stressors. *Front. Mar. Sci.* **4**, 262 (2017).
95. Ziegler, M. *et al.* Coral microbial community dynamics in response to anthropogenic impacts near a major city in the central Red Sea. *Mar. Pollut. Bull.* **105**, 629–640 (2016).
96. Gignoux-Wolfsohn, S. A. & Vollmer, S. V. Identification of candidate coral pathogens on white band disease-infected staghorn coral. *PLOS ONE* **10**, e0134416 (2015).
97. Meyer, J. L. *et al.* Microbial community shifts associated with the ongoing stony coral tissue loss disease outbreak on the Florida reef tract. *Front. Microbiol.* **10**, (2019).
98. Terzin, M. *et al.* The road forward to incorporate seawater microbes in predictive reef monitoring. *Environ. Microbiome* **19**, 5 (2024).
99. Heitzman, J. M., Caputo, N., Yang, S.-Y., Harvey, B. P. & Agostini, S. Recurrent disease outbreak in a warm temperate marginal coral community. *Mar. Pollut. Bull.* **182**, 113954 (2022).
100. Li, J., Long, L., Zou, Y. & Zhang, S. Microbial community and transcriptional responses to increased temperatures in coral *Pocillopora damicornis* holobiont. *Environ. Microbiol.* **23**, 826–843 (2021).
101. Doni, L. *et al.* Large-scale impact of the 2016 marine heatwave on the plankton-associated microbial communities of the Great Barrier Reef (Australia). *Mar. Pollut. Bull.* **188**, 114685 (2023).
102. Bourne, D. G., Morrow, K. M. & Webster, N. S. Insights into the coral microbiome: underpinning the health and resilience of reef ecosystems. *Annu. Rev. Microbiol.* **70**, 317–340 (2016).

103. Kelly, L. W. *et al.* Local genomic adaptation of coral reef-associated microbiomes to gradients of natural variability and anthropogenic stressors. *Proc. Natl. Acad. Sci.* **111**, 10227–10232 (2014).
104. Kornder, N. A. *et al.* Implications of 2D versus 3D surveys to measure the abundance and composition of benthic coral reef communities. *Coral Reefs* **40**, 1137–1153 (2021).
105. Mueller, B., Meesters, E. H. & van Duyl, F. C. DOC concentrations across a depth-dependent light gradient on a Caribbean coral reef. *PeerJ* **5**, e3456 (2017).
106. Leichter, J. J. *et al.* Biological and physical interactions on a tropical island coral reef: transport and retention processes on Moorea, French Polynesia. *Oceanography* **26**, 52–63 (2013).
107. Nelson, C. E., Alldredge, A. L., McCliment, E. A., Amaral-Zettler, L. A. & Carlson, C. A. Depleted dissolved organic carbon and distinct bacterial communities in the water column of a rapid-flushing coral reef ecosystem. *ISME J.* **5**, 1374–1387 (2011).
108. Mühlenbruch, M., Grossart, H.-P., Eigemann, F. & Voss, M. Mini-review: phytoplankton-derived polysaccharides in the marine environment and their interactions with heterotrophic bacteria. *Environ. Microbiol.* **20**, 2671–2685 (2018).
109. Skriptsova, A. V. Fucoidans of brown algae: biosynthesis, localization, and physiological role in thallus. *Russ. J. Mar. Biol.* **41**, 145–156 (2015).
110. Wang, Y. *et al.* Biological activities of fucoidan and the factors mediating its therapeutic effects: a review of recent studies. *Mar. Drugs* **17**, 183 (2019).
111. Wang, W., Wang, S.-X. & Guan, H.-S. The antiviral activities and mechanisms of marine polysaccharides: an overview. *Mar. Drugs* **10**, 2795–2816 (2012).
112. Sichert, A. *et al.* Verrucomicrobia use hundreds of enzymes to digest the algal polysaccharide fucoidan. *Nat. Microbiol.* **5**, 1026–1039 (2020).
113. Kloareg, B., Badis, Y., Cock, J. M. & Michel, G. Role and evolution of the extracellular matrix in the acquisition of complex multicellularity in eukaryotes: A macroalgal perspective. *Genes* **12**, 1059 (2021).
114. Wegley Kelly, L., Haas, A. F. & Nelson, C. E. Ecosystem microbiology of coral reefs: linking genomic, metabolomic, and biogeochemical dynamics from animal symbioses to reefscape processes. *mSystems* **3**, e00162-17, /msystems/3/2/msys.00162-17.atom (2018).
115. Allison, S. D. & Martiny, J. B. H. Resistance, resilience, and redundancy in microbial communities. *Proc. Natl. Acad. Sci.* **105**, 11512–11519 (2008).
116. Nyström, M., Graham, N. A. J., Lokrantz, J. & Norström, A. V. Capturing the cornerstones of coral reef resilience: linking theory to practice. *Coral Reefs* **27**, 795–809 (2008).
117. Ho, A., Di Lonardo, D. P. & Bodelier, P. L. E. Revisiting life strategy concepts in environmental microbial ecology. *FEMS Microbiol. Ecol.* **93**, fix006 (2017).
118. Rapport, D. J., Regier, H. A. & Hutchinson, T. C. Ecosystem behavior under stress. *Am. Nat.* **125**, 617–640 (1985).

119. Gao, Y. *et al.* Dissolved organic carbon from cultured kelp *Saccharina japonica*: production, bioavailability, and bacterial degradation rates. *Aquac. Environ. Interact.* **13**, 101–110 (2021).
120. Wada, S. *et al.* Bioavailability of macroalgal dissolved organic matter in seawater. *Mar. Ecol. Prog. Ser.* **370**, 33–44 (2008).
121. Wada, S. & Hama, T. The contribution of macroalgae to the coastal dissolved organic matter pool. *Estuar. Coast. Shelf Sci.* **129**, 77–85 (2013).
122. Watanabe, K. *et al.* Macroalgal metabolism and lateral carbon flows can create significant carbon sinks. *Biogeosciences* **17**, 2425–2440 (2020).
123. Black, K. P., Gay, S. L. & Andrews, J. C. Residence times of neutrally-buoyant matter such as larvae, sewage or nutrients on coral reefs. *Coral Reefs* **9**, 105–114 (1990).
124. Venti, A., Kadko, D., Andersson, A. J., Langdon, C. & Bates, N. R. A multi-tracer model approach to estimate reef water residence times. *Limnol. Oceanogr. Methods* **10**, 1078–1095 (2012).
125. Böhm, L., Dawson, R., Liebezeit, G. & Wefer, G. Suitability of monosaccharides as markers for particle identification in carbonate sediments*†. *Sedimentology* **27**, 167–177 (1980).
126. Strain, E. M. A., Thomson, R. J., Micheli, F., Mancuso, F. P. & Airoidi, L. Identifying the interacting roles of stressors in driving the global loss of canopy-forming to mat-forming algae in marine ecosystems. *Glob. Change Biol.* **20**, 3300–3312 (2014).
127. Smale, D. A. Impacts of ocean warming on kelp forest ecosystems. *New Phytol.* **225**, 1447–1454 (2020).
128. Turschwell, M. P. *et al.* Anthropogenic pressures and life history predict trajectories of seagrass meadow extent at a global scale. *Proc. Natl. Acad. Sci.* **118**, e2110802118 (2021).
129. Barrón, C., Apostolaki, E. T. & Duarte, C. M. Dissolved organic carbon fluxes by seagrass meadows and macroalgal beds. *Front. Mar. Sci.* **1**, (2014).
130. Barrón, C. & Duarte, C. M. Dissolved organic matter release in a *Posidonia oceanica* meadow. *Mar. Ecol. Prog. Ser.* **374**, 75–84 (2009).

Chapter 9 | General discussion

Chapter 9 | General discussion

9.1 Thesis highlights

- The pulsating soft coral *Xenia umbellata* is resistant to a variety of single and combined global and local stressors (chapters 2-5).
- Nitrate reduces the resistance of *X. umbellata* to warming, potentially by reducing organic carbon (OC) transfer from Symbiodiniaceae to coral host (chapter 2).
- Microbial fuel cells (MFCs) can detect *ex situ* OC pulses in coral reef sediments within less than one day and remain operative for over six months (chapter 6).
- Scleractinian coral phylogeny explains 70 % of variation in mucus carbohydrate compositions collected from 23 species in seven different studies (chapter 7).
- Coral exudates shaped carbohydrate- and bacterioplankton composition of reef water from an algae-dominated reef, enriching opportunistic microbes commonly considered as stress indicators (chapter 8).
- Macroalgae exudates were similar in composition to ambient reef water and did not exert any effect on the bacterioplankton community (chapter 8).

9.2 Overview

The aim of this thesis to increase our understanding of OC transfer between coral reef micro- and macro-organisms under environmental change has become more pressing in the last three years while the work was conducted. More shifts from hard coral to soft coral¹⁻⁴ and macroalgae⁵ dominance have been reported, while the current (2023-2024) marine heatwave causes global mass coral bleaching and -mortality⁶⁻⁹. With these widespread changes in coral reef composition, research- and conservation strategies may need to adjust their focus from maintaining the *status quo* to understanding and managing functions of new reef communities^{10,11}. This dissertation contributes to a broader understanding of the ecosystem function of OC cycling in coral reefs under environmental change. We provide new insights on i) the physiological response of the soft coral *Xenia umbellata* to single and combined global and local anthropogenic stressors (chapters 2-5), ii) a biological indicator tool to measure eutrophication-induced changes in OC cycling in reef sediments (chapter 6), iii) the variation of mucus carbohydrate composition within the hard corals (chapter 7), and iv) the role of carbohydrates released by hard corals and macroalgae in shaping bacterioplankton community composition and -metabolism (chapter 8).

9.3 Synoptic answers to research questions

Research question 1 | How does the pulsating soft coral *Xenia umbellata* respond to global and local environmental stressors? What are the ecological implications?

The soft coral *X. umbellata* revealed high resistance to global (i.e., warming and acidification) and local (nitrate- and phosphate eutrophication) environmental stressors in tank experiments (chapters 2 – 5, summarised in Fig. 9.1). However, results of chapter 2 revealed that nitrate eutrophication reduces the resistance of *X. umbellata* to warming by impacting growth-, pulsation-, and survival rates of coral hosts. Concomitant stable or increasing photophysiological parameters suggest a decline in OC transfer from Symbiodiniaceae to the coral host (as previously observed for soft¹² and hard corals^{13–15}). No bleaching of *X. umbellata* colonies was observed in response to any of the investigated stressors (chapters 2–5), which could be beneficial for post-stress recovery if normal OC transfer from Symbiodiniaceae to the coral hosts is restored (*sensu*¹⁶). The generally observed plastic response of polyp pulsation rates to different environmental stressors (chapters 2,3 & 5) further indicates that *X. umbellata* may be able to adapt its energy budgets to changing environmental conditions through polyp activity (*sensu*^{17,18}). Pulsation reduces the coral-water boundary layer, thus supporting photosynthetic gas exchange and filter feeding¹⁹. Water flow-induced removal of oxygen from coral tissue increases the affinity of ribulose-1,5-bisphosphate carboxylase/oxygenase (RuBisCO) to carbon dioxide (CO₂), thus reducing the formation of reactive oxygen species (ROS) and increasing photosynthetic efficiency²⁰. It was thus hypothesized that polyp pulsation may reduce coral bleaching susceptibility²¹. As such, higher pulsation rates under phosphate eutrophication may increase their resistance to warming (chapter 3), while decreasing pulsation rates may aid adaptation to ocean acidification by compensating for increased CO₂ availability (chapter 5). Combined, the high resistance of *X. umbellata* to global and local anthropogenic stressors may support their dominance over hard corals under environmental change.

While soft corals provide less structural complexity compared to some hard corals²² (except on small scales²³), they can sustain diverse fish assemblages^{24,25} and provide multiple goods and services to humans (i.e., support of fishery and aquarium trade, provision of biopharmaceuticals)^{26–28}. Results of chapter 2 thus emphasize the need to manage coastal water quality in order to sustain soft corals and their provided services under ongoing climate change. However, the effects of soft corals on benthic-pelagic coupling are still poorly understood. The soft coral genus *Xenia* can feed on dissolved and particulate OC (DOC and POC, respectively)^{29–31}, and polyp pulsation further increases their filtration capacity¹⁹ so that they can sustain heterotrophy under low waterflow conditions³⁰. Soft coral beds can be net sinks of POC³² and DOC released by soft corals may stimulate less microbial growth compared to hard corals³³. Soft coral dominance on reefs may thus have a different effect on bacterioplankton community dynamics compared to macroalgae (*sensu*³³) (i.e., soft corals may reduce²⁹, while macroalgae increase³⁴ benthic OC release). Similarly, soft coral dominance on reefs may influence nitrogen (N) cycling³⁵, as soft corals showed a lower potential for N-fixation *via* diazotrophs³⁶ and a

higher potential for denitrification³⁵ compared to hard corals. In contrast, turf algae revealed high N-fixation- and low denitrification rates which may support reef degradation by increasing N availability³⁵. To summarize, the increasing spread of soft corals on anthropogenically affected reefs may sustain some ecosystem functions like habitat provision for reef fish, while likely affecting benthic-pelagic coupling with yet poorly understood effects on microbial metabolism and reef-wide biogeochemical cycling.

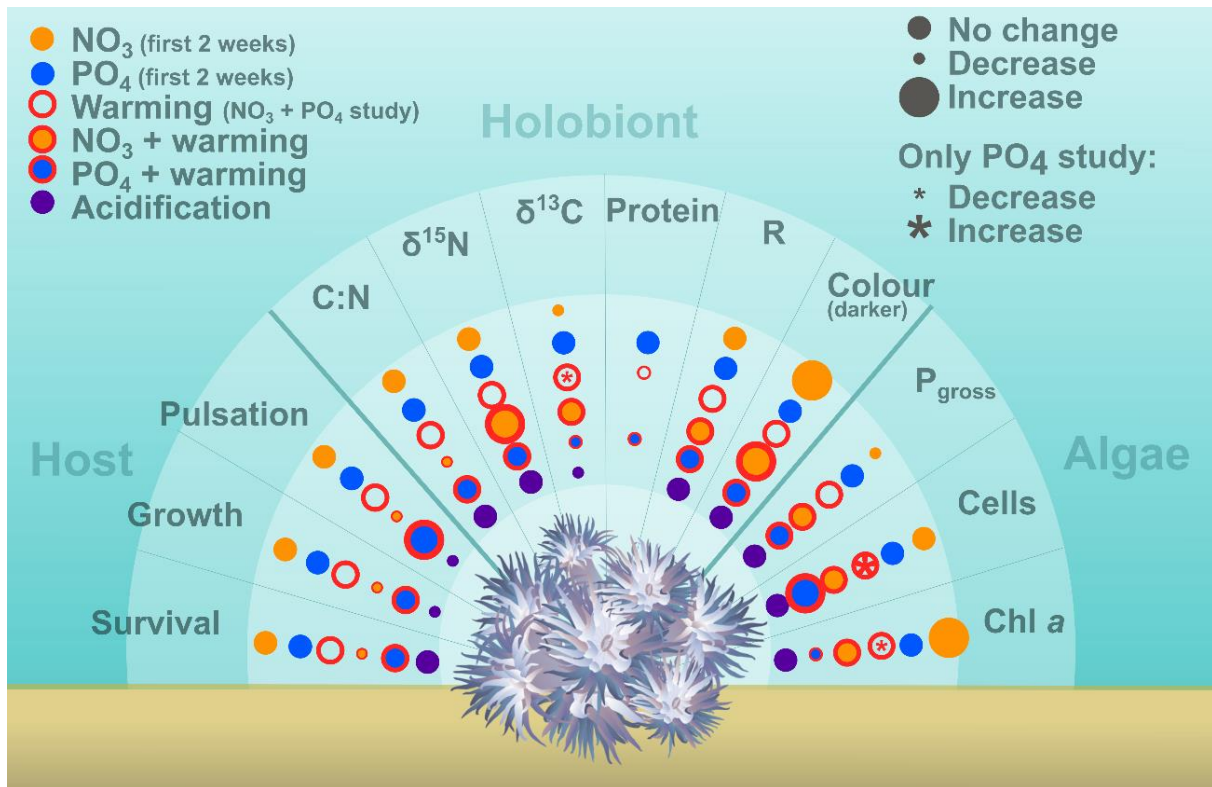


Figure 9.1. Summary of physiological response parameters of the pulsating soft coral *Xenia umbellata* to different global and local environmental stressors (chapters 2-5). C:N = carbon to nitrogen ratio, R = respiration, P_{gross} = gross photosynthesis, cells = Symbiodiniaceae cell density, Chl *a* = cellular chlorophyll *a* content of Symbiodiniaceae. Parameters are divided into three categories: host = coral host-related, algae = Symbiodiniaceae-related, holobiont = parameters directly affected several members of the coral holobiont. The single stressor warming was applied in two separate experiments: combined with nitrate, (NO_3) and phosphate (PO_4), and different outcomes of parameters in the PO_4 study (chapter 3) are marked by asterisks. The single stressors NO_3 (chapter 2) and PO_4 (chapters 3-4) were applied only for the first two weeks, with additional warming for the three consecutive weeks. Acidification (chapter 5) was applied for three weeks in total. Tissue protein content was only measured in chapter 4. Icon attribution: Integration and Application Network (ian.umces.edu/media-library).

Research question 2 | Can microbial fuel cells be used to detect OC eutrophication in coral reefs sediments? What is the ecological relevance?

The newly developed and tested microbial fuel cells (MFCs) successfully detected OC eutrophication with artificial wastewater when deployed in tanks with permeable coral reef sediment (chapter 6). Response times to OC pulses were less than one day and MFCs required low material costs and maintenance, and were operated continuously for > 6 months. These results indicate a great potential of MFCs for remote, continuous monitoring of benthic microbial metabolism in coral reef ecosystems. Wastewater discharge affects more than half of all coral reefs³⁷ and is one of the reasons for shifts in benthic communities towards macroalgae dominance and reef microbialization^{38,39}. Wastewater and

macroalgae both increase the availability of OC in reefs (Fig. 9.2) and OC degradation in coral reef sediments likely also increases on microbialized reefs, reflecting bacterioplankton dynamics⁴⁰. In addition to OC, wastewater contains inorganic phosphorus (P) and N⁴¹ which stimulate microalgae growth in the water column^{42,43} and growth of benthic cyanobacteria mats (BCMs)⁴⁴ and macroalgae⁴⁵. Microalgae detritus contributes to POC⁴² which fuels microbial metabolism in the sediment⁴⁶ and thus increases the electric current density of MFCs (chapter 6). Microalgae, BCMs and macroalgae further release DOC, stimulating bacterioplankton growth and subsequent POC formation through aggregation^{40,47}. DOC can additionally fuel sediment microbes through pore water advection^{48,49}. Sediment microbes release inorganic nutrients when degrading organic matter⁵⁰ and may thus support the formation of BCMs⁵¹ which release large amounts of DOC and further enhance reef microbialization^{52,53}. The in chapter 6 developed and tested MFCs could therefore become a valuable tool for monitoring reef sediment metabolism to detect OC eutrophication from wastewater and/or processes associated with reef microbialization.

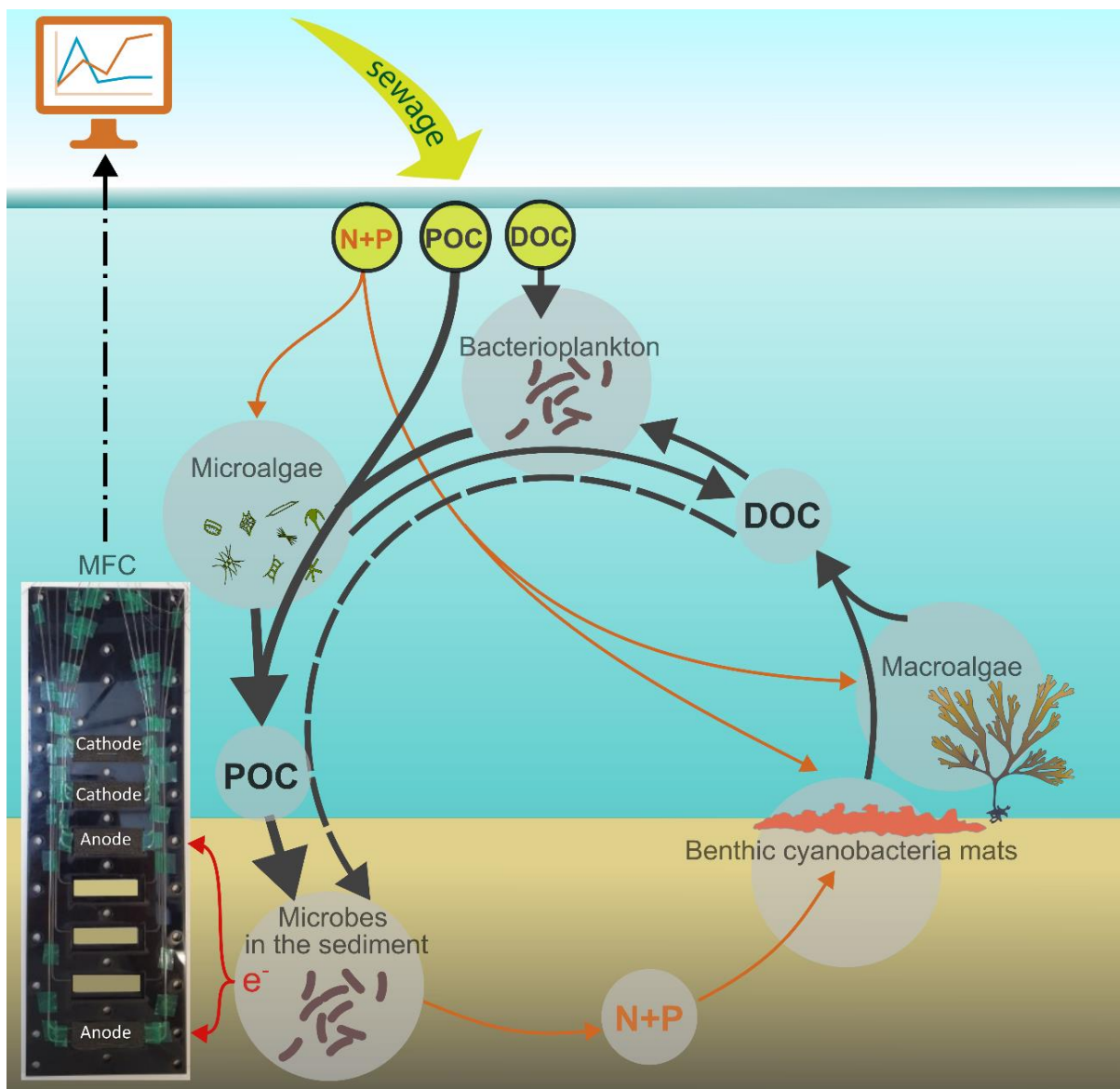


Figure 9.2. Ecological relevance of microbial fuel cells (MFCs) for the detection of organic carbon (OC) eutrophication in coral reef sediment. Sewage contains inorganic nitrogen and phosphorus (N+P),

particulate organic carbon (POC) and dissolved organic carbon (DOC). N+P input supports growth of planktonic microalgae, benthic cyanobacteria mats (BCMs) and macroalgae (orange arrows). POC (including detritus from bacterioplankton and microalgae) sinks to the sediment where it is degraded by microbes which donate electrons (e^- , red arrows) to the anode of the MFC, creating an electric signal which can be transmitted to a computer (black dashed arrow). Sediment microbes release inorganic N+P which may stimulate BCMs. DOC released by BCMs and macroalgae supports bacterioplankton growth and growth of microbes in the sediment through advective currents which transport DOC into the sediment (grey dashed arrow). Dark grey arrows indicate the flow of OC. Icon attribution: Integration and Application Network (ian.umces.edu/media-library).

Research question 3 | How does the composition of mucosal carbohydrates vary among hard coral species? What are potential implications for coral holobiont functioning?

Carbohydrate compositions of hydrolysed mucus collected from five scleractinian coral species on Curaçao and *ex situ* in Bremen were species- and genus-specific (chapter 7). Comparisons with reported data from six previous studies (i.e., a total 23 species and 10 families) further revealed that coral phylogeny explained 70 % of variation in mucus carbohydrate compositions despite other factors which could have induced variation (e.g., differences in measurement protocols between studies, different geographic origins of specimen). These results suggest co-diversification of mucus carbohydrates within scleractinian corals and support their essential function for corals. Furthermore, the pentose sugar arabinose was only present in the mucus of one of the two main hard coral lineages (i.e., the complex clade) and thus may add to the molecular-level differences between corals of the complex and robust clade (see^{54,55}) which diverged about 418 million years ago⁵⁶. Functions of mucus carbohydrates may include the regulation of coral mucus-associated microbiomes⁵⁷⁻⁵⁹. Metazoan mucus carbohydrates are increasingly recognized for their role in shaping microbial communities, e.g., through adhesion of beneficial microbes^{60,61} and bacteriophages^{62,63}, and down- or upregulation of virulence genes and quorum sensing in pathogens⁶⁴⁻⁶⁷. Additionally, metazoan carbohydrates were suggested to mediate host-symbiont coevolution⁶⁸⁻⁷⁰, which is seen in some coral symbionts⁷¹ and may thus be linked to co-diversifying mucus carbohydrates (*sensu*⁷²).

Research question 4 | How do carbohydrates exuded by hard corals and macroalgae affect bacterioplankton communities from an algae-dominated Caribbean reef? What are the ecological implications?

The carbohydrate compositions of high molecular weight (HMW) exudates from a community of hard corals were compositionally distinct from ambient reef water and enriched opportunistic microbial taxa commonly associated with corals, significantly increasing predicted metabolic functions related to coral mucus degradation (chapter 8). In contrast, brown macroalgae-derived HMW exudates were more similar to ambient reef water in carbohydrate composition and did not influence the bacterioplankton community. These results are consistent with previously reported increased respiration instead of biomass production on macroalgae exudates^{34,38,53,73} and may be explained by a shift towards less energy efficient metabolic pathways³⁸. Macroalgae exudates could additionally have increased microbial cell sizes (as shown previously⁷⁴) without affecting microbial abundance or community composition.

Furthermore, brown macroalgae-derived HMW exudates were compositionally similar to fucoidan, a complex polysaccharide which can constitute up to half of released DOC in brown algae⁷⁵ and can be highly resistant to microbial degradation^{76,77}. A fraction of brown macroalgae exudates may thus have resisted microbial degradation, while high energetic requirements for fucoidan degradation⁷⁶ could have further reduced the microbial growth efficiency. Combined, results suggest efficient uptake and growth on coral-derived HMW DOC, while brown macroalgae exudates were either inefficiently or incompletely degraded (Fig. 9.3a), both supporting the microbialization of reefs^{38,39}.

Results of chapter 8 additionally suggest that an alteration in dissolved organic matter (DOM) composition relative to ambient reef water and not *per se* the origin of DOM (i.e., coral- vs. macroalgae-derived) supports opportunistic microbes. The concept of changing environmental conditions leading to opportunism has long been established in ecology⁷⁸ and also applies to microbial ecology⁷⁹. A greater change in (HMW) DOM composition through the addition of coral exudates to seawater from an algae-dominated reef may have disrupted the stable microbial community and increased the abundance of opportunistic microbes (Fig. 9.3b). Concomitantly, the generally observed higher abundance of microbial opportunists and pathogens (e.g., Vibrionales) on algae- compared to coral-dominated reefs^{38,80,81} could still be explained by higher availability of labile DOM on degraded reefs^{82–84}. As such, green macroalgae exude carbohydrates rich in glucose⁸⁵ which is more bioavailable than fucose⁸⁶, and turf algae and BCMs release large amounts of labile DOM which contributes to reef microbialization^{52,53,73}. The rise of opportunistic microbes can impact macro-organism health, as holobionts experiencing stress may lose the ability to regulate their associated microbiome and become more vulnerable to opportunistic microbial growth and disease^{87–90}. Thus, results presented here suggest that alterations in seawater DOM composition may be one driver of the global microbialization of reefs.

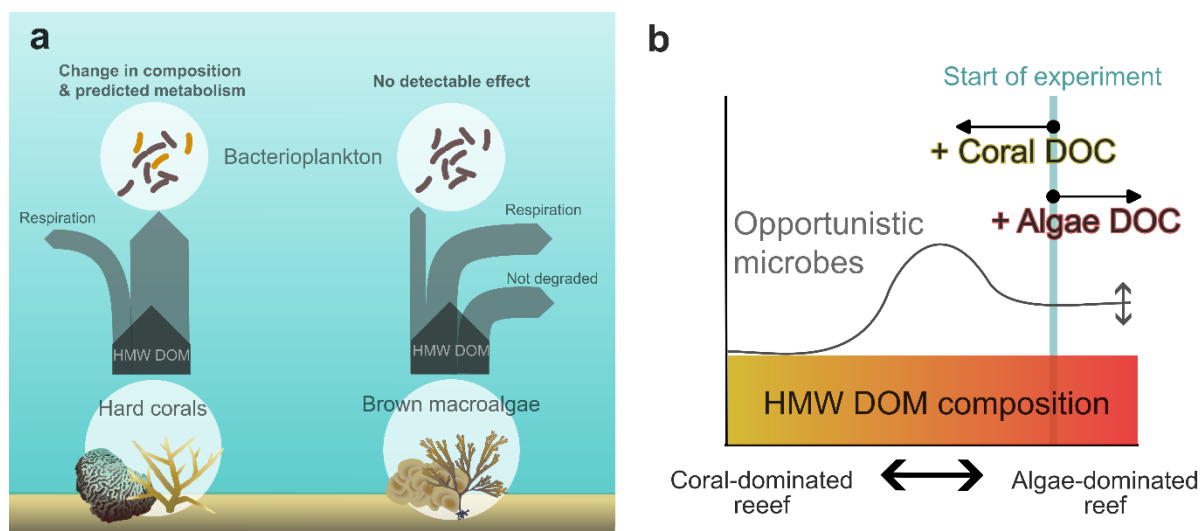


Figure 9.3. Overview of hypotheses which may explain the different responses of bacterioplankton communities to hard coral- versus macroalgae high molecular weight dissolved organic carbon (HMW DOC) (chapter 8). (a) Coral-derived HMW DOC may have resulted in higher biomass production compared to respiration of DOC, resulting in changing microbial community composition and predicted metabolism. In contrast, brown macroalgae-derived HMW DOC may have resisted microbial degradation and/or required more respiration compared to biomass production, both potentially resulting in no effect on the

bacterioplankton community composition. **(b)** The abundance of opportunistic microbes may increase due to an alteration of HMW DOC composition relative to starting conditions. Ambient reef water from an algae-dominated reef reflected algae exudate composition. Thus, the addition of algae exudates did not increase opportunistic microbes. Addition of coral exudates however altered the HMW DOC composition, supporting opportunistic microbes. Icon attribution: Integration and Application Network (ian.umces.edu/media-library).

9.4 Outlook

This thesis combined research on coral physiology, biogeochemistry, and microbial ecology to improve our understanding of coral reefs under environmental change on multiple levels of ecological organization. Overarching effects of environmental change on the scale of the coral holobiont and the reef ecosystem appear to be the shunting of OC from corals to algae (i.e., either Symbiodiniaceae or macroalgae)⁹¹ and/or from macro-organisms (i.e., either corals or higher trophic levels) to microbes (i.e., either Symbiodiniaceae^{14,15,92} or bacterioplankton^{38,39}). The work presented here provides new insights into the physiology of soft corals, proposes a new biosensor with great potential and ecological relevance for monitoring of reef eutrophication, and improves our understanding on benthic-pelagic coupling in changing coral reefs. By studying OC cycling in reefs from these diverse perspectives, new research questions arose which may connect the different aspects investigated here.

1 | Effects of soft coral dominance on reef-wide OC cycling

Results of this thesis indicate that xeniid soft corals are resistant to a range of environmental stressors (chapters 2-5) and may thus further increase in abundance on reefs affected by anthropogenic stressors^{93,94}. Future research should therefore aim to understand how these shifts influence bacterioplankton communities and ecosystem-scale OC cycling (*sensu*^{36,95}). Uptake of DOM and POM by abundant filter-feeding soft corals could potentially reduce reef microbialization, especially if soft corals compete with microbes for the same DOM components, as previously hypothesized for reef-associated sponges⁹⁶. Therefore, it will be important to not only investigate bulk DOM and POM fluxes, but also how soft corals manipulate the DOM composition of reef water through uptake and release of specific metabolites (*sensu*⁹⁷).

2 | Further development of microbial fuel cells and *in situ* tests

The here presented MFCs revealed great potential for monitoring of OC eutrophication in coral reef sediments (chapter 6). The further development of MFCs will require interdisciplinary collaboration of coral reef ecologists, electrical engineers, and computer scientists to develop wireless sensor networks (WSNs)⁹⁸ of MFCs suitable for *in situ* deployment in reef sediments (see⁹⁹). Furthermore, MFCs could be upscaled to provide sufficient electricity for transmitter systems and additional sensors (e.g.,^{100,101}) and could thus potentially become autonomous for long-term deployment. Once MFCs for *in situ* measurements are developed, they can be used to monitor OC eutrophication even in remote locations continuously and nearly in real-time. This could help to direct management and conservation strategies

to prevent changes in benthic reef composition which are often hard to reverse¹⁰² and reinforced by positive feedback loops^{103–105}.

3 | Roles of mucus carbohydrates for coral holobiont resilience

Mucus carbohydrates likely provide important functions for coral holobionts, as their compositions covary with phylogeny (chapter 7). Due to the regulating effects of mucins on microbial communities in the mammalian gut mucus layer, addition of “prebiotic mucin glycans” was recently proposed as a therapy method for gut-related diseases^{68,106,107}. Likewise, studying glycan-microbe interactions in coral mucus may provide ways to develop coral prebiotics (i.e., molecules which assist corals in selecting beneficial microbes from their environment¹⁰⁸). For instance, transplantation of sterilized mucus from healthy to stressed and/or diseased corals of the same species may reveal effects of mucins on microbial communities and host physiology. Transplantation of unsterilized mucus has previously been proposed due to beneficial probiotic effects^{109,110}, but to understand the effects of mucins alone on microbial communities, removal of microbes from the mucus prior to addition is required.

4 | Effects of changing hard coral assemblages on reef-wide OC cycling

Coral mucus carbohydrates may co-diversify with hard coral phylogeny (chapter 7) and can shape bacterioplankton communities⁸⁴, even at low concentrations (chapter 8). Changes in hard coral assemblages towards more stress-tolerant species are observed on reefs worldwide^{5,111–113}, and may affect reef water DOM- and thus, bacterioplankton compositions. Especially corals of the genus *Acropora* declined markedly on reef worldwide^{113–115} and release large amounts of DOC¹¹⁶ with mucus rich in arabinose (chapter 7). One example is *Madracis mirabilis*, which increases in relative abundance in the Caribbean¹¹¹, has low mucus carbohydrate concentrations (i.e., below the detection limit, chapter 7) and primarily takes up DOC from the water column¹¹⁷. Future studies should thus investigate how hard coral species with higher resistance to anthropogenic stressors affect benthic-pelagic coupling and OC cycling.

5 | Role of brown macroalgae-derived fucoidan in reef-wide OC cycling

Due to the high resistance of brown algae exudates to microbial degradation^{118–121} and accumulation of fucoidan during diatom blooms^{77,122}, fucoidan is hypothesized to sequester carbon in the ocean^{75,77}. Results of chapter 8 provide evidence for accumulation of fucoidan in reef water, which could reduce trophic transfer by exporting OC from the reef environment. Future studies should therefore investigate rates of fucoidan release by coral reef-associated brown macroalgae (e.g.,⁷⁵), as well as rates of microbial degradation and export of fucoidan from reef ecosystems (e.g.,^{119,120}).

6 | Role of the relative change in DOM composition in supporting opportunistic microbes

To further validate the here developed hypothesis that a change in coral reef water DOM composition promotes opportunistic microbes (chapter 8), future studies could use cross-transplantations (e.g.,¹²³)

with concentrated DOM from corals and macroalgae to bacterioplankton communities from coral- and macroalgae-dominated reefs. A recent study also reported increases in opportunistic bacterioplankton due to alterations of coral-derived DOM during thermal stress¹²⁴, which is consistent with the here proposed mechanism and suggests wider ecological relevance. Coastal ecosystems worldwide change in benthic composition due to human stressors (e.g., seagrass meadows¹²⁵, macroalgae beds¹²⁶, and kelp forests¹²⁷), and further investigations should also consider these other ecosystems.

9.5 References

1. Lallas, J. A. A., Jamodiong, E. A. & Reimer, J. D. Spatial patterns of soft coral (Octocorallia) assemblages in the shallow coral reefs of Okinawa Island, Ryukyu Archipelago, Japan: Dominance on highly disturbed reefs. *Reg. Stud. Mar. Sci.* **71**, 103405 (2024).
2. Lolis, L. A., Miranda, R. J. & Barros, F. The effects of an invasive soft coral on the structure of native benthic communities. *Mar. Environ. Res.* **183**, 105802 (2023).
3. Menezes, N. M. *et al.* New non-native ornamental octocorals threatening a South-west Atlantic reef. *J. Mar. Biol. Assoc. U. K.* **101**, 911–917 (2021).
4. Ruiz-Allais, J. P., Benayahu, Y. & Lasso-Alcalá, O. M. The invasive octocoral *Unomia stolonifera* (Alcyonacea, Xeniidae) is dominating the benthos in the Southeastern Caribbean Sea. *Mem. Fund. Salle Cienc. Nat.* **79**, (2021).
5. Alves, C. *et al.* Twenty years of change in benthic communities across the Belizean Barrier Reef. *PLOS ONE* **17**, e0249155 (2022).
6. Cantin, D. N., James, N. & Stella, D. J. *Aerial Surveys of the 2024 Mass Coral Bleaching Event on the Great Barrier Reef.* (2024).
7. Goreau, T. & Hayes, R. L. 2023 record marine heat waves: coral bleaching hotspot maps reveal global sea surface temperature extremes, coral mortality, and ocean circulation change. Preprint at <https://doi.org/10.31223/X54M5R> (2024).
8. Hoegh-Guldberg, O. *et al.* Coral reefs in peril in a record-breaking year. *Science* **382**, 1238–1240 (2023).
9. Leslie, J. & Rodgers, K. NOAA confirms 4th global coral bleaching event. *National Oceanic and Atmospheric Administration* <https://www.noaa.gov/news-release/noaa-confirms-4th-global-coral-bleaching-event> (2024).
10. Bellwood, D. R. *et al.* Coral reef conservation in the Anthropocene: confronting spatial mismatches and prioritizing functions. *Biol. Conserv.* **236**, 604–615 (2019).
11. Hughes, T. P. *et al.* Coral reefs in the Anthropocene. *Nature* **546**, 82–90 (2017).
12. Pupier, C. A. *et al.* Productivity and carbon fluxes depend on species and symbiont density in soft coral symbioses. *Sci. Rep.* **9**, 17819 (2019).
13. Allen-Waller, L. & Barott, K. L. Symbiotic dinoflagellates divert energy away from mutualism during coral bleaching recovery. *Symbiosis* **89**, 173–186 (2023).

14. Baker, D. M., Freeman, C. J., Wong, J. C. Y., Fogel, M. L. & Knowlton, N. Climate change promotes parasitism in a coral symbiosis. *ISME J.* **12**, 921–930 (2018).
15. Rådecker, N. *et al.* Heat stress destabilizes symbiotic nutrient cycling in corals. *Proc. Natl. Acad. Sci.* **118**, e2022653118 (2021).
16. Parrin, A. P. *et al.* Symbiodinium migration mitigates bleaching in three octocoral species. *J. Exp. Mar. Biol. Ecol.* **474**, 73–80 (2016).
17. Derviche, P., Menegotto, A. & Lana, P. Carbon budget trends in octocorals: a literature review with data reassessment and a conceptual framework to understand their resilience to environmental changes. *Mar. Biol.* **169**, 159 (2022).
18. Schubert, N., Brown, D. & Rossi, S. Symbiotic versus non-symbiotic octocorals: physiological and ecological implications. in *Marine Animal Forests: The Ecology of Benthic Biodiversity Hotspots* 40 (2017).
19. Kremien, M., Shavit, U., Mass, T. & Genin, A. Benefit of pulsation in soft corals. *Proc. Natl. Acad. Sci.* **110**, 8978–8983 (2013).
20. Mass, T., Genin, A., Shavit, U., Grinstein, M. & Tchernov, D. Flow enhances photosynthesis in marine benthic autotrophs by increasing the efflux of oxygen from the organism to the water. *Proc. Natl. Acad. Sci.* **107**, 2527–2531 (2010).
21. Wild, C. & Naumann, M. S. Effect of active water movement on energy and nutrient acquisition in coral reef-associated benthic organisms. *Proc. Natl. Acad. Sci.* **110**, 8767–8768 (2013).
22. Richardson, L. E., Graham, N. A. J., Pratchett, M. S. & Hoey, A. S. Structural complexity mediates functional structure of reef fish assemblages among coral habitats. *Environ. Biol. Fishes* **100**, 193–207 (2017).
23. Richardson, L. E., Graham, N. A. J. & Hoey, A. S. Cross-scale habitat structure driven by coral species composition on tropical reefs. *Sci. Rep.* **7**, 7557 (2017).
24. Epstein, H. E. & Kingsford, M. J. Are soft coral habitats unfavourable? A closer look at the association between reef fishes and their habitat. *Environ. Biol. Fishes* **102**, 479–497 (2019).
25. Moynihan, J. L., Hall, A. E. & Kingsford, M. J. Interrelationships between soft corals and reef-associated fishes on inshore-reefs of the Great Barrier Reef. *Mar. Ecol. Prog. Ser.* **698**, 15–28 (2022).
26. Lasker, H. R., Bramanti, L., Tsounis, G. & Edmunds, P. J. Chapter Thirteen - The rise of octocoral forests on Caribbean reefs. in *Advances in Marine Biology* (ed. Riegl, B. M.) vol. 87 361–410 (Academic Press, 2020).
27. Raimundo, I., Silva, S. G., Costa, R. & Keller-Costa, T. Bioactive secondary metabolites from octocoral-associated microbes—new chances for blue growth. *Mar. Drugs* **16**, 485 (2018).
28. Watson, G. J. *et al.* Can the global marine aquarium trade (MAT) be a model for sustainable coral reef fisheries? *Sci. Adv.* **9**, eadh4942 (2023).

29. Bednarz, V. N., Naumann, M. S., Niggel, W. & Wild, C. Inorganic nutrient availability affects organic matter fluxes and metabolic activity in the soft coral genus *Xenia*. *J. Exp. Biol.* **215**, 3672–3679 (2012).
30. Hill, C. E. L. *et al.* Physiology of the widespread pulsating soft coral *Xenia umbellata* is affected by food sources, but not by water flow. *Ecol. Evol.* **13**, e10483 (2023).
31. Vollstedt, S., Xiang, N., Simancas-Giraldo, S. M. & Wild, C. Organic eutrophication increases resistance of the pulsating soft coral *Xenia umbellata* to warming. *PeerJ* **8**, e9182 (2020).
32. Fabricius, K. E. & Dommissie, M. Depletion of suspended particulate matter over coastal reef communities dominated by zooxanthellate soft corals. *Mar. Ecol. Prog. Ser.* **196**, 157–167 (2000).
33. Nakajima, R. *et al.* Release of dissolved and particulate organic matter by the soft coral *Lobophytum* and subsequent microbial degradation. *J. Exp. Mar. Biol. Ecol.* **504**, 53–60 (2018).
34. Haas, A. F. *et al.* Influence of coral and algal exudates on microbially mediated reef metabolism. *PeerJ* **1**, e108 (2013).
35. El-Khaled, Y. C. *et al.* Nitrogen fixation and denitrification activity differ between coral- and algae-dominated Red Sea reefs. *Sci. Rep.* **11**, 11820 (2021).
36. Pupier, C. A. *et al.* Divergent capacity of scleractinian and soft corals to assimilate and transfer diazotrophically derived nitrogen to the reef environment. *Front. Microbiol.* **10**, (2019).
37. Tuholske, C. *et al.* Mapping global inputs and impacts from of human sewage in coastal ecosystems. *PLOS ONE* **16**, e0258898 (2021).
38. Haas, A. F. *et al.* Global microbialization of coral reefs. *Nat. Microbiol.* **1**, 16042 (2016).
39. McDole, T. *et al.* Assessing coral reefs on a pacific-wide scale using the microbialization score. *PLoS ONE* **7**, e43233 (2012).
40. Silveira, C. B. *et al.* Microbial processes driving coral reef organic carbon flow. *FEMS Microbiol. Rev.* **41**, 575–595 (2017).
41. Wear, S. L. & Vega Thurber, R. Sewage pollution: mitigation is key for coral reef stewardship. *Ann. N. Y. Acad. Sci.* **1355**, 15–30 (2015).
42. D'Angelo, C. & Wiedenmann, J. Impacts of nutrient enrichment on coral reefs: new perspectives and implications for coastal management and reef survival. *Curr. Opin. Environ. Sustain.* **7**, 82–93 (2014).
43. Furnas, M., Mitchell, A., Skuza, M. & Brodie, J. In the other 90%: phytoplankton responses to enhanced nutrient availability in the Great Barrier Reef Lagoon. *Mar. Pollut. Bull.* **51**, 253–265 (2005).
44. Kuffner, I. B. & Paul, V. J. Effects of nitrate, phosphate and iron on the growth of macroalgae and benthic cyanobacteria from Cocos Lagoon, Guam. *Mar. Ecol. Prog. Ser.* **222**, 63–72 (2001).

45. Fabricius, K. E. Factors determining the resilience of coral reefs to eutrophication: a review and conceptual model. in *Coral Reefs: An Ecosystem in Transition* (eds. Dubinsky, Z. & Stambler, N.) 493–505 (Springer Netherlands, Dordrecht, 2011). doi:10.1007/978-94-007-0114-4_28.
46. Ford, A. K. *et al.* High sedimentary oxygen consumption indicates that sewage input from small islands drives benthic community shifts on overfished reefs. *Environ. Conserv.* **44**, 405–411 (2017).
47. Cárdenas, A., Meyer, F., Schwieder, H., Wild, C. & Gärdes, A. The formation of aggregates in coral reef waters under elevated concentrations of dissolved inorganic and organic carbon: a mesocosm approach. *Mar. Chem.* **175**, 47–55 (2015).
48. Werner, U. *et al.* Spatial patterns of aerobic and anaerobic mineralization rates and oxygen penetration dynamics in coral reef sediments. *Mar. Ecol. Prog. Ser.* **309**, 93–105 (2006).
49. Wild, C. *et al.* Coral mucus functions as an energy carrier and particle trap in the reef ecosystem. *Nature* **428**, 66–70 (2004).
50. Rasheed, M., Badran, M. I. & Huettel, M. Influence of sediment permeability and mineral composition on organic matter degradation in three sediments from the Gulf of Aqaba, Red Sea. *Estuar. Coast. Shelf Sci.* **57**, 369–384 (2003).
51. Brocke, H. J. *et al.* Organic matter degradation drives benthic cyanobacterial mat abundance on Caribbean coral reefs. *PLOS ONE* **10**, e0125445 (2015).
52. Brocke, H. J. *et al.* High dissolved organic carbon release by benthic cyanobacterial mats in a Caribbean reef ecosystem. *Sci. Rep.* **5**, 8852 (2015).
53. Mueller, B. *et al.* Nocturnal dissolved organic matter release by turf algae and its role in the microbialization of reefs. *Funct. Ecol.* **36**, 2104–2118 (2022).
54. Kitahara, M. V. *et al.* The “naked coral” hypothesis revisited – evidence for and against scleractinian monophyly. *PLOS ONE* **9**, e94774 (2014).
55. Ying, H. *et al.* Comparative genomics reveals the distinct evolutionary trajectories of the robust and complex coral lineages. *Genome Biol.* **19**, 175 (2018).
56. Arrigoni, R. *et al.* A new sequence data set of SSU rRNA gene for Scleractinia and its phylogenetic and ecological applications. *Mol. Ecol. Resour.* **17**, 1054–1071 (2017).
57. Lee, S. T. M., Davy, S. K., Tang, S.-L. & Kench, P. S. Mucus sugar content shapes the bacterial community structure in thermally stressed *Acropora muricata*. *Front. Microbiol.* **7**, 371 (2016).
58. Ritchie, K. B. & Smith, G. W. Microbial communities of coral surface mucopolysaccharide layers. in *Coral Health and Disease* (eds. Rosenberg, E. & Loya, Y.) 259–264 (Springer, Berlin, Heidelberg, 2004). doi:10.1007/978-3-662-06414-6_13.
59. Tremblay, P. *et al.* Mucus composition and bacterial communities associated with the tissue and skeleton of three scleractinian corals maintained under culture conditions. *J. Mar. Biol. Assoc. U.K.* **91**, 649–657 (2011).

60. Bakshani, C. R. *et al.* Evolutionary conservation of the antimicrobial function of mucus: a first defence against infection. *Npj Biofilms Microbiomes* **4**, 1–12 (2018).
61. McLoughlin, K., Schluter, J., Rakoff-Nahoum, S., Smith, A. L. & Foster, K. R. Host selection of microbiota via differential adhesion. *Cell Host Microbe* **19**, 550–559 (2016).
62. Almeida, G. M. F., Laanto, E., Ashrafi, R. & Sundberg, L.-R. Bacteriophage adherence to mucus mediates preventive protection against pathogenic bacteria. *mBio* **10**, e01984-19 (2019).
63. Barr, J. J. *et al.* Bacteriophage adhering to mucus provide a non-host-derived immunity. *Proc. Natl. Acad. Sci.* **110**, 10771–10776 (2013).
64. Gao, C. *et al.* Coral mucus rapidly induces chemokinesis and genome-wide transcriptional shifts toward early pathogenesis in a bacterial coral pathogen. *ISME J.* **15**, 3668–3682 (2021).
65. Wang, B. X. *et al.* Host-derived O-glycans inhibit toxigenic conversion by a virulence-encoding phage in *Vibrio cholerae*. *EMBO J.* e111562 (2022) doi:10.15252/embj.2022111562.
66. Werlang, C. A. *et al.* Mucin O-glycans suppress quorum-sensing pathways and genetic transformation in *Streptococcus mutans*. *Nat. Microbiol.* **6**, 574–583 (2021).
67. Wheeler, K. M. *et al.* Mucin glycans attenuate the virulence of *Pseudomonas aeruginosa* in infection. *Nat. Microbiol.* **4**, 2146–2154 (2019).
68. Belzer, C. Nutritional strategies for mucosal health: the interplay between microbes and mucin glycans. *Trends Microbiol.* **30**, 13–21 (2022).
69. Gagneux, P., Panin, V., Hennet, T., Aebi, M. & Varki, A. Evolution of glycan diversity. in *Essentials of Glycobiology* (eds. Varki, A. *et al.*) (Cold Spring Harbor Laboratory Press, Cold Spring Harbor (NY), 2022).
70. Sichert, A. & Cordero, O. X. Polysaccharide-bacteria interactions from the lens of evolutionary ecology. *Front. Microbiol.* **12**, 705082 (2021).
71. Pollock, F. J. *et al.* Coral-associated bacteria demonstrate phyllosymbiosis and cophylogeny. *Nat. Commun.* **9**, 4921 (2018).
72. Hooper, L. V. & Gordon, J. I. Glycans as legislators of host–microbial interactions: spanning the spectrum from symbiosis to pathogenicity. *Glycobiology* **11**, 1R-10R (2001).
73. Haas, A. F. *et al.* Effects of coral reef benthic primary producers on dissolved organic carbon and microbial activity. *PLoS ONE* **6**, e27973 (2011).
74. Silveira, C. B. *et al.* Biophysical and physiological processes causing oxygen loss from coral reefs. *eLife* **8**, e49114 (2019).
75. Buck-Wiese, H. *et al.* Fucoid brown algae inject fucoidan carbon into the ocean. *Proc. Natl. Acad. Sci.* **120**, e2210561119 (2022).
76. Sichert, A. *et al.* Verrucomicrobia use hundreds of enzymes to digest the algal polysaccharide fucoidan. *Nat. Microbiol.* **5**, 1026–1039 (2020).
77. Vidal-Melgosa, S. *et al.* Diatom fucan polysaccharide precipitates carbon during algal blooms. *Nat. Commun.* **12**, 1150 (2021).

78. Rapport, D. J., Regier, H. A. & Hutchinson, T. C. Ecosystem behavior under stress. *Am. Nat.* **125**, 617–640 (1985).
79. Ho, A., Di Lonardo, D. P. & Bodelier, P. L. E. Revisiting life strategy concepts in environmental microbial ecology. *FEMS Microbiol. Ecol.* **93**, fix006 (2017).
80. Dinsdale, E. A. *et al.* Microbial ecology of four coral atolls in the Northern Line Islands. *PLOS ONE* **3**, e1584 (2008).
81. Meirelles, P. M. *et al.* Metagenomics of coral reefs under phase shift and high hydrodynamics. *Front. Microbiol.* **9**, (2018).
82. Cárdenas, A. *et al.* Excess labile carbon promotes the expression of virulence factors in coral reef bacterioplankton. *ISME J.* **12**, 59–76 (2018).
83. Kline, D., Kuntz, N., Breitbart, M., Knowlton, N. & Rohwer, F. Role of elevated organic carbon levels and microbial activity in coral mortality. *Mar. Ecol. Prog. Ser.* **314**, 119–125 (2006).
84. Nelson, C. E. *et al.* Coral and macroalgal exudates vary in neutral sugar composition and differentially enrich reef bacterioplankton lineages. *ISME J.* **7**, 962–979 (2013).
85. Haas, A. & Wild, C. Composition analysis of organic matter released by cosmopolitan coral reef-associated green algae. *Aquat. Biol.* **10**, 131–138 (2010).
86. Amon, R. M. W., Fitznar, H.-P. & Benner, R. Linkages among the bioreactivity, chemical composition, and diagenetic state of marine dissolved organic matter. *Limnol. Oceanogr.* **46**, 287–297 (2001).
87. Burge, C. A., Kim, C. J. S., Lyles, J. M. & Harvell, C. D. Special issue oceans and humans health: the ecology of marine opportunists. *Microb. Ecol.* **65**, 869–879 (2013).
88. Egan, S. & Gardiner, M. Microbial dysbiosis: rethinking disease in marine ecosystems. *Front. Microbiol.* **7**, (2016).
89. Williams, J. *et al.* Decline of a distinct coral reef holobiont community under ocean acidification. *Microbiome* **12**, 75 (2024).
90. Zaneveld, J. R. *et al.* Overfishing and nutrient pollution interact with temperature to disrupt coral reefs down to microbial scales. *Nat. Commun.* **7**, 11833 (2016).
91. Allgeier, J. E. *et al.* Rewiring coral: Anthropogenic nutrients shift diverse coral–symbiont nutrient and carbon interactions toward symbiotic algal dominance. *Glob. Change Biol.* **26**, 5588–5601 (2020).
92. Rådecker, N., Escrig, S., Spangenberg, J. E., Voolstra, C. R. & Meibom, A. Coupled carbon and nitrogen cycling regulates the cnidarian–algal symbiosis. *Nat. Commun.* **14**, 6948 (2023).
93. Norström, A., Nyström, M., Lokrantz, J. & Folke, C. Alternative states on coral reefs: beyond coral–macroalgal phase shifts. *Mar. Ecol. Prog. Ser.* **376**, 295–306 (2009).
94. Tebbett, S. B., Connolly, S. R. & Bellwood, D. R. Benthic composition changes on coral reefs at global scales. *Nat. Ecol. Evol.* **7**, 71–81 (2023).

95. Weber, L. *et al.* Benthic exometabolites and their ecological significance on threatened Caribbean coral reefs. *ISME Commun.* **2**, 1–13 (2022).
96. de Goeij, J. M., Lesser, M. P. & Pawlik, J. R. Nutrient fluxes and ecological functions of coral reef sponges in a changing ocean. in *Climate Change, Ocean Acidification and Sponges: Impacts Across Multiple Levels of Organization* (eds. Carballo, J. L. & Bell, J. J.) 373–410 (Springer International Publishing, Cham, 2017). doi:10.1007/978-3-319-59008-0_8.
97. Nelson, C. E., Wegley Kelly, L. & Haas, A. F. Microbial interactions with dissolved organic matter are central to coral reef ecosystem function and resilience. *Annu. Rev. Mar. Sci.* **15**, null (2023).
98. Förster, A. *Introduction to Wireless Sensor Networks*. (John Wiley & Sons, Hoboken, New Jersey, 2016).
99. Fattah, S., Gani, A., Ahmedy, I., Idris, M. Y. I. & Targio Hashem, I. A. A survey on underwater wireless sensor networks: requirements, taxonomy, recent advances, and open research challenges. *Sensors* **20**, 5393 (2020).
100. Donovan, C., Dewan, A., Heo, D. & Beyenal, H. Batteryless, wireless sensor powered by a sediment microbial fuel cell. *Environ. Sci. Technol.* **42**, 8591–8596 (2008).
101. Tender, L. M. *et al.* The first demonstration of a microbial fuel cell as a viable power supply: powering a meteorological buoy. *J. Power Sources* **179**, 571–575 (2008).
102. Graham, N. A. *et al.* Managing resilience to reverse phase shifts in coral reefs. *Front. Ecol. Environ.* **11**, 541–548 (2013).
103. Barott, K. L. & Rohwer, F. L. Unseen players shape benthic competition on coral reefs. *Trends Microbiol.* **20**, 621–628 (2012).
104. Dinsdale, E. A. & Rohwer, F. Fish or germs? Microbial dynamics associated with changing trophic structures on coral reefs. in *Coral Reefs: An Ecosystem in Transition* (eds. Dubinsky, Z. & Stambler, N.) 231–240 (Springer Netherlands, Dordrecht, 2011). doi:10.1007/978-94-007-0114-4_16.
105. Smith, J. E. *et al.* Indirect effects of algae on coral: algae-mediated, microbe-induced coral mortality. *Ecol. Lett.* **9**, 835–845 (2006).
106. Pruss, K. M. *et al.* Mucin-derived O-glycans supplemented to diet mitigate diverse microbiota perturbations. *ISME J.* **15**, 577–591 (2021).
107. Tolonen, A. C. *et al.* Synthetic glycans control gut microbiome structure and mitigate colitis in mice. *Nat. Commun.* **13**, 1244 (2022).
108. Voolstra, C. R. *et al.* Extending the natural adaptive capacity of coral holobionts. *Nat. Rev. Earth Environ.* **2**, 747–762 (2021).
109. Damjanovic, K., Blackall, L. L., Webster, N. S. & van Oppen, M. J. H. The contribution of microbial biotechnology to mitigating coral reef degradation. *Microb. Biotechnol.* **10**, 1236–1243 (2017).

110. Woolstra, C. R. & Ziegler, M. Adapting with microbial help: microbiome flexibility facilitates rapid responses to environmental change. *BioEssays* **42**, 2000004 (2020).
111. De Bakker, D. M., Meesters, E. H., Bak, R. P. M., Nieuwland, G. & Van Duyl, F. C. Long-term shifts in coral communities on shallow to deep reef slopes of Curaçao and Bonaire: are there any winners? *Front. Mar. Sci.* **3**, (2016).
112. Hughes, T. P. *et al.* Global warming transforms coral reef assemblages. *Nature* **556**, 492–496 (2018).
113. Pratchett, M. S., Trapon, M., Berumen, M. L. & Chong-Seng, K. Recent disturbances augment community shifts in coral assemblages in Moorea, French Polynesia. *Coral Reefs* **30**, 183–193 (2011).
114. Cramer, K. L. *et al.* Widespread loss of Caribbean acroporid corals was underway before coral bleaching and disease outbreaks. *Sci. Adv.* **6**, eaax9395 (2020).
115. Watt-Pringle, R., Smith, D. J., Ambo-Rappe, R., Lamont, T. A. C. & Jompa, J. Suppressed recovery of functionally important branching *Acropora* drives coral community composition changes following mass bleaching in Indonesia. *Coral Reefs* **41**, 1337–1350 (2022).
116. Tanaka, Y. & Nakajima, R. Dissolved organic matter in coral reefs: distribution, production, and bacterial consumption. in *Coral Reef Studies of Japan* (eds. Iguchi, A. & Hongo, C.) 7–27 (Springer, Singapore, 2018). doi:10.1007/978-981-10-6473-9_2.
117. Mueller, B. *et al.* Effect of light availability on dissolved organic carbon release by Caribbean reef algae and corals. *Bull. Mar. Sci.* **90**, 875–893 (2014).
118. Gao, Y. *et al.* Dissolved organic carbon from cultured kelp *Saccharina japonica*: production, bioavailability, and bacterial degradation rates. *Aquac. Environ. Interact.* **13**, 101–110 (2021).
119. Wada, S. *et al.* Bioavailability of macroalgal dissolved organic matter in seawater. *Mar. Ecol. Prog. Ser.* **370**, 33–44 (2008).
120. Wada, S. & Hama, T. The contribution of macroalgae to the coastal dissolved organic matter pool. *Estuar. Coast. Shelf Sci.* **129**, 77–85 (2013).
121. Watanabe, K. *et al.* Macroalgal metabolism and lateral carbon flows can create significant carbon sinks. *Biogeosciences* **17**, 2425–2440 (2020).
122. Huang, G. *et al.* Secretion of sulfated fucans by diatoms may contribute to marine aggregate formation. *Limnol. Oceanogr.* **66**, 3768–3782 (2021).
123. Xu, J. *et al.* Effect of seawater–sewage cross-transplants on bacterial metabolism and diversity. *Microb. Ecol.* **66**, 60–72 (2013).
124. Sparagon, W. J. *et al.* Coral thermal stress and bleaching enrich and restructure reef microbial communities via altered organic matter exudation. *Commun. Biol.* **7**, 1–14 (2024).
125. Turschwell, M. P. *et al.* Anthropogenic pressures and life history predict trajectories of seagrass meadow extent at a global scale. *Proc. Natl. Acad. Sci.* **118**, e2110802118 (2021).

126. Strain, E. M. A., Thomson, R. J., Micheli, F., Mancuso, F. P. & Airoidi, L. Identifying the interacting roles of stressors in driving the global loss of canopy-forming to mat-forming algae in marine ecosystems. *Glob. Change Biol.* **20**, 3300–3312 (2014).
127. Smale, D. A. Impacts of ocean warming on kelp forest ecosystems. *New Phytol.* **225**, 1447–1454 (2020).

Appendix | Supplementary material

Appendix | Supplementary material

Supplementary material to chapter 2

Supplementary figures to chapter 2

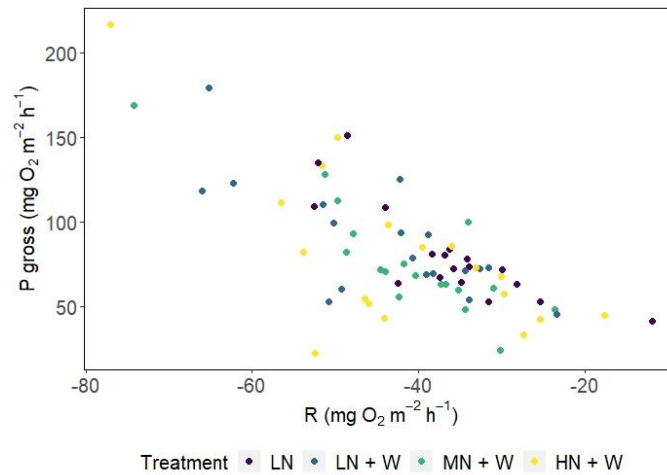


Figure S2.1. Correlation of gross photosynthesis (P_{gross}) and respiration (R) of *Xenia umbellata* colonies from control tanks with low nitrate (LN, $\sim 0.6 \mu\text{M}$) and three treatments: LN + W = low nitrate ($\sim 0.6 \mu\text{M}$) + warming from day 17; MN + W = medium nitrate eutrophication ($\sim 6 \mu\text{M}$) + warming from day 17; HN + W = high nitrate eutrophication ($\sim 37 \mu\text{M}$) + warming from day 17. Summary of all measurements conducted during the experiment. Significant negative Spearman's correlation: $r_s = -0.63$, $n = 72$, $p < 0.001$.

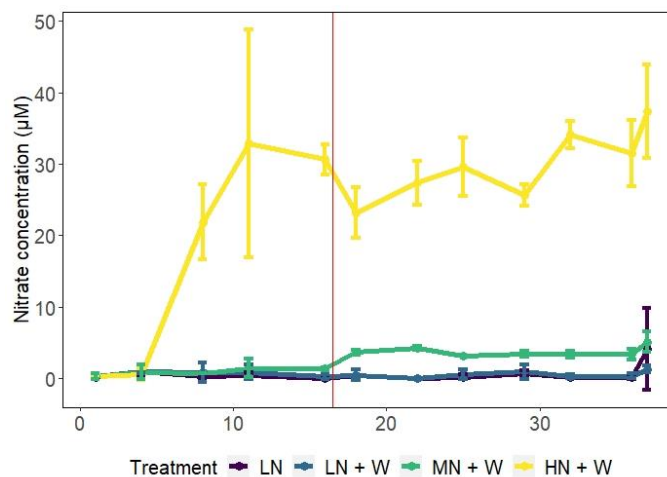


Figure S2.2. Nitrate concentrations (μM) measured in tanks before the addition of new nitrate by adjusting concentrations to $6 \mu\text{M}$ in medium nitrate (MN + W), and to $37 \mu\text{M}$ in high nitrate (HN + W) treatments. No nitrate was added to the low nitrate treatment (LN), and the low nitrate treatment with additional warming (LN + W).

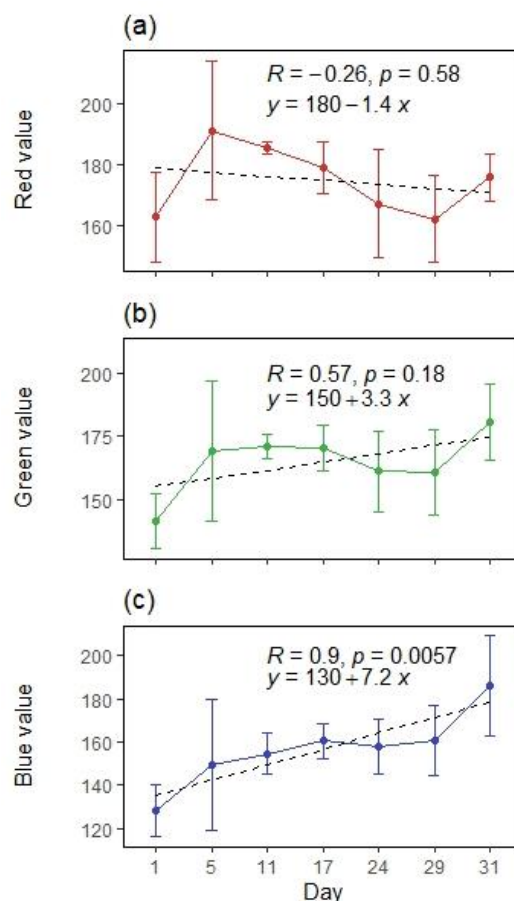


Figure S2.3. Changes in red (a), green (b), and blue (c) values derived from photograph analysis of *Xenia umbellata* colonies exposed to high nitrate eutrophication (37 μM) and gradual warming (HN + W) throughout the experiment. Error bars represent standard deviations of three replicates. Dashed lines represent linear regression line, where $R > 0.5$ indicates correlation between colour value and day of the experiment. Values were used to identify five colour scores (Table S2.2).

Supplementary tables to chapter 2

Table S2.1. Water quality parameters of experimental tanks per treatment during the experiment. Mean values \pm standard deviations for all tanks and measurements. Nitrate concentrations were measured two to three hours after nitrate enrichment to 6 μM (medium) and 37 μM (high).

Variable	LN	LN + W	MN + W	HN + W	n
NO_3 (μM)	0.30 ± 0.42	0.51 ± 0.67	2.33 ± 1.47	23.40 ± 12.54	33
PAR ($\mu\text{mol m}^{-2} \text{s}^{-1}$)	103.5 ± 7.0	112.8 ± 9.6	108.3 ± 10.3	98.2 ± 10.1	9
O_2 (mg L^{-1})	6.3 ± 0.8	6.2 ± 0.8	6.3 ± 1.1	6.6 ± 1.3	111
Salinity (‰)	35.4 ± 0.7	35.2 ± 0.5	34.8 ± 0.5	35.1 ± 0.4	111
pH	8.52 ± 0.49	8.54 ± 0.36	8.53 ± 0.28	8.60 ± 0.54	111
NO_2 (mg L^{-1})	<0.01	<0.01	<0.01	0.03 ± 0.09	111
KH	6.9 ± 1.1	6.7 ± 1.0	6.8 ± 1.0	6.6 ± 1.3	30
NH_4 (mg L^{-1})	Always below detection limit (<0.05)				30
PO_4 (μM)	Always below detection limit (<0.21)				30
SiO_4 (mg L^{-1})	0.36 ± 0.26	0.43 ± 0.27	0.27 ± 0.18	0.37 ± 0.39	30
Mg (mg L^{-1})	1316 ± 204	1312 ± 162	1316 ± 170	1352 ± 193	30
Ca (mg L^{-1})	401 ± 24	401 ± 23	387 ± 21	388 ± 21	30

Table S2.2. Definitions of colour scores by #HEX codes and red, green, and blue (RGB) values.

Score	1	2	3	4	5
#HEX code	#b69482	#b39e92	#b0a8a2	#bdb2b2	#abbd3
Red	182	179	176	173	171
Green	148	158	168	178	189
Blue	130	146	162	178	195

12	MN+W	22	100	51.6	13-19	0.00	22	-23.6	48.6	NA	NA	NA	NA	NA	NA	NA	NA	NA
1	MN+W	28	100	42.2	20-30	-0.70	29	-37.3	63.2	NA	NA	NA	NA	NA	NA	NA	NA	NA
2	HN+W	28	100	15.8	20-30	-0.48	29	-33.1	73.1	NA	NA	NA	NA	NA	NA	NA	NA	NA
3	LN+W	28	100	44.4	20-30	-0.18	29	-33.9	54.3	NA	NA	NA	NA	NA	NA	NA	NA	NA
4	LN	28	100	40.9	20-30	-0.15	29	-28.2	63.2	NA	NA	NA	NA	NA	NA	NA	NA	NA
5	LN	28	100	46.7	20-30	0.09	29	-11.8	41.6	NA	NA	NA	NA	NA	NA	NA	NA	NA
6	LN+W	28	100	36.0	20-30	0.33	29	-23.3	45.8	NA	NA	NA	NA	NA	NA	NA	NA	NA
7	MN+W	28	100	39.1	20-30	0.06	29	-41.7	75.2	NA	NA	NA	NA	NA	NA	NA	NA	NA
8	HN+W	28	100	11.3	20-30	-0.79	29	-39.6	85.1	NA	NA	NA	NA	NA	NA	NA	NA	NA
9	HN+W	28	78	7.6	20-30	-0.30	29	-30.0	67.9	NA	NA	NA	NA	NA	NA	NA	NA	NA
10	LN	28	100	46.9	20-30	0.06	29	-34.8	64.4	NA	NA	NA	NA	NA	NA	NA	NA	NA
11	LN+W	28	100	42.9	20-30	-0.24	29	-38.8	92.8	NA	NA	NA	NA	NA	NA	NA	NA	NA
12	MN+W	28	100	48.2	20-30	-0.12	29	-34.0	100.1	NA	NA	NA	NA	NA	NA	NA	NA	NA
1	MN+W	36	100	0.0	31-37	-0.45	37	-34.4	48.4	37	196670	7.6E-06	1	9.21	38.49	4.18	7.50	-22.55
2	HN+W	36	78	0.0	31-37	-10.64	37	-25.3	42.8	37	354903	6.0E-06	5	8.69	41.29	4.75	8.74	-22.95
3	LN+W	36	100	36.0	31-37	0.47	37	-49.3	60.5	37	150581	7.5E-06	1	10.56	35.33	3.35	7.50	-22.86
4	LN	36	100	46.0	31-37	0.15	37	-37.4	67.3	37	286436	3.2E-06	1	10.33	32.15	3.11	7.25	-22.13
5	LN	36	100	47.3	31-37	-0.03	37	-42.5	64.2	37	179948	4.0E-06	2	11.95	37.37	3.13	6.70	-22.74
6	LN+W	36	100	32.2	31-37	0.20	37	-50.8	52.9	37	197067	5.1E-06	2	10.34	39.62	3.83	7.12	-23.40
7	MN+W	36	100	0.0	31-37	-0.63	37	-30.2	24.2	37	167212	7.9E-06	1	9.48	35.52	3.75	7.60	-23.31
8	HN+W	36	78	0.0	31-37	-2.68	37	-46.4	55.0	37	300809	6.6E-06	5	8.44	38.04	4.51	9.29	-21.85
9	HN+W	36	67	0.0	31-37	-8.28	37	-36.0	85.8	37	325500	9.4E-06	5	6.72	35.01	5.21	8.57	-21.47
10	LN	36	100	34.4	31-37	-0.09	37	-31.5	53.0	37	255289	5.0E-06	1	12.02	34.81	2.90	6.40	-24.05
11	LN+W	36	100	1.6	31-37	0.25	37	-50.2	99.8	37	288208	3.0E-06	1	NA	NA	NA	NA	NA
12	MN+W	36	100	0.0	31-37	-0.04	37	-42.3	55.8	37	277291	3.8E-06	3	10.02	31.91	3.19	7.68	-21.87

Supplementary material to chapter 3

Supplementary tables to chapter 3

Table S3.1. Raw data for Fig. 3.1, Fig. 3.2, and Fig. 3.3.

Phosphate treatment	Tank	Time (day)	Pulsation rate (beats/minute)	Symbiodiniaceae density (cells/mg host dry weight)	Cellular chlorophyll a concentration ($\mu\text{g}/\text{algal cell}$)
control	4	0	36.44	4.06E+04	2.981E-05
control	6	0	34.89	5.24E+04	2.719E-05
control	11	0	36.67	1.96E+04	5.15E-05
low	2	0	35.78	2.73E+04	3.673E-05
low	8	0	36.22	5.60E+04	2.948E-05
low	9	0	36.67	9.02E+04	1.822E-05
medium	3	0	35.11	8.56E+04	1.271E-05
medium	7	0	32.44	9.03E+04	1.698E-05
medium	12	0	37.56	5.43E+04	1.8E-05
high	1	0	37.11	4.31E+04	1.895E-05
high	5	0	35.33	7.99E+04	1.516E-05
high	10	0	35.78	6.37E+04	1.858E-05
control	4	7	42.44	NA	NA
control	6	7	43.11	NA	NA
control	11	7	41.78	NA	NA
low	2	7	46.22	NA	NA
low	8	7	40.89	NA	NA
low	9	7	41.56	NA	NA
medium	3	7	45.33	NA	NA
medium	7	7	40.67	NA	NA
medium	12	7	44.89	NA	NA
high	1	7	43.11	NA	NA
high	5	7	42.67	NA	NA
high	10	7	43.56	NA	NA
control	4	14	44.44	5.09E+04	2.012E-05
control	6	14	41.33	7.81E+04	1.256E-05
control	11	14	40.89	4.19E+04	1.925E-05
low	2	14	45.56	4.98E+04	1.106E-05
low	8	14	40.89	5.08E+04	2.208E-05
low	9	14	43.11	9.86E+04	9.221E-06
medium	3	14	44.89	5.19E+04	9.297E-06
medium	7	14	41.78	3.73E+04	1.981E-05
medium	12	14	44.00	4.79E+04	1.36E-05
high	1	14	42.22	9.42E+04	5.549E-06
high	5	14	44.89	8.36E+04	7.576E-06
high	10	14	46.89	3.11E+04	3.285E-05
control	4	21	46.44	NA	NA
control	6	21	43.78	NA	NA
control	11	21	43.33	NA	NA
low	2	21	48.00	NA	NA
low	8	21	46.89	NA	NA
low	9	21	42.89	NA	NA
medium	3	21	49.33	NA	NA
medium	7	21	45.11	NA	NA
medium	12	21	48.89	NA	NA
high	1	21	47.78	NA	NA
high	5	21	48.44	NA	NA
high	10	21	47.33	NA	NA
control	4	28	48.00	NA	NA
control	6	28	44.44	NA	NA
control	11	28	43.56	NA	NA
low	2	28	48.44	NA	NA
low	8	28	46.44	NA	NA
low	9	28	47.56	NA	NA
medium	3	28	49.56	NA	NA
medium	7	28	49.33	NA	NA
medium	12	28	52.00	NA	NA
high	1	28	51.33	NA	NA
high	5	28	50.67	NA	NA
high	10	28	50.44	NA	NA
control	4	35	39.33	5.93E+04	1.27E-05
control	6	35	38.67	1.13E+05	3.851E-06
control	11	35	40.89	1.06E+05	5.191E-06
low	2	35	32.89	5.44E+04	1.453E-05
low	8	35	41.00	1.09E+05	1.115E-05
low	9	35	42.12	2.52E+05	4.191E-06
medium	3	35	35.33	1.65E+05	4.003E-06
medium	7	35	40.67	1.44E+05	5.736E-06
medium	12	35	44.22	9.49E+04	1.154E-05
high	1	35	43.33	5.12E+04	2.055E-05
high	5	35	47.78	1.22E+05	6.819E-06
high	10	35	41.11	9.95E+04	9.412E-06

Supplementary material to chapter 4

Supplementary figures to chapter 4

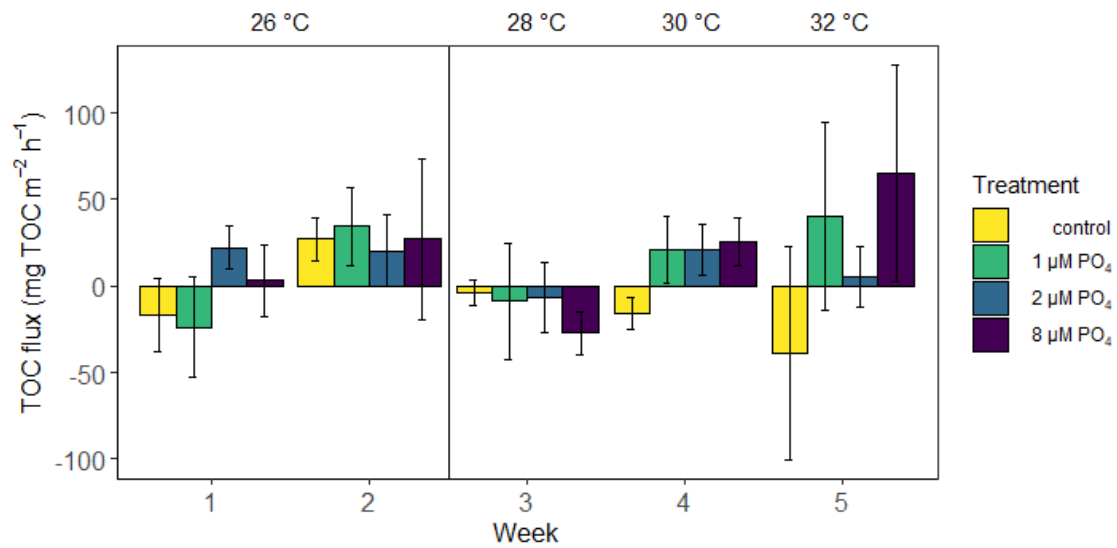


Figure S4.1. TOC fluxes of *Xenia umbellata* colonies under experimental conditions: only temperature increase without PO₄ addition (control), 1 μM PO₄ + temperature increased from week 3 onwards (1 μM PO₄), 2 μM PO₄ + temperature increased (2 μM PO₄), and 8 μM PO₄ + temperature increased (8 μM PO₄). Error bars represent standard errors. The vertical line indicates the start of the temperature treatment and the average temperature for all tanks for the different time points is given on top of the graph.

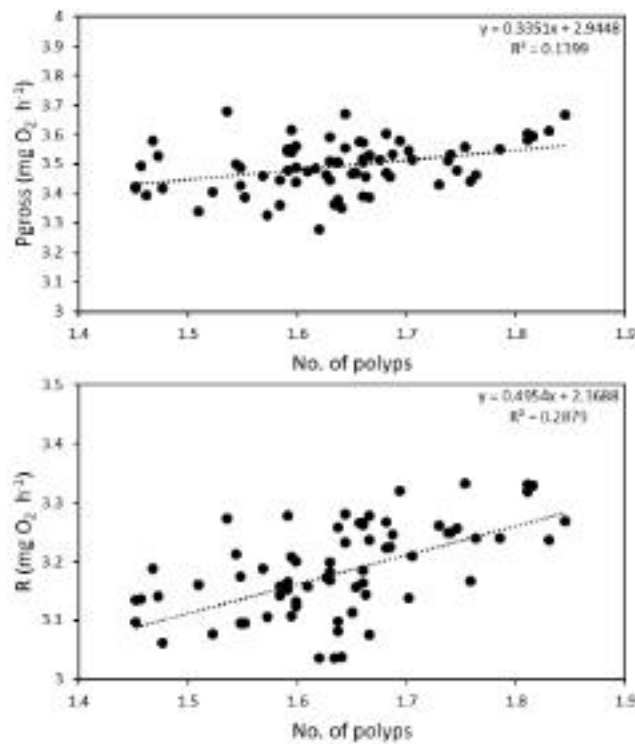


Figure S4.2. Correlation of log-transformed oxygen fluxes and number of polyps in *Xenia umbellata* colonies including all treatments.

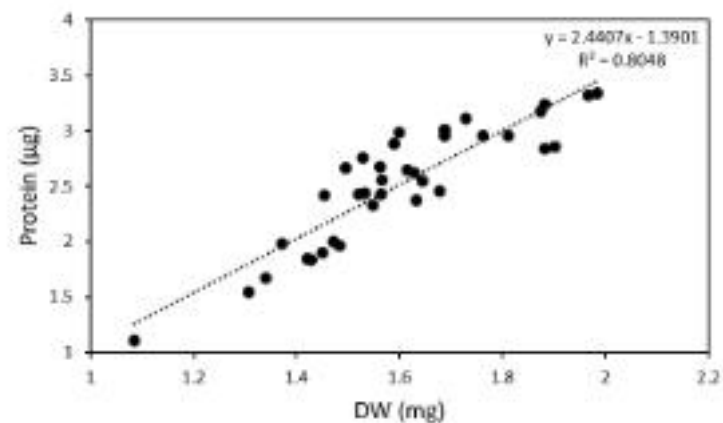


Figure S4.3. Correlation of log-transformed protein content and dry weight in *Xenia umbellata* colonies including all treatments.

Supplementary tables to chapter 4

Table S4.1. Experimental studies on effects of phosphate enrichment (PO₄) and temperature increase (Temp.) on hard corals in comparison to the present study. Only parameters similar to the ones measured in the present study were summarized. N = nitrogen source, P = phosphate source, P_{gross} = gross photosynthesis, P_{net} = net photosynthesis, R = dark respiration, P/R = photosynthesis to respiration ratio.

Study	Duration	Treatment	Coral species	Parameter	Effect
EUTROPHICATION EXPERIMENTS					
Ferrier-Pagès et al. 2000 ¹	9 weeks	2 µM PO ₄	<i>Stylophora pistillata</i>	growth	Decrease (- 60 %)
				P _{gross}	Increase (+ 100 %)
				R	Increase (+ 59 %)
				P/R	Increase (+ 47 %)
Koop et al. 2001 ²	406 days	20 µM Ammonium and/or 4µM PO ₄	<i>Stylophora pistillata</i>	P _{gross}	P: decrease (- 19 %) N+P: decrease (- 14 %)
				R	n.s.
Stambler et al. 1991 ³	28 days	0.5 and 2 µM PO ₄	<i>Pocillopora damicornis</i>	Protein	n.s.
Tanaka et al. 2017 ⁴	2 months	Nitrate: 1.4-1.9 µM PO ₄ : 0.1 µM	<i>Montipora digitata</i>	Symbiont C content	N: n.s. N+P: Increase (+ 48 %)
				Symbiont N content	N: Increase (NA) N+P: Increase (NA)
				Host C + N content	n.s.
				Host and Symbiont δ ¹³ C	N: Decrease (Host: - 6 %, Symbiont: - 5 %) N+P: n.s.
Hoegh-Guldberg et al. 2004 ⁵	406 days	20 µM Ammonium and/or 4µM PO ₃ ²⁺	<i>Heliofungia actiniformis</i>	Host δ ¹⁵ N	P: Decrease (- 68 %) N+P: Decrease (- 47 %)
				Symbiont δ ¹⁵ N	P: n.s. N+P: Decrease (- 55 %)
				δ ¹³ C	n.s.
			<i>Pocillopora damicornis</i>	Host δ ¹⁵ N	P: n.s. N+P: Decrease (- 55 %)
				Symbiont δ ¹⁵ N	P: n.s. N+P: Decrease (- 73 %)
				δ ¹³ C	n.s.
Silbiger et al. 2018 ⁶	6 weeks	medium (3.6 µmol l ⁻¹ DIN + 1.08 µmol l ⁻¹ PO ₄)	<i>Porites compressa</i>	R	Medium: Increase (+ 7 %)

); high (7.61 $\mu\text{mol l}^{-1}$ DIN + 2.6 $\mu\text{mol l}^{-1}$ PO ₄)	and <i>Montipora</i> <i>capitata</i>	High: Increase (+ 51 %)
TEMPERATURE EXPERIMENTS				
Krueger et al. 2017 ⁷	6 weeks	1-2 °C	<i>Stylophora</i> <i>pistillata</i>	P _{net} Protein Increase (+ 44 %) n.s.
Schlöder and D'Croz 2004 ⁸	30 days	1 °C	<i>Pocillopora</i> <i>damicornis</i> <i>Porites lobata</i>	Protein Protein n.s. n.s.
Gibbin et al. 2018 ⁹	7 days	2.5 °C	<i>Pocillopora</i> <i>damicornis</i>	P _{gross} R Protein $\delta^{13}\text{C}$ $\delta^{15}\text{N}$ n.s. n.s. n.s. Warm-acclimated: increase in coral gastrodermis (14 %) Warm-acclimated: decrease in coral gastrodermis (- 81 %)
Grover et al. 2011 ¹⁰	10 days	3 °C and 7°C	<i>Stylophora</i> <i>pistillata</i>	Protein P _{gross} R 3/7 °C: n.s. 3 °C: n.s. 7 °C: -200 % 3/7 °C: n.s.
Rodrigues and Grottoli 2006 ¹¹	1 month	3 °C	<i>Montipora</i> <i>capitata</i> <i>Porites</i> <i>compressa</i>	$\delta^{13}\text{C}$ (host) $\delta^{13}\text{C}$ (symbiont) $\delta^{15}\text{N}$ $\delta^{13}\text{C}$ $\delta^{15}\text{N}$ n.s. decrease (- 2 ‰) n.s. n.s. n.s.
Rodrigues and Grottoli 2007 ¹²	1 month	3 °C	<i>Montipora</i> <i>capitata</i> <i>Porites</i> <i>compressa</i>	Protein P _{gross} R Protein P _{gross} R n.s. Decrease (- 67 %) Decrease (- 45 %) Decrease (- 36 %) n.s. n.s.
Nyström et al. 2001 ¹³	24 h	4 °C	<i>Porites</i> <i>cylindrica</i>	P _{gross} R Decrease (- 50 %) Decrease (- 57 %)
Bahr et al. 2018 ¹⁴	1 day	4 °C	<i>Montipora</i> <i>capitata</i> <i>Pocillopora</i> <i>damicornis</i> <i>Leptastrea</i> <i>purpurea</i>	P _{net} R P/R P _{net} R P/R P _{net} R P/R n.s. n.s. Decrease (- 23 %) n.s. Increase (+ 40 %) Decrease (- 32 %) Decrease (- 27 %) n.s. Decrease (- 39 %)
Hoadley et al. 2015 ¹⁵	24 days	5 °C	<i>Acropora</i> <i>millepora</i> <i>Pocillopora</i> <i>damicornis</i> <i>Montipora</i> <i>monasteriata</i> <i>Turbinaria</i> <i>reniformis</i>	Protein Fv/Fm P/R R Protein Fv/Fm P/R R Protein Fv/Fm P/R R Protein Fv/Fm P/R R Decrease (- 31 %) Decrease (- 14 %) n.s. n.s. n.s. Decrease (- 10 %) n.s. Increased (+ 47 %) Decrease (- 28 %) Decrease (- 15 %) n.s. Increased (+ 62 %) Increase (+ 83 %) n.s. Increased (+ 31 %)
Petrou et al. 2018 ¹⁶	12 days	5 °C	<i>Acropora</i> <i>millepora</i>	Fv/Fm Significant decrease from day 9 onwards (- 35 %)
Béraud et al. 2013 ¹⁷	7 days	5 °C	<i>Turbinaria</i> <i>reniformis</i>	Protein P _{gross} R $\delta^{13}\text{C}$ $\delta^{15}\text{N}$ n.s. - 100 % + 64 % n.s. n.s.
Courtial et al. 2017 ¹⁸	5 weeks	5 °C	<i>Pocillopora</i> <i>damicornis</i>	Protein P _{net} Decrease (- 60 %) n.s.

				R	n.s.
			<i>Turbinaria reniformis</i>	Protein	n.s.
				P _{net}	n.s.
				R	n.s.
Ferrier-Pagès et al. 2010 ¹⁹	5 days	5 °C	<i>Stylophora pistillata</i>	Fv/Fm	Decrease (- 18 %)
				P _{gross}	Decrease (- 60 %)
				R	Decrease (- 33 %)
			<i>Turbinaria reniformis</i>	Fv/Fm	Decrease (- 11 %)
				P _{gross}	Decrease (- 75 %)
				R	Decrease (- 66 %)
			<i>Galaxea fascicularis</i>	Fv/Fm	Decrease (- 33 %)
				P _{gross}	Decrease (- 51 %)
				R	Decrease (- 33 %)
Baker et al. 2018 ²⁰	10 days	5 °C	<i>Orbicella faveolata</i> (shallow samples)	% C content	Host: Decrease (- 15 %)
					Symbiont: n.s.
				δ ¹⁵ N (host)	n.s.
				δ ¹⁵ N (symbiont)	Increase (+ 32 %)
				δ ¹³ C (host)	n.s.
				δ ¹³ C (symbiont)	Increase (+ 14 %)
Hoogenboom et al. 2012 ²¹	10-13 days	6 °C	<i>Stylophora pistillata</i>	P _{gross} (unfed)	Decrease (- 47 %)
				P _{gross} (fed)	n.s.
				R	n.s.
			<i>Turbinaria reniformis</i>	P _{gross} (unfed)	Decrease (- 39 %)
				P _{gross} (fed)	n.s.
				R	n.s.
Grottoli et al. 2017 ²²	37 days	6 °C	<i>Stylophora pistillata</i>	Protein	n.s.
				δ ¹³ C (host)	Increase (+ 2 ‰)
			<i>Pocillopora damicornis</i>	Protein	n.s.
				δ ¹³ C (host)	n.s.
			<i>Favia fava</i>	Protein	Decrease (- 48 %)
				δ ¹³ C (host)	Increase (+ 2 ‰)
COMBINED EXPERIMENTS					
Hall et al. 2018 ²³	30 days	5 °C Nutrients: nitrate+nitrite (1µM)+PO ₄ (0.0625 µM)	<i>Stylophora pistillata</i>	Fv/Fm	Temp.: decrease (NA) Nutrients: n.s. Comb.: n.s.
				P _{net}	Temp.: n.s. Nutrients: decrease (- 34 %) Comb.: n.s.
				R	n.s.
				Protein	Temp.: n.s. Nutrients: decrease (- 24 %) Comb.: n.s.
Ezzat et al. 2016 ²⁴	4 weeks eutrophication, 10 days warming	DIP: 2µM Temp.: 5 °C	<i>Pocillopora damicornis</i>	R	DIP: - 50 % Temp.: + 25 % Comb.: + 44 %
				P _{gross}	DIP: n.s. Temp.: - 50 % Comb.: - 50 %
Present study	5 weeks, Temp.: 3 weeks	PO ₄ : 1,2,8 µM Temp.: 6 °C	<i>Xenia umbellata</i>	P _{gross}	n.s.
				R	n.s.
				P/R	n.s.
				Protein	Temp.: decrease (- 62 %)
				δ ¹³ C	Temp.: Decrease (- 6.9 %)
				δ ¹⁵ N	Temp.: Decrease (- 10 %)

Table S4.2. Raw data for Fig. 4.2,4.3 & 4.4.

Sample ID	Treatment	Week	net Photosynthesis	Respiration	gross Photosynthesis	mean polyp count	DW (mg)	Protein ($\mu\text{g mg DW}^{-1}$)	$\delta^{15}\text{N}$	% N	$\delta^{13}\text{C}$	% C	C/N ratio
T1	highP	0	49.81	-19.13	68.94	47.33	74.96	20.09	8.35	3.02	-22.63	34.16	11.32
T10	highP	0	22.67	-34.22	56.89	37.33	96.53	22.58	7.85	2.90	-21.23	30.09	10.38
T11	control	0	44.70	-42.21	86.91	35.33	33.81	16.71	7.89	2.85	-20.03	28.57	10.03
T12	midP	0	32.23	-40.00	72.23	45.67	38.90	19.66	8.73	3.30	-21.08	37.34	11.30
T2	lowP	0	40.56	-35.83	76.40	33.33	39.84	24.27	7.81	3.10	-22.25	33.95	10.94
T3	midP	0	40.19	-35.21	75.40	35.33	31.34	14.69	7.62	3.23	-22.41	36.14	11.19
T4	control	0	35.07	-37.54	72.61	38.33	92.46	22.74	7.61	3.22	-22.32	37.33	11.59
T5	highP	0	15.97	-34.00	49.98	53.67	48.70	18.35	7.94	3.03	-22.30	34.97	11.52
T6	control	0	22.93	-44.77	67.71	32.33	53.69	23.97	7.12	3.37	-22.12	36.57	10.86
T7	midP	0	25.89	-37.87	63.76	56.67	57.96	15.49	7.14	3.09	-21.17	34.83	11.28
T8	lowP	0	48.64	-38.38	87.01	30.00	48.81	21.15	7.23	3.07	-20.99	32.62	10.63
T9	lowP	0	76.55	-52.60	129.15	29.33	76.28	22.70	5.72	3.42	-21.47	36.70	10.74
T1	highP	1	27.12	-32.37	59.49	54.67	NA	NA	NA	NA	NA	NA	NA
T10	highP	1	27.09	-25.68	52.77	46.33	NA	NA	NA	NA	NA	NA	NA
T11	control	1	35.43	-37.26	72.69	46.33	NA	NA	NA	NA	NA	NA	NA
T12	midP	1	36.72	-33.48	70.20	45.67	NA	NA	NA	NA	NA	NA	NA
T2	lowP	1	35.03	-34.14	69.17	39.67	NA	NA	NA	NA	NA	NA	NA
T3	midP	1	39.86	-37.49	77.35	39.00	NA	NA	NA	NA	NA	NA	NA
T4	control	1	29.55	-35.56	65.10	42.67	NA	NA	NA	NA	NA	NA	NA
T5	highP	1	24.60	-34.62	59.22	48.33	NA	NA	NA	NA	NA	NA	NA
T6	control	1	38.22	-35.28	73.51	40.67	NA	NA	NA	NA	NA	NA	NA
T7	midP	1	27.49	-32.63	60.13	65.33	NA	NA	NA	NA	NA	NA	NA
T8	lowP	1	55.27	-32.60	87.87	39.33	NA	NA	NA	NA	NA	NA	NA
T9	lowP	1	60.90	-47.78	108.68	28.67	NA	NA	NA	NA	NA	NA	NA
T1	highP	2	42.46	-27.26	69.71	50.33	64.89	13.96	7.44	2.64	-23.07	34.14	12.93
T10	highP	2	26.56	-25.01	51.57	43.67	28.40	9.29	6.44	2.69	-22.90	30.80	11.44
T11	control	2	45.11	-28.94	74.05	43.33	36.45	12.95	7.41	2.95	-21.87	33.63	11.41
T12	midP	2	33.62	-31.87	65.50	45.00	79.63	9.05	7.15	2.66	-21.42	32.09	12.05
T2	lowP	2	19.40	-26.10	45.50	41.67	34.12	7.96	8.17	2.37	-22.16	27.07	11.43
T3	midP	2	33.37	-34.88	68.25	35.67	36.70	7.22	7.28	2.75	-22.58	33.38	12.14
T4	control	2	28.39	-25.29	53.68	43.00	36.78	9.79	7.99	NA	-22.36	NA	11.41
T5	highP	2	22.53	-25.61	48.14	57.33	42.59	9.66	7.04	3.10	-22.48	33.98	10.95
T6	control	2	36.40	-29.10	65.50	44.67	76.26	8.97	7.09	2.42	-21.32	29.00	12.00
T7	midP	2	35.06	-25.44	60.50	67.67	47.71	5.98	7.17	2.65	-22.59	32.07	12.12
T8	lowP	2	49.89	-23.89	73.78	41.33	33.12	8.10	7.69	2.62	-22.81	30.71	11.73
T9	lowP	2	52.51	-32.58	85.09	29.00	41.23	10.79	7.86	2.83	-21.65	33.61	11.88
T1	highP	3	29.64	-32.23	61.87	55.00	NA	NA	NA	NA	NA	NA	NA
T10	highP	3	22.11	-31.86	53.98	45.67	NA	NA	NA	NA	NA	NA	NA
T11	control	3	31.92	-41.75	73.67	43.33	NA	NA	NA	NA	NA	NA	NA
T12	midP	3	41.79	-40.32	82.11	45.67	NA	NA	NA	NA	NA	NA	NA
T2	lowP	3	23.39	-36.25	59.64	38.33	NA	NA	NA	NA	NA	NA	NA
T3	midP	3	36.58	-41.60	78.18	37.00	NA	NA	NA	NA	NA	NA	NA
T4	control	3	41.31	-34.55	75.86	42.67	NA	NA	NA	NA	NA	NA	NA
T5	highP	3	20.24	-29.96	50.20	58.00	NA	NA	NA	NA	NA	NA	NA
T6	control	3	26.72	-34.78	61.50	48.00	NA	NA	NA	NA	NA	NA	NA
T7	midP	3	26.82	-32.23	59.06	64.67	NA	NA	NA	NA	NA	NA	NA
T8	lowP	3	44.14	-33.55	77.68	39.67	NA	NA	NA	NA	NA	NA	NA
T9	lowP	3	48.35	-44.14	92.49	28.33	NA	NA	NA	NA	NA	NA	NA
T1	highP	4	32.14	-40.89	73.03	46.33	NA	NA	NA	NA	NA	NA	NA
T10	highP	4	32.10	-30.26	62.35	46.00	NA	NA	NA	NA	NA	NA	NA
T11	control	4	42.62	-38.71	81.32	44.00	NA	NA	NA	NA	NA	NA	NA
T12	midP	4	42.45	-40.69	83.14	45.33	NA	NA	NA	NA	NA	NA	NA
T2	lowP	4	51.47	-39.99	91.46	39.67	NA	NA	NA	NA	NA	NA	NA
T3	midP	4	43.51	-46.58	90.09	35.00	NA	NA	NA	NA	NA	NA	NA
T4	control	4	33.31	-35.15	68.46	42.33	NA	NA	NA	NA	NA	NA	NA
T5	highP	4	21.83	-32.38	54.21	55.67	NA	NA	NA	NA	NA	NA	NA
T6	control	4	33.80	-36.11	69.90	48.67	NA	NA	NA	NA	NA	NA	NA

T7	midP	4	28.76	-33.13	61.89	64.67	NA	NA	NA	NA	NA	NA	NA
T8	lowP	4	52.72	-36.51	89.23	39.00	NA	NA	NA	NA	NA	NA	NA
T9	lowP	4	45.67	-48.19	93.86	28.33	NA	NA	NA	NA	NA	NA	NA
T1	highP	5	34.60	-42.30	76.90	49.33	20.31	1.74	6.34	2.42	-22.62	27.62	11.41
T10	highP	5	27.35	-27.88	55.24	43.33	26.85	2.54	6.79	3.35	-23.16	37.93	11.31
T11	control	5	62.98	-43.33	106.31	44.00	21.87	2.16	6.56	3.03	-22.42	32.59	10.76
T12	midP	5	45.14	-38.56	83.70	48.00	42.84	5.46	6.76	3.13	-23.72	34.66	11.06
T2	lowP	5	42.58	-48.49	91.07	39.00	12.16	1.04	6.37	2.99	-24.07	33.51	11.20
T3	midP	5	84.54	-54.60	139.13	34.33	26.35	2.63	6.59	2.84	-22.95	32.04	11.28
T4	control	5	54.56	-36.99	91.55	42.67	35.28	5.98	6.66	3.28	-23.09	36.85	11.23
T5	highP	5	29.75	-28.48	58.23	61.00	30.44	3.01	7.18	2.87	-23.77	32.18	11.22
T6	control	5	32.42	-31.97	64.39	50.67	44.16	7.98	7.72	3.09	-22.75	34.68	11.22
T7	midP	5	40.03	-26.51	66.53	70.00	29.60	3.35	6.31	2.97	-23.79	31.04	10.47
T8	lowP	5	64.07	-41.05	105.12	39.33	28.24	2.81	7.73	3.19	-23.24	35.80	11.22
T9	lowP	5	66.96	-46.64	113.61	29.67	23.53	4.04	7.02	3.29	-23.48	40.05	12.17

Supplementary references to chapter 4

1. Ferrier-Pagès, C., Gattuso, J. P., Dallot, S. & Jaubert, J. Effect of nutrient enrichment on growth and photosynthesis of the zooxanthellate coral *Stylophora pistillata*. *Coral Reefs* **19**, 103–113 (2000).
2. Koop, K. *et al.* ENCORE: the effect of nutrient enrichment on coral reefs. synthesis of results and conclusions. *Mar. Pollut. Bull.* **42**, 91–120 (2001).
3. Stambler, N., Popper, N., Dubinsky, Z. & Stimson, J. Effects of nutrient enrichment and water motion on the coral *Pocillopora damicornis*. *Pacific Sci.* **45**, 299–307 (1991).
4. Tanaka, Y., Grottoli, A. G., Matsui, Y., Suzuki, A. & Sakai, K. Effects of nitrate and phosphate availability on the tissues and carbonate skeleton of scleractinian corals. *Mar. Ecol. Prog. Ser.* **570**, 101–112 (2017).
5. Hoegh-Guldberg, O., Muscatine, L., Goiran, C., Siggaard, D. & Marion, G. Nutrient-induced perturbations to $\delta^{13}\text{C}$ and $\delta^{15}\text{N}$ in symbiotic dinoflagellates and their coral hosts. *Mar. Ecol. Prog. Ser.* **280**, 105–114 (2004).
6. Silbiger, N. J. *et al.* Nutrient pollution disrupts key ecosystem functions on coral reefs. *Proc. R. Soc. B Biol. Sci.* **285**, (2018).
7. Krueger, T. *et al.* Common reef-building coral in the Northern Red Sea resistant to elevated temperature and acidification. *R. Soc. Open Sci.* **4**, 170038 (2017).
8. Schlöder, C. & D’Croz, L. Responses of massive and branching coral species to the combined effects of water temperature and nitrate enrichment. *J. Exp. Mar. Bio. Ecol.* **313**, 255–268 (2004).
9. Gibbin, E. M. *et al.* Short-term thermal acclimation modifies the metabolic condition of the coral holobiont. *Front. Mar. Sci.* **5**, (2018).
10. Grover, R. *et al.* Coral uptake of inorganic phosphorus and nitrogen negatively affected by simultaneous changes in temperature and pH. *PLoS One* **6**, 1–10 (2011).
11. Rodrigues, L. J. & Grottoli, A. G. Calcification rate and the stable carbon, oxygen, and nitrogen isotopes in the skeleton, host tissue, and zooxanthellae of bleached and recovering Hawaiian corals. *Geochim. Cosmochim. Acta* **70**, 2781–2789 (2006).
12. Rodrigues, L. J. & Grottoli, A. G. Energy reserves and metabolism as indicators of coral recovery from bleaching. *Limnol. Oceanogr.* **52**, 1874–1882 (2007).
13. Nyström, M., Nordemar, I. & Tedengren, M. Simultaneous and sequential stress from increased temperature and copper on the metabolism of the hermatypic coral *Porites cylindrica*. *Mar. Biol.* **138**, 1225–1231 (2001).
14. Bahr, K. D., Rodgers, K. S. & Jokiel, P. L. Ocean warming drives decline in coral metabolism while acidification highlights species-specific responses. *Mar. Biol. Res.* **14**, 924–935 (2018).

15. Hoadley, K. D. *et al.* Physiological response to elevated temperature and pCO₂ varies across four Pacific coral species: understanding the unique host+symbiont response. *Nat. Publ. Gr.* **5**, 1–15 (2015).
16. Petrou, K., Nielsen, D. A. & Heraud, P. Single-cell biomolecular analysis of coral algal symbionts reveals opposing metabolic responses to heat stress and expulsion. *Front. Mar. Sci.* **5**, 110 (2018).
17. Béraud, E., Gevaert, F., Rottier, C. & Ferrier-Pagès, C. The response of the scleractinian coral *Turbinaria reniformis* to thermal stress depends on the nitrogen status of the coral holobiont. *J. Exp. Biol.* **216**, 2665–2674 (2013).
18. Courtial, L., Roberty, S., Shick, J. M., Houlbrèque, F. & Ferrier-Pagès, C. Interactive effects of ultraviolet radiation and thermal stress on two reef-building corals. *Limnol. Oceanogr.* **62**, 1000–1013 (2017).
19. Ferrier-Pagès, C., Rottier, C., Beraud, E. & Levy, O. Experimental assessment of the feeding effort of three scleractinian coral species during a thermal stress: effect on the rates of photosynthesis. *J. Exp. Mar. Bio. Ecol.* **390**, 118–124 (2010).
20. Baker, D. M., Freeman, C. J., Wong, J. C. Y., Fogel, M. L. & Knowlton, N. Climate change promotes parasitism in a coral symbiosis. *ISME J.* **12**, 921–930 (2018).
21. Hoogenboom, M. O., Campbell, D. A., Beraud, E., DeZeeuw, K. & Ferrier-Pagès, C. Effects of light, food availability and temperature stress on the function of photosystem II and photosystem I of coral symbionts. *PLoS One* **7**, (2012).
22. Grottoli, A. G., Tchernov, D. & Winters, G. Physiological and biogeochemical responses of super-corals to thermal stress from the Northern Gulf of Aqaba, Red Sea. *Front. Mar. Sci.* **4**, (2017).
23. Hall, E. R. *et al.* Eutrophication may compromise the resilience of the Red Sea coral *Stylophora pistillata* to global change. *Mar. Pollut. Bull.* **131**, 701–711 (2018).
24. Ezzat, L., Maguer, J.-F. F., Grover, R. & Ferrier-Pagès, C. Limited phosphorus availability is the Achilles heel of tropical reef corals in a warming ocean. *Sci. Rep.* **6**, 1–11 (2016).

Supplementary material to chapter 5

Supplementary figures to chapter 5

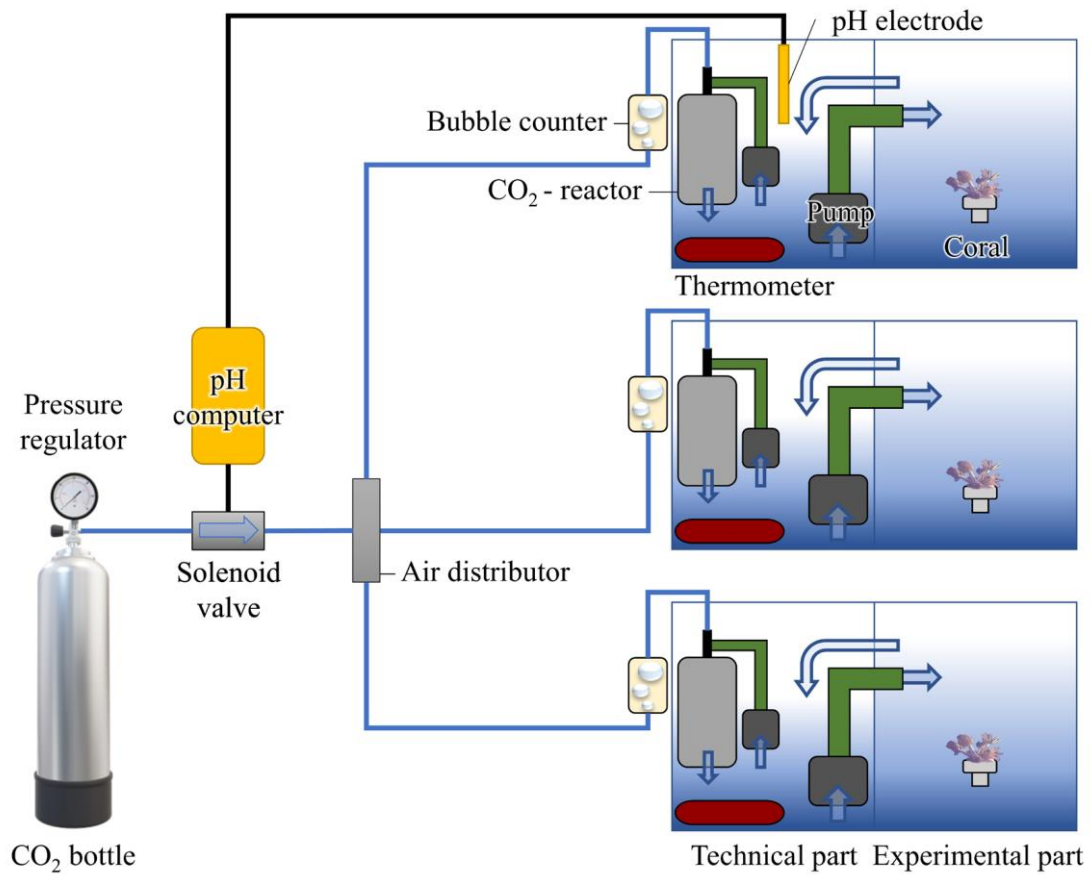


Figure S5.1 Overview of the acidification setup. A total of two of these setups acidified the water of six tanks.

Supplementary tables to chapter 5

Table S5.1. Raw data for [Fig. 5.1-5.5](#).

Tank_ID	Treatment	Day	Fig. 5.1 Pulsation (beats min ⁻¹)			Fig. 5.2 Polyp count			Fig. 5.2 Colouration			Fig. 5.4 Oxygen flux (μg cm ⁻² h ⁻¹)			Fig. 5.3 Symbiodiniaceae		Fig. 5.5 Element and isotope composition				
			Rep. 1	Rep. 2	Rep. 3	Rep. A	Rep. B	Rep. C	Red	Green	Blue	R	Pnet	Pgross	Cell density (x10 ⁶ cell s cm ⁻²)	Chl a (pg/cell)	d ¹⁵ N	d ¹³ C	% N	% C	C:N
1	Control	0	NA	NA	NA	44	59	53	NA	NA	NA	NA	NA	NA	NA	NA	NA	NA	NA	NA	NA
2	OA	0	NA	NA	NA	33	35	43	NA	NA	NA	NA	NA	NA	NA	NA	NA	NA	NA	NA	NA
3	OA	0	NA	NA	NA	42	50	45	NA	NA	NA	NA	NA	NA	NA	NA	NA	NA	NA	NA	NA
4	Control	0	NA	NA	NA	30	50	41	NA	NA	NA	NA	NA	NA	NA	NA	NA	NA	NA	NA	NA
5	Control	0	NA	NA	NA	42	52	64	NA	NA	NA	NA	NA	NA	NA	NA	NA	NA	NA	NA	NA
6	Control	0	NA	NA	NA	51	49	58	NA	NA	NA	NA	NA	NA	NA	NA	NA	NA	NA	NA	NA
7	OA	0	NA	NA	NA	44	40	64	NA	NA	NA	NA	NA	NA	NA	NA	NA	NA	NA	NA	NA
8	OA	0	NA	NA	NA	38	50	38	NA	NA	NA	NA	NA	NA	NA	NA	NA	NA	NA	NA	NA
9	OA	0	NA	NA	NA	34	36	47	NA	NA	NA	NA	NA	NA	NA	NA	NA	NA	NA	NA	NA
10	OA	0	NA	NA	NA	33	36	44	NA	NA	NA	NA	NA	NA	NA	NA	NA	NA	NA	NA	NA
11	Control	0	NA	NA	NA	45	38	43	NA	NA	NA	NA	NA	NA	NA	NA	NA	NA	NA	NA	NA
12	Control	0	NA	NA	NA	36	37	50	NA	NA	NA	NA	NA	NA	NA	NA	NA	NA	NA	NA	NA
1	Control	7	34	44	42	62	73	62	143	128	106	-3.28	14.06	17.33	4.37	NA	NA	NA	NA	NA	NA
2	OA	7	34	36	38	42	46	49	138	119	95	-2.57	12.15	14.73	6.54	NA	NA	NA	NA	NA	NA
3	OA	7	34	36	34	50	63	59	147	143	128	-3.76	15.17	18.93	2.90	NA	NA	NA	NA	NA	NA
4	Control	7	38	38	42	48	65	70	131	116	99	-3.60	16.68	20.27	6.76	NA	NA	NA	NA	NA	NA
5	Control	7	38	44	44	62	70	85	155	144	130	-4.16	11.34	15.50	6.74	NA	NA	NA	NA	NA	NA
6	Control	7	36	48	48	65	82	76	173	159	136	-3.43	10.64	14.07	4.62	NA	NA	NA	NA	NA	NA
7	OA	7	30	36	36	49	47	66	148	125	107	-3.76	11.90	15.66	3.66	NA	NA	NA	NA	NA	NA
8	OA	7	28	36	32	47	56	46	164	152	138	-3.28	14.19	17.47	6.04	NA	NA	NA	NA	NA	NA
9	OA	7	32	36	36	44	53	51	148	139	127	-2.79	11.44	14.23	3.90	NA	NA	NA	NA	NA	NA
10	OA	7	34	36	36	45	44	47	145	128	112	-3.67	14.04	17.71	7.12	NA	NA	NA	NA	NA	NA
11	Control	7	38	44	42	53	53	54	138	126	103	-3.30	14.14	17.44	6.88	NA	NA	NA	NA	NA	NA
12	Control	7	40	42	44	49	60	73	154	139	139	-3.98	18.26	22.24	5.70	NA	NA	NA	NA	NA	NA
1	Control	14	34	38	42	76	89	68	171	158	141	-2.05	7.76	9.80	8.42	NA	NA	NA	NA	NA	NA
2	OA	14	28	30	28	47	50	52	153	129	87	-2.19	8.97	11.16	6.82	NA	NA	NA	NA	NA	NA
3	OA	14	30	32	32	53	67	61	163	155	128	-3.15	11.03	14.19	4.90	NA	NA	NA	NA	NA	NA
4	Control	14	36	38	36	56	79	74	165	158	150	-3.22	9.00	12.22	7.92	NA	NA	NA	NA	NA	NA
5	Control	14	34	40	42	64	78	94	177	171	159	-2.84	6.46	9.29	5.38	NA	NA	NA	NA	NA	NA
6	Control	14	36	46	48	73	96	89	163	153	147	-4.18	10.05	14.23	8.59	NA	NA	NA	NA	NA	NA
7	OA	14	30	32	30	54	49	69	166	154	134	-2.51	9.32	11.83	6.77	NA	NA	NA	NA	NA	NA
8	OA	14	26	28	26	53	65	52	169	151	142	-3.83	15.60	19.42	9.31	NA	NA	NA	NA	NA	NA
9	OA	14	26	32	32	46	55	52	148	131	111	-2.20	7.97	10.17	5.62	NA	NA	NA	NA	NA	NA
10	OA	14	30	30	30	52	47	52	161	147	138	-4.11	11.90	16.01	4.96	NA	NA	NA	NA	NA	NA
11	Control	14	38	40	42	61	56	67	152	141	126	-4.00	14.27	18.26	10.18	NA	NA	NA	NA	NA	NA
12	Control	14	42	44	44	60	68	83	152	135	122	-2.87	11.50	14.37	6.87	NA	NA	NA	NA	NA	NA
1	Control	21	28	42	40	76	117	99	158	144	137	-2.61	7.62	10.23	4.37	4.03	8.23	-32.39	2.84	32.43	11.42
2	OA	21	22	30	30	50	50	60	149	129	105	-1.99	7.85	9.84	1.62	11.79	8.38	-22.10	2.80	27.57	9.85
3	OA	21	20	26	26	56	73	67	128	126	123	-3.41	9.02	12.43	2.03	6.57	8.49	-21.87	3.32	27.44	8.27
4	Control	21	26	34	34	61	83	92	154	148	138	-2.77	14.93	17.69	4.81	5.57	8.18	-30.99	3.04	31.50	10.36
5	Control	21	36	38	36	74	94	113	169	158	154	-3.42	15.02	18.44	4.92	7.50	8.44	-30.64	2.99	32.35	10.82
6	Control	21	34	44	44	80	102	91	162	153	144	-2.57	7.59	10.17	4.31	2.52	8.84	-30.16	2.66	24.20	9.10
7	OA	21	24	28	26	56	52	77	152	132	113	-2.93	10.55	13.48	3.62	2.52	8.34	-23.12	2.70	28.02	10.38
8	OA	21	20	24	20	59	65	57	167	152	135	-2.64	11.34	13.98	3.56	11.83	9.27	-22.63	3.08	23.79	7.72
9	OA	21	24	28	30	53	55	54	160	138	119	-2.38	7.98	10.36	2.84	2.74	8.90	-21.81	2.82	23.26	8.25
10	OA	21	24	26	28	53	48	57	153	144	127	-3.82	9.99	13.80	5.49	3.92	8.66	-22.89	3.02	28.13	9.31
11	Control	21	34	40	40	81	62	75	137	124	115	-2.26	9.31	11.57	4.48	5.55	9.01	-29.98	3.33	27.02	8.11
12	Control	21	36	44	44	82	75	91	148	127	106	-2.38	8.54	10.93	5.69	3.48	8.73	-29.95	2.86	29.18	10.20

Supplementary material to chapter 6

Supplementary figures to chapter 6

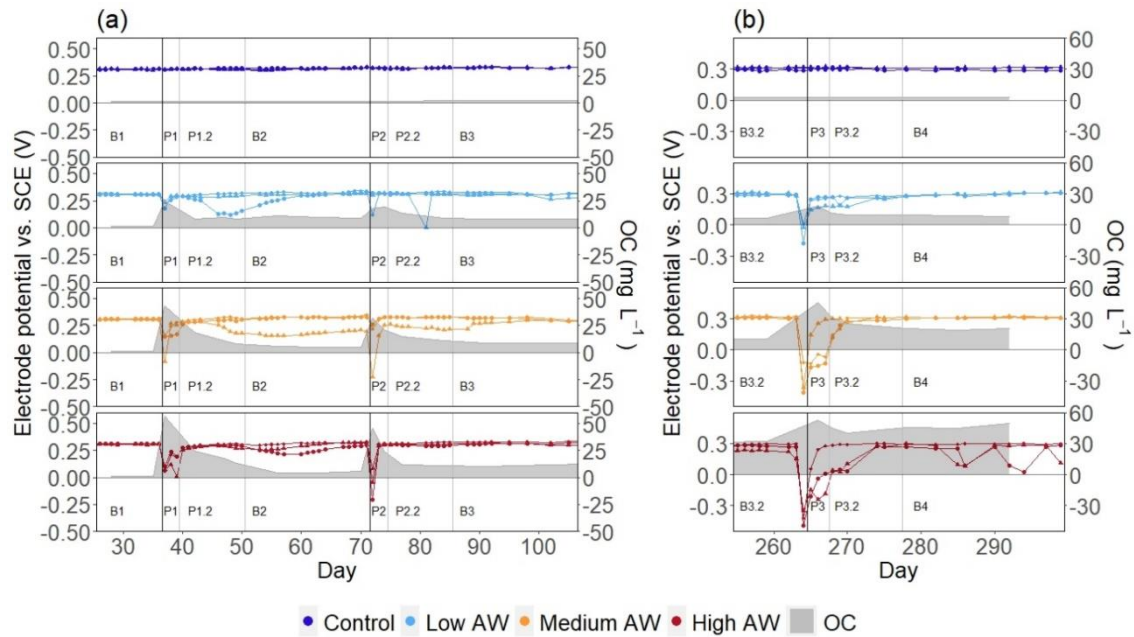


Figure S6.1. Cathode electric potentials versus Saturated Calomel Electrode (SCE) of open circuit microbial fuel cells (MFCs) and organic carbon (OC) concentrations (mg L⁻¹) from days 26 to 106 (a) and days 254 to 299 (b) at three concentrations of artificial wastewater (AW) eutrophication (measured in mg OC L⁻¹) and controls. Black vertical lines indicate eutrophication pulse initiation on days 36, 71, and 264. Black and grey vertical lines indicate distinction of experimental phases. B1-B4: baseline; P1-P3: pulse. Each line represents one replicate MFC (distinguishable by different shapes). Grey area indicates mean OC concentration in three tanks of the respective treatment. Raw data of this figure is available online in supplementary data 4 (<https://doi.org/10.1016/j.ecolind.2023.110385>).

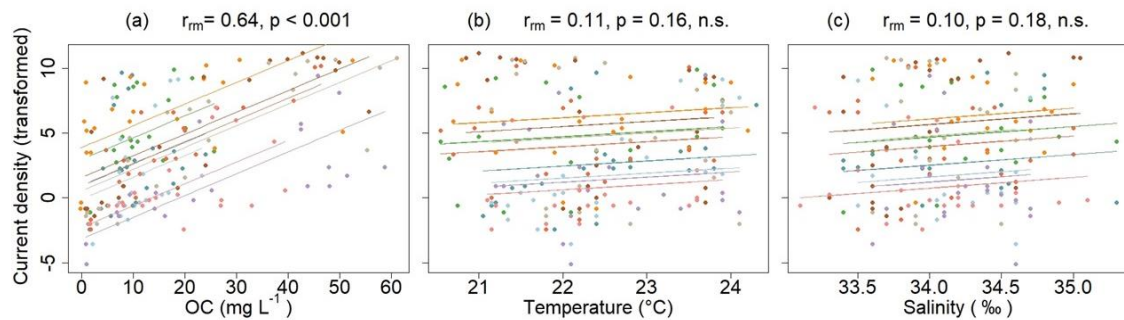


Figure S6.2. Repeated measured correlation analysis (rmcorr) of all days with simultaneous measurements of current density and (a) organic carbon (OC) concentration, (b) temperature, and (c) salinity. Current density was transformed to achieve normal distribution. Every color and corresponding regression line represents one experimental tank on different days of the experiment. Controls were excluded to enable parametric tests. Raw data of this figure is available online in supplementary data 3 (<https://doi.org/10.1016/j.ecolind.2023.110385>).

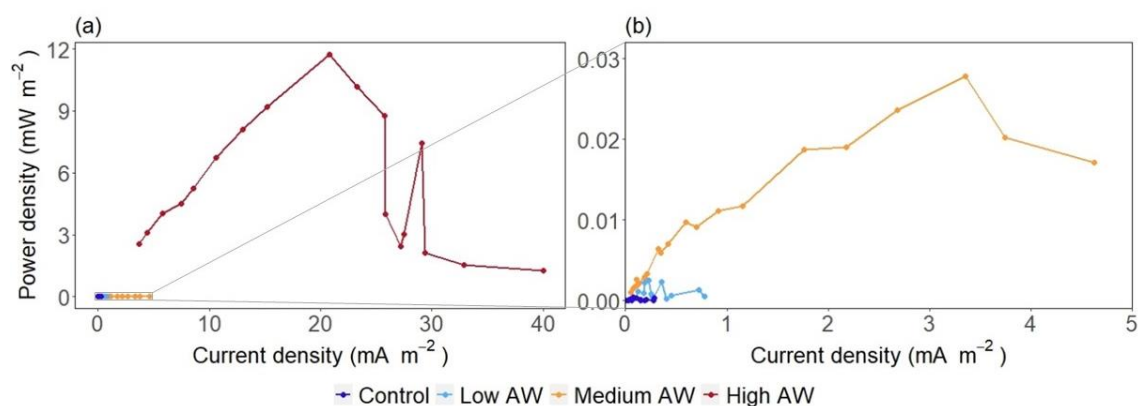


Figure S6.3. Power density over current density, for one MFC per treatment (a), and excluding the high AW treatment (b). External resistance was increased stepwise from day 223 to day 258, from 2 to 910 k Ω . Measurements were taken at nine fixed times within 24 h after the increase of the resistance, and the mean value was plotted. In the high AW treatment, with 22 k Ω , the first 6 measurements were excluded as outliers due to high variation within the first hour after exchange of the external resistance. Raw data of this figure is available online in supplementary data 5 (<https://doi.org/10.1016/j.ecolind.2023.110385>).

Supplementary tables to chapter 6

Table S6.1. Comparison of indicators for organic matter (OM)/ organic carbon (OC) eutrophication in coastal marine ecosystems.

Indicator	Finding	Benefit	Drawback	Source
Sedimentary oxygen consumption (SOC)	Sites closer to sewage sources displayed higher SOC, up to 90 m away.	Low cost and infrastructure required.	High sampling effort (2 h incubations), establishment of baselines needed.	(Ford et al., 2017) ¹
Sedimentary organic carbon content	Sediment microbial species richness declined with increasing sediment OC content.	Broad-scale comparisons and definition of thresholds.	Laboratory and analytical instruments required.	(Hyland et al., 2005) ²
Sedimentary organic matter composition	Sediment protein to carbohydrate ratio informed about trophic status and organic input.	Broad-scale comparisons and definition of thresholds.	Laboratory and analytical instruments required.	(Dell'Anno et al., 2002) ³
Microbial community composition in seawater	56% of the variation in composition was explained by environmental parameters.	Fast response times, detailed information, indicator taxa can be identified.	Laboratory and analytical instruments required, relatively higher costs than other parameters, establishment of baselines needed.	(Glasl et al., 2019) ⁴
Benthic invertebrate-based indices	Different indices can detect organic pollution.	Broad-scale comparisons (e.g., Mediterranean). Relatively fast response times (Desrosiers et al., 2013).	Taxonomic expertise required, mainly found in soft sediments, not applicable to coral reefs (Desrosiers et al., 2013).	(Simboura and Zenetos, 2002) ⁵
Microbial fuel cells (MFCs) in sediments	MFC current densities peaked after AW pulses and remained elevated during continuous OM eutrophication.	Continuous measurement, fast response times (< 1 day), low infrastructure required, low costs, low sampling effort once deployed, low maintenance.	Sensitive to fluctuations in oxygen concentrations, presence of toxins, and strong fluctuations in temperature and salinity. Qualitative information only.	Present study

Supplementary references to chapter 6

1. Ford, A. K. *et al.* High sedimentary oxygen consumption indicates that sewage input from small islands drives benthic community shifts on overfished reefs. *Environ. Conserv.* **44**, 405–411 (2017).
2. Hyland, J. *et al.* Organic carbon content of sediments as an indicator of stress in the marine benthos. *Mar. Ecol. Prog. Ser.* **295**, 91–103 (2005).
3. Dell'Anno, A., Mei, M. L., Pusceddu, A. & Danovaro, R. Assessing the trophic state and eutrophication of coastal marine systems: A new approach based on the biochemical composition of sediment organic matter. *Mar. Pollut. Bull.* **44**, 611–622 (2002).
4. Glasl, B. *et al.* Microbial indicators of environmental perturbations in coral reef ecosystems. *Microbiome* **7**, 94 (2019).
5. Simboura, N. & Zenetos, A. Benthic indicators to use in ecological quality classification of Mediterranean soft bottom marine ecosystems, including a new biotic index. *Mediterr. Mar. Sci.* **3**, 77–111 (2002).

Supplementary material to chapter 7**Supplementary tables to chapter 7**

Table S7.1. Monosaccharide concentrations (mg L⁻¹) of hydrolyzed coral mucus from five species of scleractinian corals (raw data for [Table 7.1](#)). GalN = galactosamine, Xyl = xylose, Gal = galactose, Fuc = fucose, Glc = glucose, Man = mannose, Ara = arabinose, GlcN = glucosamine.

Species	Rha	GalN	Xyl	Gal	Fuc	Glc	Man	Ara	GlcN
<i>Acropora cervicornis</i>	0.00	1.48	0.00	2.69	0.97	0.00	14.12	24.71	16.74
<i>Acropora cervicornis</i>	0.00	1.51	0.00	2.57	1.02	0.00	7.03	21.27	11.16
<i>Acropora cervicornis</i>	0.00	1.60	0.43	2.78	1.12	0.00	9.05	22.42	13.28
<i>Diploria labyrinthiformis</i>	0.00	0.05	0.00	0.00	5.45	0.08	2.58	0.00	3.53
<i>Diploria labyrinthiformis</i>	0.00	0.00	0.52	0.00	2.22	0.00	0.56	0.00	1.59
<i>Diploria labyrinthiformis</i>	0.00	0.00	0.00	0.00	0.13	0.00	0.00	0.00	0.16
<i>Meandrina meandrites</i>	0.00	0.00	0.00	0.00	1.56	0.35	0.40	0.00	1.95
<i>Meandrina meandrites</i>	0.00	0.00	0.00	0.00	0.73	0.00	0.35	0.00	1.62
<i>Montipora confusa</i>	0.00	0.00	0.00	0.00	0.00	0.00	0.00	1.43	1.93
<i>Montipora confusa</i>	0.00	0.00	0.00	0.00	0.00	0.00	0.00	1.38	2.08
<i>Montipora confusa</i>	0.00	0.00	0.00	0.00	0.00	0.00	0.00	1.35	1.83
<i>Montipora digitata</i>	0.00	0.00	0.00	0.00	0.00	0.00	0.00	1.60	2.87
<i>Montipora digitata</i>	0.00	0.00	0.00	0.00	0.00	0.00	0.00	2.65	3.89
<i>Montipora digitata</i>	0.00	0.00	0.00	0.00	0.00	0.00	0.00	1.81	2.70

Table S7.2. Data used in the heatmap (Fig. 7.1), including sources of original data and annotations concerning data preparation.

Reference	Region	Coral genus / species	Family	Clade	Replicates	Fuc	Rha	GalN /GalNAc	Ara	GlcN /GlcNAc	Gal	Glc	Man	Xyl
This study	Caribbean (Curaçao)	<i>Acropora cervicornis</i>	Acroporidae	Complex	3	2.0	0.0	2.7	48.6	24.2	4.8	0.0	17.4	0.3
This study	Caribbean (Curaçao)	<i>Meandrina meandrites</i>	Meandrinidae	Robust	2	22.4	0.0	0.0	0.0	67.7	0.0	2.7	7.2	0.0
This study	Caribbean (Curaçao)	<i>Diploria labyrinthiformis</i>	Faviidae	Robust	3	47.8	0.0	0.1	0.0	37.2	0.0	0.2	10.6	4.0
This study	From Indo-Pacific, grown in Germany	<i>Montipora confusa</i>	Acroporidae	Complex	3	0.0	0.0	0.0	46.0	54.0	0.0	0.0	0.0	0.0
This study	From Indo-Pacific, grown in Germany	<i>Montipora digitata</i>	Acroporidae	Complex	3	0.0	0.0	0.0	43.1	56.9	0.0	0.0	0.0	0.0
[†] Hadaidi et al. (2019) ¹	Central Red Sea (Shaab reef)	<i>Acropora pharaensis</i>	Acroporidae	Complex	3	1.3	1.2	0*	38.5	1.8	4.1	25.1	22.3	5.8
[†] Hadaidi et al. (2019) ¹	Central Red Sea (Shaab reef)	<i>Galaxea fascicularis</i>	Euphyllidae	Complex	3	5.6	0.0	0*	0.0	1.6	25.1	18.3	35.1	14.3
[†] Hadaidi et al. (2019) ¹	Central Red Sea (Shaab reef)	<i>Porites lobata</i>	Poritidae	Complex	3	11.2	0.6	0*	18.5	4.9	47.0	10.1	7.3	0.8
[†] Hadaidi et al. (2019) ¹	Central Red Sea (Shaab reef)	<i>Pocillopora verrucosa</i>	Pocilloporidae	Robust	3	0.0	0.0	0*	0.0	0.0	4.9	33.6	45.5	19.3
[†] Hadaidi et al. (2019) ¹	Central Red Sea (Shaab reef)	<i>Stylophora pistillata</i>	Pocilloporidae	Robust	3	0.0	0.0	0*	0.0	4.4	1.8	34.9	49.0	14.0
Lee et al. (2016) ²	Taiwan (Nan-wan)	<i>Acropora muricata</i>	Acroporidae	Complex	4	2.9	0*	0.7	8.0	30.2	10.5	20.9	10.4	6.1
Wild et al. (2010) ³	Northern Red Sea (Gulf of Aqaba)	<i>Acropora</i> sp.	Acroporidae	Complex	4-6	6.5	0.0	0.0	76.4	6.6	3.7	1.2	5.7	0.0
[†] Wild et al. (2010) ³	Northern Red Sea (Gulf of Aqaba)	<i>Fungia</i> sp.	Fungiidae	Robust	4-6	77.6	0.0	0.0	0.0	1.6	0.2	0.3	20.3	0.0
Wild et al. (2010) ³	Northern Red Sea (Gulf of Aqaba)	<i>Ctenactis</i> sp.	Fungiidae	Robust	4-6	5.2	0.0	0.0	0.0	60.8	6.0	5.9	22.1	0.0
Wild et al. (2010) ³	Sweden (Tisler Reef)	<i>Desmophyllum</i> sp.	Caryophylliidae	Robust	4-8	0.0	0.0	0.0	0.0	0.0	0.0	59.6	40.4	0.0
Wild et al. (2010) ³	Norway (Røst Reef)	<i>Desmophyllum</i> sp.	Caryophylliidae	Robust	4-8	8.0	0.0	0.0	0.0	57.2	4.7	9.8	18.8	1.5
Wild et al. (2010) ³	Norway (Røst Reef)	<i>Madrepora</i> sp.	Oculinidae	Robust	4-8	0.0	31.4	0.0	0.0	0.0	0.0	26.0	42.6	0.0
Wild et al. (2010) ³	Northern Red Sea (Gulf of Aqaba)	<i>Pocillopora</i> sp.	Pocilloporidae	Robust	4-6	25.3	0.0	0.0	0.0	0.0	0.0	25.2	49.5	0.0
[‡] Wild et al. (2010) ³	Northern Red Sea (Gulf of Aqaba)	<i>Stylophora</i> sp.	Pocilloporidae	Robust	4-6	0.0	0.0	0.0	0.0	0.0	0.0	100.0	0.0	0.0
[†] Klaus et al. (2007) ⁴	Caribbean (Curaçao)	<i>Orbicella annularis</i>	Merulinidae	Robust	36	38.5	0.0	0*	0.2	46.9	4.7	8.8	0.0	0.8
Wild et al. (2005) ⁵	Great Barrier Reef (Heron Island)	<i>Acropora pulchra</i>	Acroporidae	Complex	3	7.8	0.0	0*	25.4	10.7	2.9	32.2	11.1	9.8
Wild et al. (2005) ⁵	Great Barrier Reef (Heron Island)	<i>Acropora digitifera</i>	Acroporidae	Complex	3	5.0	2.8	0*	13.9	16.4	5.3	40.5	12.0	4.0
Wild et al. (2005) ⁵	Great Barrier Reef (Heron Island)	<i>Acropora robusta</i>	Acroporidae	Complex	3	6.6	8.0	0*	24.9	10.6	5.9	22.1	13.4	4.7
Wild et al. (2005) ⁵	Great Barrier Reef (Heron Island)	<i>Acropora aspera</i>	Acroporidae	Complex	3	5.5	0.0	0*	50.8	13.7	6.2	13.2	10.6	0.0
Wild et al. (2005) ⁵	Great Barrier Reef (Heron Island)	<i>Acropora millepora</i>	Acroporidae	Complex	3	0.0	0.0	0*	63.2	7.9	5.3	12.5	11.1	0.0
Wild et al. (2005) ⁵	Great Barrier Reef (Heron Island)	cf. <i>Acropora muricata</i>	Acroporidae	Complex	3	5.6	0.0	0*	36.7	17.2	5.4	22.2	12.8	0.0
Meikle et al. (1988) ⁶	Great Barrier Reef (Magnetic Island)	<i>Acropora muricata</i>	Acroporidae	Complex	1	2.0	0*	1.0	47.0	29.0	2.0	1.0	18.0	0.0
Meikle et al. (1988) ⁶	Great Barrier Reef (Magnetic Island)	<i>Pachyseris speciosa</i>	Agariciidae	Complex	1	14.0	0*	2.0	16.0	10.0	46.0	0.0	12.0	0.0
Meikle et al. (1988) ⁶	Great Barrier Reef (Magnetic Island)	<i>Fungia fungites</i>	Fungiidae	Robust	1	41.0	0*	7.0	2.0	22.0	4.0	3.0	19.0	2.0

*Study did not report the absence of GalN/GalNAc or Rha, but value was set to zero because the method used (see Table S7.3) generally enables the detection.

[†] Study included additional monosaccharides which were not included in the analysis of the present study, and mole % values were adjusted accordingly.

[‡] Three separate measurements of *Fungia* sp. from different seasons were averaged.

[§] *Stylophora* sp. was not included in the heatmap (Fig. 7.1) because only Glc was detected, indicating low carbohydrate concentrations in general, which likely lead to over-estimation of the relative proportion of Glc.

Table S7.3. Overview of methods for mucus collection and monosaccharide measurement. PAD = pulsed amperometric detector; HPLC = high performance liquid chromatography; HPAEC = high-performance anion exchange chromatography; GC = gas chromatography; GC-MS = combined gas chromatography/mass spectrometry; TMS = per-O-trimethylsilyl.

Reference	Mucus collection	Measurement of monosaccharides
Meikle et al. (1988) ⁶	Drawn from the colony surface after chilling corals for 20 h at 4 °C under toluene	Dialysis, centrifugation, acid hydrolysis of the supernatant, GC-MS of alditol acetate derivatives
Wild et al. (2005) ⁵	"milked" colonies by exposing them to air for 2 minutes and collecting the dripping mucus	Dialysis (10 kDa), lyophilization, acid hydrolysis, GC-MS of TMS derivatives, analysis done at the Center of Complex Carbohydrate Research (CCCR) of the University of Georgia in Athens, Georgia, USA
Klaus et al. (2007) ⁴	Drawn from the colony surface	Dialysis (1 kDa), acid hydrolysis, HPAEC-PAD
Wild et al (2010) ³	"milked" for 2 minutes	Dialysis (100-500 Da), lyophilization, acid methanolysis, GC-MS of TMS derivatives, analysis done at the CCCR
Lee et al. (2016) ²	"milked" for 5 minutes	Dialysis (100-500 Da), acid hydrolysis, HPLC-MS of TMS derivatives
Hadaidi et al. (2019) ¹	Drawn from colony surface <i>in situ</i>	Dialysis (50 kDa), acid methanolysis, GC-MS of TMS derivatives, analysis done at the CCCR
Present study	"milked" for 2 minutes	Acid hydrolysis, 1:100 dilution, centrifugation, HPAEC-PAD

Table S7.4. Species list for phylogenetic tree based on mitochondrial COI (cytochrome *c* oxidase subunit I) gene.

Species	Location	Length (bp)	Accession no.*	Reference
<i>Acropora aspera</i>	Unknown	657 bp	KX664114	Unpublished
<i>Acropora cervicornis</i>	Caribbean	658 bp	AY451340	Shearer and Coffroth (2008) ⁷
<i>Acropora digitifera</i>	Unknown	681 bp	KR401100	Unpublished
<i>Acropora millepora</i>	Sabah, Malaysia	658 bp	MG383848	Robert et al. (2019) ⁸
<i>Acropora muricata</i>	Sabah, Malaysia	657 bp	KX664143	Unpublished
<i>Acropora pharaonis</i>	Unknown	664 bp	MK309942	Unpublished
<i>Acropora pulchra</i>	Sabah, Malaysia	658 bp	MG383851	Robert et al. (2019) ⁸
<i>Acropora robusta</i>	Unknown	590 bp	MN413872	Unpublished
<i>Ctenactis crassa</i>	Indo-Pacific	504 bp	LC191439	Oku et al. (2017) ⁹
<i>Desmophyllum dianthus</i>	Mediterranean	512 bp	JQ611389	Addamo et al. (2012) ¹⁰
<i>Diploria labyrinthiformis</i>	Atlantic	630 bp	AB117224	Fukami et al. (2004) ¹¹
<i>Fungia fungites</i>	Nansei Island group, southern Japan	505 bp	LC484536	Oku et al. (2020) ¹²
<i>Galaxea fascicularis</i>	Unknown	590 bp	MN413859	Unpublished
<i>Madrepora oculata</i>	Mediterranean	512 bp	JQ611395	Addamo et al. (2012) ¹⁰
<i>Meandrina meandrites</i>	Atlantic	630 bp	AB117296	Fukami et al. (2004) ¹¹
<i>Montipora undata</i>	Sodwana Bay, South-Africa	590 bp	MN413817	Unpublished
<i>Montipora digitata</i>	Indo-Pacific	657 bp	KF492662	Swain et al. (2016) ¹³
<i>Orbicella annularis</i>	Caribbean	658 bp	AY451352	Shearer and Coffroth (2008) ⁷
<i>Pachyseris speciosa</i>	Unknown	590 bp	MN413852	Unpublished
<i>Pocillopora verrucosa</i>	Unknown	590 bp	MN413871	Unpublished
<i>Porites lobata</i>	Islas Marias Biosphere Reserve, Mexico	627 bp	MN005655	Santiago-Valentín et al. (2020) ¹⁴
<i>Stylophora pistillata</i>	Unknown	590 bp	MN413851	Unpublished

bp = basepairs

*All sequences were obtained from the NCBI GenBank database

Supplementary references to chapter 7

1. Hadaidi, G., Gegner, H. M., Ziegler, M. & Voolstra, C. R. Carbohydrate composition of mucus from scleractinian corals from the central Red Sea. *Coral Reefs* **38**, 21–27 (2019).
2. Lee, S. T. M., Davy, S. K., Tang, S.-L. & Kench, P. S. Mucus sugar content shapes the bacterial community structure in thermally stressed *Acropora muricata*. *Front. Microbiol.* **7**, 371 (2016).
3. Wild, C., Naumann, M., Niggel, W. & Haas, A. Carbohydrate composition of mucus released by scleractinian warm- and cold-water reef corals. *Aquat. Biol.* **10**, 41–45 (2010).

4. Klaus, J. S., Janse, I., Heikoop, J. M., Sanford, R. A. & Fouke, B. W. Coral microbial communities, zooxanthellae and mucus along gradients of seawater depth and coastal pollution. *Environ. Microbiol.* **9**, 1291–1305 (2007).
5. Wild, C., Woyt, H. & Huettel, M. Influence of coral mucus on nutrient fluxes in carbonate sands. *Mar. Ecol. Prog. Ser.* **287**, 87–98 (2005).
6. Meikle, P., Richards, G. N. & Yellowlees, D. Structural investigations on the mucus from six species of coral. *Mar. Biol.* **99**, 187–193 (1988).
7. Shearer, T. L. & Coffroth, M. A. DNA barcoding: barcoding corals: limited by interspecific divergence, not intraspecific variation: DNA barcoding. *Mol. Ecol. Resour.* **8**, 247–255 (2008).
8. Robert, R., Rodrigues, K. F., Waheed, Z. & Kumar, S. V. Extensive sharing of mitochondrial COI and CYB haplotypes among reef-building staghorn corals (*Acropora* spp.) in Sabah, North Borneo. *Mitochondrial DNA Part A* **30**, 16–23 (2019).
9. Oku, Y., Naruse, T. & Fukami, H. Morpho-molecular evidence for polymorphism in the mushroom coral *Cycloseris hexagonalis* (Scleractinia: Fungiidae), with a new phylogenetic position and the establishment of a new genus for the species. *Zoolog. Sci.* **34**, 242–251 (2017).
10. Addamo, A. M., Reimer, J. D., Taviani, M., Freiwald, A. & Machordom, A. *Desmophyllum dianthus* (Esper, 1794) in the scleractinian phylogeny and its intraspecific diversity. *PLoS ONE* **7**, e50215 (2012).
11. Fukami, H. et al. Conventional taxonomy obscures deep divergence between Pacific and Atlantic corals. *Nature* **427**, 832–835 (2004).
12. Oku, Y. et al. *Fungia fungites* (Linnaeus, 1758) (Scleractinia, Fungiidae) is a species complex that conceals large phenotypic variation and a previously unrecognized genus. *Contrib. Zool.* **89**, 188–209 (2020).
13. Swain, T. D. et al. Skeletal light-scattering accelerates bleaching response in reef-building corals. *BMC Ecol.* **16**, 10 (2016).
14. Santiago-Valentín, J. D., Rodríguez-Troncoso, A. P., Bautista-Guerrero, E., López-Pérez, A. & Cupul-Magaña, A. L. Settlement ecology of scleractinian corals of the Northeastern Tropical Pacific. *Coral Reefs* **39**, 133–146 (2020).

Supplementary material to chapter 8

Supplementary methods to chapter 8

Carbohydrate microarray analysis

Macroalgae tissue extracts were analysed using carbohydrate microarrays, as described by Vidal-Melgosa et al.¹. Shortly, AIR-washed tissue powder was sequentially extracted using autoclaved UW, 50 mM EDTA pH 7.5, and 4 M NaOH with 0.1 % w/v NaBH₄ and stored at -20 °C until further

processing. UW- and EDTA extracts were additionally diluted by a factor of 1:2 to adjust viscosity. Extracts were vortexed (5 sec), centrifuged (10 min at $16,000 \times g$), and transferred into 384-microwell plates for printing of microarrays. Printing was done in four concentrations (1:2, 1:10, 1:20 and 1:40) per extract, diluted with printing buffer (ArrayJet, Roslin, UK), and printed using a microarray robot (Sprint, ArrayJet, Roslin, UK) on nitrocellulose membrane ($0.45 \mu\text{m}$, Whatmann). All solvents were also printed on the microarrays and did not result in unspecific signals. Printed microarrays were first incubated for 1 h in phosphate buffered saline (PBS, 1x) with 5 % (w/v) non-fat milk powder (MPBS), and then for 2 h with monoclonal antibodies (mAbs) in MPBS which bind specifically to epitopes present in sulphated fucan (i.e., BAM1, BAM2, BAM3 and BAM4). Microarrays were then washed in PBS, incubated for 2 h with secondary control antibodies (anti-rat, anti-mouse and anti-His conjugated to alkaline phosphatase, all not resulting in any signals) in MPBS and afterwards washed in deionised water. Microarrays were developed in a solution of 5-bromo-4-chloro-3-indolylphosphate and nitro blue tetrazolium in alkaline phosphatase buffer (100 mM NaCl, 5 mM MgCl₂, 100 mM Tris-HCl, pH 9.5) and probe binding signal intensity was analysed using the software Array-Pro Analyzer 6.3 (Media Cybernetics). The highest signal intensity of the dataset (which included 27 other mAbs and carbohydrate binding modules (CBMs)) was set to 100, all other signals were adjusted accordingly, and low arbitrary units were removed by applying a cut-off of 5. Binding intensities cannot be compared between species, nor between mAbs, because binding efficiencies may differ.

Fucoidan extraction from biomass

Up to 2 g of dried algae biomass powder (i.e., oven-dried *Lobophora* and *Dictyota* thalli) were weighed and resuspended in a final concentration of 25 mM EDTA (pH= 8) in 1 L of ultrapure water (UW). The suspension was autoclaved at 123 °C for 25 min and afterwards filtered over a glass fibre filter ($0.7 \mu\text{m}$) and cellulose nitrate filter ($0.45 \mu\text{m}$) prior to polyvinylpyrrolidon (PVPP, Merck/Sigma Aldrich) treatment. To bind polyphenols, 1 L of sample was mixed with 50 g of PVPP and 1 M phosphate buffer at a final concentration of 50 mM (pH= 6), stirred for 1 hour at room temperature and filtered again over a glass fibre filter. 10 μL of alginate lyase (Sigma) was added to the solution and incubated at 37 °C for 24 h. The filtrate was run over a 30 kDa Biomax ultrafiltration membrane (Merck Millipore) using an Amicon filtration device, washed 3 times against UW, resuspended in 200 mL UW and mixed with 1M Tris-HCl, pH 7.5 at a final concentration of 50 mM. The sample was passed through an anion exchange column, which had been conditioned with 2 column volumes of 0.5 M NaCl and 20 mM Tris-HCl at 5 mL min⁻¹ flow rate, 2 column volumes of 5 M NaCl and 20 mM Tris-HCl at 5 mL min⁻¹ flow rate and again 2 column volumes of 0.5 M NaCl and 20 mM Tris-HCl at 5 mL min⁻¹ flow rate. The sample was loaded to the column and washed with 3 column volumes of 0.5 M NaCl and 20 mM Tris-HCl prior to eluting fucoidan in 5 M NaCl and 20 mM Tris-HCl at a 5 mL min⁻¹ flow rate. The sample was dialysed against three times UW and concentrated using a 30 kDa ultrafiltration membrane with an Amicon filtration device. The final solution was freeze dried to obtain fucoidan powder. From the fucoidan

powder, 5 mg L⁻¹ solutions were prepared in UW. 500 µL of these stocks were added to 500 µL of 2 M HCl in pre-combusted glass ampoules (450 °C, 4.5 h), acid-hydrolysed at 100 °C for 24 h, dried in an acid-resistant vacuum concentrator, re-suspended in 1 mL of UW, and further processed for HPAEC-PAD analyses (see main methods section).

Supplementary figures to chapter 8

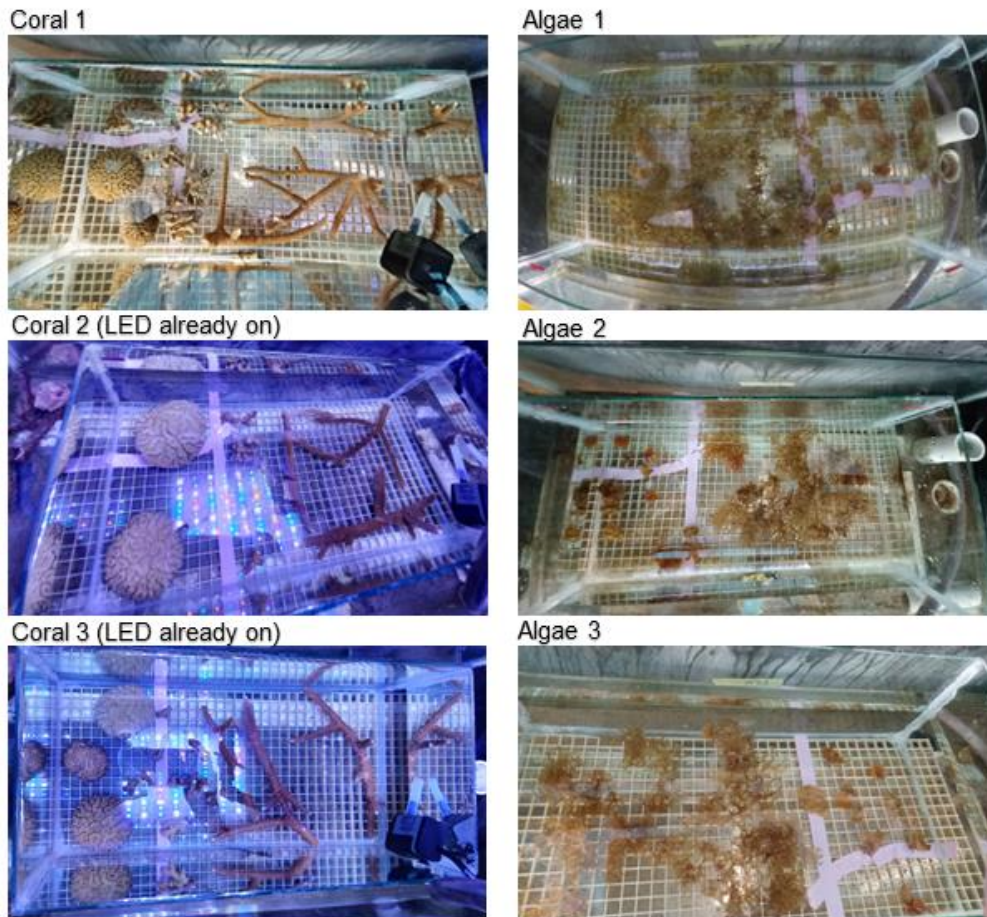


Figure S8.1. Pictures taken at the start of the exudate incubations with corals (left) and macroalgae (right). Mean relative cover of the aquarium floor was 34 % (\pm 5 sd) for coral- and 50 % (\pm 14 sd) for macroalgae incubations (analyzed with ImageJ).

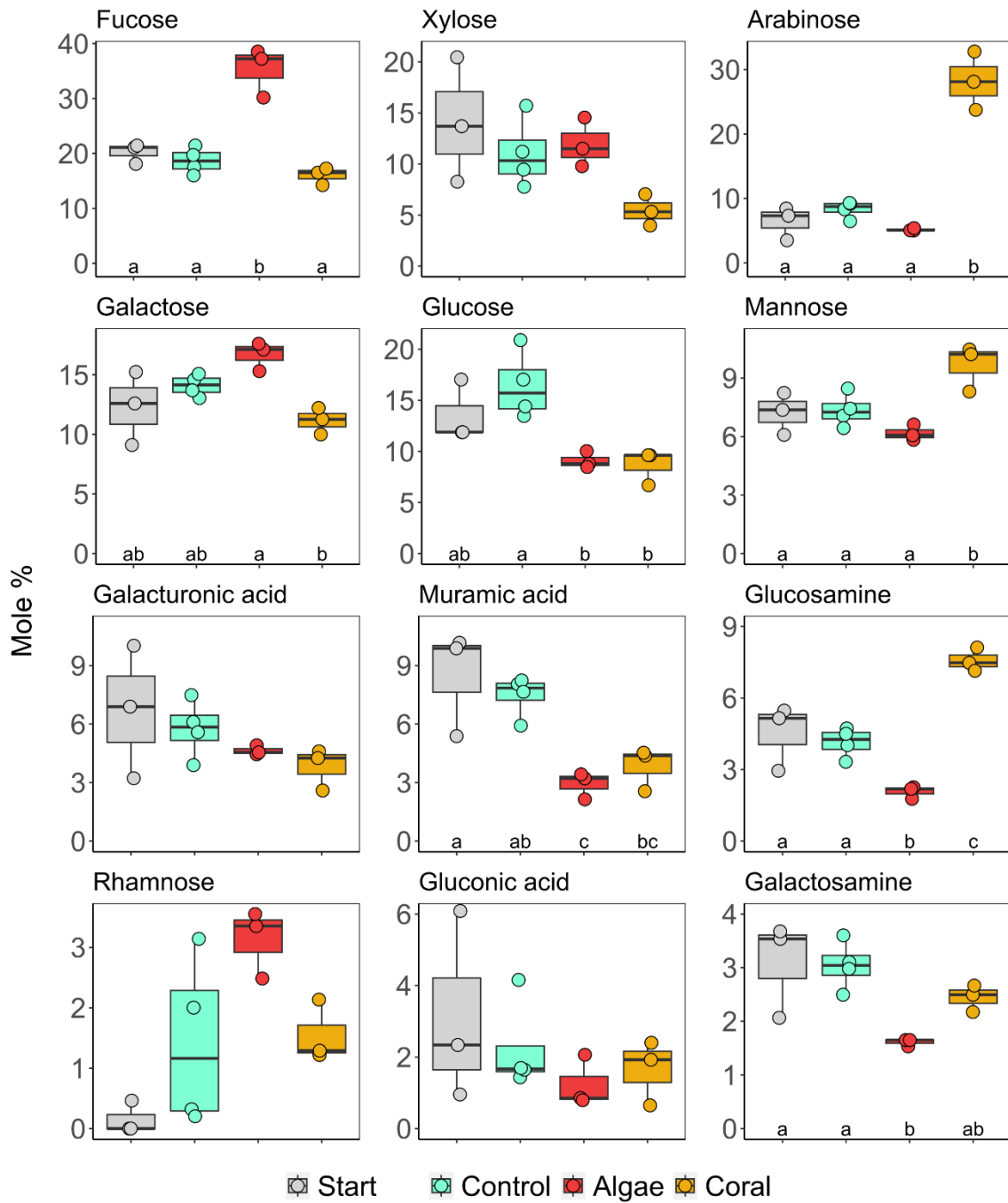


Figure S8.2. Carbohydrates released by corals and macroalgae in mole %. Boxes represent median \pm 95 % confidence intervals, and points represent replicates. Letters indicate significant differences between treatments (HSD test). See results of statistical tests (Analysis of Variance or Kruskal-Wallis tests) in [Table 8.2](#). Raw data to this figure is available in [Supplementary Table S8.4](#).

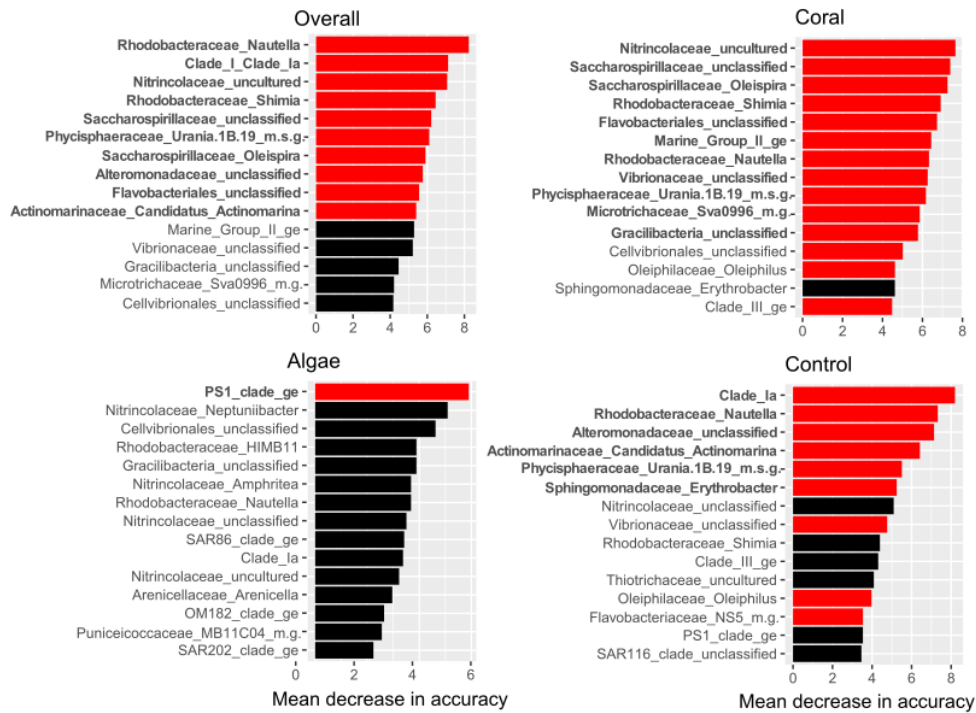


Figure S8.3. *RFpermute* variable importance plots of the bacterioplankton community composition after one day of bacterioplankton incubation. A high mean decrease in accuracy (MDA) of the model when a specific variable (genus) is removed equals a high importance in classification of the overall model, coral, algae, and control samples. Red bars indicate significant ($p < 0.05$) contribution to permutational random forest classification. Bold genera were significant and had an MDA score > 5 .

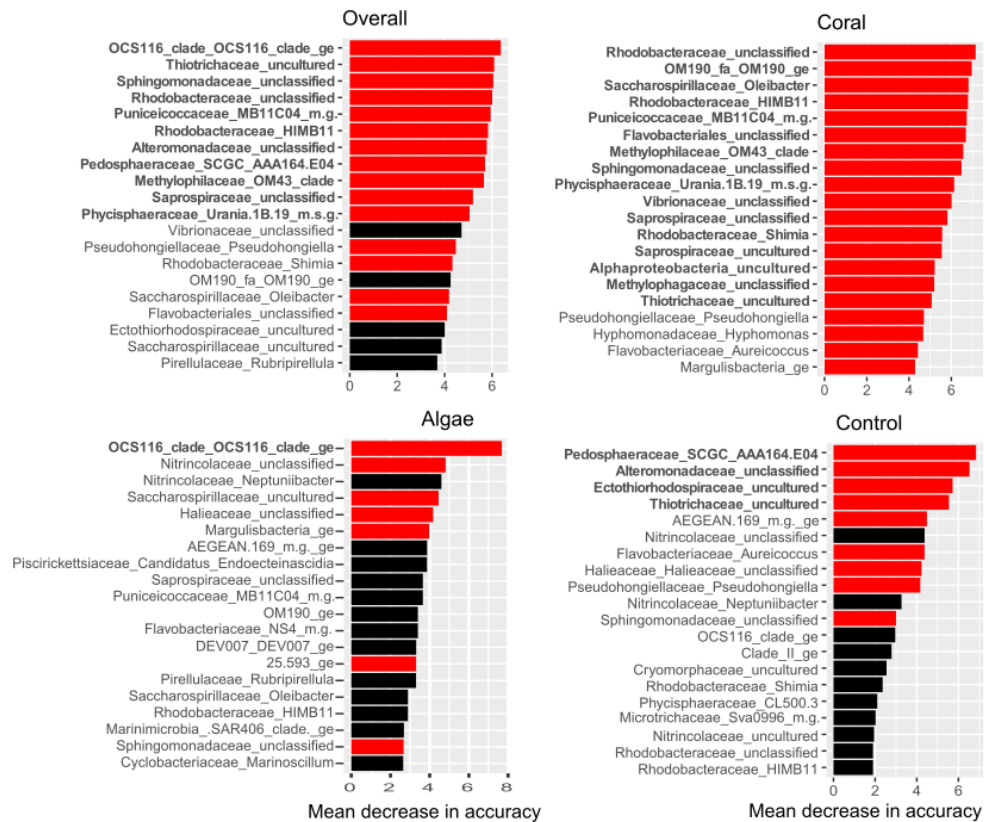


Figure S8.4. *RFpermute* variable importance plots of the bacterioplankton community composition after four days of bacterioplankton incubation. A high mean decrease in accuracy (MDA) of the model when a

specific variable (genus) is removed equals a high importance in classification of the overall model, coral, algae, and control samples. Red bars indicate significant ($p < 0.05$) contribution to permutational random forest classification. Bold genera were significant and had an MDA score > 5 .

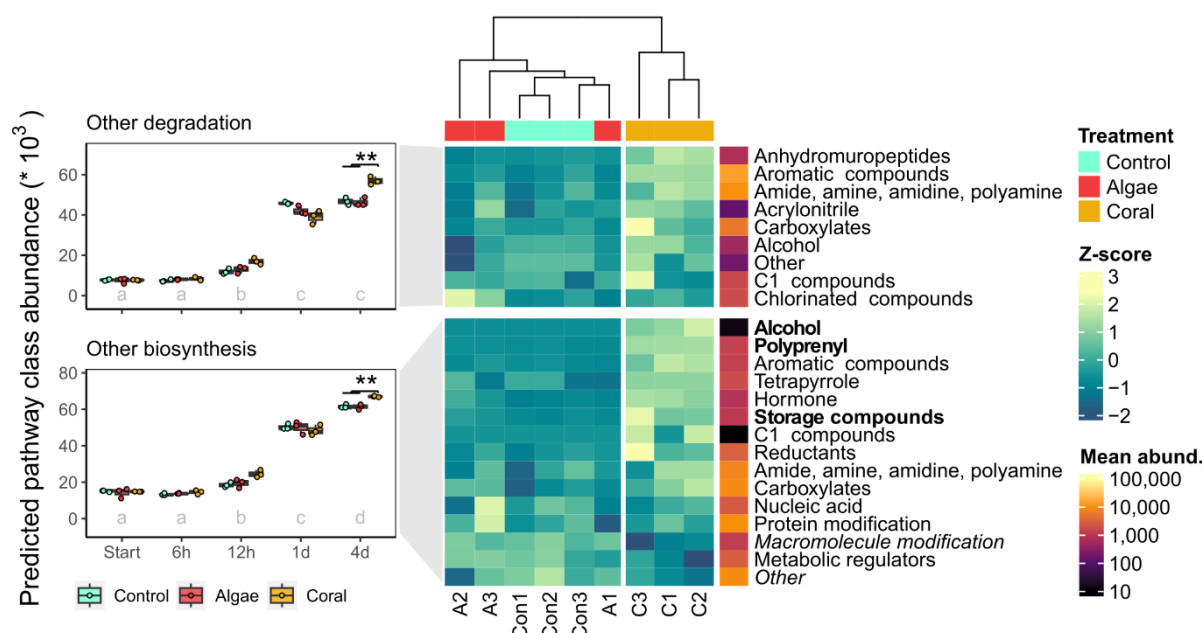


Figure S8.5. (a) Development of other predicted metabolic degradation and biosynthesis pathways during bacterioplankton incubations with algae and coral HMW DOM and background HMW DOM (controls). Different letters indicate significant differences between times ($p < 0.05$, pairwise t -tests, Bonferroni adjusted). Asterisks indicate significant differences between treatments (* $p < 0.05$, *** $p < 0.001$, **** $p < 0.0001$, pairwise t -tests, Bonferroni adjusted). Predictions are based on the MicFunPred analysis tool, using the MetaCyc database. (b) Predicted pathway abundance by type as Z-scores after four days of dark incubation. The dendrogram on the top represents the Euclidean distance between samples including all pathway types of all classes. SYN = biosynthesis, DEG = degradation. Bold pathway types in (b) indicate a significant increase in coral treatments compared to controls (fdr-corrected $p < 0.001$, log₂ fold change > 0.5 , *DESeq2* on all pathway types), and italicized types a significant decrease.

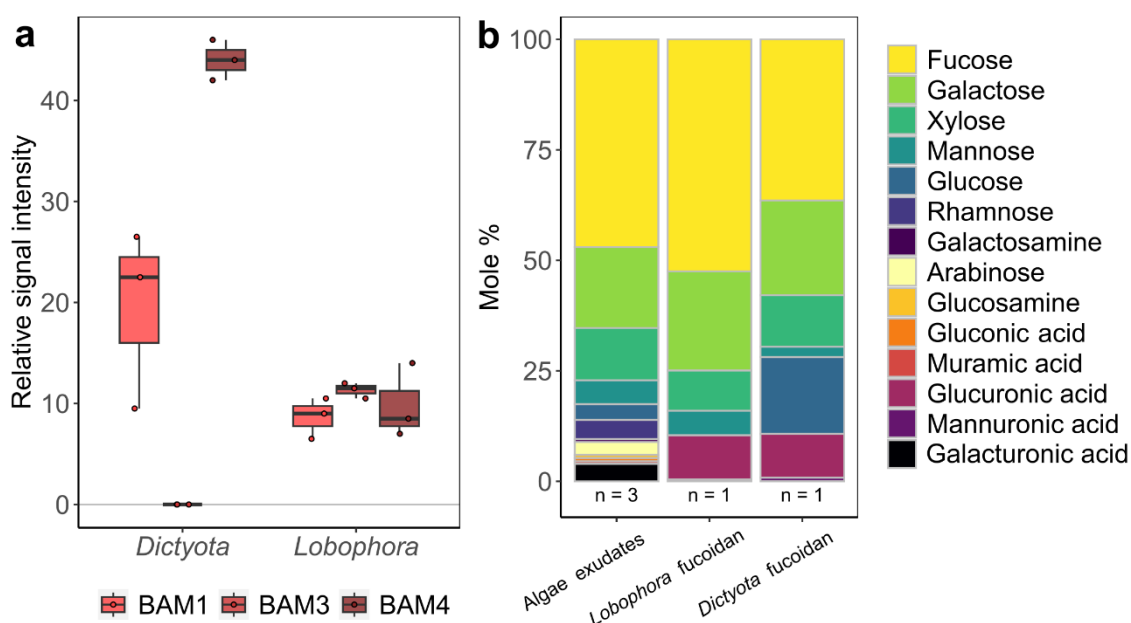


Figure S8.6. Evidence for fucoidan contribution to brown macroalgae HMW DOM. (a) Relative signal intensity of monoclonal antibodies binding to epitopes present in sulphated fucan for macroalgae tissue

extracts of *Dictyota* sp. and *Lobophora* sp. (sum of signals from UW, EDTA, and NaOH extracts). BAM2 was not detected in any sample. **(b)** Hydrolysable monosaccharide composition of algae exudates (control-corrected) and fucoidan extracted from dried tissue of macroalgae used in the present study. Relative signal intensity **(a)** cannot be compared among monoclonal antibodies, nor between algae species, because of different binding efficiencies.

Supplementary tables to chapter 8

Table S8.1. RFpermute model confusion matrix for classification after one and four days. LCI_0.95 / UCI_0.95 = lower / upper 95 % confidence interval. RF models are based on 5,000 trees each, with 16 variables tried at each split and 100 permutational replicates.

	Algae	Control	Coral	percent correct	LCI_0.95	UCI_0.95
1 day						
Algae	0	2	1	0.0	0.0	70.8
Control	2	1	0	33.3	0.8	90.6
Coral	0	0	3	100.0	29.2	100.0
Overall	NA	NA	NA	44.4	13.7	78.8
4 days						
Algae	0	3	0	0.0	0.0	70.8
Control	3	0	0	0.0	0.0	70.8
Coral	0	0	3	100.0	29.2	100.0
Overall	NA	NA	NA	33.3	7.5	70.1

Table S8.2. Microbial orders significantly enriched with coral exudates in the present study, and their previously described associations with coral mucus, coral exudates, coral disease and stress, and algae exudates. Numbers refer to supplementary references.

	Order	Found in coral mucus	Increase in seawater with coral mucus / exudates	Increase with coral disease / stress	Increase in seawater with algae exudates
Alpha-proteobacteria	Rhodobacterales	2-5	6-9	10-12	6
Gammaproteobacteria	Vibrionales	5,13	7,8,14	11,12,15,16	6
	Oceanospirillales	2,5,13	8		6
	Thiotrichales	4		17	
	Ectothiotrichales				
Bacteroidetes	Flavobacteriales	2-4	7,8	11,12,15	6
Planctomycetes	Chromatiales			18,19	
	OM190		6		

Table S8.3. Raw data to Fig. 8.2.

Name	Treatment	Fig. 8.2a DOC (µM)	Fig. 8.2b HMW DOC (µM)	Fig. 8.2c HMW DOC as CH (µM)	Fig. 8.2d HMW DOC as CH (%)
A1	Start	69.84	NA	NA	NA
A2	Start (1)	71.36	1.60	0.39	24.42
A3	Start	73.85	NA	NA	NA
C1	Start	72.03	NA	NA	NA
C2	Start	73.62	NA	NA	NA
C3	Start (2)	70.70	1.98	0.57	25.55
Con1	Start (3)	69.36	2.31	1.10	47.51
Con2	Start	74.08	NA	NA	NA
Con3	Start	75.57	NA	NA	NA
Con4	Start	69.16	NA	NA	NA
A1	Algae	84.85	2.28	1.75	76.71
A2	Algae	80.03	2.33	1.78	76.53
A3	Algae	79.81	3.65	2.50	68.56
C1	Coral	85.78	3.34	2.64	79.01
C2	Coral	79.74	2.71	1.38	70.71
C3	Coral	73.39	2.38	1.19	49.78
Con1	Control	76.58	2.82	0.99	35.23
Con2	Control	76.73	1.95	0.67	34.52
Con3	Control	75.91	1.87	0.66	35.41
Con4	Control	72.28	NA	0.87	NA

Table S8.4. Raw data for Fig. 8.3 & S8.2. Fuc = fucose, Rha = rhamnose, GalN = galactosamine, Ara = arabinose, GlcN = glucosamine, Gal = galactose, Glc = glucose, Man = mannose, Xyl = xylose, GlcA = gluconic acid, MurA = muramic acid, GalA = galacturonis acid.

Time	Name	Treatment	Fuc	Rha	GalN	Ara	GlcN	Gal	Glc	Man	Xyl	GlcA	MurA	GalA
Fig. 8.3 - $\mu\text{g L}^{-1}$														
Start	S1	Start	2.19	0.00	0.40	0.33	0.62	1.43	1.35	0.84	0.78	0.75	1.61	1.23
Start	S2	Start	2.80	0.00	0.62	1.19	0.87	2.58	2.01	1.03	1.93	0.18	2.34	1.26
Start	S3	Start	6.56	0.14	0.69	2.05	0.98	3.06	5.72	2.77	5.72	0.85	2.52	1.17
End	A1	Algae	18.74	1.63	0.81	2.24	0.94	9.13	4.69	3.53	4.34	0.50	1.59	2.56
End	A2	Algae	18.37	1.22	0.89	2.28	1.22	8.28	4.58	3.15	5.18	1.22	2.42	2.86
End	A3	Algae	21.01	2.47	1.25	3.43	1.66	13.45	7.66	4.63	9.25	0.66	3.64	3.74
End	C1	Coral	12.58	1.63	1.81	22.82	6.75	8.35	5.58	8.74	3.70	0.59	2.98	2.33
End	C2	Coral	5.56	0.47	1.06	10.02	3.18	4.82	4.12	4.37	1.42	1.12	2.61	2.12
End	C3	Coral	5.77	0.43	0.97	7.25	2.60	4.48	3.53	3.05	2.15	0.77	2.32	1.68
End	Con1	Control	4.83	0.09	0.75	2.09	1.00	3.93	6.30	2.13	3.94	0.47	2.49	1.26
End	Con2	Control	3.91	0.36	0.72	1.53	0.94	2.92	2.69	1.49	1.29	0.36	2.24	1.32
End	Con3	Control	2.86	0.56	0.61	1.06	0.79	2.96	2.83	1.66	1.55	0.89	2.25	1.58
End	Con4	Control	4.67	0.05	0.77	2.01	1.16	3.56	4.43	1.67	2.42	0.48	2.77	1.56
Fig. S8.2 - Mole %														
Start	S1	Start	28.64	0.00	4.80	4.75	7.42	17.09	16.10	9.99	11.20	8.25	13.79	13.59
Start	S2	Start	22.01	0.00	4.47	10.25	6.27	18.52	14.44	7.40	16.64	1.16	12.01	8.38
Start	S3	Start	24.08	0.52	2.32	8.21	3.31	10.23	19.13	9.25	22.95	2.62	6.04	3.62
End	A1	Algae	41.66	3.62	1.65	5.44	1.91	18.50	9.50	7.15	10.56	0.92	2.31	4.80
End	A2	Algae	41.49	2.77	1.84	5.63	2.52	17.04	9.43	6.49	12.79	2.30	3.58	5.47
End	A3	Algae	33.10	3.89	1.81	5.92	2.40	19.30	11.00	6.65	15.94	0.87	3.75	4.98
End	C1	Coral	17.55	2.27	2.31	34.80	8.62	10.61	7.10	11.11	5.64	0.69	2.71	2.75
End	C2	Coral	16.08	1.37	2.82	31.71	8.44	12.71	10.86	11.53	4.48	2.71	4.94	5.19
End	C3	Coral	19.33	1.44	2.99	26.59	8.00	13.68	10.79	9.30	7.88	2.16	5.07	4.76
End	Con1	Control	19.80	0.36	2.81	9.38	3.75	14.70	23.54	7.96	17.69	1.61	6.67	4.39
End	Con2	Control	25.48	2.38	4.28	10.88	5.61	17.33	16.00	8.83	9.22	1.95	9.56	7.25
End	Con3	Control	19.98	3.92	3.87	8.07	5.02	18.82	17.98	10.56	11.79	5.19	10.28	9.34
End	Con4	Control	23.20	0.24	3.50	10.93	5.29	16.10	20.02	7.57	13.16	1.99	9.00	6.56

Table S8.5. Raw data for Fig. 8.4. Values in mole % of algae tissue extracts, coral mucus, control-corrected fluxes (exudates), or ambient reef water.

Name	Treatment	Fucose	Rhamnose	Galactosamine	Arabinose	Glucosamine	Galactose	Glucose	Mannose	Xylose
Lob1	Lobophora tissue	33.86	0.63	0.15	0.00	1.68	15.35	12.56	10.73	10.61
Lob2	Lobophora tissue	31.60	0.41	0.03	0.00	1.76	16.74	18.72	9.88	9.44
Lob3	Lobophora tissue	34.97	1.03	0.17	0.00	2.08	19.13	7.50	10.93	11.91
Dic1	Dictyota tissue	23.31	1.29	0.00	0.00	1.10	14.55	14.11	4.53	7.56
Dic2	Dictyota tissue	17.12	0.37	0.00	0.00	0.83	16.45	13.61	4.50	7.11
Dic3	Dictyota tissue	24.94	0.79	0.00	0.00	1.03	15.70	7.91	3.80	8.38
Acr1	Acropora mucus	1.61	0.00	2.25	45.04	25.57	4.08	0.00	21.44	0.00
Acr2	Acropora mucus	2.28	0.00	3.09	52.11	22.91	5.26	0.00	14.35	0.00
Acr3	Acropora mucus	2.22	0.00	2.89	48.53	24.08	5.01	0.00	16.32	0.94
Dipl1	Diploria mucus	48.88	0.00	0.41	0.00	28.98	0.00	0.63	21.10	0.00
Dipl2	Diploria mucus	46.58	0.00	0.00	0.00	30.58	0.00	0.00	10.80	12.03
Dipl3	Diploria mucus	47.85	0.00	0.00	0.00	52.15	0.00	0.00	0.00	0.00
Mea1	Meandrina mucus	38.67	0.00	0.00	0.00	44.43	0.00	7.96	8.94	0.00
Mea2	Meandrina mucus	28.61	0.00	0.00	0.00	58.64	0.00	0.00	12.75	0.00
Algae1	Algae exudates	53.53	4.97	0.34	2.25	0.00	19.25	2.09	5.96	8.15
Algae2	Algae exudates	52.01	3.49	0.59	2.42	0.81	16.37	1.73	4.69	11.45
Algae3	Algae exudates	35.47	4.62	1.04	4.03	1.33	19.27	6.87	5.52	15.91
Coral1	Coral exudates	15.68	2.50	1.85	42.59	9.74	8.40	2.55	11.75	2.82
Coral2	Coral exudates	8.21	1.15	1.78	50.31	11.16	7.42	0.28	13.24	0.00
Coral3	Coral exudates	13.78	1.34	1.95	49.51	12.14	8.40	0.00	9.67	0.00
Reef	Ambient	20.11	4.28	3.01	9.47	3.89	14.31	14.45	7.31	14.43
Start1	Ambient	21.11	0.00	3.54	3.50	5.47	12.60	11.87	7.37	8.26
Start2	Ambient	18.11	0.00	3.68	8.43	5.15	15.24	11.88	6.09	13.69
Start3	Ambient	21.44	0.46	2.06	7.31	2.95	9.11	17.04	8.24	20.44

Table S8.6. Raw data for Fig. 8.5. Microbial cell counts, DOC- and nutrient concentrations.

Name	Treatment	Time	Microbes (mL ⁻¹)	DOC (µM)	NO2+NO3 (µM)	PO4 (µM)
A1	Algae	Start	713986	86.19	0.58	0.012
A2	Algae	Start	673311	NA	0.46	0.012
A3	Algae	Start	597027	88.06	0.51	0.012
C1	Coral	Start	645743	87.29	0.52	0.015
C2	Coral	Start	635878	NA	0.48	0.016
C3	Coral	Start	595000	87.05	0.49	0.014
Con1	Control	Start	752635	90.84	0.33	0.015
Con2	Control	Start	638041	86.89	NA	NA
Con3	Control	Start	706622	87.52	0.54	0.009
A1	Algae	6 h	807365	77.56	0.52	0.010
A2	Algae	6 h	756959	NA	0.46	0.011
A3	Algae	6 h	720878	81.86	0.58	0.013
C1	Coral	6 h	709910	80.12	0.56	0.014
C2	Coral	6 h	668694	NA	0.46	0.015
C3	Coral	6 h	733288	79.85	0.50	0.012
Con1	Control	6 h	762635	84.49	0.60	0.012
Con2	Control	6 h	721149	82.18	0.51	0.009
Con3	Control	6 h	675203	83.07	0.51	0.010
A1	Algae	12 h	916630	82.30	0.51	0.006
A2	Algae	12 h	802507	NA	0.45	0.009
A3	Algae	12 h	791630	80.59	0.60	0.009
C1	Coral	12 h	1298080	77.50	0.48	0.008
C2	Coral	12 h	823225	NA	0.44	0.011
C3	Coral	12 h	676571	79.09	0.54	0.013
Con1	Control	12 h	1256920	81.60	0.57	0.006
Con2	Control	12 h	1099529	80.94	0.58	0.015
Con3	Control	12 h	1048804	81.75	0.56	0.009
A1	Algae	1 day	1081884	79.97	0.52	0.005
A2	Algae	1 day	928261	NA	0.41	0.005
A3	Algae	1 day	1166558	80.54	0.62	0.007
C1	Coral	1 day	1174239	78.10	NA	NA
C2	Coral	1 day	1000580	NA	0.34	0.008
C3	Coral	1 day	1057283	79.73	0.37	0.010
Con1	Control	1 day	1044493	82.74	0.53	0.004
Con2	Control	1 day	1076522	79.97	0.54	0.005
Con3	Control	1 day	1044964	82.32	0.51	0.005
A1	Algae	4 days	783423	81.84	0.19	0.012
A2	Algae	4 days	827883	NA	0.07	0.011
A3	Algae	4 days	844910	83.49	0.18	0.008
C1	Coral	4 days	762568	80.43	0.19	0.009
C2	Coral	4 days	782973	NA	0.07	0.010
C3	Coral	4 days	897973	83.08	0.19	0.005
Con1	Control	4 days	773784	79.99	0.16	0.006
Con2	Control	4 days	776351	76.24	0.15	0.008
Con3	Control	4 days	808919	79.41	0.21	0.018

Table S8.7. Results of *DESeq2* analyses for 1 and 4 days; raw data to Fig. 8.7. Only genera with significant *p* adjust are shown (out of a total of 101 and 111 genera detected after 1 and 4 days, respectively).

Time	Family_Genus	base Mean	log2Fold Change	lfcSE	stat	p-value	p adj
1 day	Rhodobacteraceae_Nautella	26.64	2.86	0.67	4.29	0.0000	0.0009
1 day	Saccharospirillaceae_Oleispira	8.32	2.61	0.88	2.95	0.0032	0.0459
1 day	Vibrionaceae_unclassified	24.11	2.00	0.60	3.35	0.0008	0.0203
1 day	Flavobacteriales_unclassified	48.69	1.89	0.41	4.57	0.0000	0.0005
1 day	Phycisphaeraceae_Urania-1B-19_m.s.g.	30.65	1.12	0.35	3.16	0.0016	0.0266
1 day	Oleiphilaceae_Oleiphilus	178.98	0.96	0.30	3.22	0.0013	0.0261
1 day	Marine_Group_II_ge	14.46	-3.10	0.77	-4.05	0.0001	0.0017
4 days	Phycisphaeraceae_Urania-1B-19_m.s.g.	37.50	2.10	0.45	4.63	0.0000	0.0001
4 days	Flavobacteriales_unclassified	20.57	1.88	0.48	3.91	0.0001	0.0026
4 days	Rhodobacteraceae_Shimia	38.43	1.71	0.48	3.60	0.0003	0.0059
4 days	Saprospiraceae_uncultured	20.29	1.52	0.54	2.83	0.0047	0.0377
4 days	Vibrionaceae_unclassified	19.04	1.34	0.50	2.68	0.0075	0.0488
4 days	Ectothiorhodospiraceae_uncultured	39.71	1.30	0.38	3.44	0.0006	0.0091
4 days	Phycisphaeraceae_CL500-3	73.65	1.25	0.42	2.98	0.0029	0.0294
4 days	Thiotrichaceae_uncultured	29.93	1.24	0.40	3.11	0.0019	0.0207
4 days	Rhodobacteraceae_unclassified	589.73	1.14	0.22	5.29	0.0000	0.0000
4 days	OM190_ge	110.63	0.87	0.24	3.64	0.0003	0.0059

4 days	Alphaproteobacteria uncultured ge	48.73	-1.20	0.44	-2.73	0.0063	0.0449
4 days	Saccharospirillaceae Oleibacter	32.11	-1.49	0.53	-2.82	0.0048	0.0377
4 days	Puniceococcaceae MB11C04 m.g.	13.47	-1.68	0.57	-2.92	0.0035	0.0323
4 days	Methylophilaceae OM43 clade	14.58	-2.37	0.75	-3.16	0.0016	0.0196
4 days	Marine Group III ge	5.81	-3.78	1.39	-2.72	0.0065	0.0449
4 days	Methylophagaceae Marine Methylophilic g 3	128.28	-4.20	1.29	-3.25	0.0012	0.0162
4 days	Methylophagaceae unclassified	188.58	-5.40	1.14	-4.73	0.0000	0.0001

Table S8.8. Raw data to Fig. 8.8a. Predicted pathway class abundance (MicFunPred).

Treatment	Time	ID	Energy Metabolism	Amino Acids	Carbo-hydrates	Fatty Acids and Lipids	Secondary metabolites
Algae	Start	A1	22418	16161	12280	7283	6275
Algae	Start	A2	24080	16505	13337	7542	6797
Algae	Start	A3	17407	6183	4745	6091	4099
Coral	Start	C1	21875	15384	12107	6904	6228
Coral	Start	C2	22273	14722	12049	8598	6196
Coral	Start	C3	21520	15854	11824	7032	6049
Control	Start	Con1	23357	14893	12714	7176	6534
Control	Start	Con2	21502	14485	11824	6774	6033
Control	Start	Con3	22830	15331	12395	7037	6310
Algae	6 h	A1	20381	13707	11532	6878	5625
Algae	6 h	A2	21169	14016	11793	6889	5830
Algae	6 h	A3	20428	14200	11201	7830	5570
Coral	6 h	C1	21431	13220	8224	7832	4824
Coral	6 h	C2	20647	12673	8224	7372	4648
Coral	6 h	C3	19755	11293	10952	6691	4810
Control	6 h	Con1	19188	13575	10605	7771	5423
Control	6 h	Con2	17746	11509	6943	6603	4095
Control	6 h	Con3	20571	14180	11565	6902	5659
Algae	12 h	A1	22081	13772	6762	9164	4978
Algae	12 h	A2	29227	18064	16758	10997	7140
Algae	12 h	A3	27705	18324	8497	12048	6305
Coral	12 h	C1	38139	29902	21315	16766	10232
Coral	12 h	C2	32902	27765	18184	15542	11611
Coral	12 h	C3	29686	21593	12218	12718	6672
Control	12 h	Con1	22550	13381	6786	9512	5108
Control	12 h	Con2	23941	16870	9744	9947	5403
Control	12 h	Con3	25483	17648	7853	11136	5842
Algae	1 day	A1	59208	54291	23458	32083	16586
Algae	1 day	A2	55333	47963	25357	28216	13175
Algae	1 day	A3	58839	53391	27857	31068	15787
Coral	1 day	C1	53193	44657	19633	28543	14082
Coral	1 day	C2	68107	63784	41621	38413	19439
Coral	1 day	C3	62118	57683	40751	30384	18282
Control	1 day	Con1	64309	61930	44629	38378	19007
Control	1 day	Con2	62822	62119	45274	33379	19152
Control	1 day	Con3	59046	52004	23821	33019	17238
Algae	4 days	A1	69145	54011	24819	37645	16050
Algae	4 days	A2	72811	55480	25648	38644	16116
Algae	4 days	A3	75085	57666	27013	38131	18389
Coral	4 days	C1	90982	81437	56127	42236	26523
Coral	4 days	C2	92795	80717	55062	48205	25573
Coral	4 days	C3	88055	85263	53059	50319	31733
Control	4 days	Con1	68873	54646	25517	37476	16597
Control	4 days	Con2	70014	61847	25749	38811	16857
Control	4 days	Con3	72704	55836	26483	36924	18049

Supplementary references to chapter 8

1. Vidal-Melgosa, S. *et al.* Diatom fucan polysaccharide precipitates carbon during algal blooms. *Nature Comm.* **12**, 1150 (2021).
2. Apprill, A., Weber, L. G. & Santoro, A. E. Distinguishing between microbial habitats unravels ecological complexity in coral microbiomes. *mSystems* **1**, e00143-16 (2016).

3. Lima, L. F. O. *et al.* Coral and seawater metagenomes reveal key microbial functions to coral health and ecosystem functioning shaped at reef scale. *Microb. Ecol.* **86**, 392–407 (2023).
4. Marchioro, G. M. *et al.* Microbiome dynamics in the tissue and mucus of acroporid corals differ in relation to host and environmental parameters. *PeerJ* **8**, e9644 (2020).
5. Zou, Y., Chen, Y., Wang, L., Zhang, S. & Li, J. Differential responses of bacterial communities in coral tissue and mucus to bleaching. *Coral Reefs* **41**, 951–960 (2022).
6. Nelson, C. E. *et al.* Coral and macroalgal exudates vary in neutral sugar composition and differentially enrich reef bacterioplankton lineages. *ISME J* **7**, 962–979 (2013).
7. Taniguchi, A., Kuroyanagi, Y., Aoki, R. & Eguchi, M. Community structure and predicted functions of actively growing bacteria responsive to released coral mucus in surrounding seawater. *Microb. Environ.* **38**, ME23024 (2023).
8. Taniguchi, A., Yoshida, T., Hibino, K. & Eguchi, M. Community structures of actively growing bacteria stimulated by coral mucus. *J. Exp. Mar. Biol. Ecol.* **469**, 105–112 (2015).
9. Weber, L. *et al.* Benthic exometabolites and their ecological significance on threatened Caribbean coral reefs. *ISME Commun.* **2**, 1–13 (2022).
10. Bourne, D. G., van der Zee, M. J. J., Botté, E. S. & Sato, Y. Sulfur-oxidizing bacterial populations within cyanobacterial dominated coral disease lesions. *Environ. Microbiol. Rep.* **5**, 518–524 (2013).
11. McDevitt-Irwin, J. M., Baum, J. K., Garren, M. & Vega Thurber, R. L. Responses of coral-associated bacterial communities to local and global stressors. *Front. Mar. Sci.* **4**, 262 (2017).
12. Meyer, J. L. *et al.* Microbial community shifts associated with the ongoing stony coral tissue loss disease outbreak on the Florida reef tract. *Front. Microbiol.* **10**, 2244 (2019).
13. Lee, S. T. M., Davy, S. K., Tang, S.-L., Fan, T.-Y. & Kench, P. S. Successive shifts in the microbial community of the surface mucus layer and tissues of the coral *Acropora muricata* under thermal stress. *FEMS Microbiol. Ecol.* **91**, fiv142 (2015).
14. Allers, E., Niesner, C., Wild, C. & Pernthaler, J. Microbes enriched in seawater after addition of coral mucus. *AEM* **74**, 3274–3278 (2008).
15. Gignoux-Wolfsohn, S. A. & Vollmer, S. V. Identification of candidate coral pathogens on white band disease-infected staghorn coral. *PLOS ONE* **10**, e0134416 (2015).
16. Lee, S. T. M., Davy, S. K., Tang, S.-L. & Kench, P. S. Mucus sugar content shapes the bacterial community structure in thermally stressed *Acropora muricata*. *Front. Microbiol.* **7**, 371 (2016).
17. Heitzman, J. M., Caputo, N., Yang, S.-Y., Harvey, B. P. & Agostini, S. Recurrent disease outbreak in a warm temperate marginal coral community. *Mar. Pollut. Bull.* **182**, 113954 (2022).
18. Li, J., Long, L., Zou, Y. & Zhang, S. Microbial community and transcriptional responses to increased temperatures in coral *Pocillopora damicornis* holobiont. *Environ. Microbiol.* **23**, 826–843 (2021).

19. Ziegler, M., Seneca, F. O., Yum, L. K., Palumbi, S. R. & Voolstra, C. R. Bacterial community dynamics are linked to patterns of coral heat tolerance. *Nat. Commun.* **8**, 14213 (2017).

Universität Bremen
Fachbereich 2
Prüfungsamt Chemie
z. Hd. Frau Frauke Ernst
Leobener Straße

28359 Bremen
Deutschland

Prüfungsamt
Chemie

Frauke Ernst
Geschäftsstelle
Fachbereich 02
Leobener Str. / NW2
D-28359 Bremen

Verwaltungspavillon 06
Tel. 0421 218-62802
Fax 0421 218-9862802
frauke.ernst@uni-bremen.de
www.fb2.uni-bremen.de

Versicherung an Eides Statt

Name, Vorname	Thobor, Bianca M.
Matrikel-Nr.	
Straße	Hamburger Str. 29G
Ort, PLZ	Bremen, 28205

Ich, Bianca M. Thobor

versichere an Eides Statt durch meine Unterschrift, dass ich die vorstehende Arbeit selbständig und ohne fremde Hilfe angefertigt und alle Stellen, die ich wörtlich dem Sinne nach aus Veröffentlichungen entnommen habe, als solche kenntlich gemacht habe, mich auch keiner anderen als der angegebenen Literatur oder sonstiger Hilfsmittel bedient habe.

Ich versichere an Eides Statt, dass ich die vorgenannten Angaben nach bestem Wissen und Gewissen gemacht habe und dass die Angaben der Wahrheit entsprechen und ich nichts verschwiegen habe.

Die Strafbarkeit einer falschen eidesstattlichen Versicherung ist mir bekannt, namentlich die Strafandrohung gemäß § 156 StGB bis zu drei Jahren Freiheitsstrafe oder Geldstrafe bei vorsätzlicher Begehung der Tat bzw. gemäß § 161 Abs. 1 StGB bis zu einem Jahr Freiheitsstrafe oder Geldstrafe bei fahrlässiger Begehung.

Ort, Datum / Unterschrift